



NASA-CR-184317

(UAH-5-32640) ADVANCED ELECTRIC MOTOR
TECHNOLOGY: FLUX MAPPING Final Technical
Report, Apr. 1992 (Alabama Univ.) 303 p

CSCL 09C

G3

11/33

N92-24047

Unclas
0086909

**Research Institute
The University of Alabama in Huntsville**

NASANational Aeronautical and
Space Agency**Report Document Page**

1. Report No.	2. Government Accession No.	3. Recipient's Catalog No.	
4. Title and Subtitle "Advanced Electric Motor-Flux Mapping"		5. Report Due April 10, 1992	
		6. Performing Organization Code Research Institute, UAH	
7. Author(s) Dr. George Doane III, Dr. Warren Campbell and Mr. Larry Brantley		8. Performing Organization Report No. Delivery Order 121	
		10. Work Unit No. 5-32640	
9. Performing Organization Name and Address UAH Research Institute RI E-47 Huntsville, AL 35899		11. Contract or Grant No. NAS8-36955, D.O. 121	
		13. Type of report and Period covered Final Technical Report April 1992	
12. Sponsoring Agency Name and Address National Aeronautics and Space Administration Washington, D.C. 20546-001 Marshall Space Flight Center, AL 35812		14. Sponsoring Agency Code	
		15. Supplementary Notes	
16. Abstract Research into optimizing the electric motor to be used in space vehicle control; for example-thrust vector control. Consideration given to optimum gear ratios and the use of the latest computer techniques and materials to design the motor.			
17. Key Words (Suggested by Authors(s)) electromagnetic actuators, optimum gear trains, use of latest magnetic materials		18. Distribution Statement TBD	
19. Security Class. (of this report) Unclassified	20. Security Class. (of this page) Unclassified	21. No. of pages	22. Price TBA

ABSTRACT

This report contains the assumptions, mathematical models, design methodology and point designs involved with the design of an electromechanical actuator (EMA) suitable for directing the thrust vector of a large MSFC/NASA launch vehicle. Specifically the design of such an actuator for use on the upcoming liquid fueled National Launch System (NLS) is considered culminating in a point design of both the servo system and the electric motor needed. A major thrust of the work is in selecting spur gear and roller screw reduction ratios (in consort with a given load and various motors from which to choose) to achieve simultaneously wide bandwidth, maximum power transfer and disturbance rejection while meeting specified horsepower requirements at a given stroking speed as well as a specified maximum stall force. An innovative feedback signal is utilized in meeting these diverse objectives.

ACKNOWLEDGEMENT

The authors gratefully acknowledge being given access to the data from previous hydraulic actuator designs. These data were made available by Messrs Cornelius, Harbison, Lominick, Sharkey and our technical coordinator Ms. Weir. These data concerning previous designs were very valuable especially in establishing realistic requirements and responses for the EMA. In addition, conversations with MSFC personnel at various points in time during this investigation were both helpful and quite insightful.

PREFACE

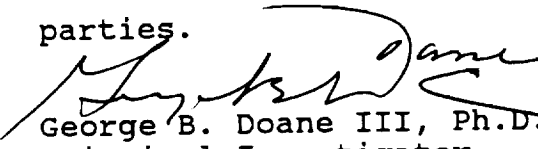
This technical report was prepared by the Space Systems and Technology Laboratory (SSTL) of the University of Alabama in Huntsville Research Institute. This is the final report of technical work performed under contract number NAS8-36955, Delivery Order Number 121.

The principal investigator was Dr. George B. Doane III, coordinator of the SSTL. Much of the technical work was contributed by Mr. Larry W. Brantley and by Mr. Garvin Dean.

Ms. Rae Ann Weir of the Control Mechanisms and Propellant Delivery Branch, Component Development Division, Propulsion Laboratory, MSFC/NASA was the technical coordinator for MSFC.

The views, opinions and/or findings contained in this report are those of the authors and should not be construed as an official MSFC position, policy or finding unless so specified by other MSFC/NASA documentation.

Except as may be otherwise authorized this report and its findings require MSFC approval before release to third parties.


George B. Doane III, Ph.D., P.E.
Principal Investigator

Approval:


Research Institute

TABLE OF CONTENTS

ABSTRACT.....	ii
ACKNOWLEDGEMENTS.....	iii
PREFACE.....	iv
 I. INTRODUCTION.....	 1-1
 II. STATEMENT OF RESEARCH PROBLEM AREA.....	 2-1
 III. APPROACH USED.....	 3-1
 IV. DETAILED ANALYSIS.....	 4-1
A. System Inertia Considerations.....	4-2
B. Selection Of Optimum Bandwidth Gear Ratio (n) And Lead (l).....	4-10
C. Final Selection Of Gear Ratio (n) and Lead (l) For Point Design.....	4-63
D. Development Of Simulation Model.....	4-67
E. Servoloop Design Procedures.....	4-74
F. Non-Linear Model.....	4-92
G. Controller Reconfiguration To Minimize Effects Of Start/Stop Transient Disturbance Forces..	4-103
H. Unloaded Actuator Operation.....	4-110
I. Effects Of Mechanical Stops.....	4-122
J. Friction Modeling.....	4-144
K. Electric Motor Design.....	4-167
 V. DISCUSSION OF RESULTS.....	 5-1
 VI. CONCLUSIONS AND RECOMMENDATIONS.....	 6-1
 VII. APPENDICES.....	 7-1
A. Maximum Power Transfer Considerations.....	7-2
B. Why A Small Motor And A Large Gear Train May Not Be What Is Wanted.....	7-19
C. Various Roller Screw Relationships.....	7-25
D. Load Analysis.....	7-36
E. NASA/MSFC Specifications.....	7-38
F. Geometrical And Disturbance Calculations...	7-45
G. Demonstration Of Optimality Of Final Selection Of Gear Ratio(n) And Lead(l) For Point Design.....	7-61

CONTRACTOR REPORT

ADVANCED ELECTRIC MOTOR
TECHNOLOGY
FLUX MAPPING

Dr. George B. Doane III
Dr. Warren Campbell
Mr. Larry W. Brantley
Mr. Garvin Dean

CONTRACT NO./DELIVERY ORDER NO. NAS8-36955/121

MARCH 1992

INTRODUCTION

INTRODUCTION

This report contains the design considerations attendant to furnishing an electromechanical actuator (EMA) for the control of the thrust vector of new large liquid fueled NASA launch vehicles. In particular the point designs shown herein are based on Space Shuttle Main Engine (SSME) or, as it became available, national launch system (NLS) engineering parameters. It is interesting to note that the first large US launch vehicle (the REDSTONE missile) used electromechanical actuators to develop its vehicle control moments i.e. control of the carbon vane rocket engine exhaust deflectors and the ganged aerodynamic fin deflections. These first actuators functioned all right but they were plagued by the high repair rate of the multistage electromechanical relay boxes used to control the flow of electrical power to the low inertia electric motors. These motors were in turn attached to a rod which pivoted the carbon vanes and the aerodynamic surfaces (on the same shaft) which became active as the vehicle gained air speed.

To overcome the problems encountered in the REDSTONE EMAs and to make use of technology developed in the aircraft industry subsequent launch vehicles have used hydraulic actuators; typically a double acting ram cylinder for actuators used in swiveling the entire rocket engine to achieve thrust vector control and also reversible rotary

actuators for propellant flow control. While their success is manifest for all to see one could eliminate one whole system with all of its logistics i.e. the hydraulic one with its mandatory supplies of very clean oil, filters for micron sized contamination particles, system purge requirements etc. if electromechanical actuators could once again be used. After all there will be a supply of electricity on board any foreseeable large launch system. The enabling technology that has developed in recent times is the ability of semiconductor based amplifiers using pulse techniques to handle and control relatively large amounts of electrical power (e.g. 200 Amps) from the proposed 270 Volt DC (nominal) power system of the NLS (previous launch systems used nominal 28 Volt DC systems).

This report points out some of the similarities between the design of an hydraulic thrust vector control system and an electromechanical one as well as the dissimilarities which are very real. The accompanying figure lays out the steps required in such a design study. In the body of the report it is pointed out how very important it is to consider the design as an integrated whole if high performance is to be obtained. It is relatively easy to design an actuator which will traverse in and out on command. However, it is quite another task to consider the compliance of the engine and structure, the masses of the elements involved, the desired speed of response, the maximum required force, resistance to

```
graph TD
    SSReq([STEADY STATE REQUIREMENTS]) --> OverallReq[OVERALL PERFORMANCE REQUIREMENTS]
    DynReq([DYNAMIC REQUIREMENTS]) --> OverallReq
    OverallReq --> IntegrateReq[INTEGRATE REQUIREMENTS AND CONFIGURATION DATA]
    IntegrateReq --> CreateModel[CREATE GENERAL SYSTEM ANALYTICAL MODEL]
    CreateModel --> PerformDesign[PERFORM POINT DESIGNS FOR VARIOUS ELECTRIC MOTOR AND GEAR TRAIN SELECTIONS]
    PerformDesign --> EvalDesign[EVALUATE POINT DESIGNS]
    EvalDesign --> PerformDesign
    PerformDesign --> DesignCtrl[DESIGN & FABRICATE CONTROLLER]
    DesignCtrl --> AssembleMotors[ASSEMBLE MOTORS IN TEST ACTUATOR & TEST IN LOAD FIXTURE]
    AssembleMotors --> DesignCtrl
    
    FormFit[FORM/FIT CONSTRAINTS] --> MechConfig[MECHANICAL CONFIGURATION]
    Redundancy[REDUNDANCY REQUIREMENTS] --> MechConfig
    MechConfig --> IntegrateReq
    
    RocketEng[RCKET ENGINE MASS AND COMPLIANCE] --> MaxAcc([MAXIMIZE LOAD ACCELERATION FOR GIVEN MOTOR INERTIAS])
    StructComp[STRUCTURAL COMPLIANCE] --> MaxAcc
    MaxAcc --> EstParams[ESTABLISH VARIOUS MOTORS' ELECTROMECHANICAL PARAMETERS]
    EstParams --> DesignMotors[DESIGN ELECTRIC MOTORS OPTIMIZING INERTIA, TORQUE AND TEMPERATURE CHARACTERISTICS]
    DesignMotors --> AssembleMotors
```

expected disturbances and produce an optimized or even acceptable design.

A particularly interesting feature of this design effort is the use of finite element methods (FEM) (implemented by means of the magnetic analysis option of the ANSYS digital computer program) to design the magnetic circuits of the requisite electric motor. This approach allows direct control of the motor magnetic flux paths, trade studies involving different magnetic material characteristics, the calculation of torque developed as a function of torque angle for a given design e.g. for a given set of permanent magnets, thermal considerations and so on without having to build and test the various configurations. This approach allows tailoring a motor design to meet the demands of the optimized actuator. It should be noted though that the beginning points of the motor design are premised on existing motor designs so that unreasonable parameters are not specified.

**STATEMENT OF RESEARCH
PROBLEM AREA**

STATEMENT OF RESEARCH PROBLEM AREA

To be investigated in this work were the factors necessary to use electromagnetic actuators (EMAs) as the thrust vector control (TVC) actuators for the upcoming National Launch System (NLS). Development of the gearing specifications, overall coupled dynamics of the actuator and load (the rocket engine and support structure), a suitable multiloop servomechanism design and particularly the accompanying electric motor design needed to be addressed. For the most part numerical engineering parameters were obtained from the Space Shuttle Main Engine (SSME) system because most of the NLS engineering parameter numbers are yet to be determined.

The first task accomplished was establishing a methodology by which designs of an EMA could be performed methodically. This allows at any time in the future new designs to be accomplished without further research to identify the methods to be employed and the issues to be addressed.

Another area researched was the establishment of a design procedure which produces maximum system bandwidth with a given electric motor and load (rocket engine and attach structure). This involves, as one of its facets, developing the gearing ratios optimization technique. Another part of this effort required the development of the overall dynamic

system equations and the multiloop servomechanism design procedures to achieve the required bandwidth.

The major area investigated was that of the design of the electric motor itself. This area involves requirements developed in the first two areas alluded to above. The motor design involves creating a finite element model (FEM) of the magnetic and thermal flux flows in the motor and tailoring each to this application. The results of the first two areas of effort supply the numerical values of the parameters e.g. motor inertia, motor back emf/torque constant, maximum torque, resistance and so forth that the motor design must meet. Various pertinent properties of permanent magnet and back iron material were to be assembled. Liaison with the electronic controller designers and accumulating awareness of the proposed electric power bus were to be accomplished.

APPROACH USED

APPROACH USED

A three pronged approach was used in solving the actuator design problems addressed in this research.

The first problem solution undertaken was to determine a methodology which, given the load and a range of possible electric motor characteristics, could be used to obtain the optimum spur gear and roller gear reduction factors (from the motor to the tailstock) that should be used in a given design. In the course of this work the object was to choose the factors in such a way as to maximize the acceleration of the load utilizing the least amount of power possible. The resulting design had to be capable of being built.

After obtaining the solution to the first problem the servoloop design methodology was established by means of an example (using classical techniques and simulation) in which a multiloop servo was designed that met all of MSFC/NASA's known dynamic performance requirements. This design was tested in a number of different scenarios (output disturbance, nonloaded operation, end of travel dynamics) to determine how well it performed in off-nominal and nonlinear operation.

Having established both the power train and servoloop design methodologies and having exercised them in a

realistic example they were applied to the major design effort, i.e. that of the electric motor. The results of the first two solution methodologies pointed the way in determining the characteristics (e.g. torque to inertia ratio) most conducive to optimum actuator operation. It was decided to use finite element methods to design the electric motor's electromagnetic circuits and also to use it to analyze the temperature distribution and heat flow within the proposed motor configurations. The finite element analysis system chosen was ANSYS. This involved securing the manuals, obtaining access to this resource and learning the ANSYS analysis methods as well as the language of ANSYS.

DETAILED ANALYSIS

**SYSTEM INERTIA
CONSIDERATIONS**

A. SYSTEM INERTIA CONSIDERATIONS

Introduction

For this design, three 15 HP-3000 RPM motors were chosen. The number of motors was determined by MSFC and most likely was based upon redundancy considerations. The horsepower rating and the RPM rating of the motors was chosen to meet the MSFC requirements of 40,000 lbs at 5 in/sec and 60,000 lbs at stall. It is clear that several combinations of horsepower and RPM ratings could be chosen to meet the two above requirements, however, the 15 HP-3000 RPM motor was chosen because it provides maximum acceleration of the load for a given torque (Refer to Page 4-53 for details).

Calculation Of Motor Inertia

The inertia of a permanent magnet motor is given by the following equation (obtained from MSFC)

$$J_{\text{Motor}} = \frac{(565)(\text{HP})^{3/2}}{(\text{RPM})^{5/3}} \text{ in-lbs-sec}^2$$

where HP = Horsepower and RPM = Revolutions Per Minute. For three motors this becomes

$$J_{3\text{-Motor}} = \frac{(3)(565)(\text{HP})^{3/2}}{(\text{RPM})^{5/3}} \text{ in-lbs-sec}^2$$

A motor specifications sheet received from MSFC/EP-64 contained a description of an actual permanent magnet motor that had a motor inertia ten times smaller than the motor inertia given by the above equation. Therefore, it was assumed that a 15 HP-3000 RPM permanent magnet motor could be designed and built to have a motor inertia five times smaller

than that given by the above equation. Using this assumption, the inertia of the three permanent magnet motors is now given by

$$J_{3\text{-Motor}} = \frac{(3)(565)(\text{HP})^{3/2}}{(5)(\text{RPM})^{5/3}} \text{ in-lbs-sec}^2$$

Reflected Inertia Seen By The Motor

From the preceding section, the inertia of the three permanent magnet motors used in this design is given by the following equation

$$J_{3\text{-Motor}} = \frac{(3)(565)(\text{HP})^{3/2}}{(5)(\text{RPM})^{5/3}} = \frac{(3)(565)(15)^{3/2}}{(5)(3000)^{5/3}} = 0.0315598 \text{ in-lbs-sec}^2$$

Other inertias and masses included in this system were:

$$J_{3\text{-Pinion Gear}} = (3)(J_{\text{Pinion Gear}}) = (3)(4.768 \times 10^{-5}) = 1.4304 \times 10^{-4} \text{ in-lbs-sec}^2$$

$$J_{\text{Bull Gear}} = n^4 J_{\text{Pinion Gear}} = (4.28)^4 (4.768 \times 10^{-5}) = 0.0159997 \text{ in-lbs-sec}^2$$

$$J_{\text{Roller Screw}} = 0.016 \text{ in-lbs-sec}^2$$

$$M_{\text{Tailstock}} = 0.257998 \frac{\text{lbs-sec}^2}{\text{in}}$$

$$M_{\text{Engine}} = 55 \frac{\text{lbs-sec}^2}{\text{in}}$$

The values for the pinion gear inertia, the roller screw inertia, the mass of the tailstock, and the mass of the engine were obtained directly from MSFC (The value of 4.28 used for n was calculated on Page 4-55). The inertia of the pinion gears can be added directly to the inertia of the motors; however, the inertias of the bull gear and roller screw, the mass of the tailstock, and the mass of the engine must be reflected through the gear train and roller screw in the correct manner.

The inertia of the bull gear and the roller screw can be reflected to the motor shaft by dividing by the square of the gear ratio, or

$$\frac{J_{\text{Bull Gear}}}{n^2}$$

$$\frac{J_{\text{Roller Screw}}}{n^2}$$

The mass of the tailstock and the engine can be reflected to the motor shaft by dividing by the square of the overall gear ratio, or

$$\frac{M_{\text{Tailstock}}}{\left[\frac{2 \pi n}{l}\right]^2}$$

$$\frac{M_{\text{Engine}}}{\left[\frac{2 \pi n}{l}\right]^2}$$

Therefore, the reflected inertia seen by the motors is given by the following equation:

$$\text{Reflected Inertia} = J_{3\text{-Motor}} + J_{3\text{-Pinion Gear}} + \frac{J_{\text{Bull Gear}} + J_{\text{Roller Screw}}}{n^2} + \frac{M_{\text{Tailstock}} + M_{\text{Engine}}}{\left[\frac{2 \pi n}{l}\right]^2}$$

Dominant Inertia Of This System

To determine the dominant inertia of this system, compare the inertia of each component as n (gear ratio) and l (lead) vary over a certain range (n varies from 1-10 and l varies from 0.01-1).

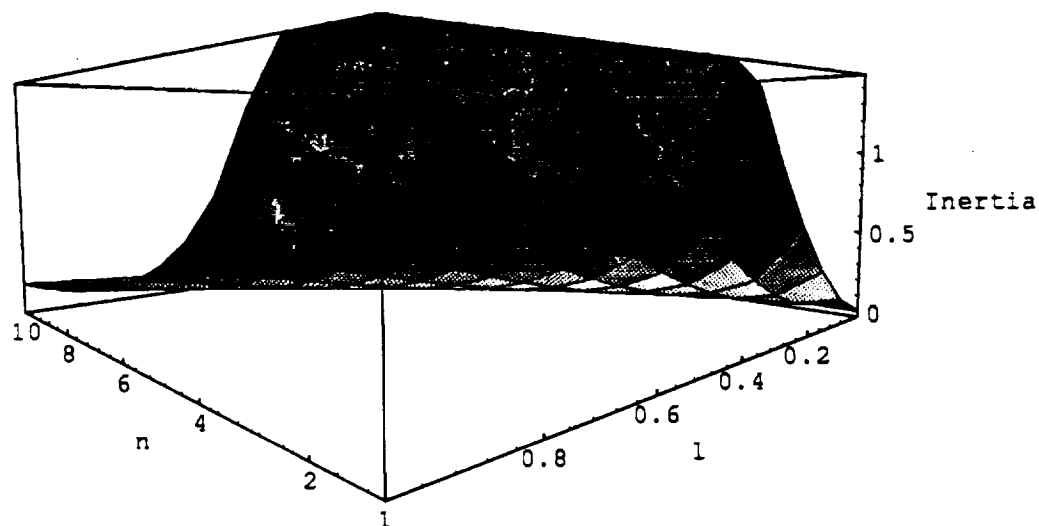
The motor speed (due to the rate requirement of 5 in/sec for the load) can be expressed as

$$S_{\text{Motor}} = \left(\frac{5 \text{ in}}{\text{sec}}\right) \left(\frac{2\pi}{1}\right) (n) \left(\frac{60 \text{ sec}}{\text{min}}\right) \left(\frac{1 \text{ rev}}{2\pi \text{ rad}}\right) = 47.7465 \left(\frac{2\pi}{1}\right) (n)$$

Substituting into the equation for motor inertia yields

$$J_{3\text{-Motor}} = \frac{(3)(565)(\text{HP})^{3/2}}{(\text{RPM})^{5/3}} = \frac{(3)(565)(\text{HP})^{3/2}}{[47.7465 \left(\frac{2\pi}{1}\right) (n)]^{5/3}} = \frac{(3)(0.899)(15)^{3/2}}{\left[\frac{2\pi n}{1}\right]^{5/3}}$$

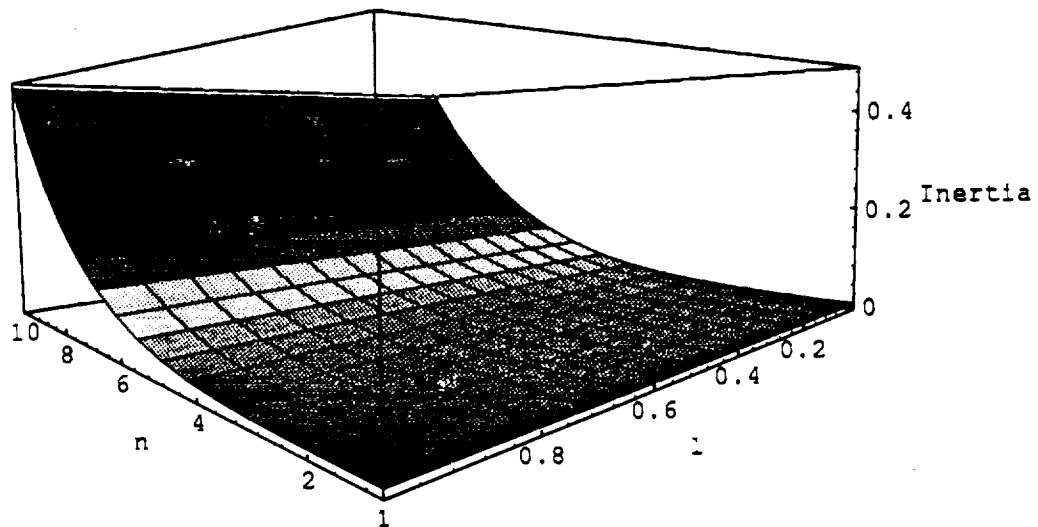
Plotting the above equation as n and l vary



The bull gear inertia is related to the pinion gear inertia in the following manner:

$$J_{\text{Bull Gear}} = n^4 J_{\text{Pinion Gear}} = 0.00004768 n^4$$

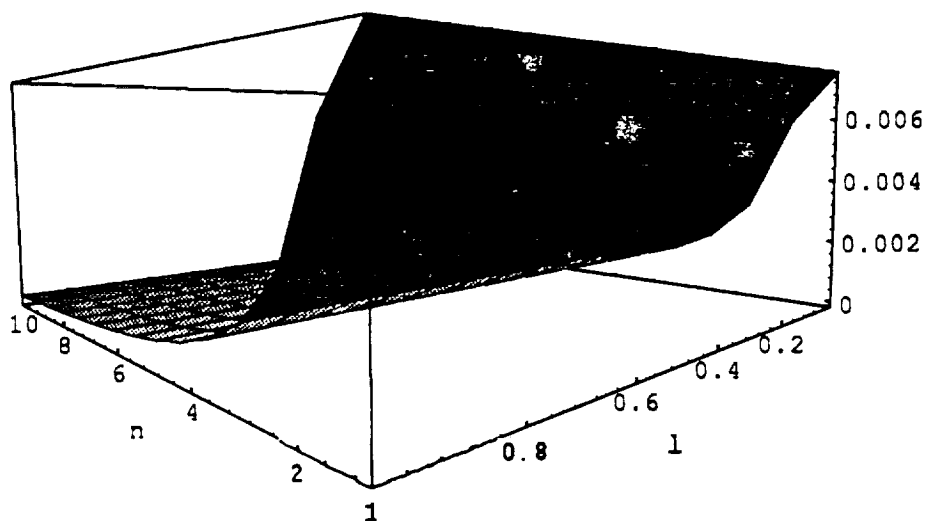
Plotting the above equation as n and l vary



The roller screw inertia is reflected to the motor shaft by

$$\frac{J_{\text{Roller Screw}}}{n^2}$$

Plotting the above equation as n and l vary



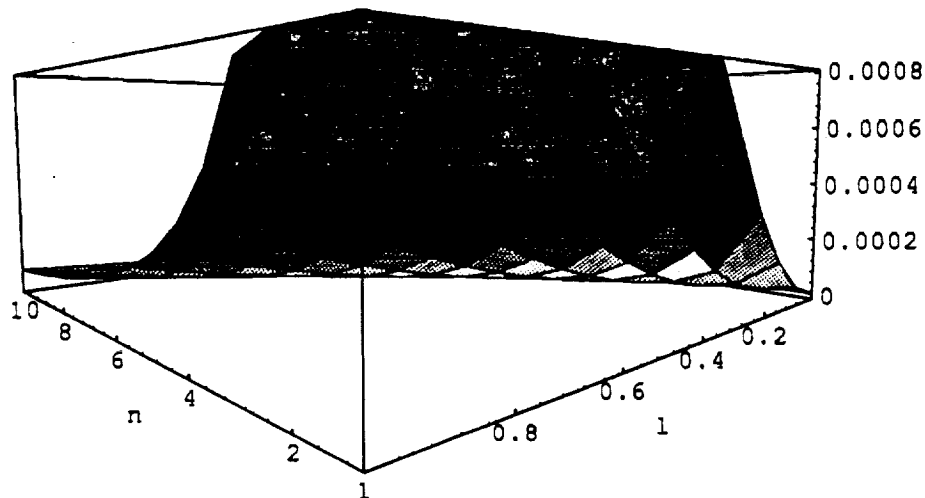
The tailstock mass is given by

$$M_{\text{Tailstock}} = \frac{100 \text{ lbs}_f}{\left(\frac{32.2 \text{ ft}}{\text{sec}^2}\right)\left(\frac{12 \text{ in}}{1 \text{ ft}}\right)} = \frac{0.257998 \text{ lbs}_f \cdot \text{sec}^2}{\text{in}}$$

The inertia seen at the motor shaft due to the tailstock is given by

$$\frac{M_{\text{Tailstock}}}{\left[\frac{2 \pi n}{l}\right]^2}$$

Plotting the above equation as n and l vary



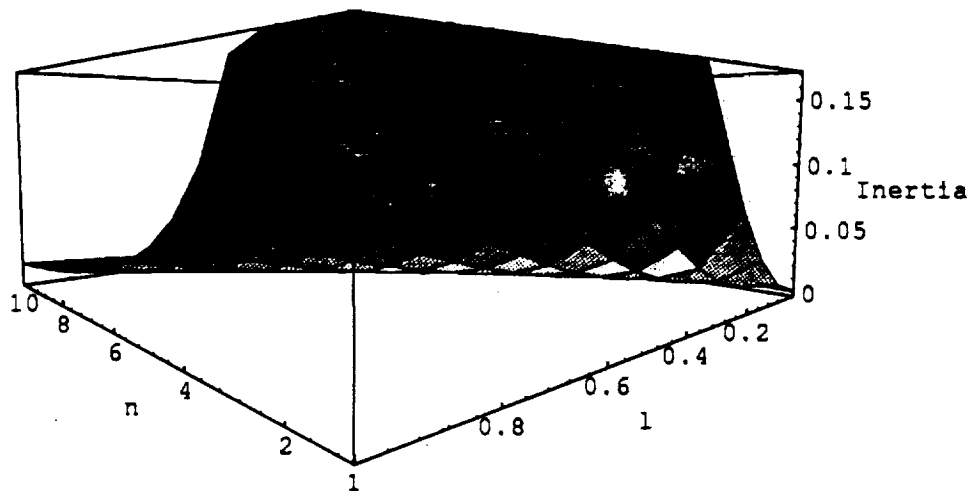
The engine mass is given as

$$M_{\text{Engine}} = \frac{55 \text{ lbs}_f \cdot \text{sec}^2}{\text{in}}$$

The inertia seen at the motor shaft due to the engine is given by

$$\frac{M_{\text{Engine}}}{\left[\frac{2\pi n}{l}\right]^2}$$

Plotting the above equation as n and l vary



The motor and engine inertias have the greatest effect on the overall inertia of this system. However, by the proper choice of n (gear ratio) and l (lead), the "Source" inertia may be matched to the "Load" inertia. The "Source" inertia is defined to be the sum of the motor inertias, the pinion gear inertias, the bull gear inertia reflected to the motor shaft, the roller screw inertia reflected to the motor shaft, and the mass of the tailstock reflected to the motor shaft. The "Load" inertia is defined to be the mass of the engine reflected to the motor shaft. The choice of n (gear ratio) and l (lead) which matches the "Source" inertia to the "Load" inertia also provides the maximum possible acceleration of the engine which is a MSFC requirement. (Refer to Appendix A for details).

SELECTION OF OPTIMUM BANDWIDTH
GEAR RATIO(n) AND LEAD(l)

B. Gear Train Optimization

In contradistinction to hydraulic actuators EMAs need a gear train to couple the electric motor to the tailstock of the actuator. This is because in the case of hydraulics a highly pressurized (typically 3000 psi at this time) fluid bears on an appropriate piston surface area to produce the desired force (which may be quite high; e.g. 100kips); while in the case of the EMA the torque (perhaps tens of foot pounds) of the electric motor needs to be multiplied and converted to linear motion by a gear train to reach these magnitudes of axially directed output force. The power delivered by either type of actuator is the same in a given application and therefore the electric motor must rotate at some considerable speed to develop the required output power when the actuator is in motion whereas the hydraulic actuator has only to move in consort with the load and therefore at the same speed as the load to develop the same power.

Given then that there is a necessity for gearing in an EMA (if for no other reason than to convert rotary to linear motion) the question quite naturally arises as to what form this gearing should take and what gearing parameters should be used. Two common types of gears that convert rotary to linear motion are the ball screw and the roller screw. The former type of screw is used widely in automobiles in the steering system. However, in comparison with the loads encountered in automotive service the EMA will experience much greater loads in performing the Thrust Vector Control (TVC) function and therefore the roller screw was chosen instead. This type of gearing is used in military service to launch aircraft and presumably for other arduous service as well and was recommended by the manufacturer for this application. Thus it was chosen as the output element gear. It was also decided to have the electric motor drive directly a spur gear pass, the output of which in turn drives the roller screw.

Having thus chosen a two pass (i.e. spur gear - roller screw) configuration the question arises as to how to choose the two gear pass ratios involved. The answer lies in the integration of several requirements. These include the requirement to produce a given amount of force at stall (the maximum developed whether hydraulic or electric actuators are used), the requirement to produce a maximum amount of power (also generally known as the actuator's rated power) at a given actuator stroking velocity and the desire to maximize the load acceleration or actuator bandwidth.

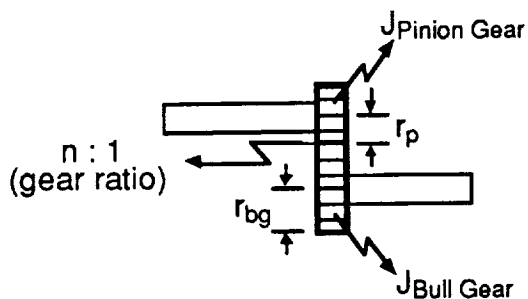
Hence the criteria used to judge the gear pass ratio selections are that of achieving **maximum load or engine acceleration** with a given electric motor (and hence with a given torque capacity and inertia) *and specified load combination* while being able to produce the required stall torque and power rating. Note that the acceleration of the motor is NOT the acceleration to be maximized. A little reflection will show that the highest gear ratio possible will serve to maximize the motor acceleration while as direct a drive as possible will maximize the load acceleration. The case at hand lies, clearly, in between these two extremes. The work reported upon in this section will show the solution to the problem of selecting the ratios.

Relationship Between The Pinion Gear And The Bull Gear Inertia

In the paper "Predicting Minimum Inertia Gear Trains" by Daniel P. Petersen (Machine Design, June 1954, pgs. 161-167), the following assumption was made

$$J_{\text{Bull Gear}} = n^4 J_{\text{Pinion Gear}}$$

The following development verifies analytically that this relationship is valid. Given a simple one-pass gear train



where

r_p - Radius Of Pinion Gear

r_{bg} - Radius Of Bull Gear

$J_{\text{Pinion Gear}}$ - Inertia Of Pinion Gear

$J_{\text{Bull Gear}}$ - Inertia Of Bull Gear

Note that the gear ratio is equal to

$$n = \frac{r_{bg}}{r_p} \Rightarrow r_{bg} = n r_p$$

If the pinion gear is treated as a right circular cylinder, then the polar mass moment of inertia is given by the following equation

$$J_{\text{Pinion Gear}} = \frac{Mr_p^2}{2}$$

where

$$M = \rho \pi r_p^2 l$$

ρ - Mass Density Of The Gear Material

l - Length Of The Cylinder

Substituting for M yields

$$J_{\text{Pinion Gear}} = \frac{(\rho \pi r_p^2 l) r_p^2}{2} = \frac{(\rho \pi l) r_p^4}{2}$$

Treating the bull gear as a right circular cylinder, then the inertia is

$$J_{\text{Bull Gear}} = \frac{Mr_{bg}^2}{2}$$

where

$$M = \rho \pi r_{bg}^2 l$$

ρ - Mass Density Of The Gear Material

l - Length Of The Cylinder

Substituting for M yields

$$J_{\text{Bull Gear}} = \frac{(\rho \pi r_{bg}^2 l) r_{bg}^2}{2} = \frac{(\rho \pi l) r_{bg}^4}{2}$$

Substitute

$$r_{bg} = n r_p$$

Then

$$J_{\text{Bull Gear}} = \frac{(\rho \pi l) r_{bg}^4}{2} = \frac{(\rho \pi l) (n r_p)^4}{2} = \frac{(\rho \pi l r_p^4)}{2} n^4$$

Recalling that

$$J_{\text{Pinion Gear}} = \frac{(\rho \pi l) r_p^4}{2}$$

yields

$$J_{\text{Bull Gear}} = \frac{(\rho \pi l r_p^4)}{2} n^4 = J_{\text{Pinion Gear}} n^4$$

Data supplied by MSFC about a spur gear pass used in their first EMA supports the validity of this relationship. The data and calculations are as follows:

$$J_{\text{Pinion Gear}} = 0.00004768 \text{ in-lbs-sec}^2$$

$$J_{\text{Bull Gear}} = 0.5 \text{ in-lbs-sec}^2$$

$$n = \frac{96 \text{ teeth}}{10 \text{ teeth}} = 9.6$$

Substituting into the relationship yields

$$J_{\text{Bull Gear}} = (0.00004768 \text{ in-lbs-sec}^2)(9.6^4) = 0.404968 \text{ in-lbs-sec}^2$$

$$n = \sqrt[4]{\frac{J_{\text{Bull Gear}}}{J_{\text{Pinion Gear}}}} = \sqrt[4]{\frac{0.5 \text{ in-lbs-sec}^2}{0.00004768 \text{ in-lbs-sec}^2}} = \sqrt[4]{10486.6} = 10.1195$$

$$\% \text{ difference} = \left[\frac{10.1195 - 9.6}{9.6} \right] [100] = 5.41146 \%$$

MOTOR - LOAD COUPLING

In this section is presented an investigation into the best possible values which can be chosen for reduction (gear) ratios (combining both a spur gear and a roller screw in various combinations) in a two pass power train when the intent is to maximize the acceleration (and hence bandwidth) possible from the train. The investigation is pursued by building a hierarchy of combinations starting with a relatively simple single pass case and progressing in eleven steps to the one spur gear and one roller screw solution used elsewhere in the design process. In the course of this investigation a unique solution for the reduction ratios was found for one relationship of spur gear mass moments of inertia between the pinion and the mating (bull) gear. Absent this relationship only local maxima can be found i.e. given a priori one or the other reduction ratio the other can be found but the combination is not necessarily the best possible of all the infinite number of solutions available.

In the work to follow extensive use is made of the computer program MATHEMATICA developed and sold by Wolfram Research. It is used herein to perform the symbolic calculus e.g. differentiation and algebra e.g. solution of nonlinear algebraic equations involved in maximizing the acceleration expressions. The latest version available at this time is 2.0. Unfortunately this version has a problem with its Solve

routine that renders some of the solutions exhibited below unattainable. If it is desired to reproduce all of the work shown below use of version 1.2 will be necessary. Wolfram has been notified and they say that the section of their code in question was completely rewritten between the two versions noted above and that they will look into the problem.

As mentioned above eleven cases of interest were investigated. Case one assumes that motor and load polar mass moments of inertia are given and that the task is to maximize the acceleration of the load by choosing the reduction ratio of a one pass system. The MATHEMATICA program is given below. J_m is the motor inertia, J_l the load inertia and n is the reduction ratio. The analytical course followed was to minimize the denominator of the expression for load acceleration. The denominator is called den (see In[21]), its derivative with respect to n is performed in the operation $D[\text{den}, n]$ (see In[24]) and the resulting algebraic equation used to determine n the reduction ratio by use of the $\text{Solve}[D1==0]$ command. The result is that n should be equal to the square root of the load to motor inertia. This result is entirely analogous to matching loads or impedances across a transformer for maximum power transfer. This example sets the stage for the solutions to follow.

Case I

Single-gear pass system

Motor inertia and load inertia

In[21]:=

den=n*(Jm+Jl/(n^2.))

Out[21]=

$$(J_m + \frac{J_l}{n^2}) n$$

In[24]:=

D1=D[den,n]

Out[24]=

$$J_m - \frac{J_l}{n^2}$$

In[27]:=

Solve[D1==0,n]

Out[27]=

$$\left\{ \left\{ n \rightarrow \frac{J_l}{J_m} \right\} \right\}$$

Case two follows the same methodology as did case one. It represents however the case wherein both the spur gear and the roller screw reductions are considered. The same symbols are used as in case one with the following additions. π is the constant 3.14159265 and l is the roller screw ratio. $den1$ denotes the denominator (see In[30]), its derivative with respect to n is obtained by the `D[den1,n]` command and the simplified result displayed in Out[33]. A similar procedure produces the derivative with respect to n and is displayed in Out[35]. Two solutions are then obtained by using the `Solve` command. Out[38] displays n as a function of l (and the fixed parameters, while Out[37] displays l as a function of n and the fixed parameters. Thus given one or the other ratio (i. e. either n or l) the companion ratio may be calculated. The topological nature of this solution is shown in the accompanying typical three dimensional and contour plots of the denominator function ($den1$). The MATHEMATICA code has been included in case it is desired to reproduce these plots. The ranges of n and l , 0.1 to 10 and 0.1 to 1 respectively, are believed, based upon information from MSFC technical personnel to represent reasonable ranges of these reduction ratios. From inspection of the plots it is seen that there is no global minimum to the function. Rather the most that can be done is to pick either an n or an l and determine the other parameter; this is of course the same result as that obtained from the algebraic solution.

Case II

Single-gear pass and roller screw system

Motor inertia and load inertia

In[30]:=

den1=(2*PI*n/1)*(Jm+(Jl/((2*PI*n/1)^(2))))

Out[30]=

$$\frac{2 \text{ PI } (J_m + \frac{J_l}{4 \text{ PI }^2 n})}{1}$$

In[31]:=

Simplify[den1]

Out[31]=

$$\frac{J_l}{2 \text{ PI } n} + \frac{2 J_m \text{ PI } n}{1}$$

In[32]:=

D2=D[den1,n]

Out[32]=

$$\frac{2 \text{ PI } (J_m + \frac{J_l}{4 \text{ PI }^2 n})}{1} - \frac{J_l}{2 \text{ PI } n^2}$$

In[33]:=

Simplify[D2]

Out[33]=

$$\frac{2 J_m \text{ PI}}{1} - \frac{J_l}{2 \text{ PI } n^2}$$

In[34]:=

D3=D[den1,1]

Out[34]=

$$\frac{\frac{J1}{PI n} - \frac{J1^2}{4 PI^2 n^2}}{2 PI (Jm + \frac{J1^2}{4 PI^2 n^2}) n}$$

In[35]:=

Simplify[D3]

Out[35]=

$$\frac{J1}{2 PI n} - \frac{J1^2}{4 PI^2 n^2}$$

In[38]:=

Solve[{D2==0,D3==0},{n,1}]

Out[38]=

$$\left\{ \left\{ n \rightarrow \frac{\sqrt{J1}}{2 \sqrt{Jm} PI}, \left\{ n \rightarrow \frac{-(\sqrt{J1})}{2 \sqrt{Jm} PI} \right\} \right\} \right\}$$

In[37]:=

Solve[{D2==0,D3==0},{1,n}]

Out[37]=

$$\left\{ \left\{ 1 \rightarrow \frac{2 \sqrt{Jm} PI n}{\sqrt{J1}}, \left\{ 1 \rightarrow \frac{-2 \sqrt{Jm} PI n}{\sqrt{J1}} \right\} \right\} \right\}$$

In[16]:=

```
Jl=55
Jm=.157799
PI=3.1415926
den1=(2*PI*n/l)*(Jm+(Jl/((2*PI*n/l)^(2))))
Plot3D[den1,{n,.1,10},{l,.1,1}]
```

Out[16]=

55

Out[17]=

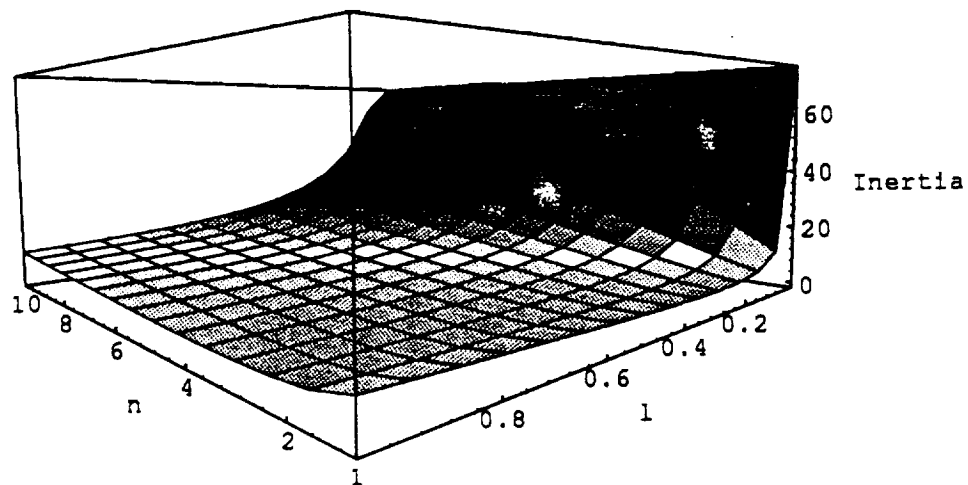
0.157799

Out[18]=

3.1415926

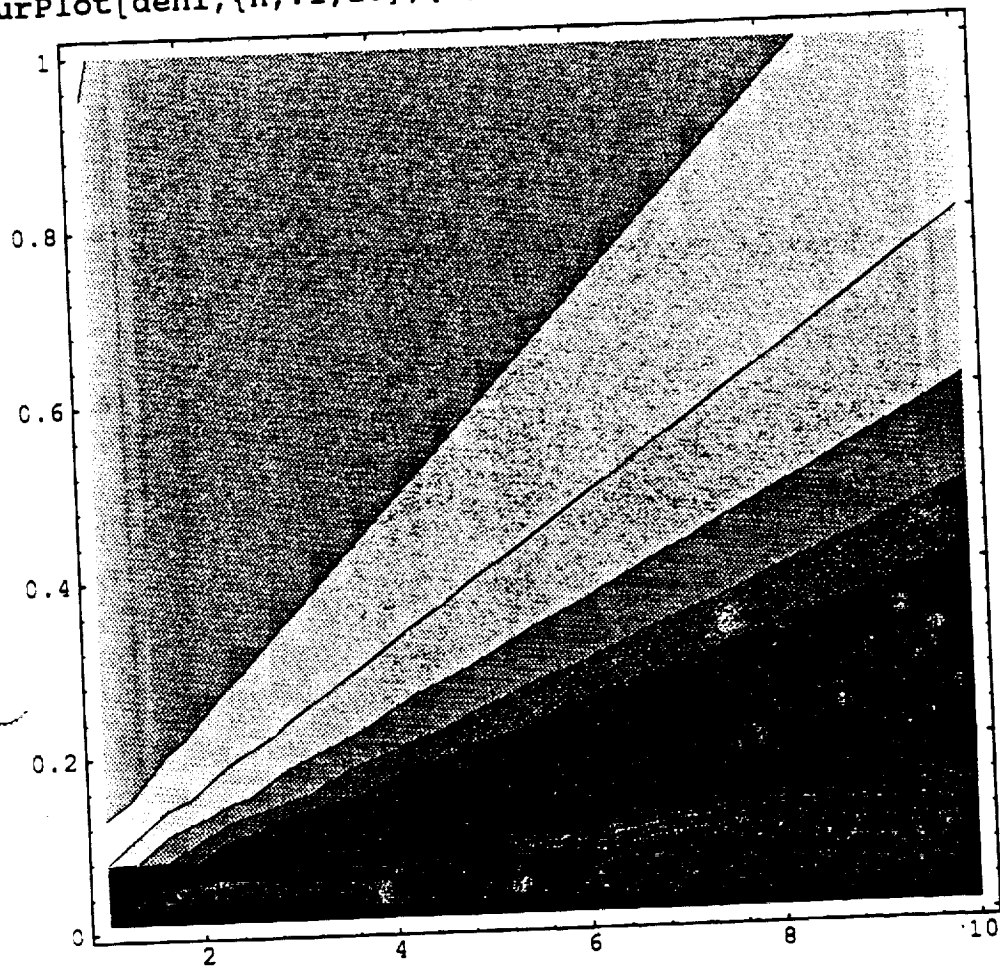
Out[19]=

$$\frac{6.28319 \left(0.157799 + \frac{1.39317 l^2}{n^2} \right) n}{1}$$



Out[20]=

Plot[den1,{n,.1,10},{1,.1,1}]



Case three is essentially a repeat of case two with one difference in formulation. Inspection of the expression for the denominator quickly reveals that the ratio of n to l always appears, never one of the ratios i.e. neither n nor l as a stand alone (it is also multiplied by 2 PI). Thus in the third case the denominator was formulated by substituting

$$B = (2 \text{ PI } n)/l$$

in the expression. The problem was solved as before with the result shown in Out[55]. Comparison of this result with the result of case one shows the same form of result except that B takes the place of n in the first case. Thus at least a consistency is observed to be present in the results.

Case III (Case II revised)

Single-gear pass and roller screw system

Motor inertia and load inertia

den1=(2*PI*n/l)*(Jm+(Jl/((2*PI*n/l)^(2))))

***Let B=2*PI*n/l, then**

In[53]:=

den2=B*(Jm+(Jl/(B^2)))

Out[53]=

$$B \left(\frac{Jl}{B^2} + Jm \right)$$

In[54]:=

D3=D[den2,B]

Out[54]=

$$-\left(\frac{Jl}{B^2} \right) + Jm$$

In[55]:=

Solve[D3==0,B]

Out[55]=

$$\left\{ \left\{ B \rightarrow \frac{\sqrt{Jl}}{\sqrt{Jm}} \right\}, \left\{ B \rightarrow -\left(\frac{\sqrt{Jl}}{\sqrt{Jm}} \right) \right\} \right\}$$

In the preceding three cases mass was attributed only to the motor and the load. In case four the pinion gear was given a mass J_p and the solution process repeated as before. The results are presented in Out[67] and Out[68]. It is noted that once again n may be found as a function of l and the fixed parameters or l as a function of n and the fixed parameters. Thus case four repeats previous results in that no unique minimum occurs. Thus once again no global minimum exists.

Case IV

Single-gear pass and roller screw system

Motor inertia, pinion inertia, and load inertia

In[58]:=

den3=(2*PI*n/l)*((Jm+Jp)+(Jl/((2*PI*n/l)^(2))))

Out[58]=

$$\frac{2 \text{ PI } (J_m + J_p + \frac{J_l l^2}{4 \text{ PI } n^2})}{l}$$

In[62]:=

Expand[den3]

Out[62]=

$$\frac{J_l l}{2 \text{ PI } n} + \frac{2 J_m \text{ PI } n}{1} + \frac{2 J_p \text{ PI } n}{1}$$

In[63]:=

D4=D[den3,n]

Out[63]=

$$\frac{2 \text{ PI } (J_m + J_p + \frac{J_l l^2}{4 \text{ PI } n^2})}{l} - \frac{J_l l}{\text{PI } n^2}$$

In[64]:=

Simplify[D4]

Out[64]=

$$\frac{2 J_m \text{ PI}}{1} + \frac{2 J_p \text{ PI}}{1} - \frac{J_l l}{2 \text{ PI } n^2}$$

In[65]:=

D5=D[den3,1]

Out[65]=

$$\frac{\frac{J1}{PI \cdot n} - \frac{2 \cdot PI \cdot (Jm + Jp + \frac{J1}{4 \cdot PI \cdot n^2})}{1}}{1}$$

In[66]:=

Simplify[D5]

Out[66]=

$$\frac{J1}{2 \cdot PI \cdot n} - \frac{2 \cdot Jm \cdot PI \cdot n}{1} - \frac{2 \cdot Jp \cdot PI \cdot n}{1}$$

In[67]:=

Solve[{D4==0,D5==0},{n,1}]

Out[67]=

$$\left\{ \left\{ n \rightarrow \frac{\sqrt{J1}}{2 \sqrt{Jm \cdot PI^2 + Jp \cdot PI^2}} \right\}, \left\{ n \rightarrow \frac{-(\sqrt{J1})}{2 \sqrt{Jm \cdot PI^2 + Jp \cdot PI^2}} \right\} \right\}$$

In[68]:=

Solve[{D4==0,D5==0},{1,n}]

Out[68]=

$$\left\{ \left\{ 1 \rightarrow \frac{\sqrt{4 \cdot Jm + 4 \cdot Jp} \cdot PI \cdot n}{\sqrt{J1}} \right\}, \left\{ 1 \rightarrow -\frac{\sqrt{4 \cdot Jm + 4 \cdot Jp} \cdot PI \cdot n}{\sqrt{J1}} \right\} \right\}$$

Case five is case four repeated in the same manner that case three repeated case two. Once again the same substitution was made (B) and the problem resolved. The results are wholly consistent with all the previous ones.

Case V (Case IV revised)

Single-gear pass and roller screw system

Motor inertia, pinion inertia, and load inertia

den3=(2*PI*n/l)*((Jm+Jp)+(Jl/((2*PI*n/l)^(2))))

***Let B=2*PI*n/l, then**

In[69]:=

den3=B*(Jm+Jp+(Jl/(B^2)))

Out[69]=

$$\frac{Jl}{B \left(\frac{--}{2} + Jm + Jp \right)}$$

In[70]:=

D6=D[den3,B]

Out[70]=

$$-\frac{Jl}{B \left(\frac{--}{2} + Jm + Jp \right)}$$

In[71]:=

Solve[D6==0,B]

Out[71]=

$$\left\{ \left\{ B \rightarrow \frac{\text{Sqrt}[Jl]}{\text{Sqrt}[Jm + Jp]} \right\}, \left\{ B \rightarrow -\frac{\text{Sqrt}[Jl]}{\text{Sqrt}[Jm + Jp]} \right\} \right\}$$

Case six and case seven (with the substitution B made as previously) now includes the inertia of the "bull" gear. The solution was made as before with the results shown in Out[88] and Out[87] for case six and Out[92] and Out[93] for case seven. Again unique solutions for n and l were not available.

Case VI

Single-gear pass and roller screw system

Motor inertia, pinion inertia, bull gear inertia, and load inertia

In[73]:=

den4=(2*PI*n/l)*(Jm+Jp+(Jbg/(n^2))+(Jl/((2*PI*n/l)^(2))))

Out[73]=

$$\frac{2 \text{ PI } (J_m + J_p + \frac{J_{bg}}{n^2} + \frac{J_l l^2}{4 \text{ PI } n^2})}{1}$$

In[75]:=

Expand[den4]

Out[75]=

$$\frac{2 J_{bg} \text{ PI}}{1 n} + \frac{J_l l^2}{2 \text{ PI } n} + \frac{2 J_m \text{ PI } n}{1} + \frac{2 J_p \text{ PI } n}{1}$$

In[76]:=

D7=D[den4,n]

Out[76]=

$$\frac{2 \text{ PI } (J_m + J_p + \frac{J_{bg}}{n^2} + \frac{J_l l^2}{4 \text{ PI } n^2})}{1} + \frac{2 \text{ PI } (\frac{-2 J_{bg}}{n^3} - \frac{J_l l^2}{2 \text{ PI } n^3})}{1} n$$

In[77]:=

Simplify[D7]

Out[77]=

$$\frac{2 J_m \text{ PI}}{1} + \frac{2 J_p \text{ PI}}{1} - \frac{2 J_{bg} \text{ PI}}{1 n} - \frac{J_l l^2}{2 \text{ PI } n}$$

In[78]:=

D8=D[den4,1]

Out[78]=

$$\frac{J1 \cdot \sqrt{2 \pi (Jm + Jp + \frac{Jbg}{n} + \frac{J1}{4 \pi n})}}{\pi n \sqrt{1}}$$

In[80]:=

Expand[D8]

Out[80]=

$$\frac{J1 \sqrt{2 \pi n} + 2 Jbg \pi + 2 Jm \pi n + 2 Jp \pi n}{2 \pi n \sqrt{1} + 2 \pi n \sqrt{1} + 2 \pi n \sqrt{1}}$$

In[88]:=

Solve[{D7==0,D8==0},{n,1}]

Out[88]=

$$\left\{ \left\{ n \rightarrow \frac{\sqrt{4 Jbg \pi + J1}}{2 \sqrt{Jm \pi + Jp \pi}}, -\sqrt{4 Jbg \pi + J1} \right\} \right\}$$

In[87]:=

Solve[{D7==0,D8==0},{1,n}]

Out[87]=

$$\{ \{1 \rightarrow \frac{\text{PI Sqrt}[-4 \text{Jbg} + 4 \text{Jm n}^2 + 4 \text{Jp n}^2]}{\text{Sqrt}[J1]} \},$$

$$\{1 \rightarrow -(\frac{\text{PI Sqrt}[-4 \text{Jbg} + 4 \text{Jm n}^2 + 4 \text{Jp n}^2]}{\text{Sqrt}[J1]}) \} \}$$

Case VII (Case VI revised)

Single-gear pass and roller screw system

Motor inertia, pinion inertia, bull gear inertia, and load inertia

den4=(2*PI*n/l)*(Jm+Jp+(Jbg/(n^2))+(Jl/((2*PI*n/l)^(2))))

***Let B=2*PI*n/l, then**

In[89]:=

den4=B*(Jm+Jp+(Jbg/(n^2))+(Jl/(B^2)))

Out[89]=

$$B \left(\frac{Jl}{B^2} + Jm + Jp + \frac{Jbg}{n^2} \right)$$

In[91]:=

Expand[den4]

Out[91]=

$$\frac{Jl}{B} + B Jm + B Jp + \frac{B Jbg}{n^2}$$

In[92]:=

D9=D[den4,B]

Out[92]=

$$-\left(\frac{Jl}{B^2}\right) + Jm + Jp + \frac{Jbg}{n^2}$$

In[93]:=

Solve[D9==0,B]

Out[93]=

$$\left\{ \left\{ B \rightarrow \frac{\text{Sqrt}[J1] \, n}{\sqrt{J_{bg} + J_m n^2 + J_p n^2}} \right\}, \right.$$

$$\left. \left\{ B \rightarrow -\left(\frac{\text{Sqrt}[J1] \, n}{\sqrt{J_{bg} + J_m n^2 + J_p n^2}} \right) \right\} \right\}$$

Case eight is the first example in which all the power train inertias are included in the formulation (here the addition is the roller screw inertia). Proceeding as before MATHEMATICA was unable to find a solution for either n or l , even as a function of other parameters or each other. Case nine is of interest in that making the ubiquitous B substitution MATHEMATICA was able to find a solution for B as a function of n and the fixed system parameters. However one notes that B itself is a function of n so something of a tautology is implied. Representative plots of the topology are presented below so that the function may be studied. This study shows that the function possesses similar characteristics to previous non unique solutions. Probably the functional relationships are just too complicated for MATHEMATICA to achieve a closed form for n as a function of l as before; even the "solution" for B in case nine is polemical as already noted.

Case VIII

Single-gear pass and roller screw system

Motor inertia, pinion inertia, bull gear inertia, roller screw inertia, and load inertia

In[164]:=

```
den5=(2*PI*n/1)*(Jm+Jp+((Jbg+Jrs)/(n^2))+
(Jl/((2*PI*n/1)^(2))))
```

Out[164]=

$$\frac{2 \text{ PI } (J_m + J_p + \frac{J_{bg} + J_{rs}}{n^2} + \frac{J_l}{4 \text{ PI } n^2})}{1}$$

In[165]:=

Expand[den5]

Out[165]=

$$\frac{2 J_{bg} \text{ PI}}{1 n} + \frac{2 J_{rs} \text{ PI}}{1 n} + \frac{J_l}{2 \text{ PI } n} + \frac{2 J_m \text{ PI } n}{1} + \frac{2 J_p \text{ PI } n}{1}$$

In[166]:=

D10=D[den5,n]

Out[166]=

$$\frac{2 \text{ PI } (J_m + J_p + \frac{J_{bg} + J_{rs}}{n^2} + \frac{J_l}{4 \text{ PI } n^2})}{1} + \frac{2 \text{ PI } (-\frac{2 (J_{bg} + J_{rs})}{n^3} - \frac{J_l}{2 \text{ PI } n^3})}{1}$$

In[167]:=

Simplify[D10]

Out[167]=

$$\frac{2 J_m P I}{1} + \frac{2 J_p P I}{1} - \frac{2 J_{bg} P I}{1 n} - \frac{2 J_{rs} P I}{1 n} - \frac{J_l 1}{2 P I n}$$

In[168]:=

D11=D[den5,1]

Out[168]=

$$\frac{J_l}{P I n} - \frac{2 P I (J_m + J_p + \frac{J_{bg} + J_{rs}}{2 n} + \frac{J_l 1}{4 P I n})}{1}$$

In[169]:=

Expand[D11]

Out[169]=

$$\frac{J_l}{2 P I n} - \frac{2 J_{bg} P I}{1 n} - \frac{2 J_{rs} P I}{1 n} - \frac{2 J_m P I n}{1} - \frac{2 J_p P I n}{1}$$

In[171]:=

Solve[{D10==0,D11==0},{n,1}]

Out[171]=

{}

In[1]:=

```
PI = 3.1415926
Jl=55
Jm=0.157799
Jp=4.768*10^-5
Jrs=0.016
Jbg=Jp*4.28^4
den5=(2*PI*n/l)*(Jm+Jp+((Jbg+Jrs)/(n^2)))+(Jl/((2*PI*n/l)^(2)))
Plot3D[den5,{n,0.1,10},{l,0.1,1.0}]
```

Out[1]=

3.1415926

Out[2]=

55

Out[3]=

0.157799

Out[4]=

0.00004768

Out[5]=

0.016

Out[6]=

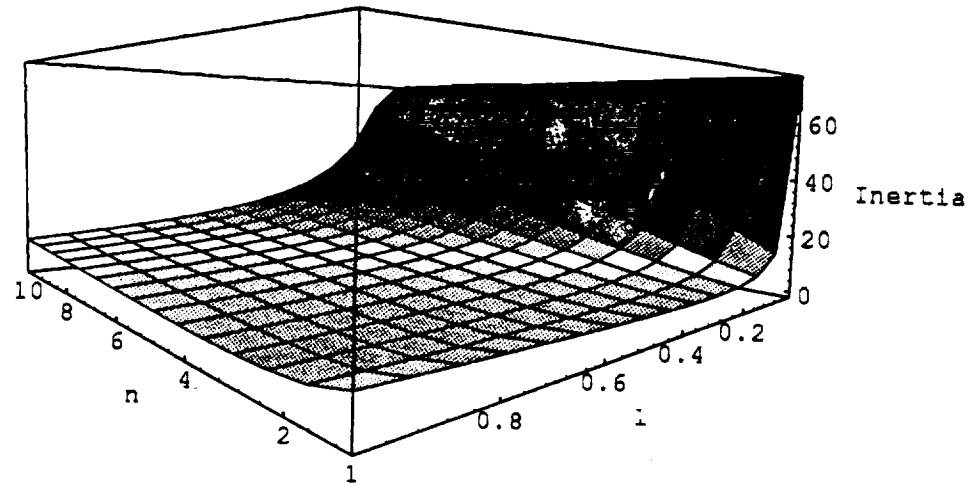
0.0159997

Out[7]=

$$\frac{6.28319 \left(0.157847 + \frac{0.0319997}{n^2} + \frac{1.39317}{n^2} \right) n^2}{1}$$

Out[8]=

-SurfaceGraphics-

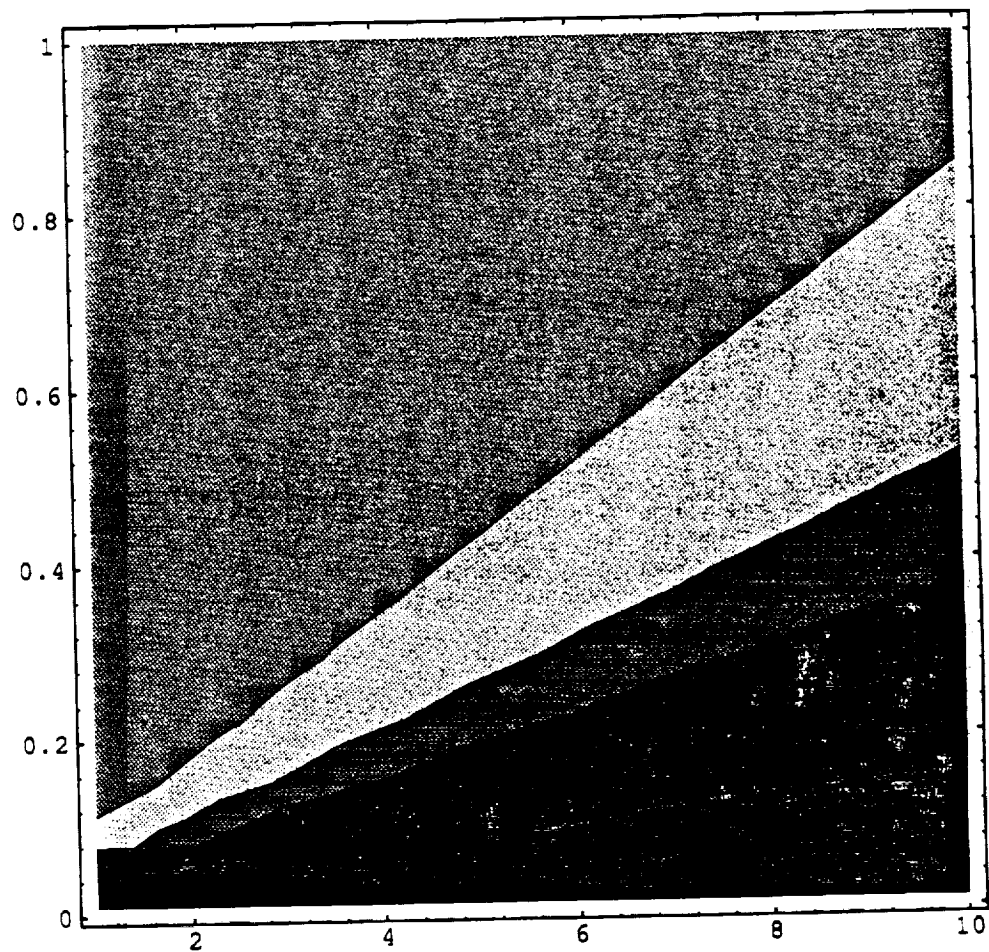


`Out[8]=`

`-SurfaceGraphics-`

ln(9):=

`ContourPlot[den5,{n,0.1,10},{l,0.1,1.0}]`



This page intentionally left blank

Case IX (Case VIII revised)

Single-gear pass and roller screw system

Motor inertia, pinion inertia, bull gear inertia, roller screw inertia, and load inertia

$$\text{den5} = (2\pi n/l) * (J_m + J_p + ((J_{bg} + J_{rs}) / (n^2)) + (J_l / ((2\pi n/l)^2)))$$

***Let $B = 2\pi n/l$, then**

In[156]:=

$$\text{den5} = B * (J_m + J_p + ((J_{bg} + J_{rs}) / (n^2)) + (J_l / (B^2)))$$

Out[156]=

$$B \left(\frac{J_l}{B^2} + J_m + J_p + \frac{J_{bg} + J_{rs}}{n^2} \right)$$

In[157]:=

Expand[den5]

Out[157]=

$$\frac{J_l}{B} + B J_m + B J_p + \frac{B J_{bg}}{n^2} + \frac{B J_{rs}}{n^2}$$

In[158]:=

D12=D[den5,B]

Out[158]=

$$-\left(\frac{J_l}{B^2}\right) + J_m + J_p + \frac{J_{bg} + J_{rs}}{n^2}$$

PRECEDING PAGE BLANK NOT FILMED

In[159]:=

Solve[D12==0,B]

Out[159]=

$$\left\{ \left\{ B \rightarrow \frac{\text{Sqrt}[J1] n}{\text{Sqrt}[Jbg + Jrs + Jm n^2 + Jp n^2]} \right\}, \right. \\ \left. \left\{ B \rightarrow -\left(\frac{\text{Sqrt}[J1] n}{\text{Sqrt}[Jbg + Jrs + Jm n^2 + Jp n^2]} \right) \right\} \right\}$$

Case ten represents a breakthrough. In this case not only are all the inertias explicitly included in the formulation but also a crucial relationship between the pinion gear inertia and the bull gear inertia is introduced. The relationship is

$$J_{bg} = J_p n^4$$

This relationship was suggested by Petersen in his seminal paper and is easily derived under the assumption that both gears are right circular cylinders of the same material e.g. steel. Once this key constraint is imposed (see In[203]) the solution proceeds as always. The result appears in Out[209] as a series of roots of the algebraic equation. Knowing that $\sqrt{}$ in the MATHEMATICA language signifies the square root of minus one and that n and l must be positive real quantities shows that there is one physically useful to the equation. Representative graphs are shown below and the results are used elsewhere in the report during the design process. Case eleven employs the B substitution but seems to add little more to the discussion and was included for completeness sake.

Case X

Single-gear pass and roller screw system

Motor inertia, pinion inertia, bull gear inertia, roller screw inertia, and load inertia

***Using the substitution $J_{bg}=J_p*n^4$ ***

In[203]:=

den6=(2*PI*n/l)*(Jm+Jp+(Jp*(n^2))+(Jrs/(n^2))+(Jl/((2*PI*n/l)^(2))))

Out[203]=

$$\frac{2 \text{ PI } n \left(J_m + J_p + \frac{J_{rs}}{n^2} + \frac{J_l l^2}{4 \text{ PI } n^2} + J_p n^2 \right)}{1}$$

In[204]:=

Expand[den6]

Out[204]=

$$\frac{2 J_{rs} \text{ PI}}{l n} + \frac{J_l l^2}{2 \text{ PI } n} + \frac{2 J_m \text{ PI } n}{1} + \frac{2 J_p \text{ PI } n}{1} + \frac{2 J_p \text{ PI } n^3}{1}$$

In[205]:=

D13=D[den6,n]

Out[205]=

$$\frac{2 \text{PI} n \left(\frac{-2 \text{Jrs}}{n^3} - \frac{\text{Jl}^2}{2 \text{PI} n^2} + 2 \text{Jp} n \right)}{1} + \frac{2 \text{PI} \left(\text{Jm} + \text{Jp} + \frac{\text{Jrs}}{n^2} + \frac{\text{Jl}^2}{4 \text{PI} n^2} + \text{Jp} n^2 \right)}{1}$$

In[206]:=

Simplify[D13]

Out[206]=

$$\frac{2 \text{Jm} \text{PI}}{1} + \frac{2 \text{Jp} \text{PI}}{1} - \frac{2 \text{Jrs} \text{PI}}{1 n^2} - \frac{\text{Jl}^2}{2 \text{PI} n^2} + \frac{6 \text{Jp} \text{PI} n^2}{1}$$

In[207]:=

D14=D[den6,1]

Out[207]=

$$\frac{\text{Jl}}{\text{PI} n} - \frac{2 \text{PI} n \left(\text{Jm} + \text{Jp} + \frac{\text{Jrs}}{n^2} + \frac{\text{Jl}^2}{4 \text{PI} n^2} + \text{Jp} n^2 \right)}{1}$$

In[208]:=

Expand[D14]

Out[208]=

$$\frac{J1}{2 \text{ PI } n} - \frac{2 \text{ Jrs PI}}{2} - \frac{2 \text{ Jm PI } n}{2} - \frac{2 \text{ Jp PI } n}{2} - \frac{2 \text{ Jp PI } n^3}{2}$$

In[209]:=

Solve[{D13==0,D14==0},{n,1}]

Out[209]=

$$\left\{ \left\{ 1 \rightarrow \frac{4 \text{ Jm Sqrt[Jrs]} \text{ Sqrt} \left[\frac{4 \text{ Jm Sqrt[Jrs]} \text{ Sqrt[Jp]} \text{ Sqrt[Jrs]} + 8 \text{ Jrs} \right] \text{ PI}}{\text{Sqrt[Jp]} \text{ Sqrt[J1]}}, \right. \right.$$

$$\left. \left\{ 1 \rightarrow \frac{1/4 \text{ Jrs}}{1/4 \text{ Jp}} \right\} \right\}$$

$$\left\{ \left\{ 1 \rightarrow \frac{4 \text{ Jm Sqrt[Jrs]} \text{ Sqrt} \left[\frac{4 \text{ Jm Sqrt[Jrs]} \text{ Sqrt[Jp]} \text{ Sqrt[Jrs]} + 8 \text{ Jrs} \right] \text{ PI}}{\text{Sqrt[Jp]} \text{ Sqrt[J1]}}, \right. \right.$$

$$\left. \left\{ 1 \rightarrow \frac{1/4 \text{ Jrs}}{1/4 \text{ Jp}} \right\} \right\}$$

$$\left\{ \left\{ 1 \rightarrow \frac{-4 \text{ Jm Sqrt[Jrs]} \text{ Sqrt} \left[\frac{-4 \text{ Jm Sqrt[Jrs]} \text{ Sqrt[Jp]} \text{ Sqrt[Jrs]} + 8 \text{ Jrs} \right] \text{ PI}}{\text{Sqrt[Jp]} \text{ Sqrt[J1]}}, \right. \right.$$

$$\left. \left\{ 1 \rightarrow \frac{1/4 \text{ Jrs}}{1/4 \text{ Jp}} \right\} \right\}$$

$$n \rightarrow \frac{1/4}{Jp}, \{1 \rightarrow$$

$$\frac{\text{Sqrt}[-\frac{-4 Jm \text{Sqrt}[Jrs]}{\text{Sqrt}[Jp]} - 4 \text{Sqrt}[Jp] \text{Sqrt}[Jrs] + 8 Jrs] \text{PI}}{-(\frac{\text{Sqrt}[Jp]}{\text{Sqrt}[Jl]}),$$

$$n \rightarrow \frac{I Jrs}{Jp}, \{1 \rightarrow$$

$$\frac{\text{Sqrt}[-\frac{4 Jm \text{Sqrt}[Jrs]}{\text{Sqrt}[Jp]} + 4 \text{Sqrt}[Jp] \text{Sqrt}[Jrs] + 8 Jrs] \text{PI}}{\text{Sqrt}[Jl],$$

$$n \rightarrow -(\frac{Jrs}{Jp}), \{1 \rightarrow$$

$$\frac{\text{Sqrt}[-\frac{4 Jm \text{Sqrt}[Jrs]}{\text{Sqrt}[Jp]} + 4 \text{Sqrt}[Jp] \text{Sqrt}[Jrs] + 8 Jrs] \text{PI}}{-(\frac{\text{Sqrt}[Jp]}{\text{Sqrt}[Jl]}),$$

$$n \rightarrow -(\frac{Jrs}{Jp}), \{1 \rightarrow$$

$$\frac{\text{Sqrt}[-\frac{-4 Jm \text{Sqrt}[Jrs]}{\text{Sqrt}[Jp]} - 4 \text{Sqrt}[Jp] \text{Sqrt}[Jrs] + 8 Jrs] \text{PI}}{\text{Sqrt}[Jl],$$

$$\begin{aligned}
 & \frac{1}{4} \\
 & -I \text{ Jrs} \\
 n \rightarrow & \frac{\quad}{Jp}, \{1 \rightarrow \\
 & \frac{1}{4} \\
 & \text{Jp} \\
 & -4 \text{ Jm Sqrt[Jrs]} \\
 & \text{Sqrt}[\frac{\quad}{\text{Sqrt[Jp]} - 4 \text{ Sqrt[Jp] Sqrt[Jrs] + 8 Jrs} \text{ PI}} \\
 & -(\frac{\quad}{\text{Sqrt[J1]}},
 \end{aligned}$$

$$\begin{aligned}
 & \frac{1}{4} \\
 & -I \text{ Jrs} \\
 n \rightarrow & \frac{\quad}{Jp} \} \} \\
 & \frac{1}{4} \\
 & \text{Jp}
 \end{aligned}$$

```

*Case XI (Case X revised)*

*Single-gear pass and roller screw system*

*Motor inertia, pinion inertia, bull gear inertia, roller
  screw inertia, and load inertia*

*Using the substitution Jbg=Jp*n^4*

den6=(2*PI*n/l)*(Jm+Jp+(Jp*(n^2))+(Jrs/(n^2))+
  (Jl/((2*PI*n/l)^(2))))

*Let B=2*PI*n/l, then

In[199]:=
den6=B*(Jm+Jp+(Jp*(n^2))+(Jrs/(n^2))+(Jl/(B^2)))

Out[199]=
      Jl          Jrs      2
      B ( -- + Jm + Jp + --- + Jp n )
          2          2
          B          n

In[200]:=
Expand[den6]

Out[200]=
      Jl          B Jrs      2
      -- + B Jm + B Jp + ---- + B Jp n
      B          2
          n

In[201]:=
D15=D[den6,B]

Out[201]=
      Jl          Jrs      2
      - ( -- ) + Jm + Jp + --- + Jp n
          2          2
          B          n

```

In[202]:=

Solve[D15==0,B]

Out[202]=

$$\left\{ \left\{ B \rightarrow \frac{\sqrt{J1} n}{\sqrt{Jrs + Jm n^2 + Jp n^2 + Jp n^4}}, \right. \right. \\ \left. \left. B \rightarrow -\left(\frac{\sqrt{J1} n}{\sqrt{Jrs + Jm n^2 + Jp n^2 + Jp n^4}} \right) \right\} \right\}$$

Calculation Of Optimum Bandwidth n (Gear Ratio) And l (Lead) For Point Design Parameters

Given a specific spur gear train - roller screw configuration, there is **one** choice for n (gear ratio) and l (lead) that will provide maximum acceleration for any given torque. The following analysis is the step-by-step procedure used to determine the value for n (gear ratio) and l (lead) (Refer to Case X in the previous section).

The acceleration of the load is

$$\alpha_{\text{Load}} = \frac{\alpha_{\text{Motor}}}{(n)\left(\frac{2\pi}{l}\right)} = \left(\frac{l}{2\pi n}\right)\alpha_{\text{Motor}}$$

where

$$\alpha_{\text{Motor}} = \frac{\text{Torque}}{J_T}$$

The torque in the above equation is the combined torque provided by three motors. The denominator term is the total inertia seen by the motor. There are three motors and three pinion gears in this system. The inertias of each of these elements has to be accounted for when calculating the total inertia of this system.

$$J_T = J_{3\text{-Motor}} + J_{3\text{-Pinion Gear}} + \frac{J_{\text{Bull Gear}}}{n^2} + \frac{J_{\text{Roller Screw}}}{n^2} + \frac{M_{\text{Engine}}}{\left[(n)\left(\frac{2\pi}{l}\right)\right]^2}$$

Substituting for motor acceleration and total inertia yields

$$\alpha_{\text{load}} = \frac{\text{Torque}}{\left[(n)\left(\frac{2\pi}{l}\right)\right]J_T} = \frac{\text{Torque}}{\left[(n)\left(\frac{2\pi}{l}\right)\right]\left[J_{3\text{-Motor}} + J_{3\text{-Pinion Gear}} + \frac{J_{\text{Bull Gear}}}{n^2} + \frac{J_{\text{Roller Screw}}}{n^2} + \frac{M_{\text{Engine}}}{\left[(n)\left(\frac{2\pi}{l}\right)\right]^2}\right]}$$

Note:

$$\frac{J_{\text{Bull Gear}}}{n^2} = n^4 J_{\text{Pinion Gear}}$$

Thus,

$$\alpha_{\text{Load}} = \frac{\text{Torque}}{J_{3\text{-Motor}} \left[\frac{2\pi n}{1} \right] + [J_{\text{Pinion Gear}}(3 + n^2)] \left[\frac{2\pi n}{1} \right] + J_{\text{Roller Screw}} \left[\frac{2\pi}{n1} \right] + M_{\text{Engine}} \left[\frac{1}{2\pi n} \right]}$$

For the three-motor case,

$$J_{3\text{-Motor}} = \frac{(3)(565)(15)^{3/2}}{(5)(3000)^{5/3}} = 0.0315598 \text{ in-lbs-sec}^2$$

$$J_{\text{Pinion Gear}} = 0.00004768 \text{ in-lbs-sec}^2$$

$$J_{\text{Roller Screw}} = 0.016 \text{ in-lbs-sec}^2$$

$$M_{\text{Engine}} = 55 \frac{\text{lbs} \cdot \text{sec}^2}{\text{in}}$$

Substituting,

$$\alpha_{\text{Load}} = \frac{\text{Torque}}{[0.0315598] \left[\frac{2\pi n}{1} \right] + [(0.00004768)(3 + n^2)] \left[\frac{2\pi n}{1} \right] + [0.016] \left[\frac{2\pi}{n1} \right] + [55] \left[\frac{1}{2\pi n} \right]}$$

To maximize the acceleration, we must minimize the denominator of the above equation. Let den = denominator then,

$$\text{den} = \frac{2\pi n 0.0315598}{1} + \frac{2\pi n 0.00004768 (3 + n^2)}{1} + \frac{2\pi 0.016}{n1} + \frac{55}{2\pi n}$$

Take the derivative of the denominator with respect to n

$$D1 = \frac{0.198296}{1} - \frac{0.100531}{1 \cdot n} - \frac{8.75352 \cdot 1}{n^2} + \frac{0.000599165 \cdot n^2}{1} + \frac{0.000299582 (3. + n)^2}{1}$$

Take the derivative of the denominator with respect to l

$$D2 = \frac{8.75352}{n} - \frac{0.100531}{1 \cdot n^2} - \frac{0.198296 \cdot n}{1} - \frac{0.000299582 \cdot n^2 (3. + n)^2}{1}$$

Set both D1 and D2 equal to zero and solve for l and n

$$\{l \rightarrow 0.663194, n \rightarrow 4.28002\}$$

Thus, for maximum acceleration an n(gear ratio) of 4.28 and an l(lead) of 0.6632 inches should be chosen.

SENSITIVITY OF THE LOAD ACCELERATION TO VARIATIONS IN THE VALUE OF THE PINION GEAR POLAR MASS MOMENT OF INERTIA

In the work described in section V.tbd covering the maximization of the load acceleration by the proper choice of spur gear and roller screw reduction ratios it was assumed that the value of the spur gear polar mass moment of inertia was known. This is a good assumption if there is some a priori idea of the range of probable gear ratio values for the spur gear pass and the loads which it is to transmit. To test how sensitive the present design is to this ratio the following numerical experiment was performed. The maximum load acceleration was formulated as a function of the two reduction ratios and the rest of the system physical parameters. Then a plot was made of the load acceleration as J_p was varied from one half to double its nominal value. This plot is presented below. Inspection of this plot indicates that there is minimum load acceleration sensitivity in the range of J_p variations to be expected in this design (i.e. with the set of numerical parameters proposed for this design). Close inspection reveals that as expected a little more acceleration occurs when J_p is halved and a little less when it is doubled but the amount of change is very small. Probably this is because the gearing, as calculated elsewhere, is not a dominant factor at all in this system's total inertia. Once again the MATHEMATICA programs are included in case it is desired to perform this type of experiment independently.

In[1]:=

$$Jm = (3 * 565 * (15)^{(1.5)}) / (5 * ((3000)^{(5./3.)}))$$

Out[1]=

0.0315598

In[2]:=

$$Tmax = N[3 * 10 * 550 * 12 / (3000 * 2 * Pi / 60)]$$

Out[2]=

630.254

In[3]:=

$$d = N[((2.*Pi*n/1)*(Jm)) + ((2.*Pi*n/1)*(Jp)*(3.+(n^2))) + ((2.*Pi/(n*1))*(0.016)) + (55.*1/(2.*Pi*n))]$$

Out[3]=

$$\frac{0.100531}{1 \ n} + \frac{8.75352 \ 1}{n} + \frac{0.198296 \ n}{1} + \frac{6.28319 \ Jp \ n \ (3. + n^2)}{1}$$

In[4]:=

$$I1 = 1./d$$

Out[4]=

$$1. / \left(\frac{0.100531}{1 \ n} + \frac{8.75352 \ 1}{n} + \frac{0.198296 \ n}{1} + \frac{6.28319 \ Jp \ n \ (3. + n^2)}{1} \right)$$

In[5]: =

acc=N[Tmax*I1]

Out[5]=

$$630.254 / \left(\frac{0.100531}{1 \ n} + \frac{8.75352 \ 1}{n} + \frac{0.198296 \ n}{1} + \frac{6.28319 \ Jp \ n \ (3. + n^2)}{1} \right)$$

In[6]: =

n=4.28

Out[6]=

4.28

In[7]: =

l=0.6632

Out[7]=

0.6632

In[8]: =

acc

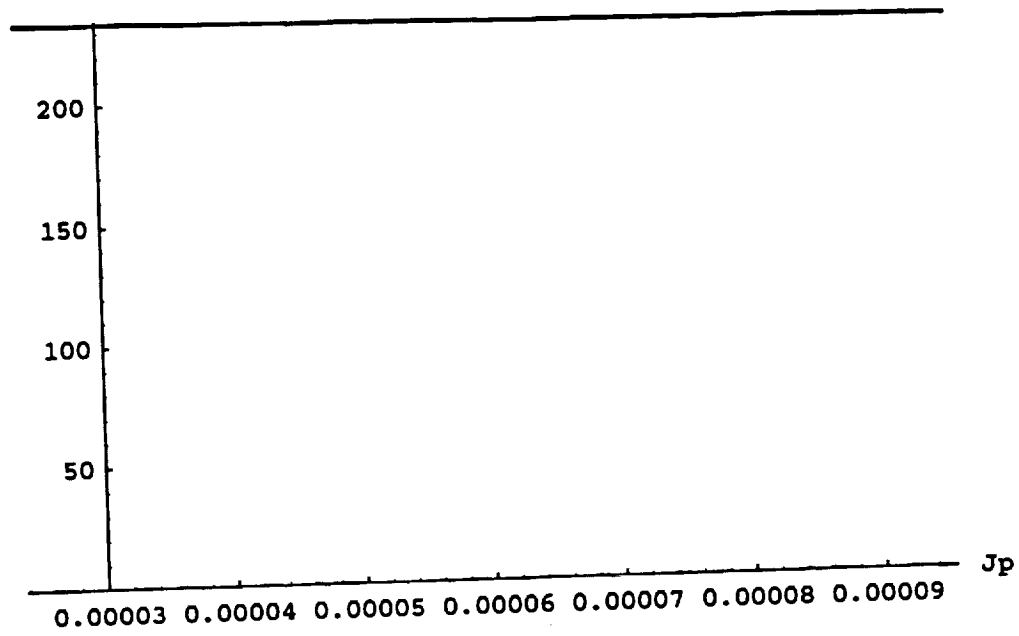
Out[8]=

$$\frac{630.254}{2.67152 + 864.438 \ Jp}$$

In[26]:=

```
Plot[acc, {Jp, 0.00002384, 0.00009536}, AxesLabel->
{"Jp", "Acceleration"}, PlotRange->
{{0.00002384, 0.00009536}, {0, 235}}]
```

Acceleration



Verification That Optimum n (Gear Ratio) And l (Lead) Results In The Matching Of The "Source" Inertia With The "Load" Inertia

The MSFC requirements include maximizing the bandwidth of the system (i.e. acceleration of the engine) and minimizing the power demands on the system (i.e. maximizing the power transfer). It is shown in Appendix A that **both** the bandwidth and the power requirements of the system are satisfied when the source inertia is matched with the load inertia.

The components that are included in the source inertia are:

$J_{3\text{-Motor}}$; $J_{3\text{-Pinion Gear}}$; $J_{\text{Bull Gear}}$; $J_{\text{Roller Screw}}$

The bull gear and the roller screw inertia must be reflected through the gear train to the motor shaft before they can be summed with the motor and pinion gear inertia. This yields

$$J_{\text{Source}} = J_{3\text{-Motor}} + J_{3\text{-Pinion Gear}} + \frac{J_{\text{Bull Gear}}}{n^2} + \frac{J_{\text{Roller Screw}}}{n^2}$$

The components that are included in the load inertia are:

M_{Engine}

The mass of the engine must be reflected through the gear train and the roller screw to the motor shaft which yields

$$J_{\text{Load}} = \frac{M_{\text{Engine}}}{\left[\frac{2\pi n}{1} \right]^2}$$

The parameter values are

$$J_{3\text{-Motor}} = \frac{(3)(565)(15)^{3/2}}{(5)(3000)^{5/3}} = 0.315598 \text{ in-lbs-sec}^2$$

$$J_{3\text{-Pinion Gear}} = (3)(0.00004768) = 0.00014304 \text{ in-lbs-sec}^2$$

$$J_{\text{Bull Gear}} = n^4 J_{\text{Pinion Gear}} \text{ in-lbs-sec}^2$$

$$J_{\text{Roller Screw}} = 0.016 \text{ in-lbs-sec}^2$$

$$M_{\text{Engine}} = 55 \frac{\text{lbs-sec}^2}{\text{in}}$$

$$n = 4.28$$

$$l = 0.6632 \text{ in}^{-1}$$

The reflected source inertia is

$$J_{\text{Source}} = [0.0315598] + [0.00014304] + \left[\frac{(4.28)^4 (0.00004768)}{4.28^2} \right] + \left[\frac{0.016}{4.28^2} \right]$$

$$J_{\text{Source}} = 0.0334497 \text{ in-lbs-sec}^2$$

The reflected load inertia is

$$J_{\text{Load}} = \frac{55}{\left[\frac{2\pi(4.28)^2}{(0.6632)} \right]} = 0.0334506 \text{ in-lbs-sec}^2$$

Therefore, the source inertia and the load inertia are matched for this choice of gear ratio(n) and lead(l). Recall that the values for n and l were chosen to maximize the speed of response (i.e. bandwidth) of this system.

**FINAL SELECTION OF GEAR
RATIO (n) AND LEAD (l)
FOR POINT DESIGN**

C. FINAL SELECTION OF GEAR RATIO(n) AND LEAD(l) FOR POINT DESIGN

Calculation Of Overall Gear Ratio To Meet The 5 in/sec Rate Requirement

Heretofore, only maximized acceleration and best power transfer have been considered in the selection of n(gear ratio) and l(lead). Covered below are additional requirements which lead to final n(gear ratio) and l(lead) choices.

Recall that

$$\dot{\theta}_{\text{Motor}} = \left[\frac{2 \pi n}{l} \right] \dot{x}_{\text{Engine}}$$

Rearranging terms

$$\left[\frac{2 \pi n}{l} \right] = \frac{\dot{\theta}_{\text{Motor}}}{\dot{x}_{\text{Engine}}}$$

From the above equation it is clear that the overall gear ratio (2pn/l) is a function of the motor speed and the load speed. For this design the motor speed is 3000 RPM and the load speed is 5 in/sec. Substituting into the equation yields

$$\left[\frac{2 \pi n}{l} \right] = \frac{(3000 \frac{\text{rev}}{\text{min}})(2 \pi \frac{\text{rad}}{\text{rev}})(\frac{1 \text{ min}}{60 \text{ sec}})}{5 \frac{\text{in}}{\text{sec}}} = 62.8318 \text{ in}^{-1}$$

Remember that n(gear ratio) is equal to 4.28 (for the given pinion gear and roller screw) and solve for l(lead) in the above equation

$$l = \frac{2 \pi (4.28)}{62.8318 \text{ in}^{-1}} = 0.428 \text{ inches}$$

Thus, a given motor and load speed requirement will set the value for l (lead) which will set the value of the overall gear ratio.

Calculation Of Overall Gear Ratio To Meet The 40,000 lbs Requirement Given A Specific Available Torque

To verify the results obtained in the preceding section, the following calculations were made.

Recall that

$$T(\text{in-lbs}) = [\text{Force (lbs)}] \left[\frac{l \text{ in}}{2 \pi n} \right]$$

Rearranging terms

$$\frac{2 \pi n}{l \text{ in}} = \frac{\text{Force (lbs)}}{T(\text{in-lbs})}$$

From the above equation it is clear that the overall gear ratio ($2\pi n/l$) is a function of the required output force and the available torque. The required output force is 40,000 lbs. The available torque of a motor providing 10 Horsepower is

$$T_{\text{Available}} = \frac{(3)(10 \text{ HP}) \left(\frac{550 \text{ ft-lbs}}{1 \text{ HP}} \right) \left(\frac{12 \text{ in}}{1 \text{ ft}} \right)}{(3000 \frac{\text{rev}}{\text{min}}) \left(\frac{2 \pi \text{ rad}}{1 \text{ rev}} \right) \left(\frac{1 \text{ min}}{60 \text{ sec}} \right)} = 630.254 \text{ in - lbs}$$

Substituting yields

$$\frac{2 \pi n}{l \text{ in}} = \frac{40,000 \text{ lbs}}{630.254 \text{ in - lbs}} = 63.4665 \text{ in}^{-1}$$

Remember that n (gear ratio) is equal to 4.28 (for the given pinion gear and roller screw) and solve for l (lead) in the above equation

$$l = \frac{2 \pi (4.28)}{63.4665 \text{ in}^{-1}} = 0.42372 \text{ inches}$$

Thus, a given output force requirement and a specific available torque will set the value for the l (lead) which will set the value of the overall gear ratio.

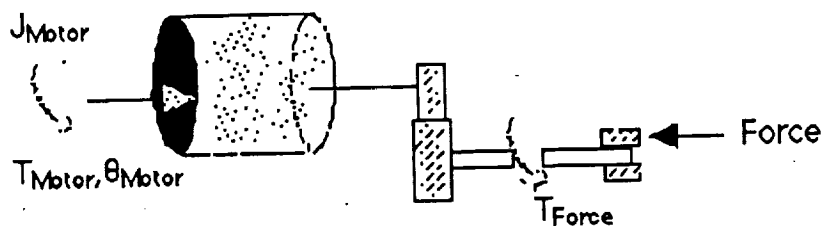
Notice that the values calculated for l (lead) in each of the two cases are very similar. This is not a coincidence. One value for l (lead) must satisfy both requirements at the same time: The 5 in/sec rate requirement and the 40,000 lbs force requirement.

**DEVELOPMENT OF
SIMULATION MODEL**

D. PHYSICAL MODEL USED TO DEVELOP EQUATIONS OF MOTION FOR THIS SYSTEM

As discussed previously the first analytical effort was to construct an analytical model of the "plant" i.e. the mechanical portions of the actuator-rocket engine combination. This had to be accomplished in such a way as to render available the variables to be measured and fed back. The method of free bodies was chosen and Newtonian physics (d'Alembert's Principal) applied. This is shown below.

Treat Model In Two Parts



First

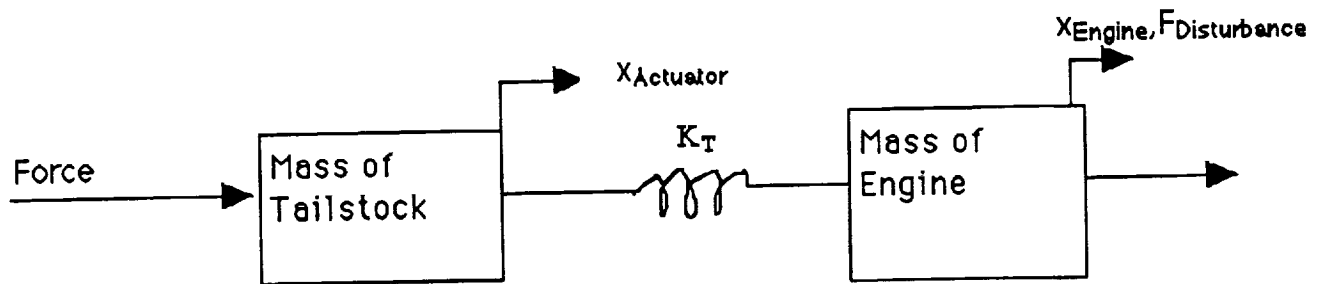
$$T_{\text{Force}} = \frac{IF}{2\pi}$$

Refer T_{Force} and Rotary Inertia to Motor

$$J_{\Sigma} = J_{\text{Motor}} + J_{\text{Pinion Gear}} + \frac{J_{\text{Bull Gear}}}{n^2} + \frac{J_{\text{Roller Screw}}}{n^2}$$

$$T_{\text{Motor}} = \frac{IF}{2\pi} = J_{\Sigma} \ddot{\theta}_{\text{Motor}} \quad (1)$$

Second



$$m_{\text{Tailstock}} \ddot{x}_{\text{Actuator}} = F - K_T(x_{\text{Actuator}} - x_{\text{Engine}}) \quad (2)$$

$$m_{\text{Engine}} \ddot{x}_{\text{Engine}} = K_T(x_{\text{Actuator}} - x_{\text{Engine}}) + F_{\text{Disturbance}} \quad (3)$$

Constraint

$$x_{\text{Actuator}} = \frac{l \theta_{\text{Motor}}}{2\pi n} \quad (4)$$

Substitute (4) \rightarrow (2) \rightarrow (1)

$$J_{\Sigma} \ddot{\theta}_{\text{Motor}} = T_{\text{Motor}} - \left(\frac{1}{2\pi n} \right) \left(m_{\text{Tailstock}} \frac{1}{2\pi n} \ddot{\theta}_{\text{Motor}} + K_T \left(\frac{1}{2\pi n} \theta_{\text{Motor}} - x_{\text{Engine}} \right) \right)$$

Substitute (4) \rightarrow (3)

$$m_{\text{Engine}} \ddot{x}_{\text{Engine}} = K_T \left(\frac{1}{2\pi n} \theta_{\text{Motor}} - x_{\text{Engine}} \right) + F_{\text{Disturbance}}$$

Combine Terms and Rearrange

$$\left\{ J_{\Sigma} + \left(\frac{1}{2\pi n} \right)^2 m_{\text{Tailstock}} \right\} \ddot{\theta}_{\text{Motor}} = T_{\text{Motor}} - \left(\frac{1}{2\pi n} \right)^2 K_T \theta_{\text{Motor}} + \frac{1}{2\pi n} K_T x_{\text{Engine}}$$

$$m_{\text{Engine}} \ddot{x}_{\text{Engine}} = F_{\text{Disturbance}} + \left(\frac{1}{2\pi n} \right) K_T \theta_{\text{Motor}} - K_T x_{\text{Engine}}$$

$$\text{Let } \lambda = \frac{1}{2\pi n}$$

$$\text{Let } J_{EQ} = J_{\Sigma} + \left(\frac{1}{2\pi n}\right)^2 m_{\text{Tailstock}}$$

Then

$$\ddot{\theta}_{\text{Motor}} = \frac{T_{\text{Motor}}}{J_{EQ}} - \frac{\lambda^2}{J_{EQ}} K_T \theta_{\text{Motor}} + \frac{\lambda K_T}{J_{EQ}} x_{\text{Engine}}$$

$$\ddot{x}_{\text{Engine}} = \frac{F_{\text{Disturbance}}}{m_{\text{Engine}}} + \frac{\lambda K_T}{m_{\text{Engine}}} \theta_{\text{Motor}} - \frac{K_T}{m_{\text{Engine}}} x_{\text{Engine}}$$

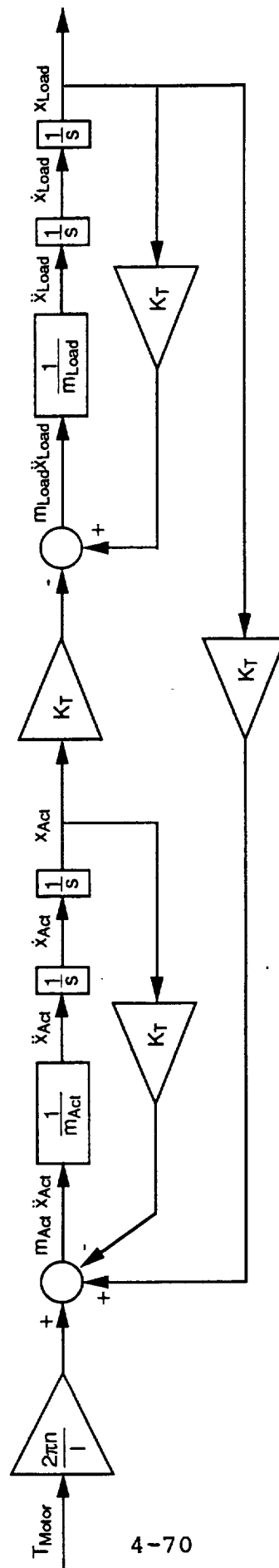
Transform To Rectilinear Coordinates

$$\theta_{\text{Motor}} = \frac{x_{\text{Actuator}}}{\lambda}$$

Substituting $J_{EQ} = \lambda^2 M_{EQ}$ Yields Equations Used To Develop Block Diagram

$$\ddot{x}_{\text{Actuator}} = \frac{T_{\text{Motor}}}{\lambda M_{EQ}} - \frac{K_T x_{\text{Actuator}}}{M_{EQ}} + \frac{K_T x_{\text{Engine}}}{M_{EQ}}$$

$$\ddot{x}_{\text{Engine}} = \frac{F_{\text{Disturbance}}}{m_{\text{Engine}}} + \frac{K_T}{m_{\text{Engine}}} x_{\text{Actuator}} - \frac{K_T}{m_{\text{Engine}}} x_{\text{Engine}}$$



Simulation Model Developed From The Equations Of Motion

MODEL PARAMETERS

The parameters used in this model were chosen based on gear-train optimization work, system dynamic response requirements, and system steady-state requirements. The values for n and l were calculated in Section C.

$$n(\text{Gear Ratio}) = 4.28$$

$$l(\text{Lead}) = 0.428 \text{ in}^{-1}$$

$$\frac{2\pi n}{l}(\text{Overall Gear Ratio}) = \frac{2\pi(4.28)}{0.428} = 62.832 \text{ in}^{-1}$$

The bull gear inertia and the reciprocal actuator mass were calculated on Page 4-15 and in Appendix D, respectively.

$$J_{\text{Bull Gear}}(\text{Bull Gear Inertia}) = n^4 J_{\text{Pinion Gear}} = 0.01599 \text{ in-lb-sec}^2$$

$$\text{Reciprocal Actuator Mass} = 0.00755796 \frac{\text{in}}{\text{lb-sec}^2}$$

The values used for mechanical damping and the mass of the tailstock were estimates generated by Dr. George Doane based on his past experience with actuators.

$$\text{Mechanical damping in load loop} = 0.6 \frac{\text{in/sec}^2}{\text{in/sec}}$$

$$W_{\text{Tailstock}} = 100 \text{ lbs}_f$$

$$M_{\text{Tailstock}} = \frac{100 \text{ lbs}_f}{(32.2 \frac{\text{ft}}{\text{sec}^2})(12 \frac{\text{in}}{\text{ft}})} = 0.258799 \frac{\text{lb-sec}^2}{\text{in}}$$

The values for the motor inertia, the roller screw inertia, the pinion gear inertia, the engine mass, and the spring constant were supplied by MSFC

$$J_{3\text{-Motor}}(\text{Motor Inertia}) = \frac{(3)(565)(\text{HP})^{3/2}}{(\text{RPM})^{5/3}} = \frac{(3)(565)(15)^{3/2}}{(3000)^{5/3}} \text{ in-lb-sec}^2$$

$$J_{\text{Roller Screw}}(\text{Roller Screw Inertia}) = 0.016 \text{ in-lb-sec}^2$$

$$J_{\text{Pinion Gear}}(\text{Pinion Gear Inertia}) = 0.00004768 \text{ in-lb-sec}^2$$

$$M_{\text{Engine}}(\text{Engine Mass}) = 55 \frac{\text{lbs-sec}^2}{\text{inches}}$$

$$K_T(\text{Spring Constant}) = 139,000 \text{ lbs/in}$$

**SERVOLOOP DESIGN
PROCEDURES**

E. SERVOLOOP DESIGN PROCEDURES

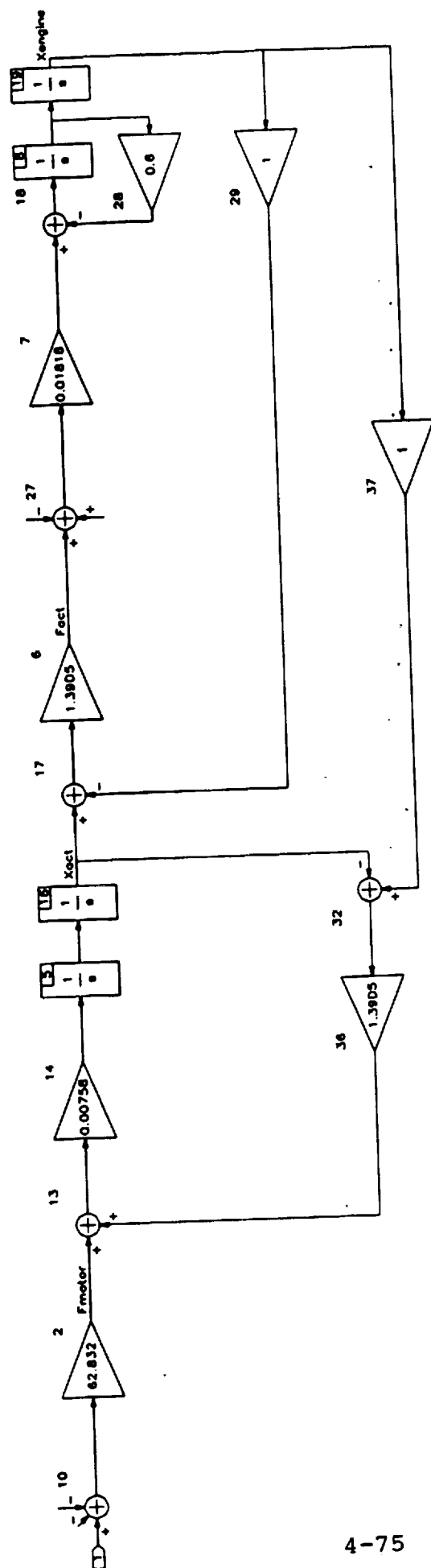
The work reported upon in the previous section developed the overall dynamic model of the actuator (the plant in control vernacular). This model is shown in the first figure in this section as a block diagram which was in fact used to program the digital simulation. The servoloop design methodology had to produce a controller which causes good tracking of the load to reference commands even though there is no possibility of measuring directly any of the load's states i.e. its position or velocity. Following the approach developed long ago in the control of hydraulic actuators it was decided to measure the force in the tailstock (i.e. the force applied to the load) and feed it back as a first loop. The other loops employed were to feed back the actuator position as a second loop and lastly to feed back a signal proportional to actuator velocity (which also proved useful in overcoming start/stop induced transients in a reconfigured controller).

As explained in the included text below a mixture of frequency response and root locus methods were used in conjunction with the linear model to design the loops. Extensive use was made of the MATRIxx environment to generate frequency response plots, root loci and time response plots. These are included below.

Continuous Super-Block
 Cl ent Linear Model

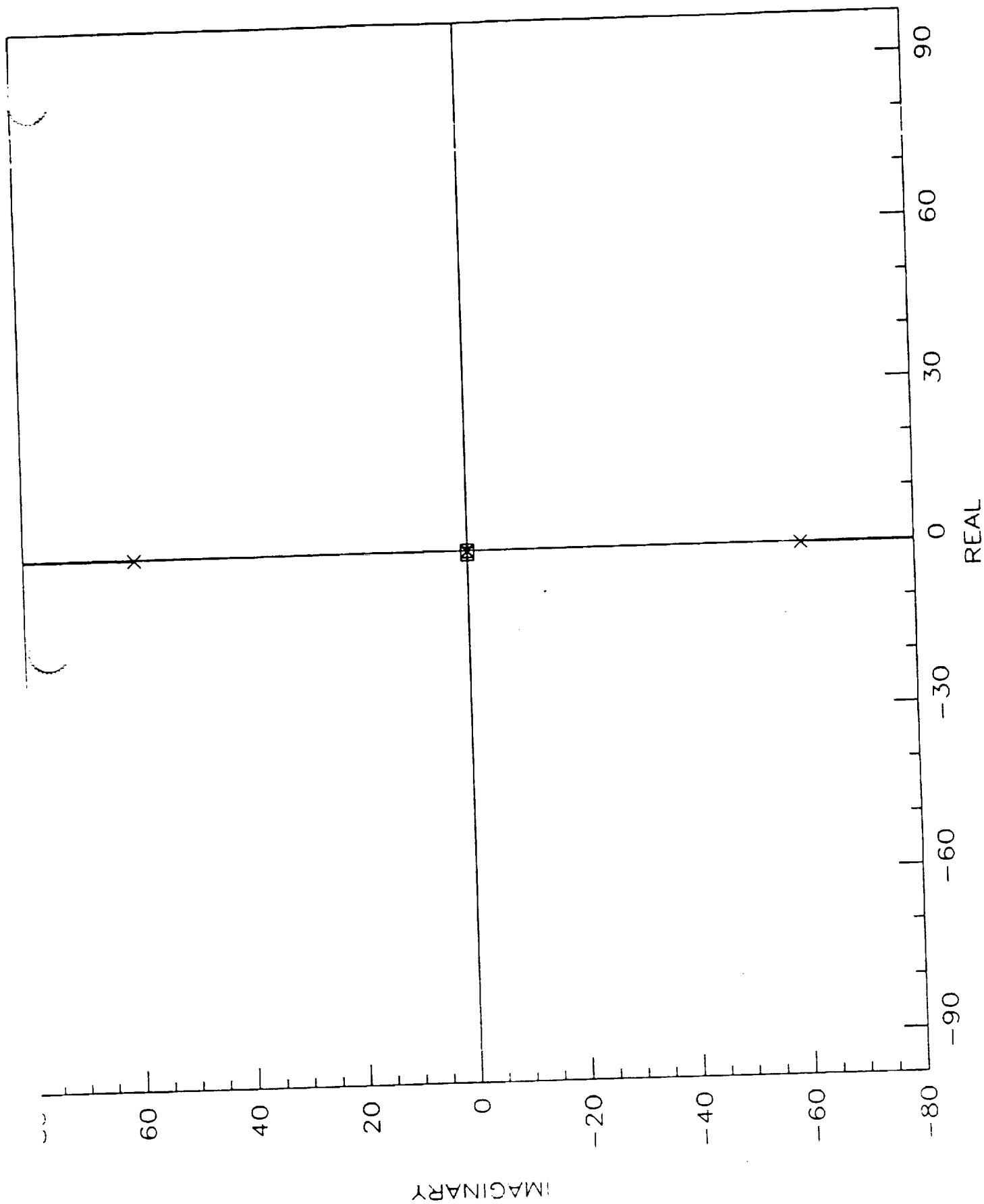
Ext.In
 1

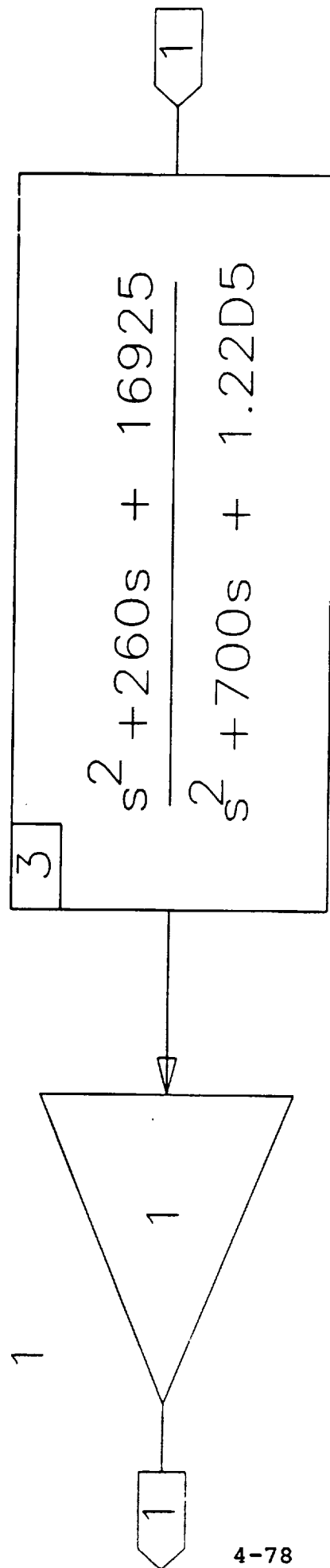
Ext.Ou
 0

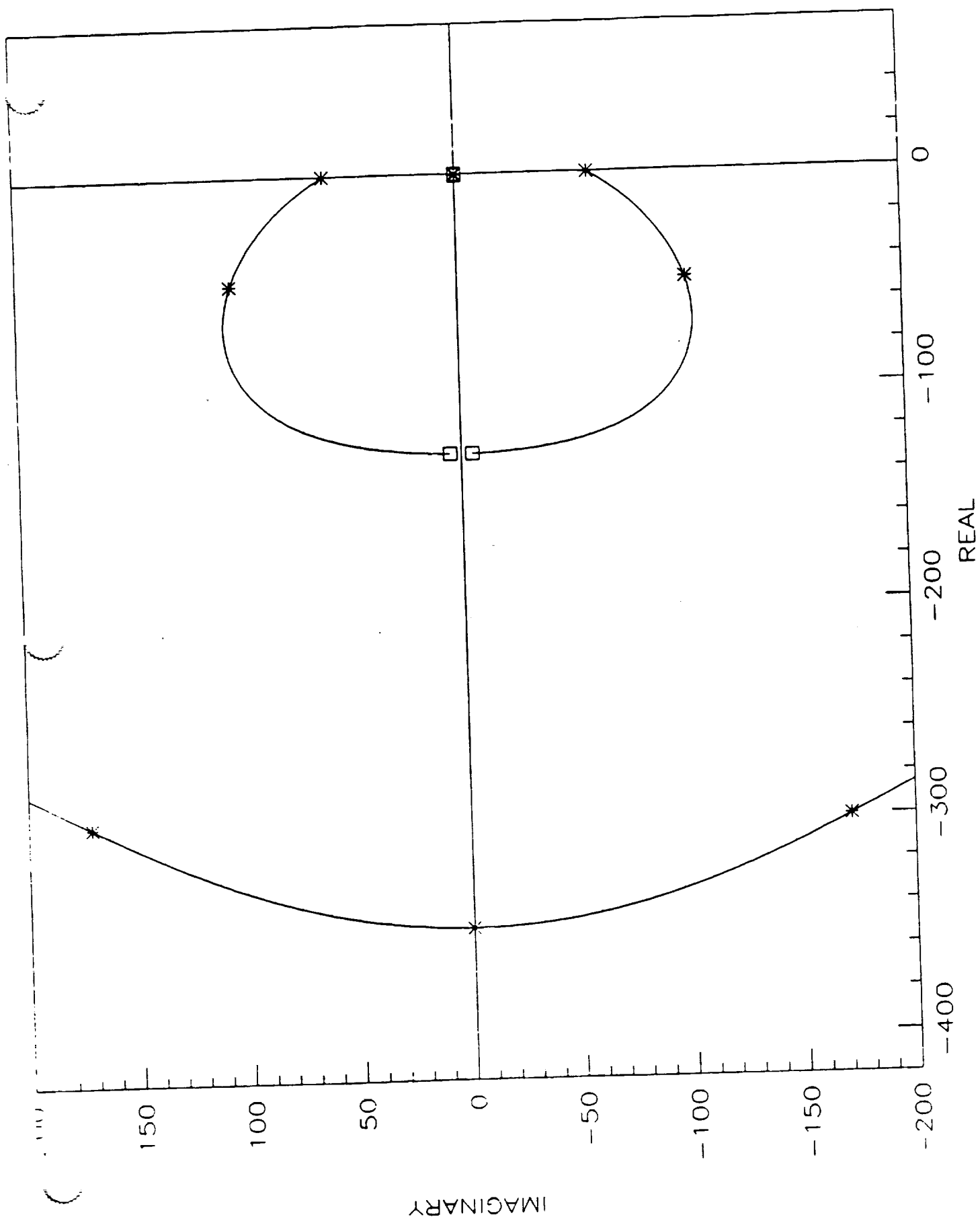


FORCE FEEDBACK LOOP

The force feedback loop is the first loop closed. The Figure on Page 4-77 shows the migration of the poles as a function of loop gain. Although the open loop undamped system is neutrally stable, the present system response is unacceptable. The force compensator shown on Page 4-78 was used to close the force loop. The Figure on Page 4-79 shows the migration of the poles (with the force loop compensator included) as a function of the loop gain. Clearly, the system is now more stable and the system response is faster (i.e. , the poles are in the LHP). However, the bandwidth and phase lag of this system does not meet specifications, so a phase stabilized loop was closed next using the position output.

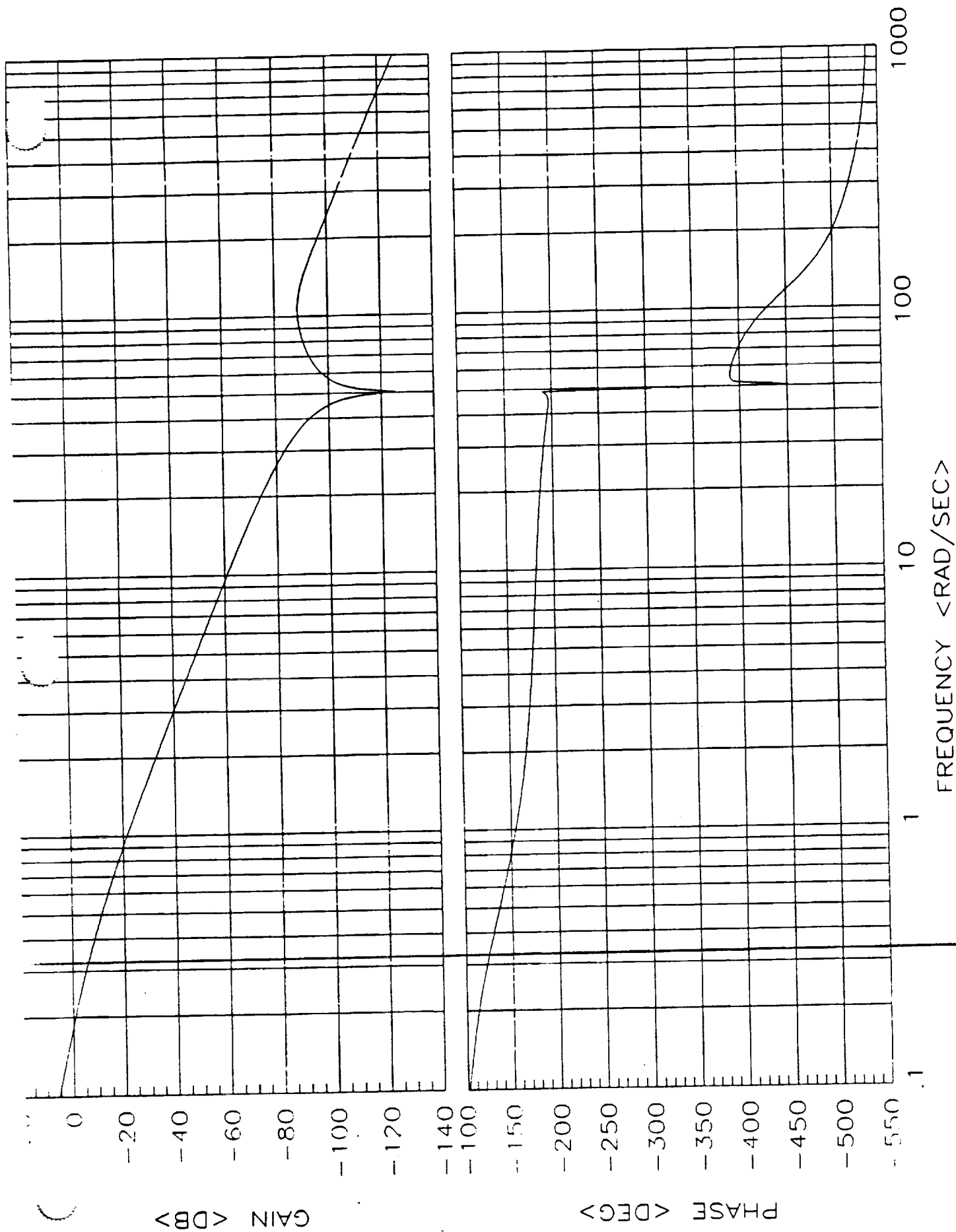


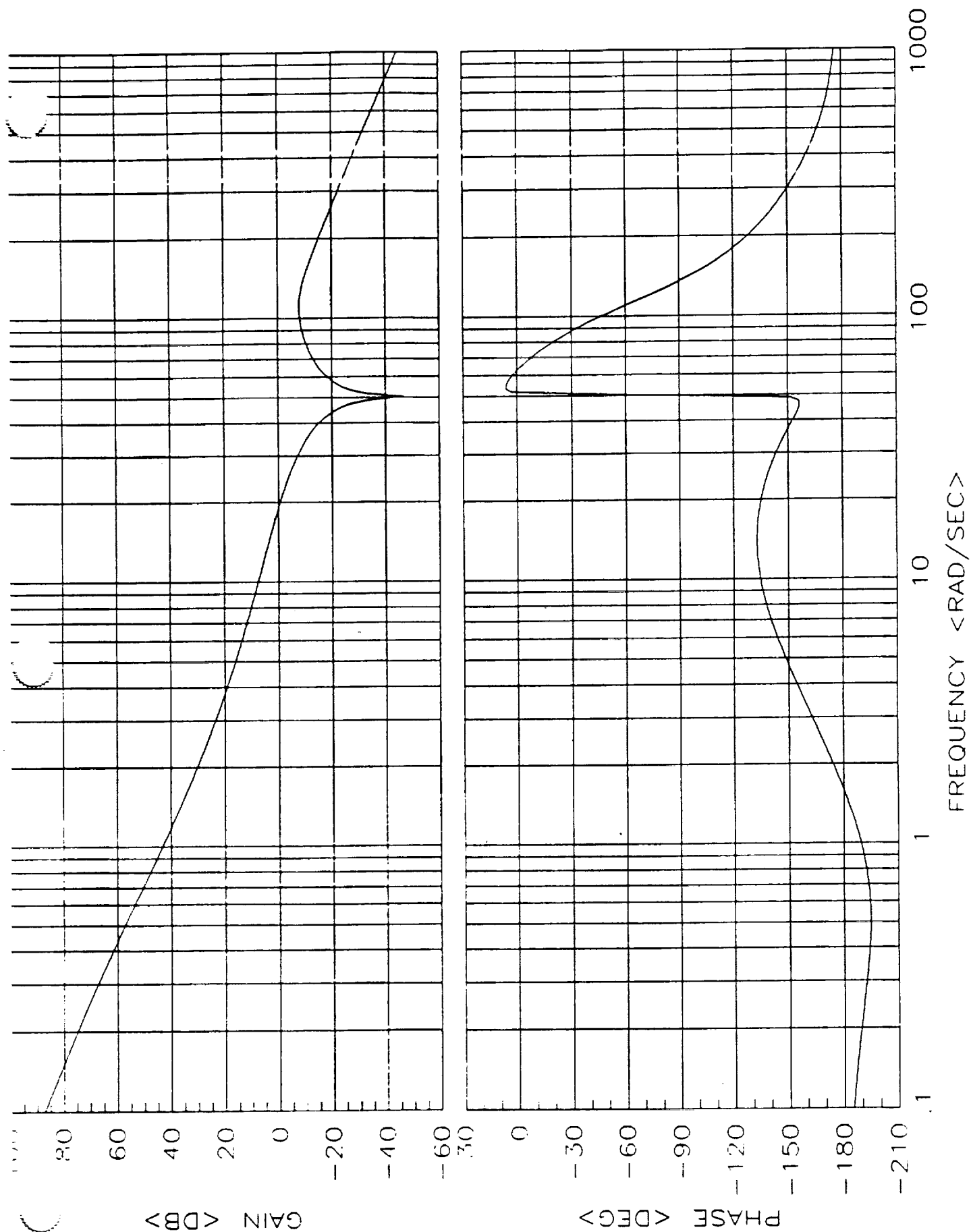




ACTUATOR POSITION FEEDBACK LOOP

The Figure on Page 4-81 shows the open-loop frequency response between the actuator position and the input command. To achieve the required bandwidth of 4.2 Hz, the 0-db cross-over frequency was set at approximately 20 rad/sec (which corresponds to a gain requirement of 12000 or 80 db). To meet the phase requirement, 54.8 degrees of phase lead (i.e., a single stage pole-zero spread of 10) was added to the system. In addition, an integrator was added to minimize the errors caused by low frequency disturbances and inputs. The Figure on Page 4-82 shows the resulting open-loop frequency response between actuator position and the input command. The position compensator (shown on Page 4-83) was put in the forward path of this loop so the actuator position would track the input command. Note that switching from the feedback path to the forward path does not affect the stability of the loop. To fine tune the time response of this system, a velocity loop (with a simple gain) was closed around the system.

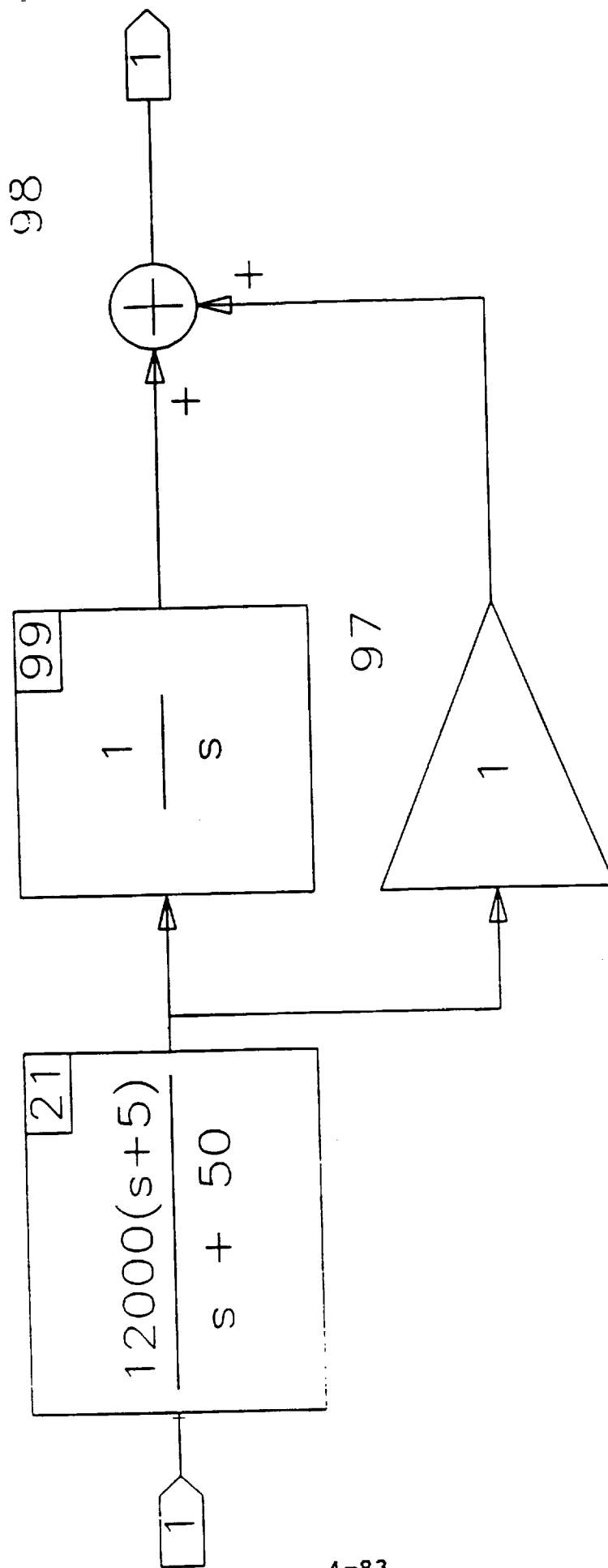




Continuous Super-Block
Position Compensator

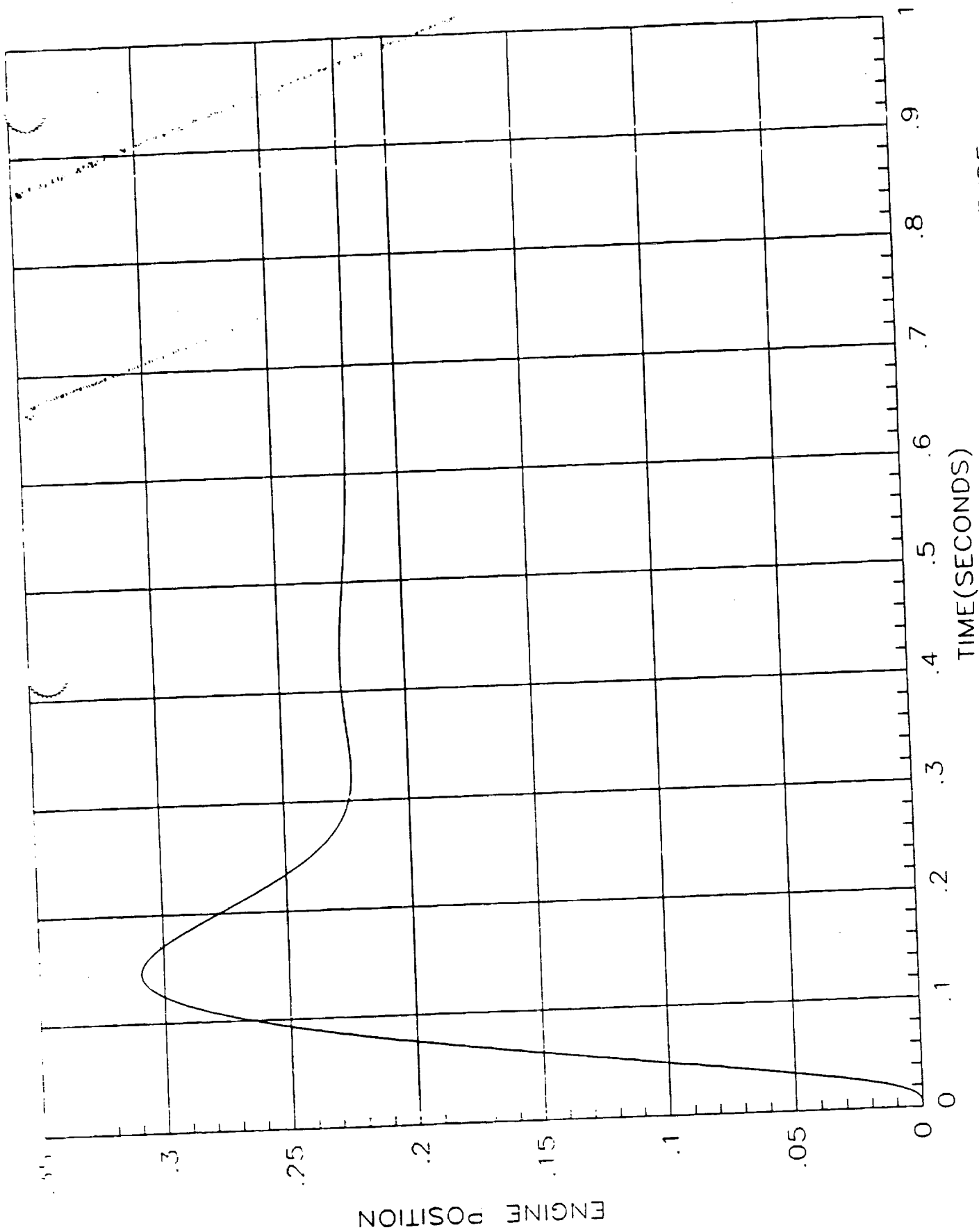
Ext. In 1

Ext. Out 1

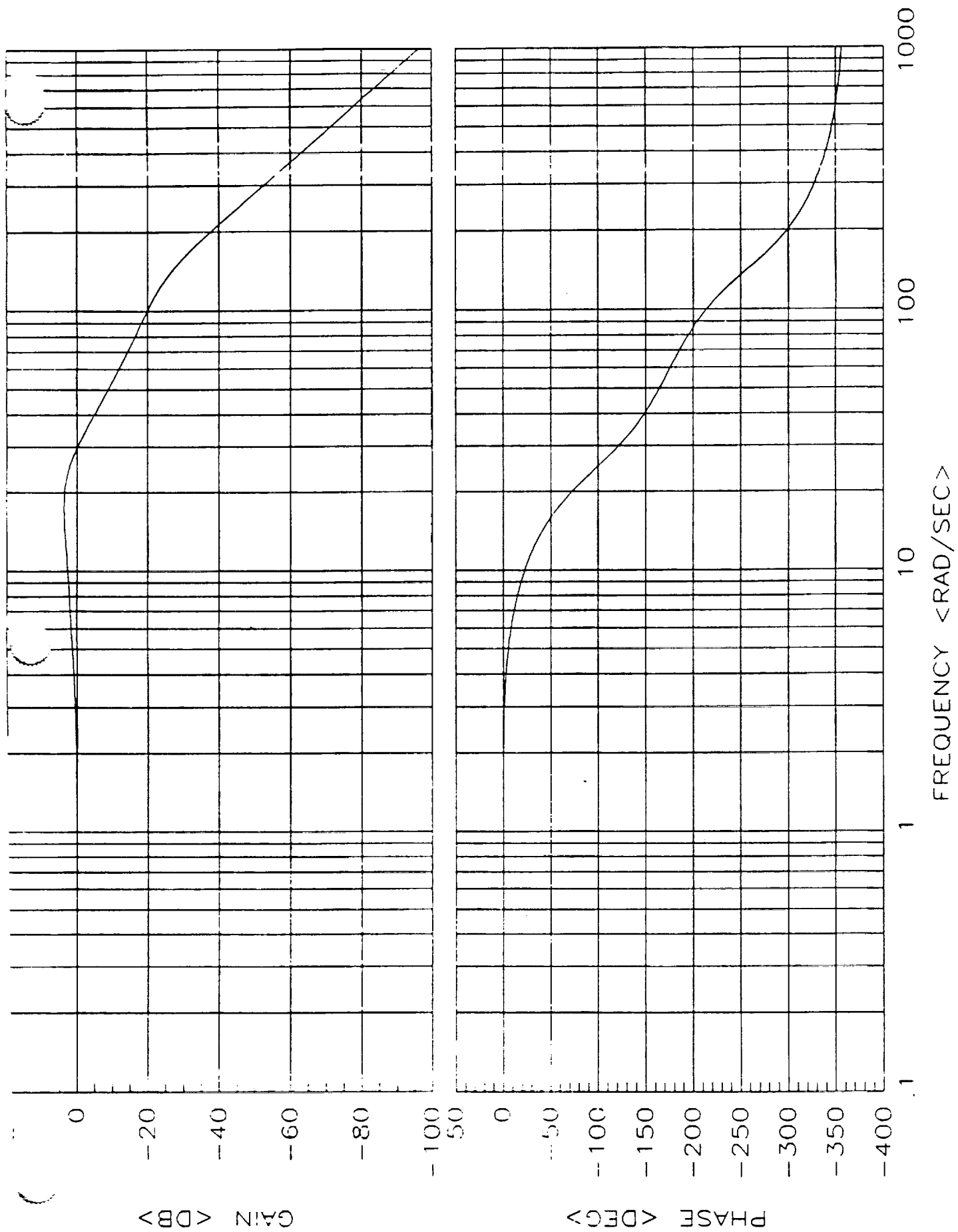


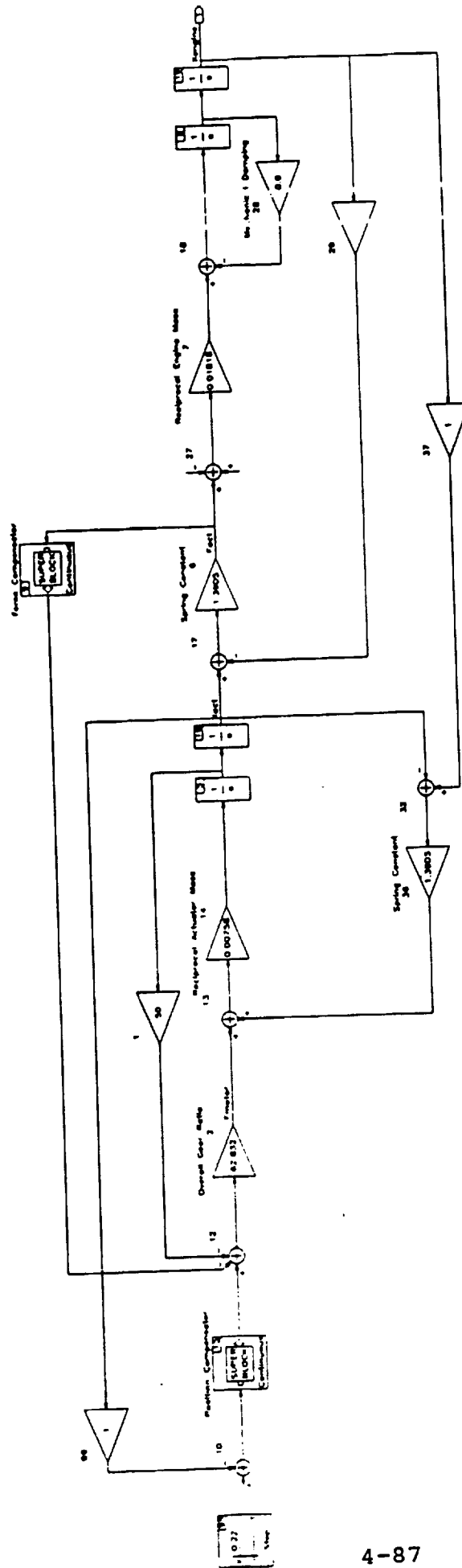
ACTUATOR VELOCITY FEEDBACK LOOP

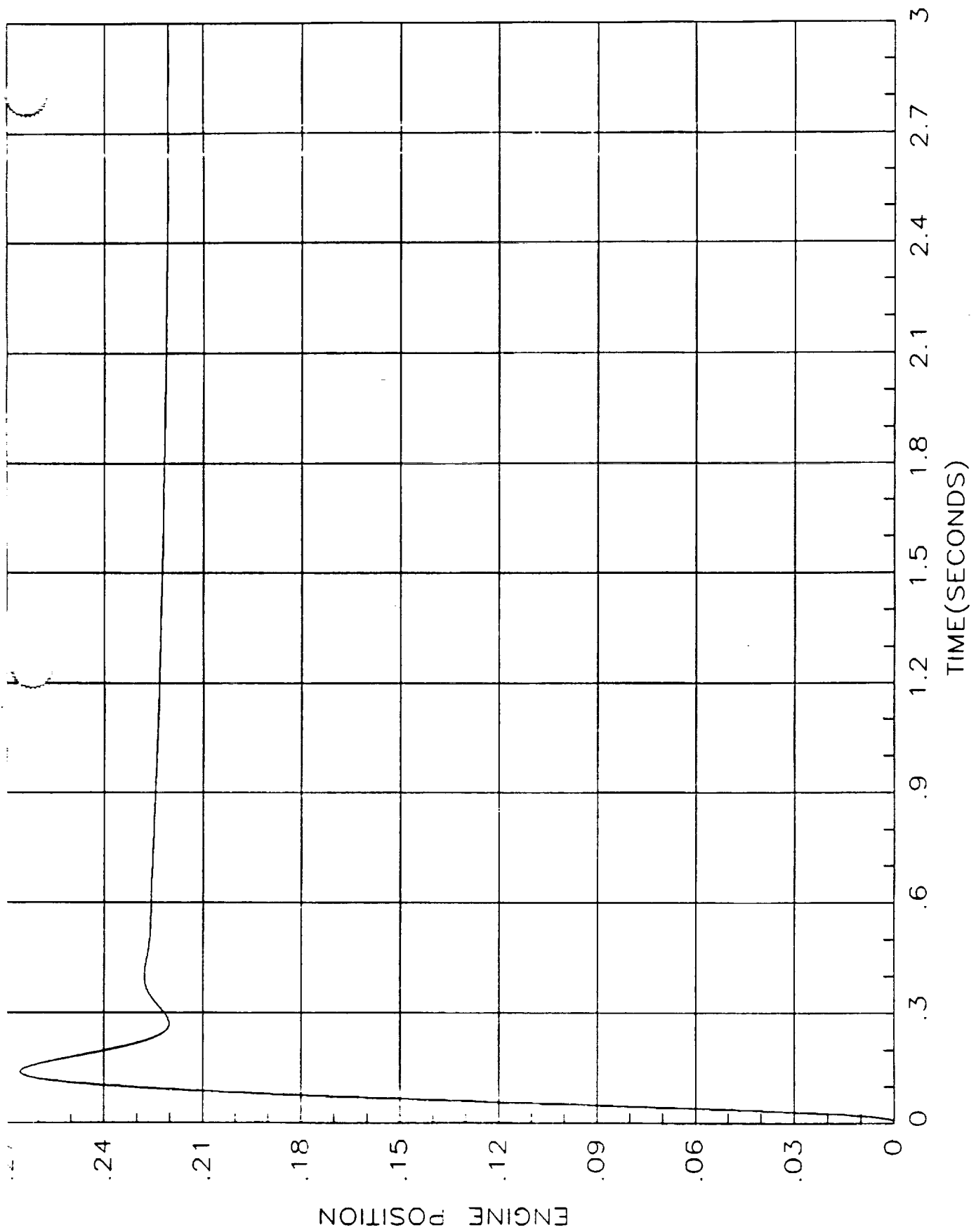
The Figures on Pages 4-85 and 4-86 show the time response and the frequency response, respectively between the engine position and the input command of the system without the velocity loop closed. By closing the velocity loop and adjusting the gain, the system overshoot in the time domain and peaking in the frequency domain were reduced while still maintaining less than 20 degrees phase lag at 1 Hz and less than 90 degrees phase lag at 4.2 Hz. The Figure on Page 4-87 shows the current linear system model. The Figures on Pages 4-88 through 4-90 show the time-response of the engine position and the frequency-response between the engine position and the input command. Comparison to NASA's performance specifications will reveal that the performance of this system does meet both time-domain and frequency-domain requirements.



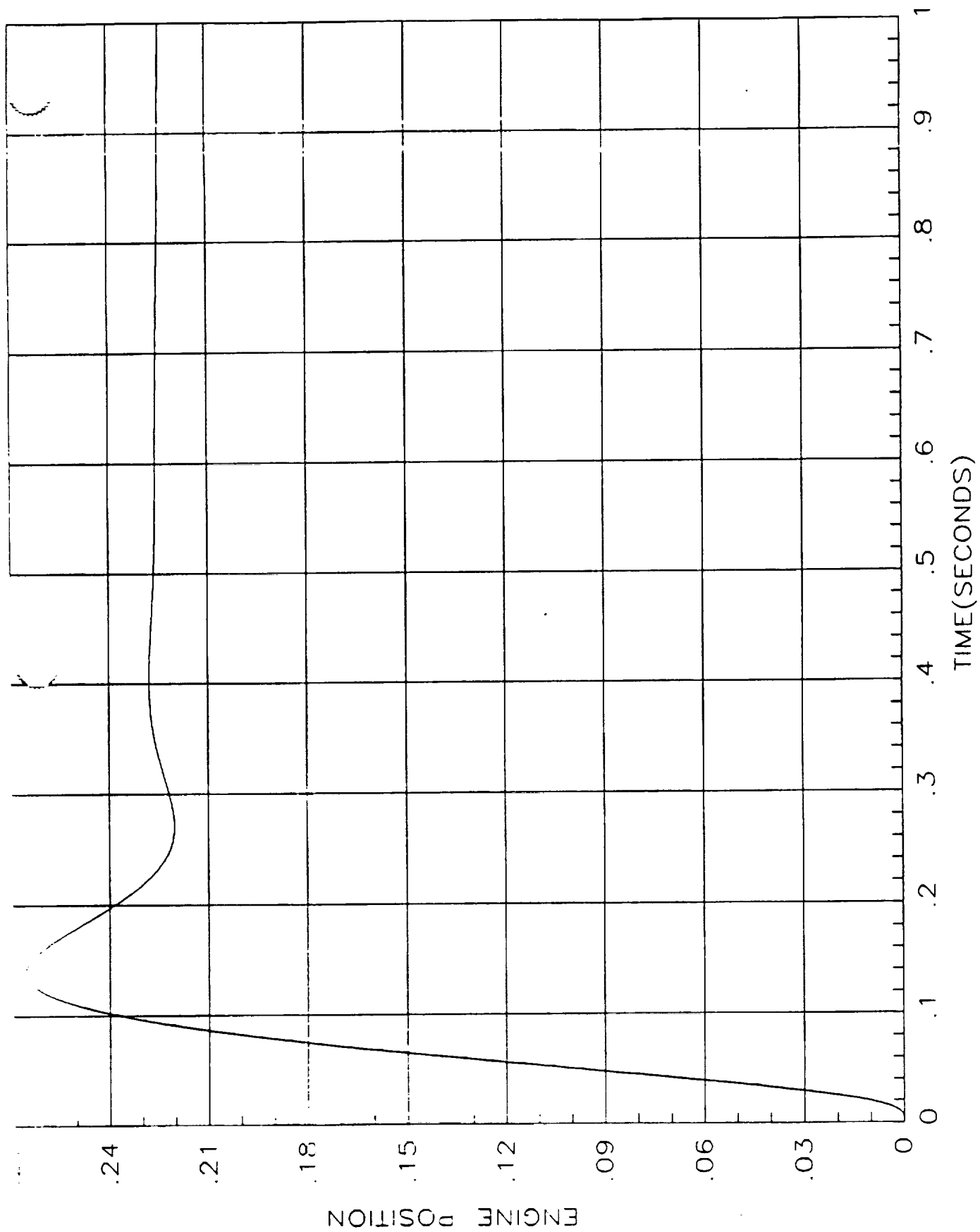
STEP CHANGE IN INPUT COMMAND AT 4% INPUT AMPLITUDE



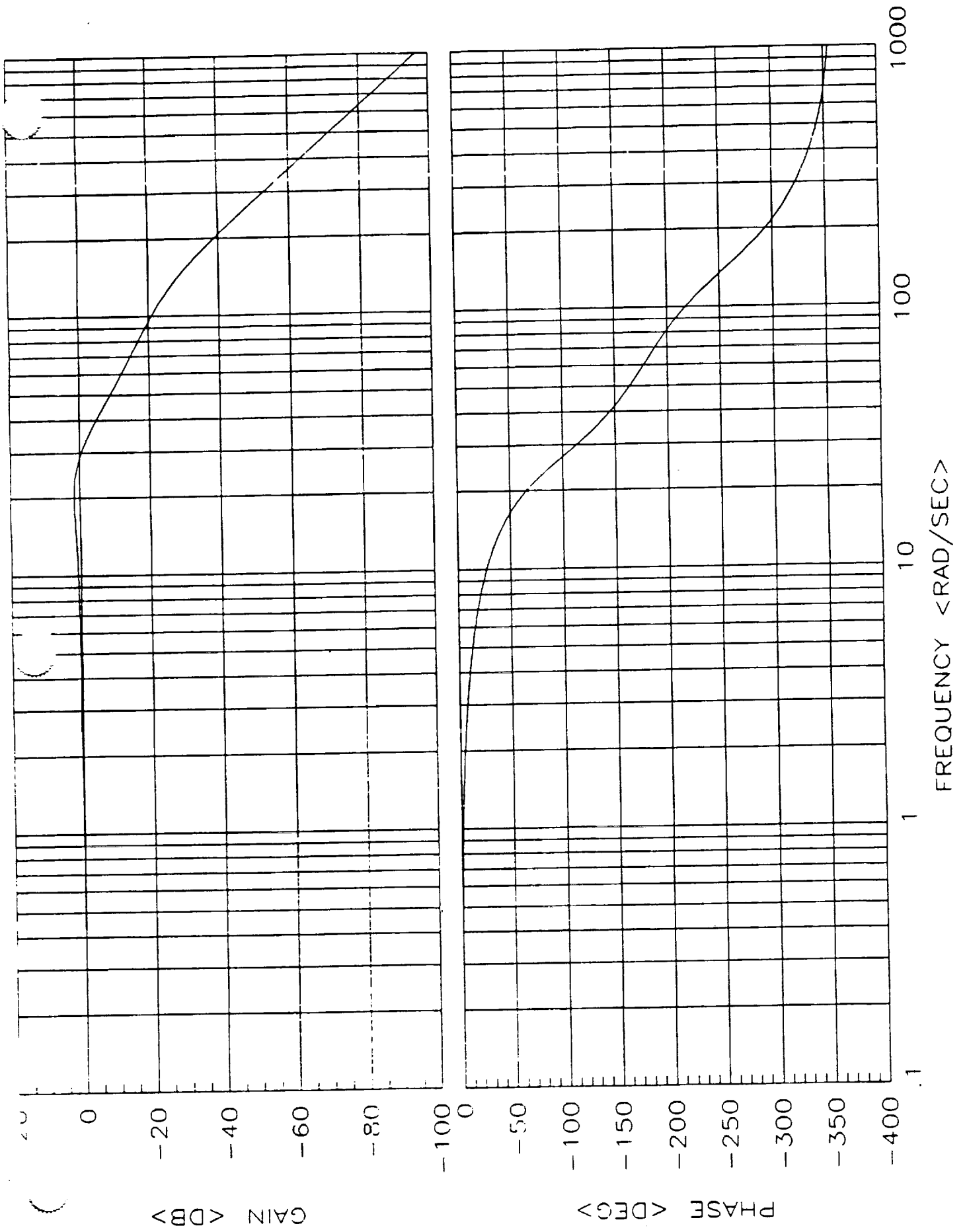




STEP CHANGE IN INPUT COMMAND AT 4% INPUT AMPLITUDE



STEP CHANGE IN INPUT COMMAND AT 4% INPUT AMPLITUDE

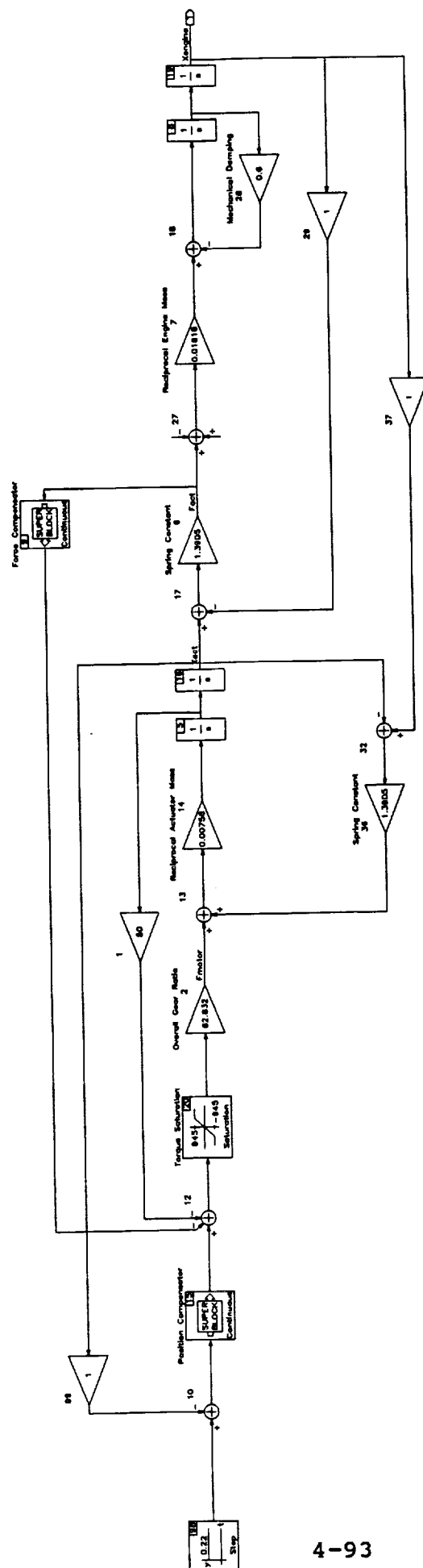


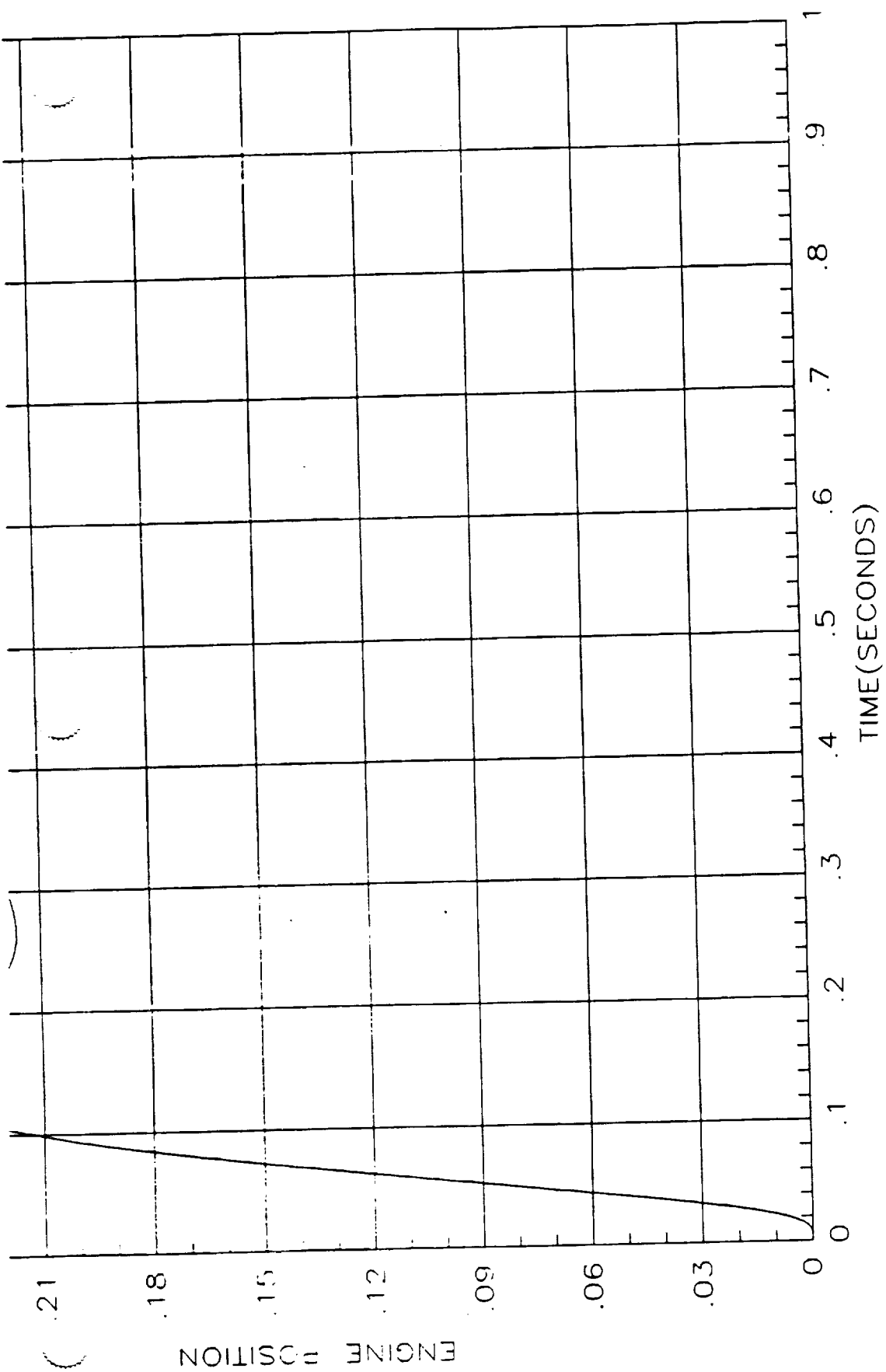
NON-LINEAR

MODEL

NON-LINEAR MODEL

After a linear model was developed, a saturation limit was introduced to model the current limit inherent in the motor drive power amplifier. The Figure on Page 4-93 shows the present non-linear system model. The Figures on Pages 4-94 through 4-96 show the time-response of the engine position and the frequency-response between the engine position and the input command. Comparison to NASA's performance specifications reveals that the performance of this system does meet both time-domain and frequency-domain requirements.

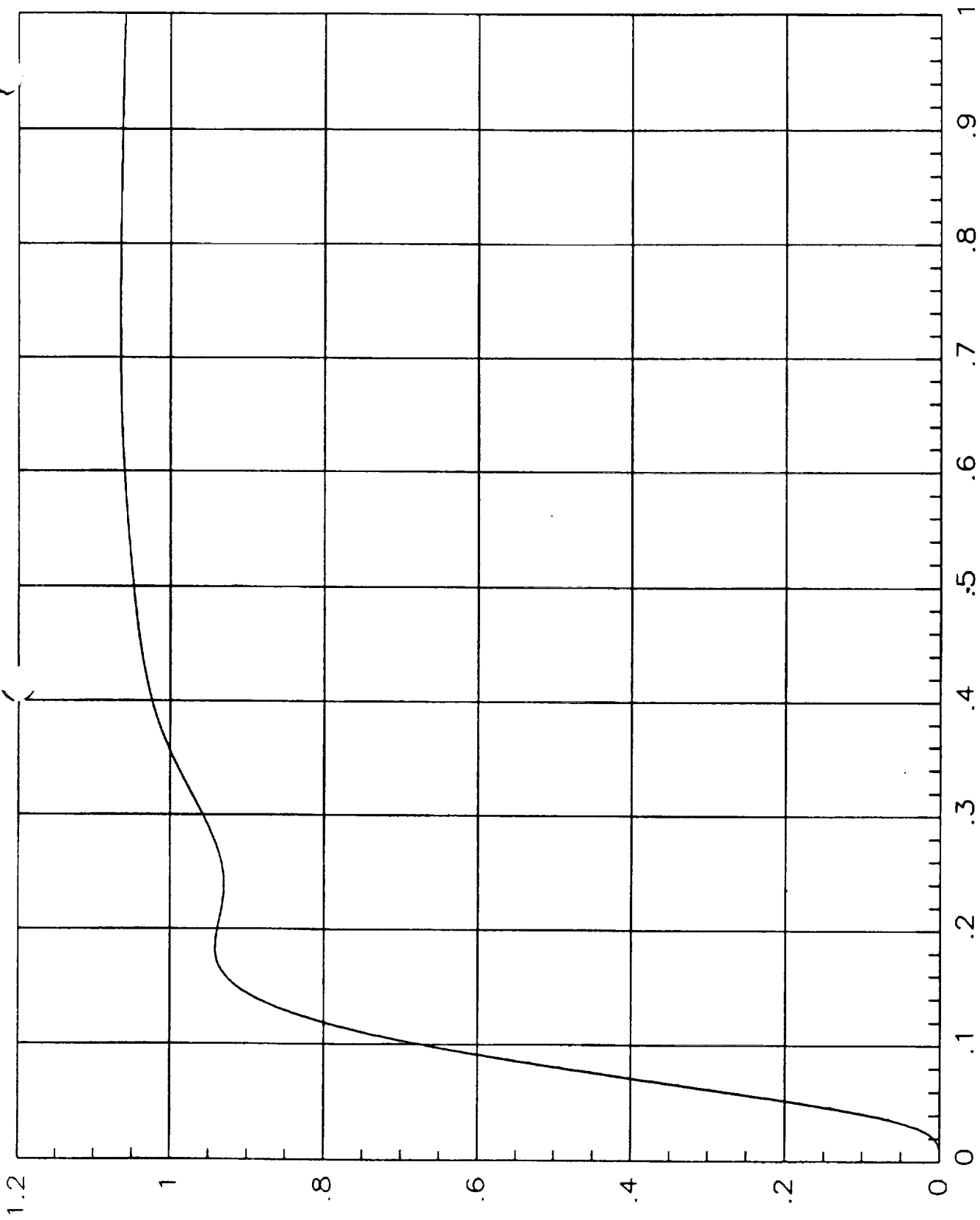




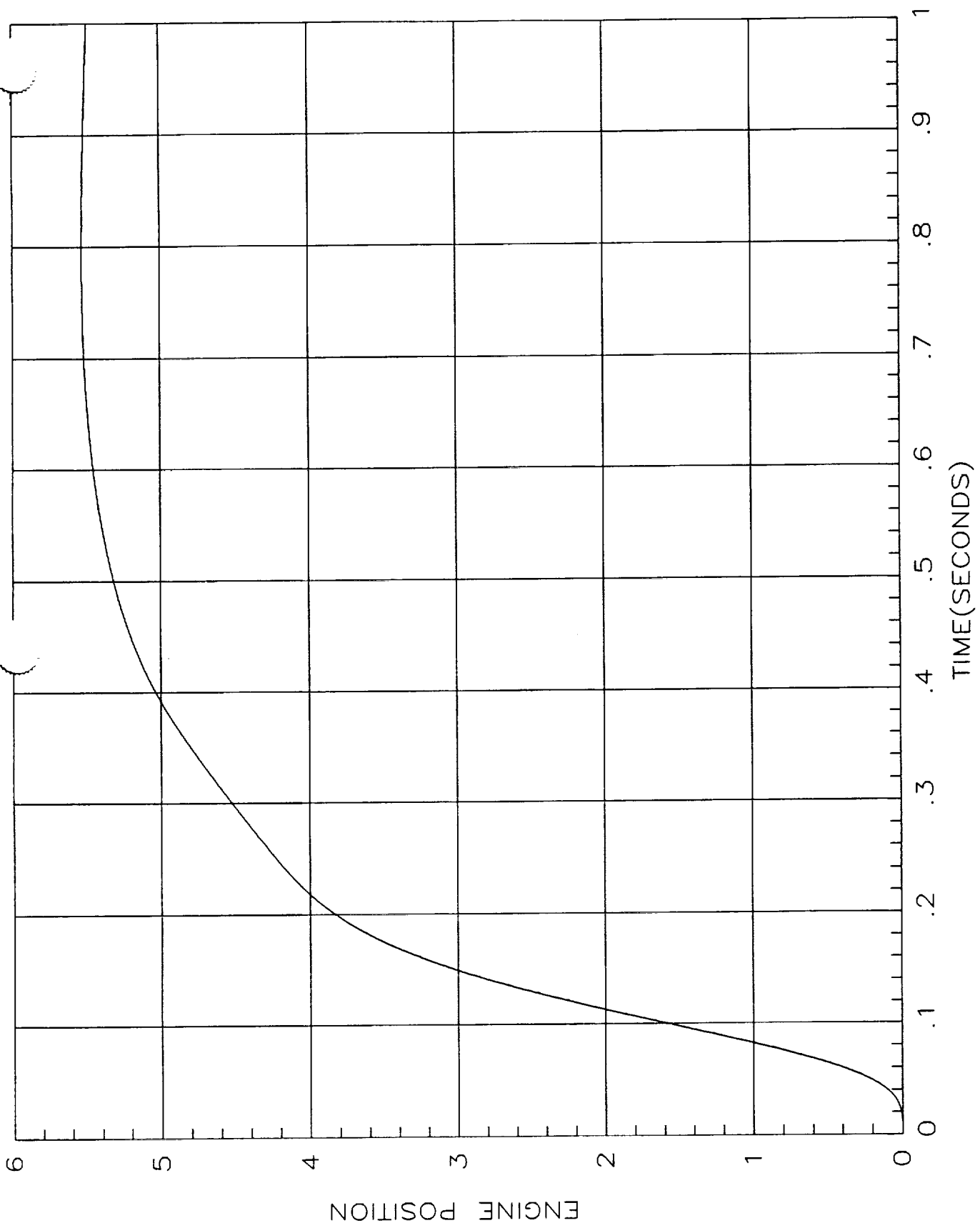
STEP CHANGE IN INPUT COMMAND AT 4% INPUT AMPLITUDE

TIME(SECONDS)
RESPONSE TO 1 INCH STEP COMMAND

ENGINE POSITION



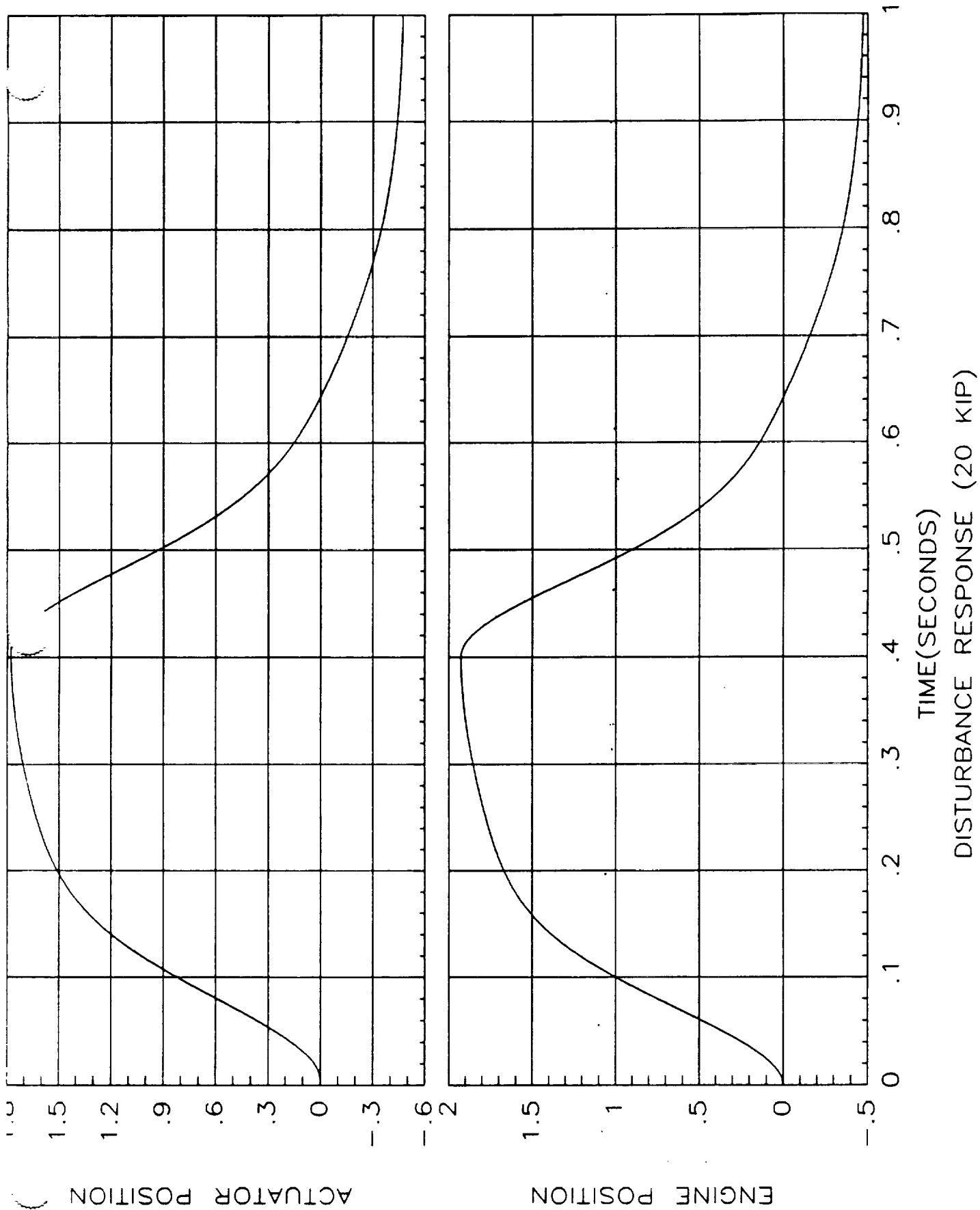
TIME(SECONDS)
RESPONSE TO 1 INCH STEP COMMAND

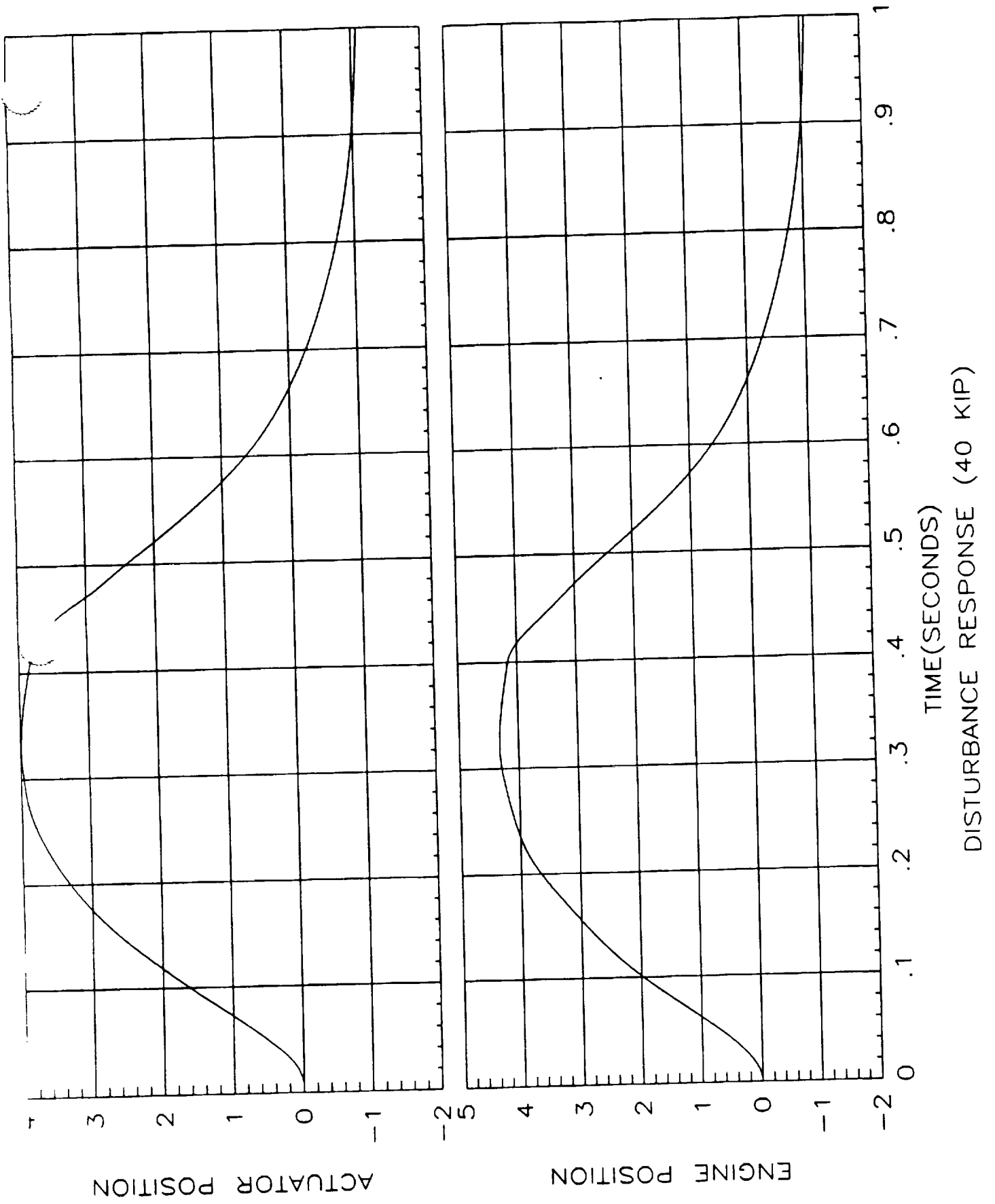


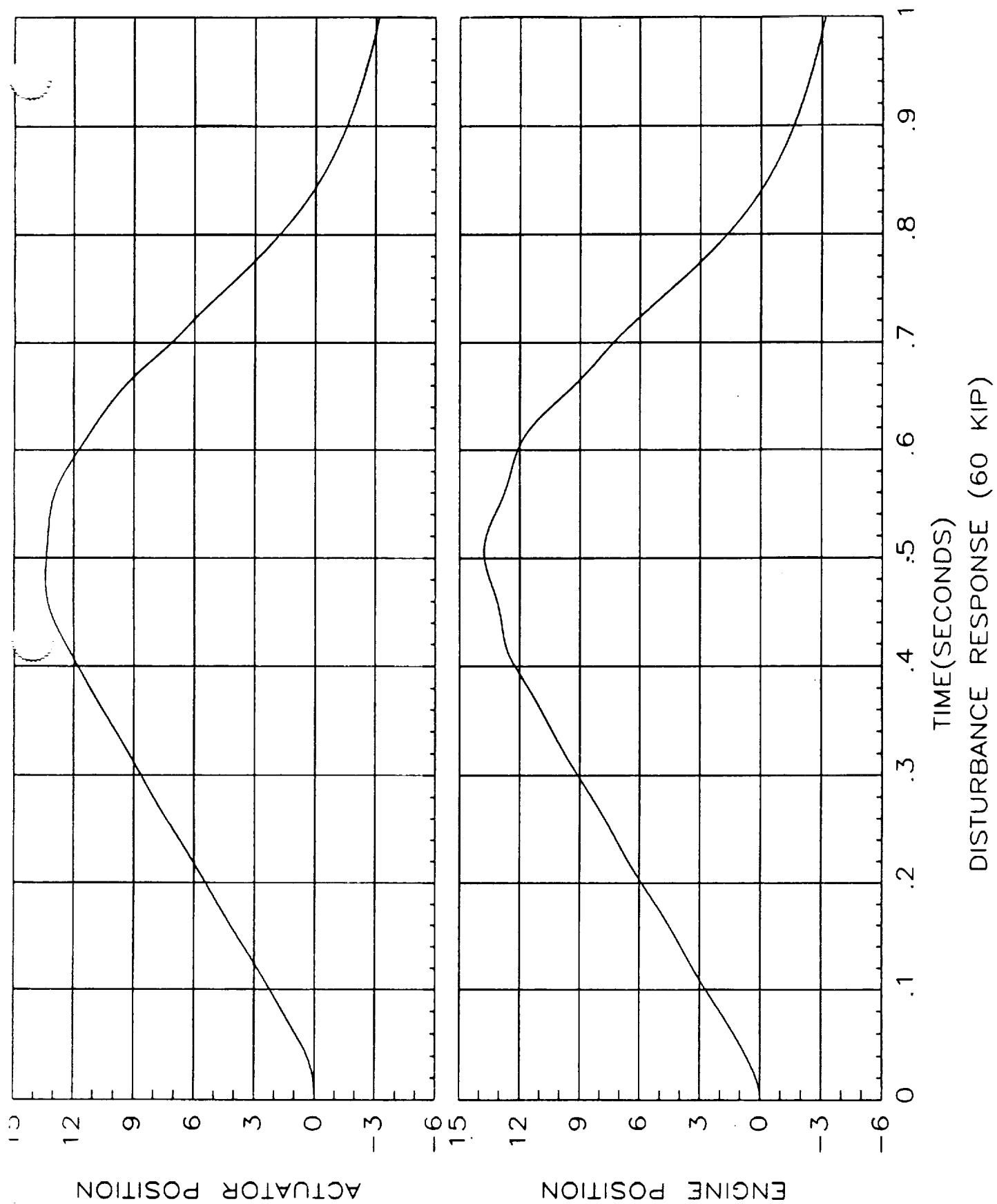
RESPONSE TO 5 INCH STEP COMMAND

The Figure on Page 4-98 shows the simulation model used to analyze the system response to disturbance inputs applied at the engine. A 0.4 second duration pulse train with a large period and various amplitudes (20,000 lbs, 40,000 lbs, and 60,000 lbs) was applied to the system. This disturbance function was suggested as a rocket engine start/stop disturbance force model by MSFC. The Figure on Page 4-99 shows the engine response to a 20,000 lb disturbance input. This type of response is probably acceptable, however, the Figures on Pages 4-100 and 4-101 show engine deflections exceeding 4-14 inches which is completely unacceptable. The following section presents a proposed solution to this disturbance problem.









**CONTROLLER RECONFIGURATION TO
MINIMIZE EFFECTS OF START/STOP
TRANSIENT DISTURBANCE FORCES**

G. CONTROLLER RECONFIGURATION TO MINIMIZE EFFECTS OF START/STOP TRANSIENT DISTURBANCE FORCES

In a previous section it was shown that the controller designed to handle the normal actuator function when the rocket engine is running is not capable of handling safely the anticipated large start/stop transient forces. The most severe force suggested by MSFC as a disturbance model was a square shouldered pulse of 60KIPS lasting for 400 milliseconds. The load displacement resulting from this force was too large when using the designed controller.

It was speculated that the delay time around the position and force loops caused by their somewhat complex dynamic nature prevented the motor from counteracting the disturbance in a timely way. With this in mind a discussion was held with the electronics designers in which they agreed that it would be relatively easy to reconfigure the power amplifier so that it would work as a current limited "short circuit". With this assurance it was decided to reconfigure the amplifier for the short transient time period of the start/stop disturbance force by disconnecting the force and position loops (in practice perhaps turning the gain in these loops way down might be the ultimate solution) and increasing the gain in the velocity or rate feed back loop. This was done and the satisfactory results are displayed below. The physical explanation of what is going on is merely that a shorted motor with separate field excitation,

such as proposed here, will resist motion when its armature circuit is shorted, i.e. it becomes a shorted generator without any time delays.

**G. CONTROLLER RECONFIGURATION TO MINIMIZE EFFECTS OF
START/STOP TRANSIENT DISTURBANCE FORCES**

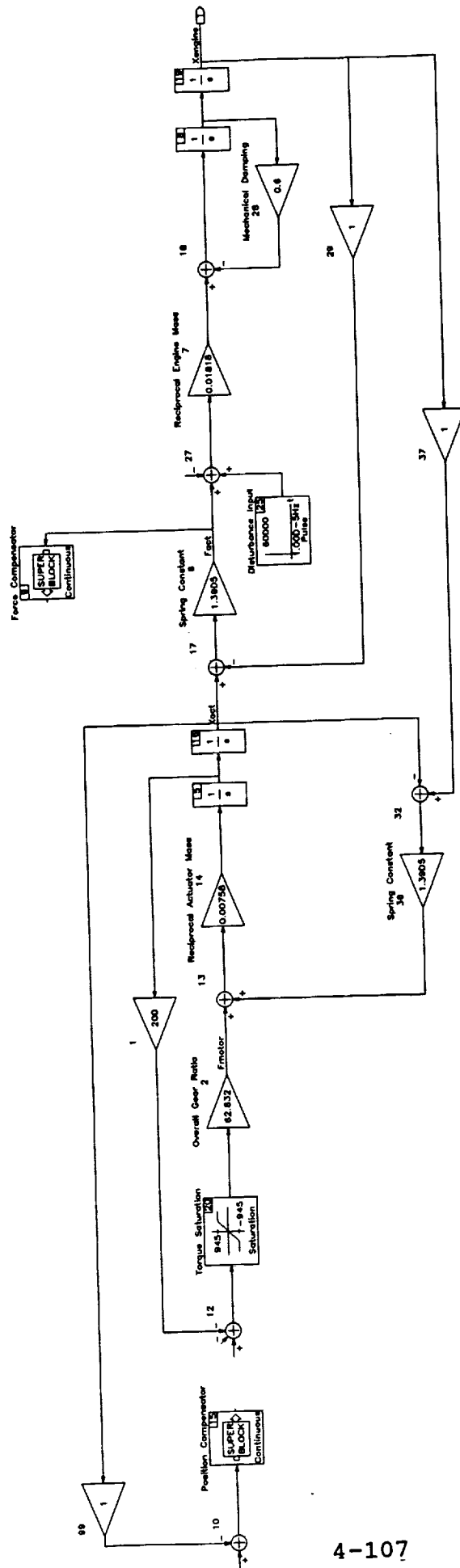
In a previous section it was shown that the controller designed to handle the normal actuator function when the rocket engine is running is not capable of handling safely the anticipated large start/stop transient forces. The most severe force suggested by MSFC as a disturbance model was a square shouldered pulse of 60KIPS lasting for 400 milliseconds. The load displacement resulting from this force was too large when using the designed controller.

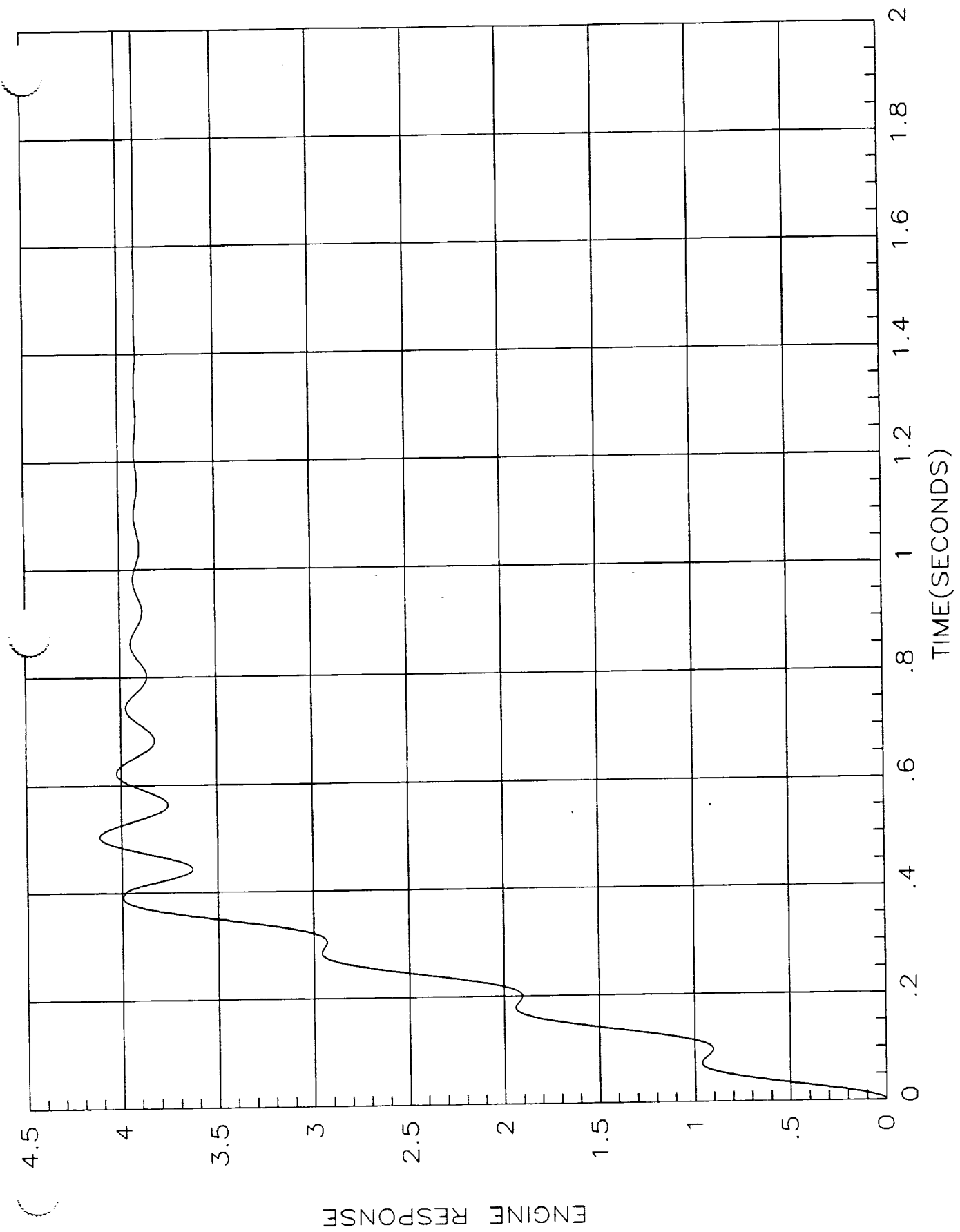
It was speculated that the delay time around the position and force loops caused by their somewhat complex dynamic nature prevented the motor from counteracting the disturbance in a timely way. With this in mind a discussion was held with the electronics designers in which they agreed that it would be relatively easy to reconfigure the power amplifier so that it would work as a current limited "short circuit". With this assurance it was decided to reconfigure the amplifier for the short transient time period of the start/stop disturbance force by disconnecting the force and position loops (in practice perhaps turning the gain in these loops way down might be the ultimate solution) and increasing the gain in the velocity or rate feed back loop. This was done and the satisfactory results are displayed below. The physical explanation of what is going on is merely that a shorted motor with separate field excitation,

such as proposed here, will resist motion when its armature circuit is shorted, i.e. it becomes a shorted generator without any time delays.

Continuous Super-Block
Start Stop Disturbance Model

Ext.In (0
t.Out 1





ENGINE RESPONSE TO A 60,000 LB DISTURBANCE INPUT

**UNLOADED ACTUATOR
OPERATION**

H. OPERATION WITHOUT A LOAD ATTACHED TO THE ACTUATOR

There will be times when it is desired to exercise the actuator without having an external load i.e. the load simulator or the actual engine attached to the actuator. This may be the case after initial assembly or during various verification operations. Therefore it is necessary to investigate operation of the actuator system without a load but with the position and velocity loops closed (the force loop would not have any effect under this condition) and with the loop compensation present which was designed under the assumption that the actuator was attached to a specific engine-structure combination.

During design of the various compensators one of the design guidelines followed was that no conditionally stable loops were permitted. It turns out when analyzing the no load case that the position loop is slightly conditionally stable at the low gain values (see accompanying root locus) if the velocity loop is not simultaneously closed. Of course the saturation nonlinearity is also present. The analytical investigation of this situation would involve the use of describing functions. This course has not been followed as of yet. Rather the simulation with both loops closed was exercised under strenuous conditions i.e. with increasingly large commands. As shown in the accompanying simulation results the system exhibited no tendency to oscillate or

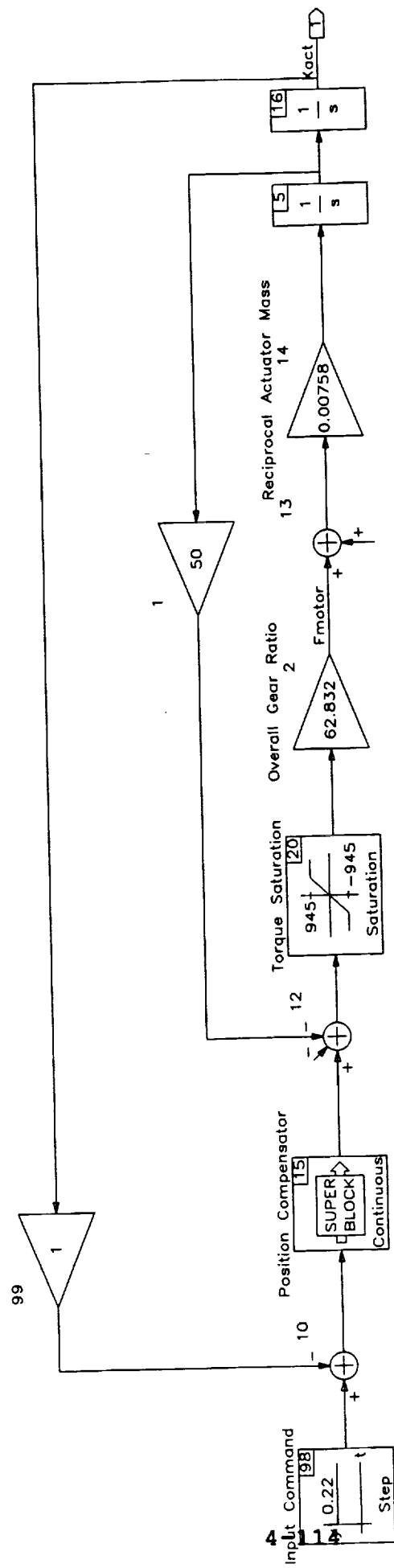
lose control even when driven by absurdly large commands. Thus it seems that at this stage of analysis and investigation there is no suggestion of a problem during no load operation as long as both the position and velocity loops are both closed during no load operation. One should also note how the form of the response to a step command changes from what it is when operating into the design load.

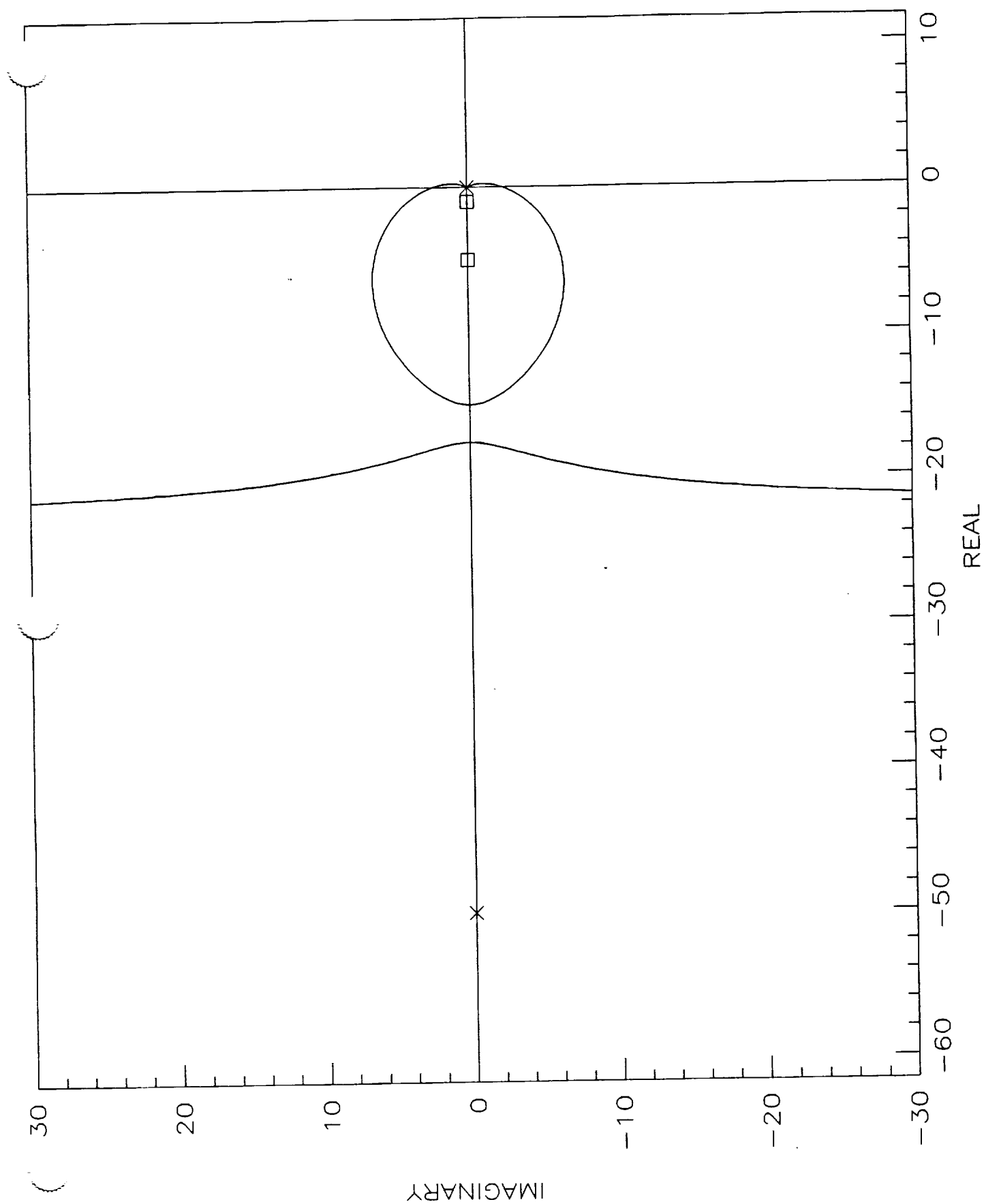
H. OPERATION WITHOUT A LOAD ATTACHED TO THE ACTUATOR

There will be times when it is desired to exercise the actuator without having an external load i.e. the load simulator or the actual engine attached to the actuator. This may be the case after initial assembly or during various verification operations. Therefore it is necessary to investigate operation of the actuator system without a load but with the position and velocity loops closed (the force loop would not have any effect under this condition) and with the loop compensation present which was designed under the assumption that the actuator was attached to a specific engine-structure combination.

During design of the various compensators one of the design guidelines followed was that no conditionally stable loops were permitted. It turns out when analyzing the no load case that the position loop is slightly conditionally stable at the low gain values (see accompanying root locus) if the velocity loop is not simultaneously closed. Of course the saturation nonlinearity is also present. The analytical investigation of this situation would involve the use of describing functions. This course has not been followed as of yet. Rather the simulation with both loops closed was exercised under strenuous conditions i.e. with increasingly large commands. As shown in the accompanying simulation results the system exhibited no tendency to oscillate or

lose control even when driven by absurdly large commands. Thus it seems that at this stage of analysis and investigation there is no suggestion of a problem during no load operation as long as both the position and velocity loops are both closed during no load operation. One should also note how the form of the response to a step command changes from what it is when operating into the design load.

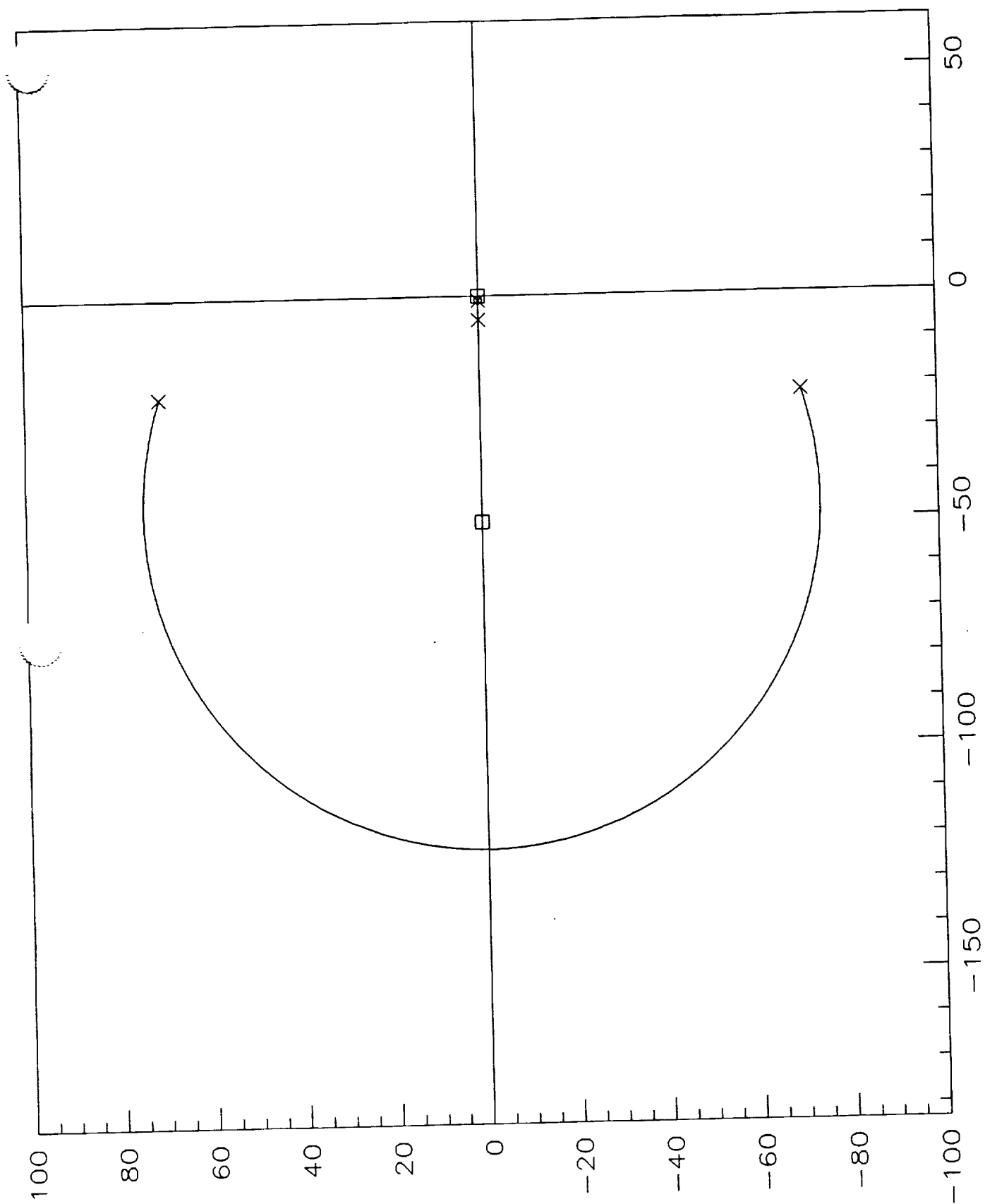
Ext.Out
1

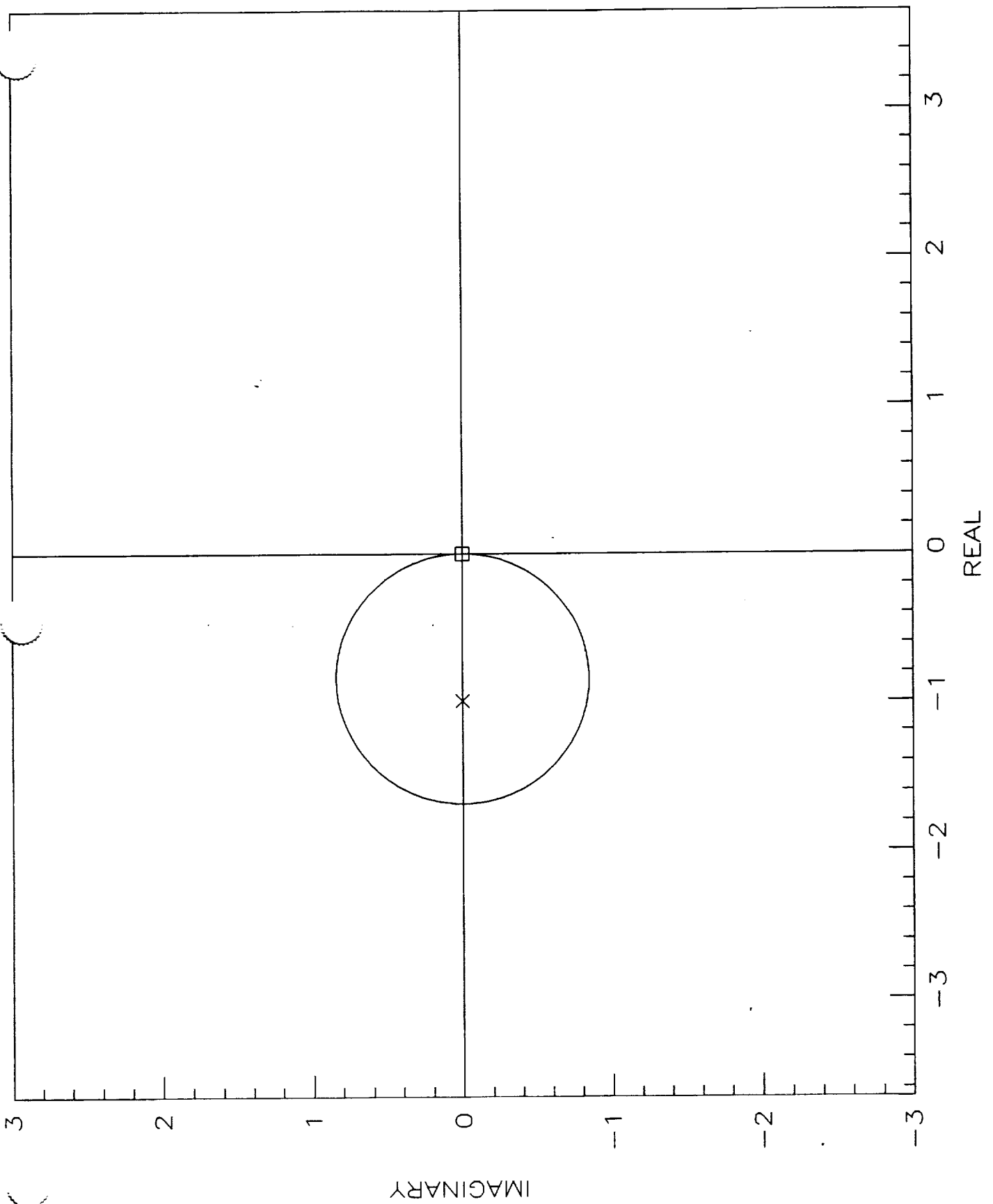


IMAGINARY

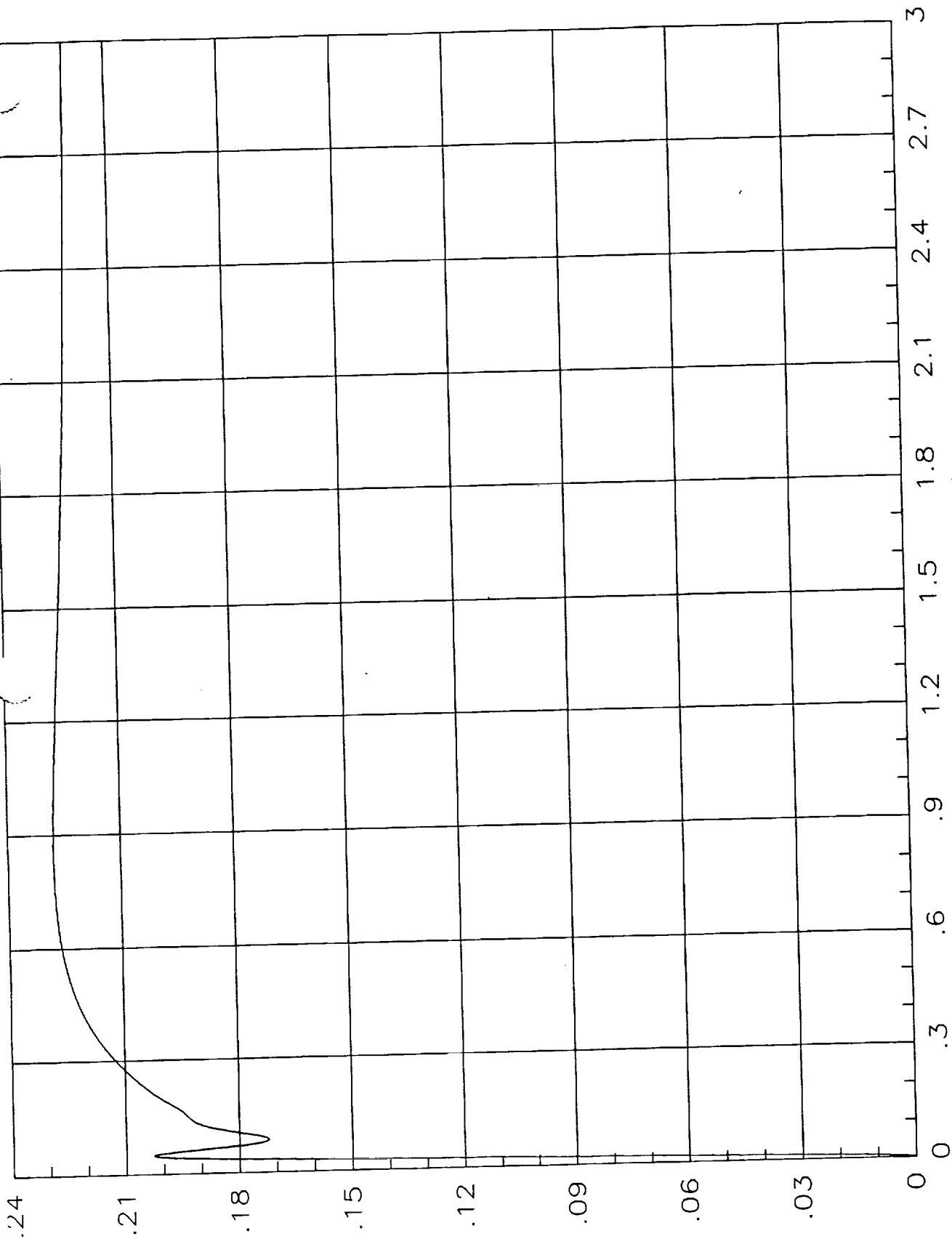
4-116

REAL



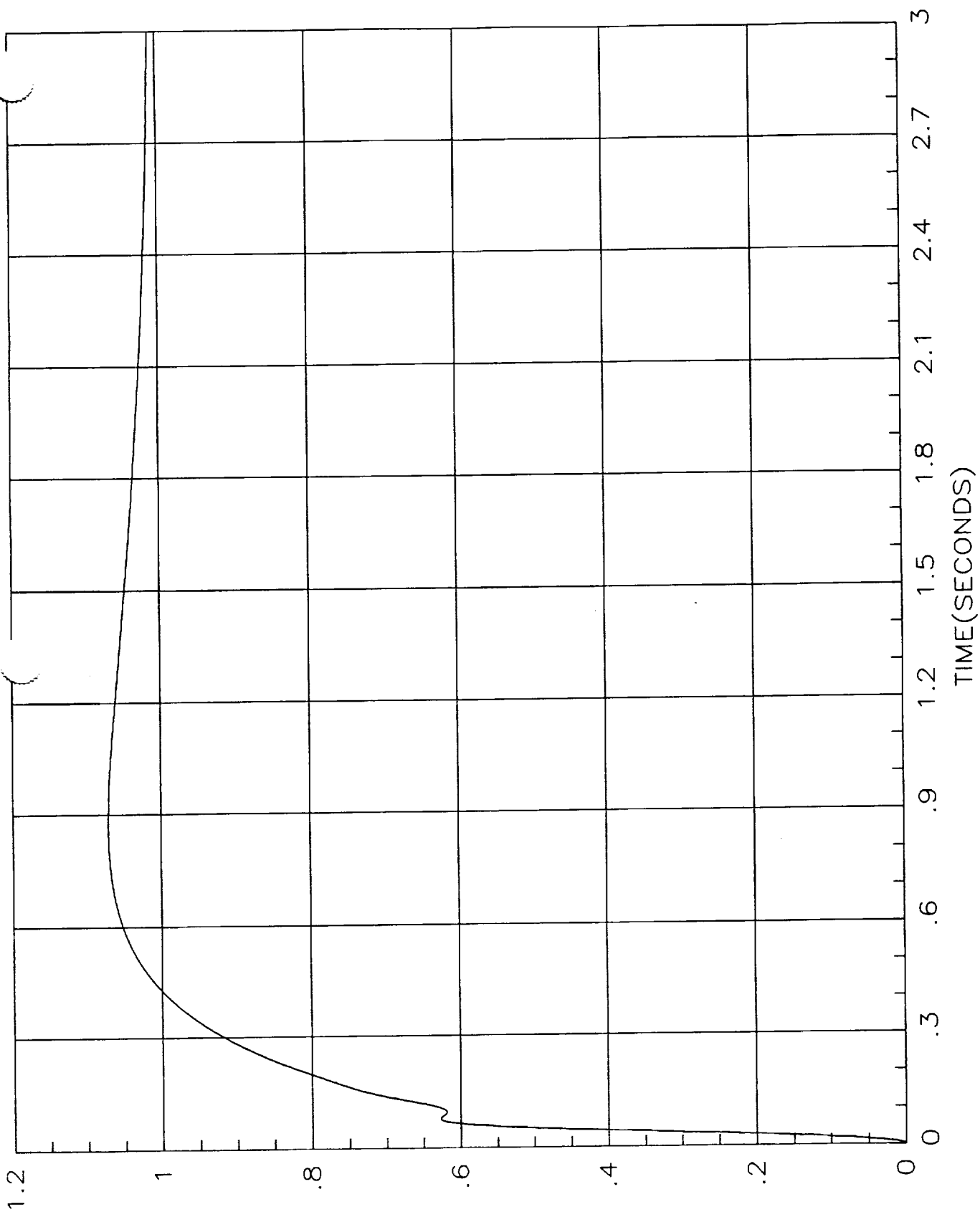


ACTUATOR POSITION

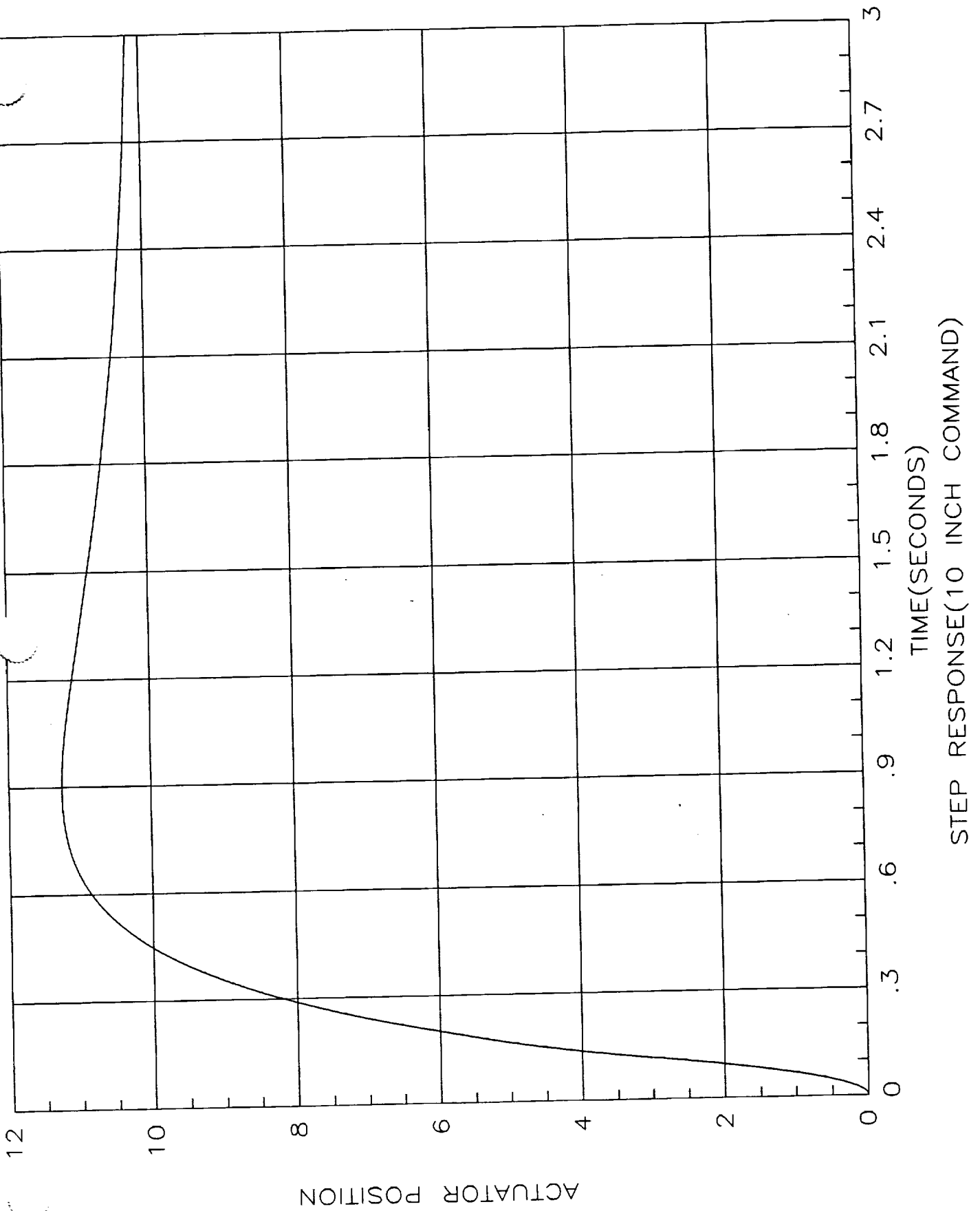


STEP CHANGE IN INPUT COMMAND AT 4% INPUT AMPLITUDE

ACTUATOR POSITION



STEP RESPONSE(1 INCH COMMAND)



**EFFECTS OF
MECHANICAL STOPS**

I. THE EFFECTS OF MECHANICAL STOPS

Although it is anticipated that software limits or the input circuitry of the servo electronics will be configured so that no commands will be given or received which would command the actuator to attempt to extend into the mechanical limits or stops there is always the possibility that such might happen. Therefore a preliminary investigation was performed to determine what the effects might be. A simple model was used. It consisted of an elastic stop or spring which was contacted by the actuator as it neared end of stroke. Of course more elaborate models could be constructed by the use of function generators which could have a nonlinear functional relationship between the force and the near end of stroke displacement of the actuator. It did not seem worthwhile to attempt this sort of more complicated modeling at this stage of design (i.e. before the mechanical configuration is proposed or known) because of the myriad of possible stop designs.

The results of this simple model and its implementation are given in the following figures. The first figure shows the block diagram of the MATRIXx model used. One notes the elastic stop model super block fed back around from the actuator position to the force summer on the actuator mass. The super block contents are shown before each of the three cases investigated. The difference between the cases is the

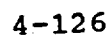
spring constant modeled into the stop. The first results exhibited correspond to a spring constant of 1.4×10^6 pounds per inch. The time domain plot and the succeeding three phase plane plots (for 1, 3 and 10 seconds of time) show the response to a 5 inch command. Clearly the response is unstable and in the case of the 10 second plot reaches absurd values. Clearly this is unacceptable behavior.

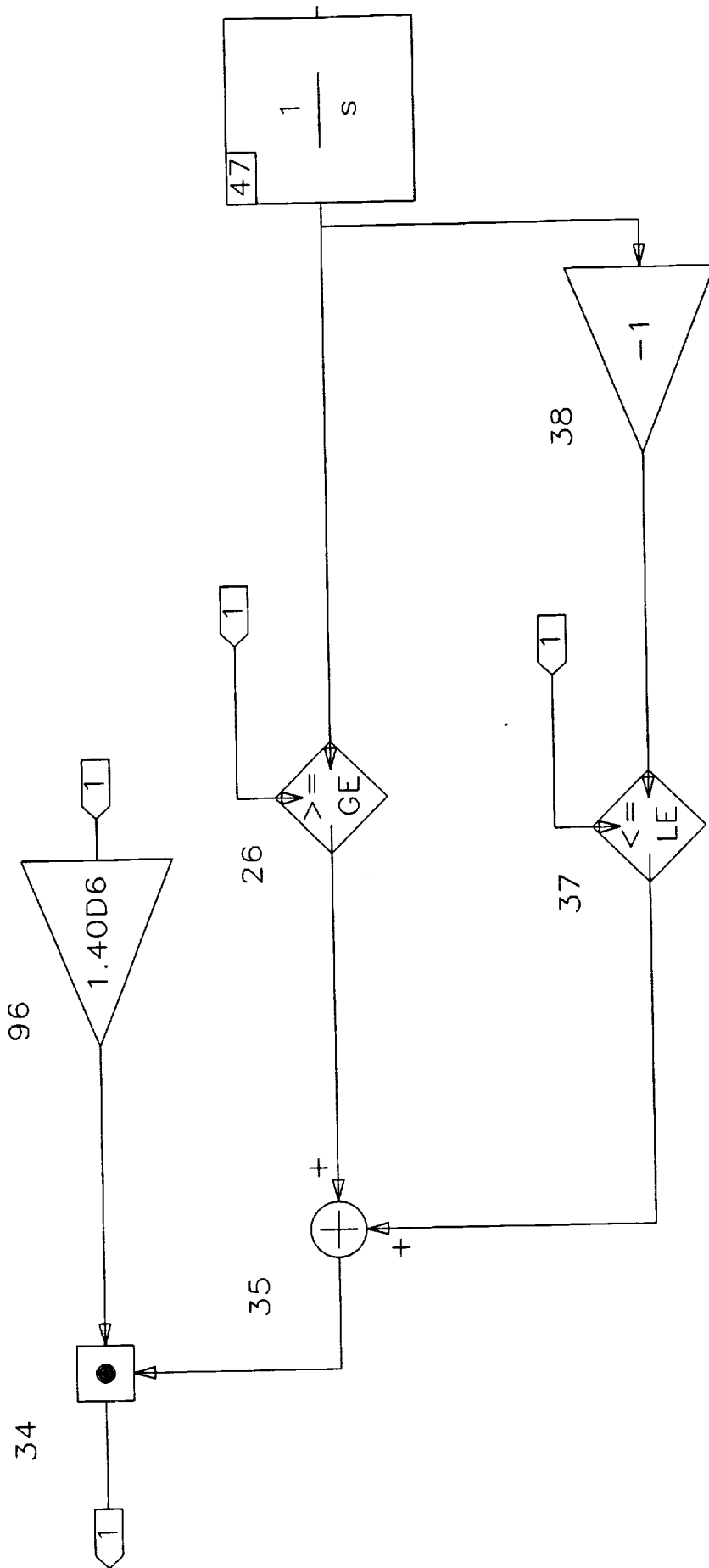
I. THE EFFECTS OF MECHANICAL STOPS

Although it is anticipated that software limits or the input circuitry of the servo electronics will be configured so that no commands will be given or received which would command the actuator to attempt to extend into the mechanical limits or stops there is always the possibility that such might happen. Therefore a preliminary investigation was performed to determine what the effects might be. A simple model was used. It consisted of an elastic stop or spring which was contacted by the actuator as it neared end of stroke. Of course more elaborate models could be constructed by the use of function generators which could have a nonlinear functional relationship between the force and the near end of stroke displacement of the actuator. It did not seem worthwhile to attempt this sort of more complicated modeling at this stage of design (i.e. before the mechanical configuration is proposed or known) because of the myriad of possible stop designs.

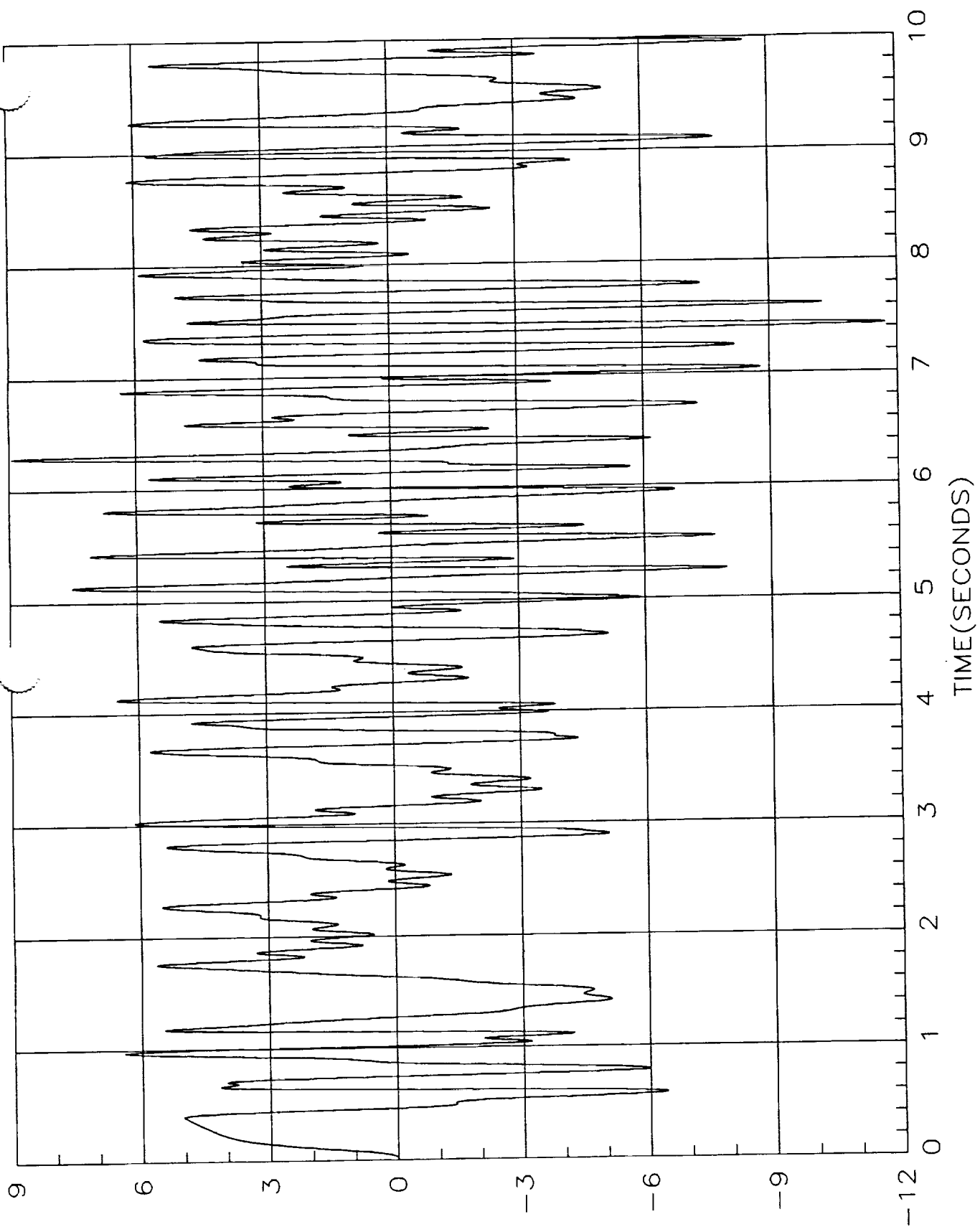
The results of this simple model and its implementation are given in the following figures. The first figure shows the block diagram of the MATRIXx model used. One notes the elastic stop model super block fed back around from the actuator position to the force summer on the actuator mass. The super block contents are shown before each of the three cases investigated. The difference between the cases is the

spring constant modeled into the stop. The first results exhibited correspond to a spring constant of 1.4 times 10^6 pounds per inch. The time domain plot and the succeeding three phase plane plots (for 1, 3 and 10 seconds of time) show the response to a 5 inch command. Clearly the response is unstable and in the case of the 10 second plot reaches absurd values. Clearly this is unacceptable behavior.

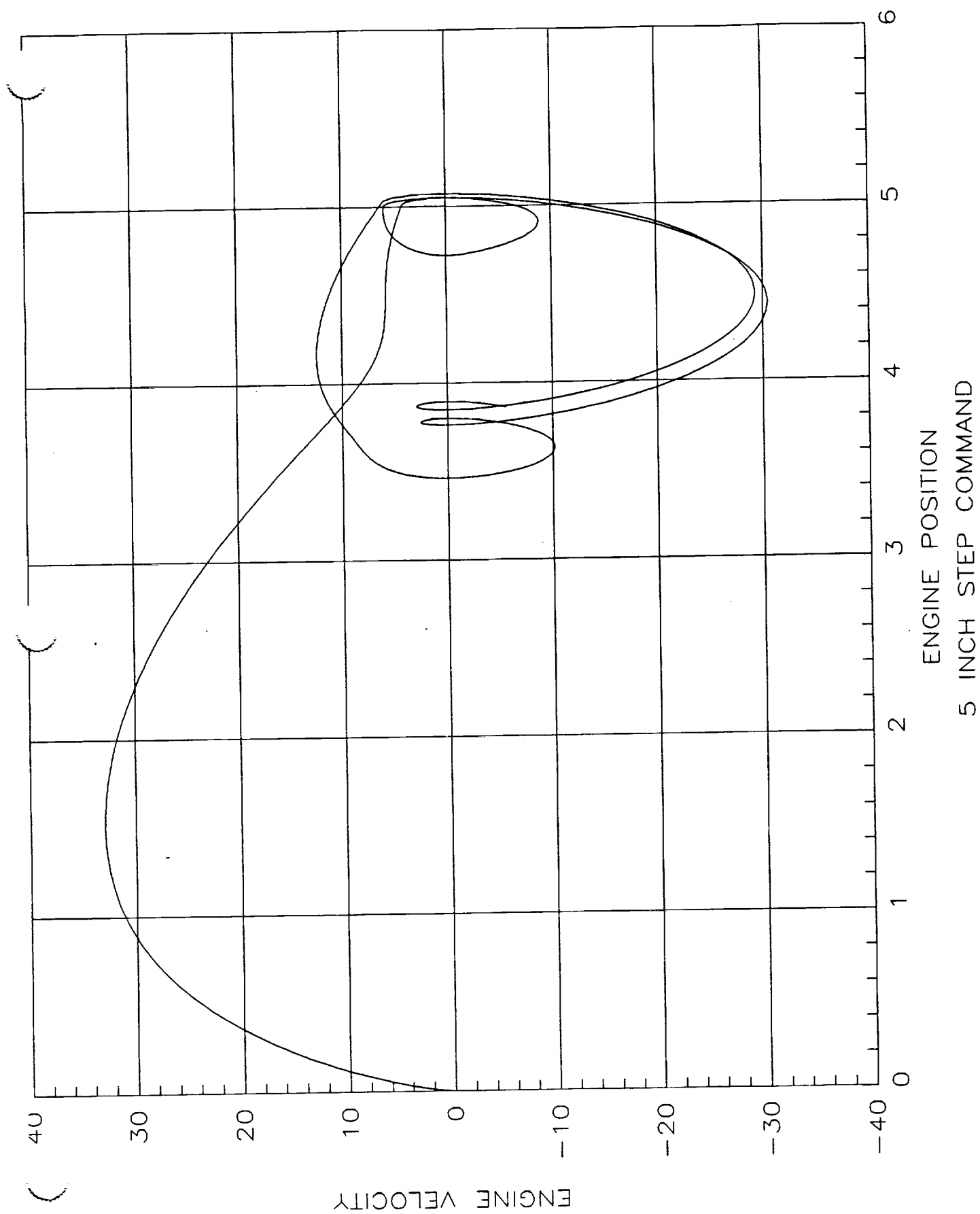


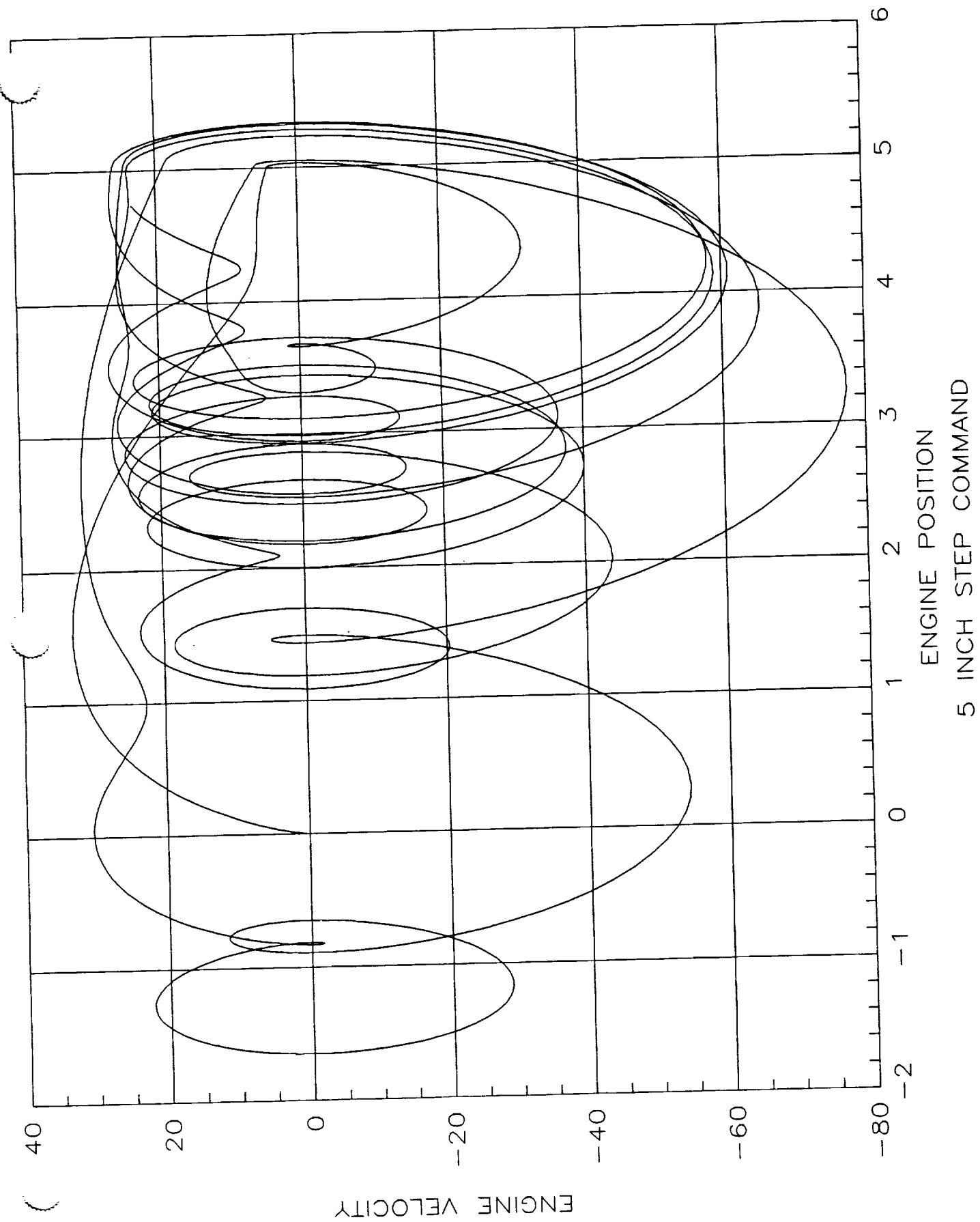


ENGINE POSITION



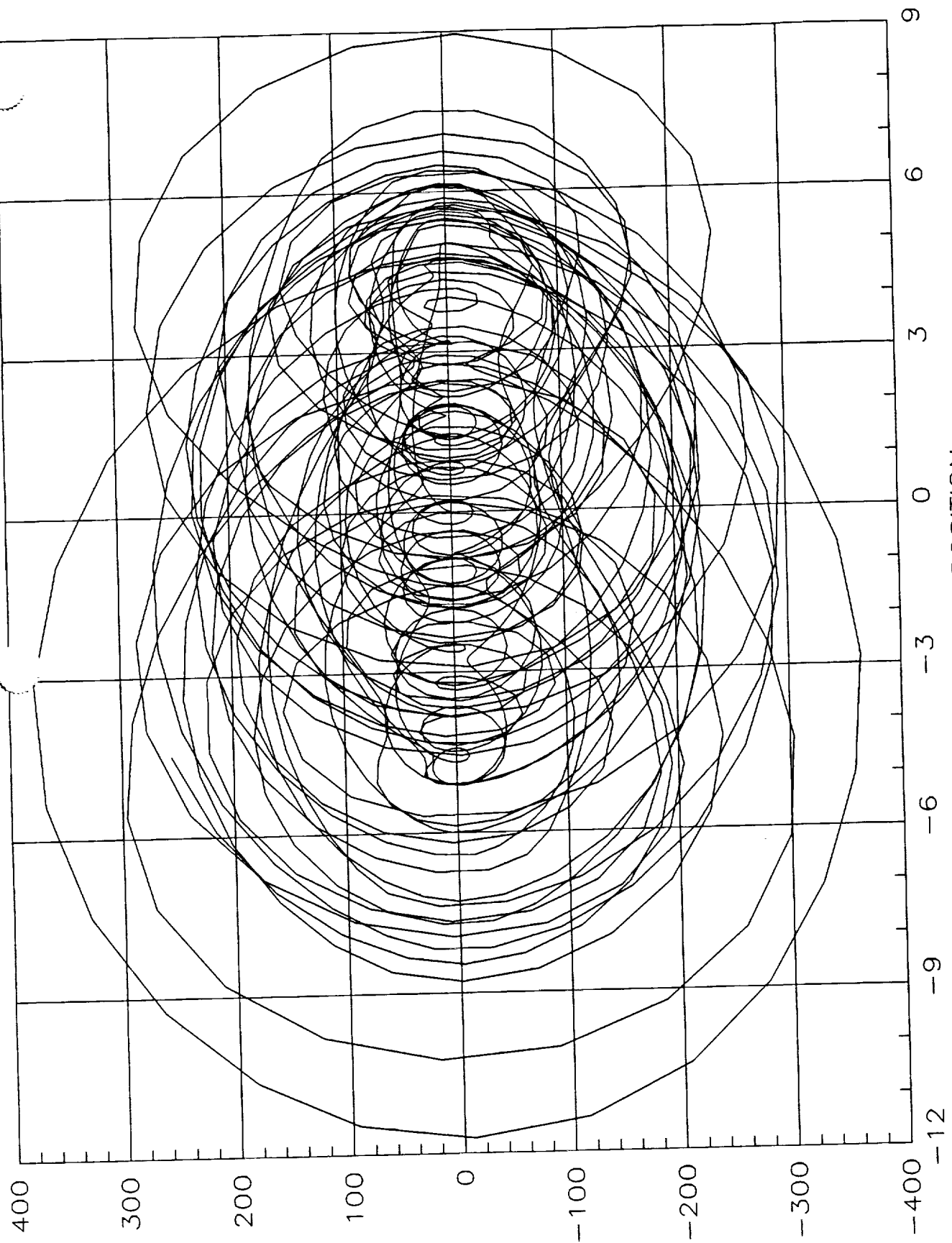
5 INCH STEP COMMAND





ENGINE VELOCITY

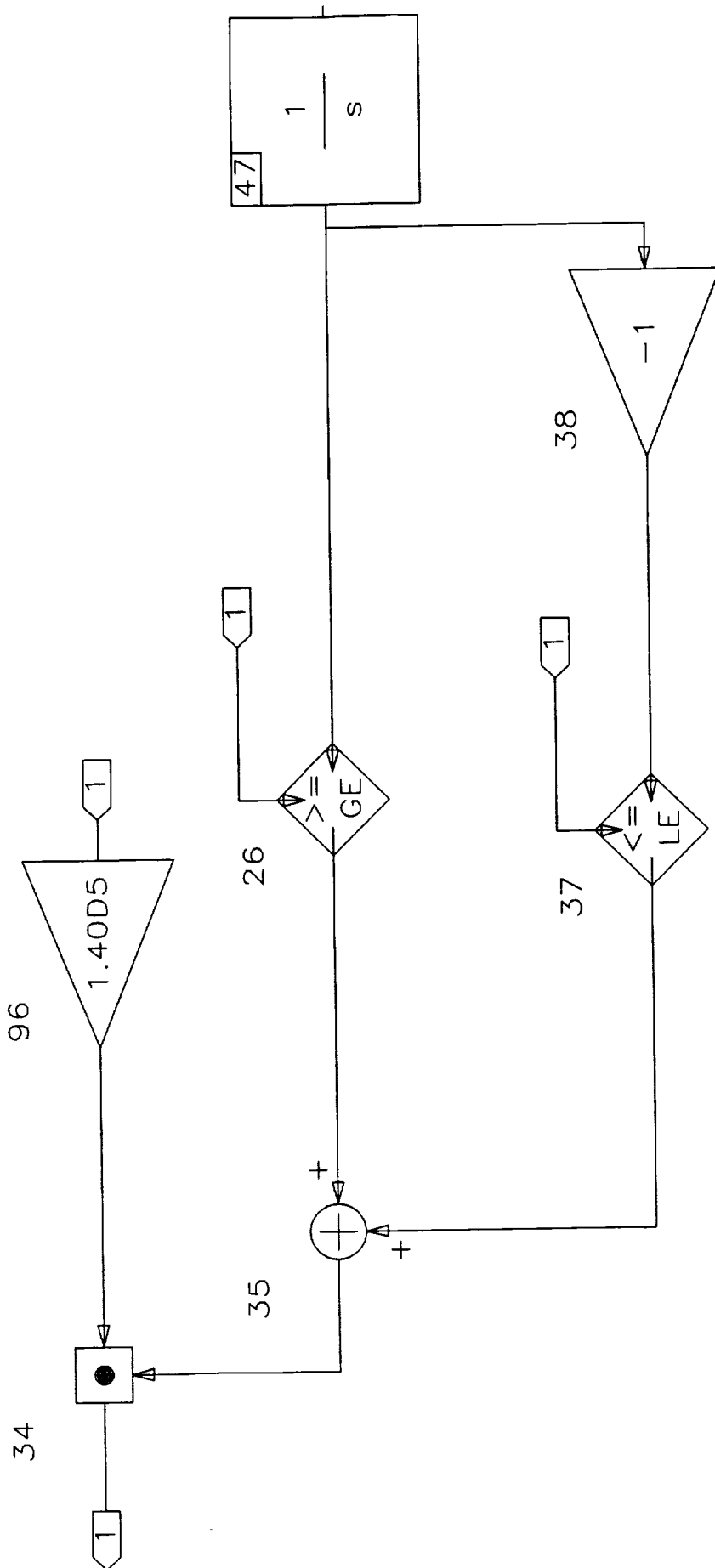
4-131

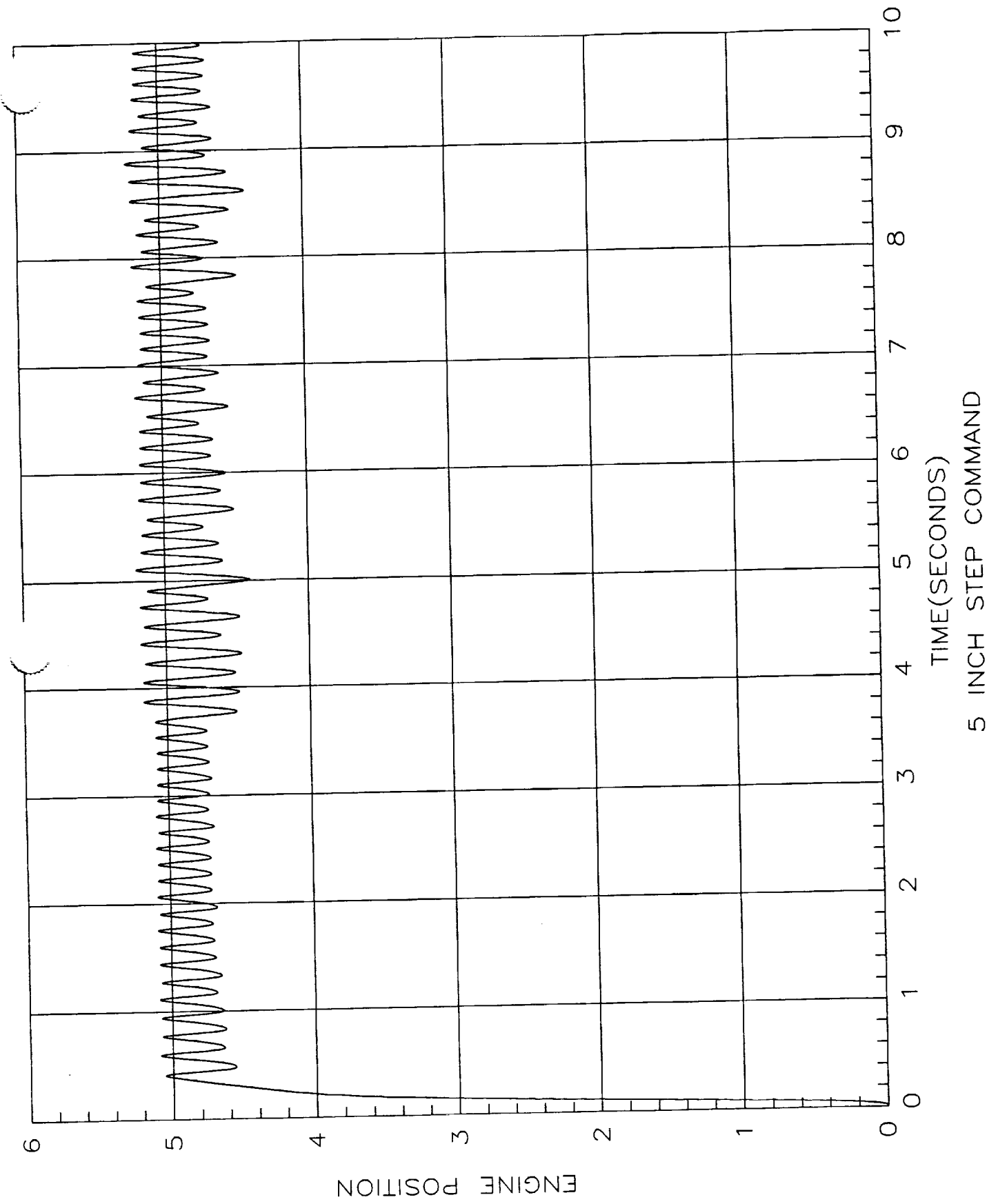


ENGINE POSITION
5 INCH STEP COMMAND

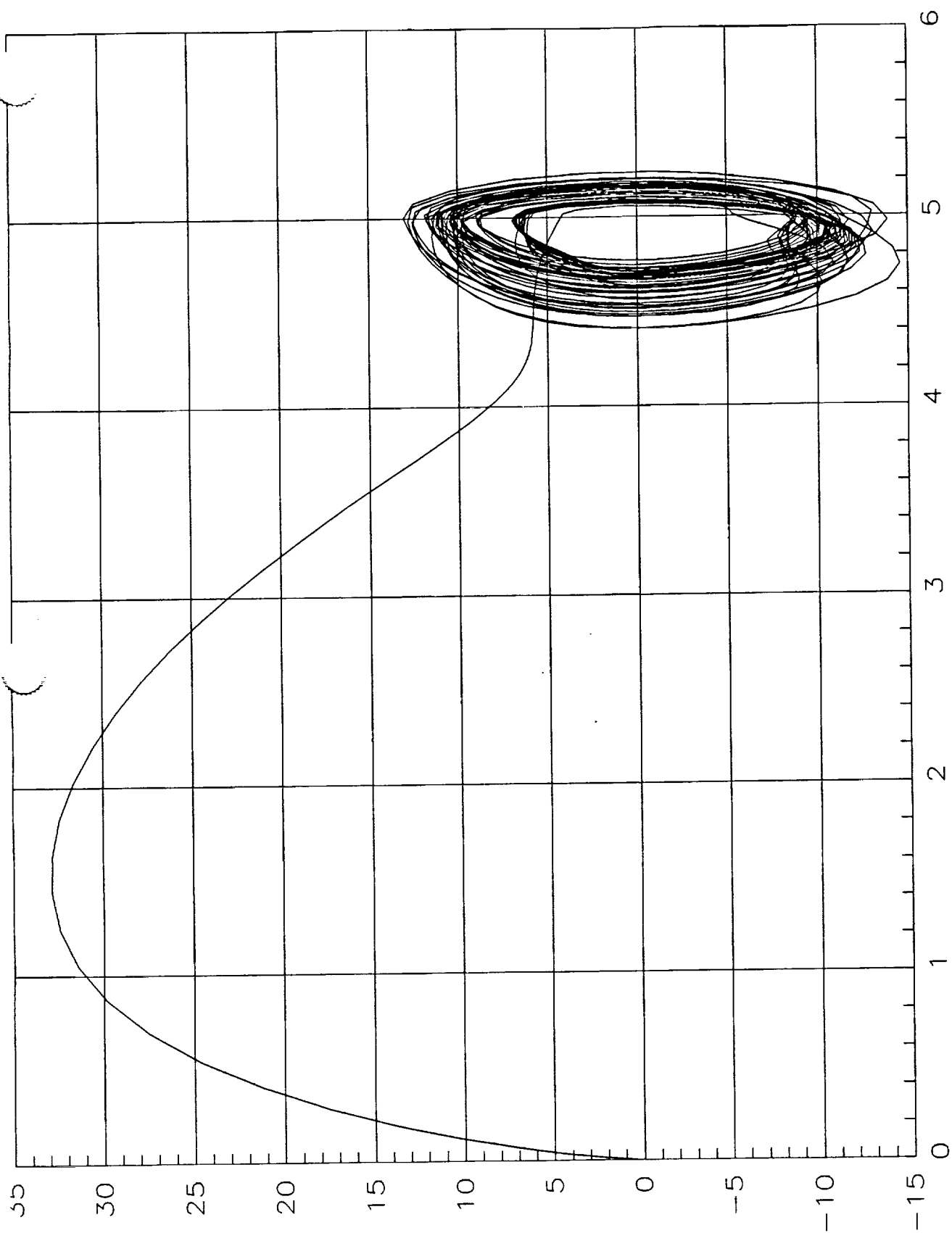
This next group of plots were constructed with a spring constant an order of magnitude less than in the first case run (1.4×10^5 pounds per inch). Once again the super block is shown in the first figure. The time domain response to plot to a 5 inch command shows a slower approach to instability build up as does the last figure, a phase plane plot with the amplitude of the oval in the phase plane growing with time. Clearly this is unacceptable but the trend has been established that softer stops than originally modeled are tending toward a stable condition.

This next group of plots were constructed with a spring constant an order of magnitude less than in the first case run (1.4×10^5 pounds per inch). Once again the super block is shown in the first figure. The time domain response to plot to a 5 inch command shows a slower approach to instability build up as does the last figure, a phase plane plot with the amplitude of the oval in the phase plane growing with time. Clearly this is unacceptable but the trend has been established that softer stops than originally modeled are tending toward a stable condition.



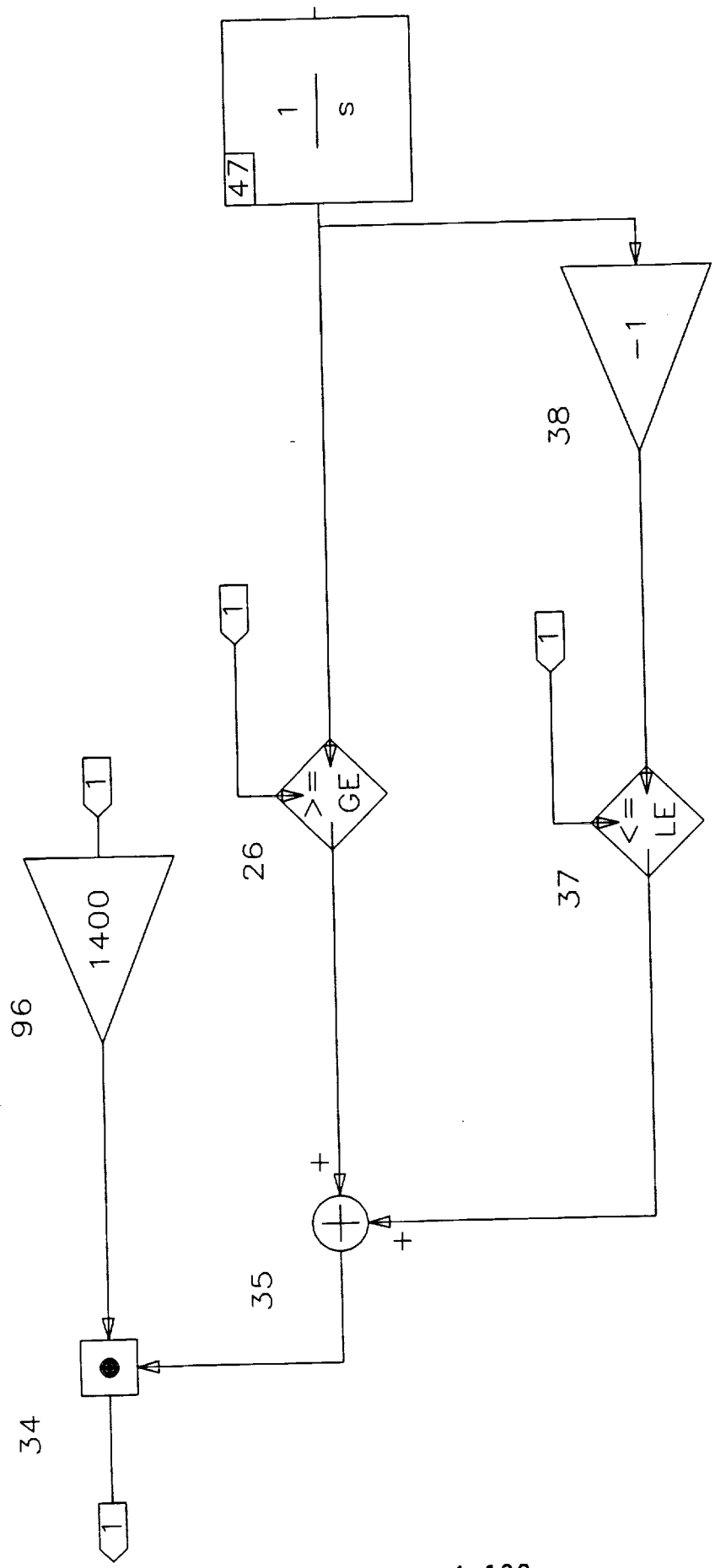


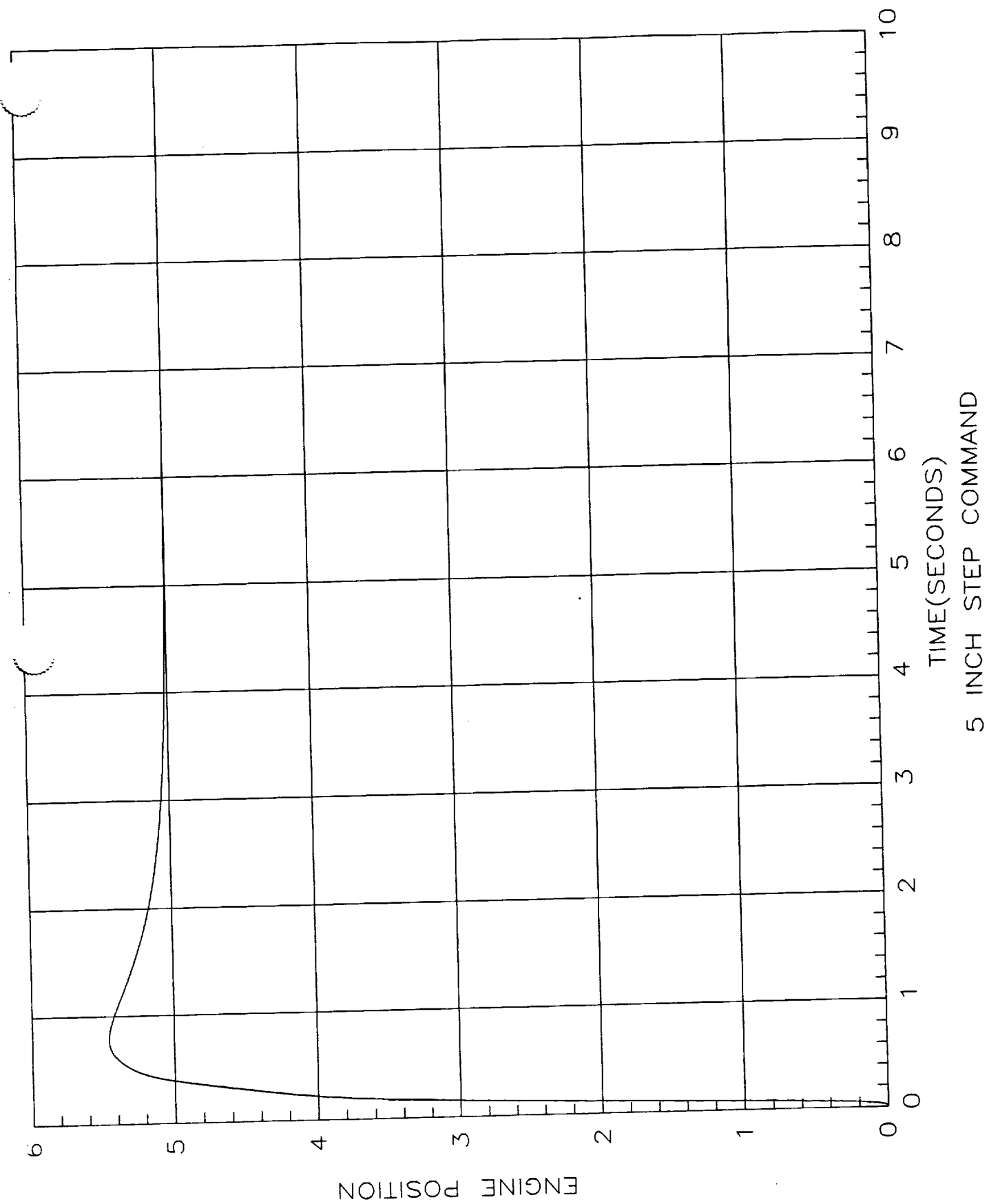
ENGINE VELOCITY



ENGINE POSITION
5 INCH STEP COMMAND

The last group of plots once again show the super block configuration for a spring constant an order of magnitude smaller than the second case i.e. 1400 pounds per inch. The time domain and the phase plane plot show clearly that this case leads to a stable situation. Thus the value of the spring constant leading to a stable condition for this model lies somewhere between the values use in the latter two models.





ENGINE VELOCITY

35
30
25
20
15
10
5
0
-5

6

5

4

3

2

1

ENGINE POSITION

5 INCH STEP COMMAND

Initial conclusions from this investigation are that a soft stop should probably be built into the actuator to thwart any tendency to oscillate when or if the actuator is commanded into the stop. Of course more elaborate models of the stop might lead to different stiffness values than those found here but this would have to be ascertained when more is known about the proposed or actual design. How the appropriate spring would be mechanized is a matter for the mechanical designer (coil or cantilever springs come to mind but it is unknown at this juncture what would be practical).

Initial conclusions from this investigation are that a soft stop should probably be built into the actuator to thwart any tendency to oscillate when or if the actuator is commanded into the stop. Of course more elaborate models of the stop might lead to different stiffness values than those found here but this would have to be ascertained when more is known about the proposed or actual design. How the appropriate spring would be mechanized is a matter for the mechanical designer (coil or cantilever springs come to mind but it is unknown at this juncture what would be practical).

**FRICTION
MODELING**

I. FRICTION MODELING

It is a certainty that friction will exist in the thrust vector control (TVC) system. Indeed some amount of friction has been noticed already in the laboratory (MSFC building 4656) during experiments with the first MSFC electromagnetic actuator (EMA) in the load fixture.

Modeling friction analytically or in a simulation depends upon knowledge of the properties of the friction. These properties are usually given in the form of some relationship between friction caused force or torque and relative velocity between two mating or rubbing surfaces. A major difficulty in dealing with friction at any level of analysis or simulation is determining what the functional relationship is for the particular system under consideration. It is hoped that as time progresses laboratory experimentation will guide the EMA investigations in this regard.

During the course of this initial development it was assumed that no friction or other energy losses were present in the system. This was done for several reasons. One is that this probably poses the most stringent control problem at least from the exponential stability viewpoint (although friction will exacerbate the bandwidth attainment problem and could under certain circumstances cause instability of and by its

presence). Another was that no knowledge (certain or otherwise) of the friction characteristics to be expected was available. A third was that many of the friction models slow the execution of a simulation palpably and in the light of the uncertainty regarding the applicable friction model it was not deemed to be an efficient thing to do in this first design phase.

What was done was to investigate two models of friction hoping that when the time comes one of them would prove adequately descriptive of the "real world" friction.

The first of these is due to Mr. Philip Dahl of the Aerospace Corporation who developed his model while studying the friction associated with ball bearings (see the following references: Aerospace Corporation Report Number TOR-0158(3107-18)-1, "A Solid Friction Model", May, 1968; "Solid Friction Damping of Mechanical Vibrations, "AIAA Journal, 14, (12), 1675-1682 (December 1976); "Solid Friction Damping of Spacecraft Oscillations," Paper No. 75-1104, Paper presented at the AIAA Guidance and control Conference Boston, Mass., August 1975). The next seven figures deal with the development of the simulation model of the Dahl friction. The first three deal with the MATRIXx computer blocks developed to implement the model. The next four show the double valued function (hysteresis like) of friction versus relative velocity typical of Dahl friction

(and which was found in the ball bearing experiments which motivated his model, see page 22 of the first cited reference). The plots were generated by driving the model with a quarter Hertz sawtooth wave which simulates the relative velocity of interest. The amplitude of the friction was set to remain between approximately plus and minus 12,000 lbs and the parameters of the simulation changed to demonstrate more or less area within the hysteresis like loop. When used in a simulation the actual amplitude and area would be set according to hardware test data.

I. FRICTION MODELING

It is a certainty that friction will exist in the thrust vector control (TVC) system. Indeed some amount of friction has been noticed already in the laboratory (MSFC building 4656) during experiments with the first MSFC electromagnetic actuator (EMA) in the load fixture.

Modeling friction analytically or in a simulation depends upon knowledge of the properties of the friction. These properties are usually given in the form of some relationship between friction caused force or torque and relative velocity between two mating or rubbing surfaces. A major difficulty in dealing with friction at any level of analysis or simulation is determining what the functional relationship is for the particular system under consideration. It is hoped that as time progresses laboratory experimentation will guide the EMA investigations in this regard.

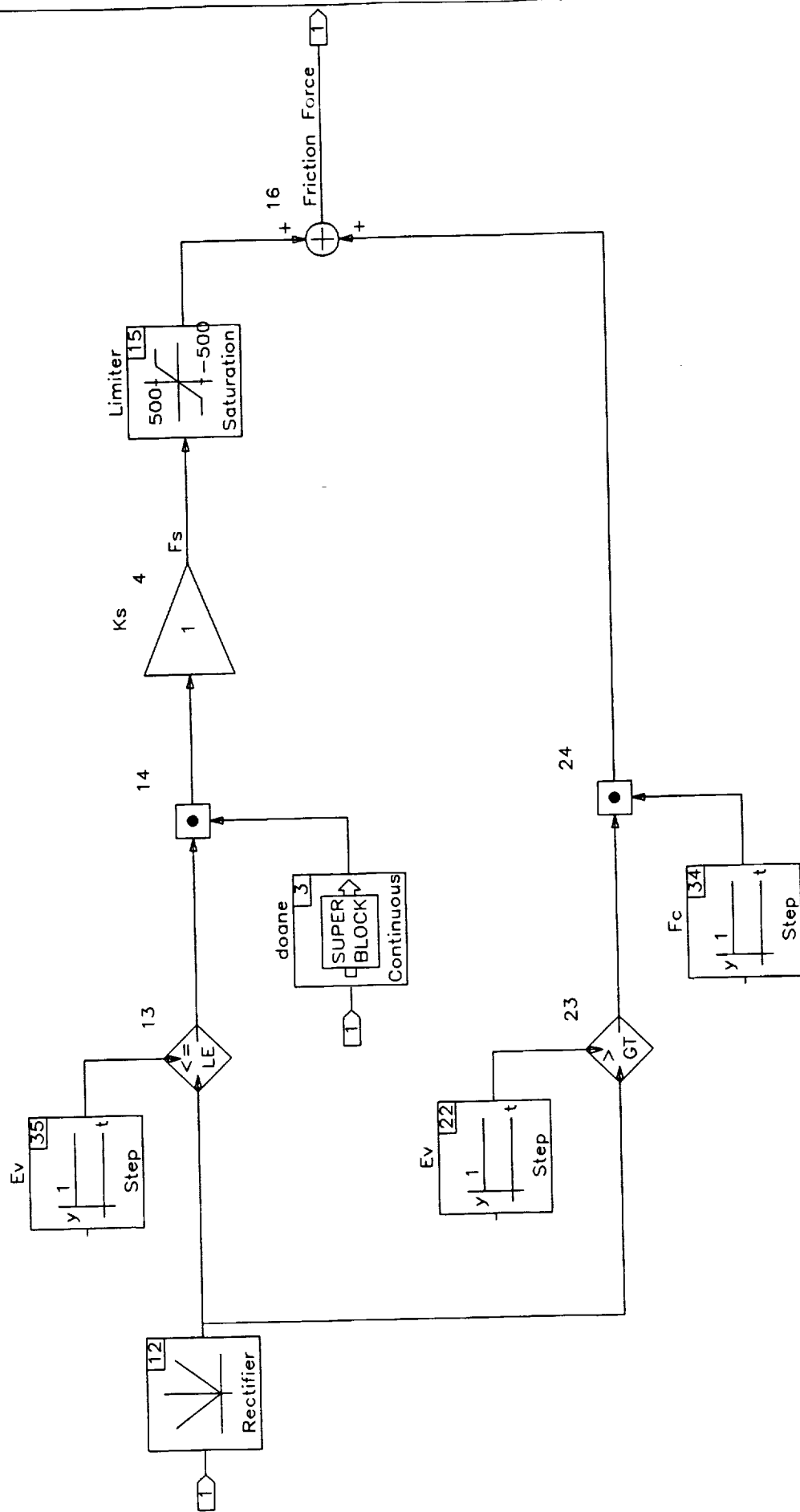
During the course of this initial development it was assumed that no friction or other energy losses were present in the system. This was done for several reasons. One is that this probably poses the most stringent control problem at least from the exponential stability viewpoint (although friction will exacerbate the bandwidth attainment problem and could under certain circumstances cause instability of and by its

presence). Another was that no knowledge (certain or otherwise) of the friction characteristics to be expected was available. A third was that many of the friction models slow the execution of a simulation palpably and in the light of the uncertainty regarding the applicable friction model it was not deemed to be an efficient thing to do in this first design phase.

What was done was to investigate two models of friction hoping that when the time comes one of them would prove adequately descriptive of the "real world" friction.

The first of these is due to Mr. Philip Dahl of the Aerospace Corporation who developed his model while studying the friction associated with ball bearings (see the following references: Aerospace Corporation Report Number TOR-0158(3107-18)-1, "A Solid Friction Model", May, 1968; "Solid Friction Damping of Mechanical Vibrations, "AIAA Journal, 14, (12), 1675-1682 (December 1976); "Solid Friction Damping of Spacecraft Oscillations," Paper No. 75-1104, Paper presented at the AIAA Guidance and control Conference Boston, Mass., August 1975). The next seven figures deal with the development of the simulation model of the Dahl friction. The first three deal with the MATRIXx computer blocks developed to implement the model. The next four show the double valued function (hysteresis like) of friction versus relative velocity typical of Dahl friction

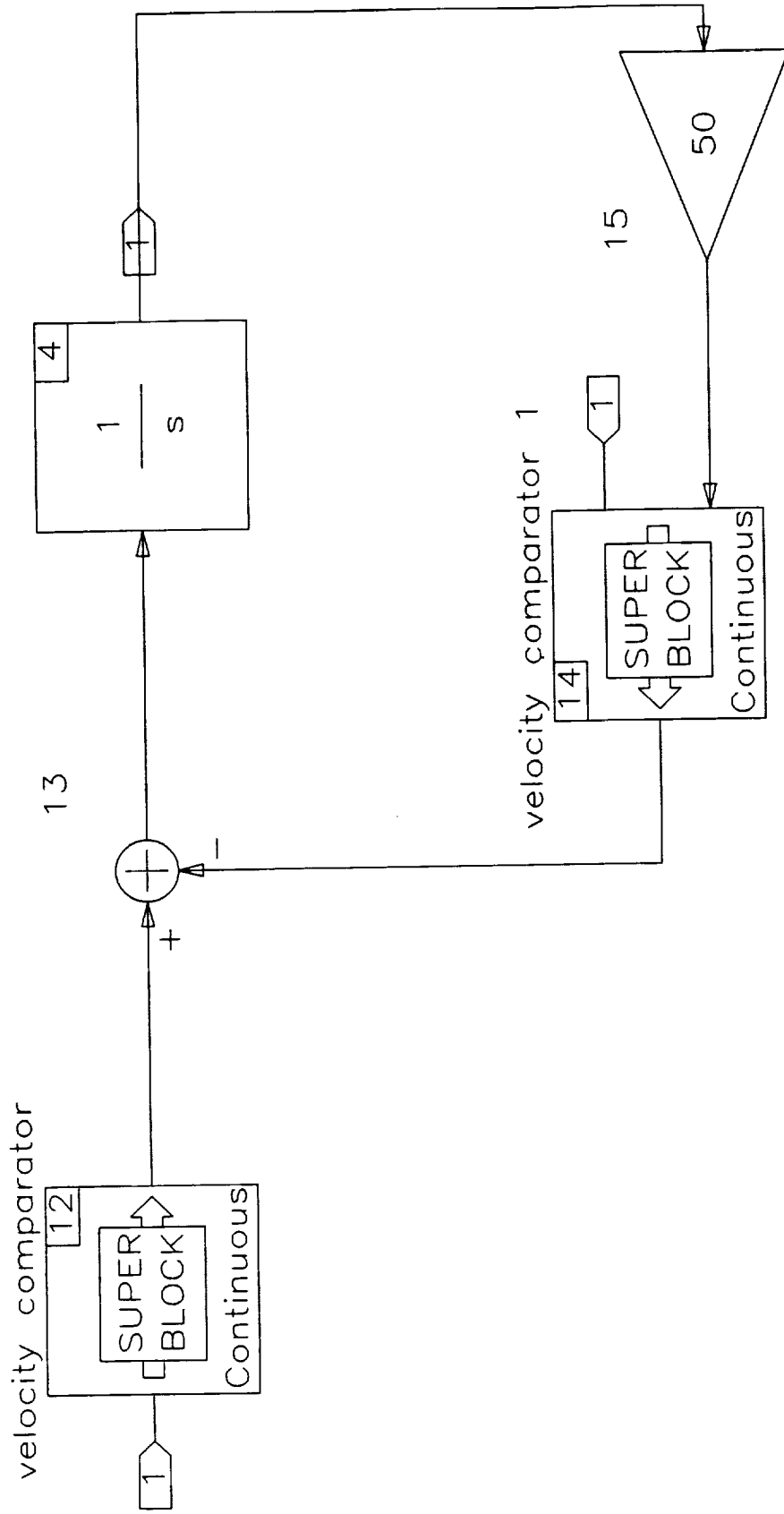
(and which was found in the ball bearing experiments which motivated his model, see page 22 of the first cited reference). The plots were generated by driving the model with a quarter Hertz sawtooth wave which simulates the relative velocity of interest. The amplitude of the friction was set to remain between approximately plus and minus 12,000 lbs and the parameters of the simulation changed to demonstrate more or less area within the hysteresis like loop. When used in a simulation the actual amplitude and area would be set according to hardware test data.

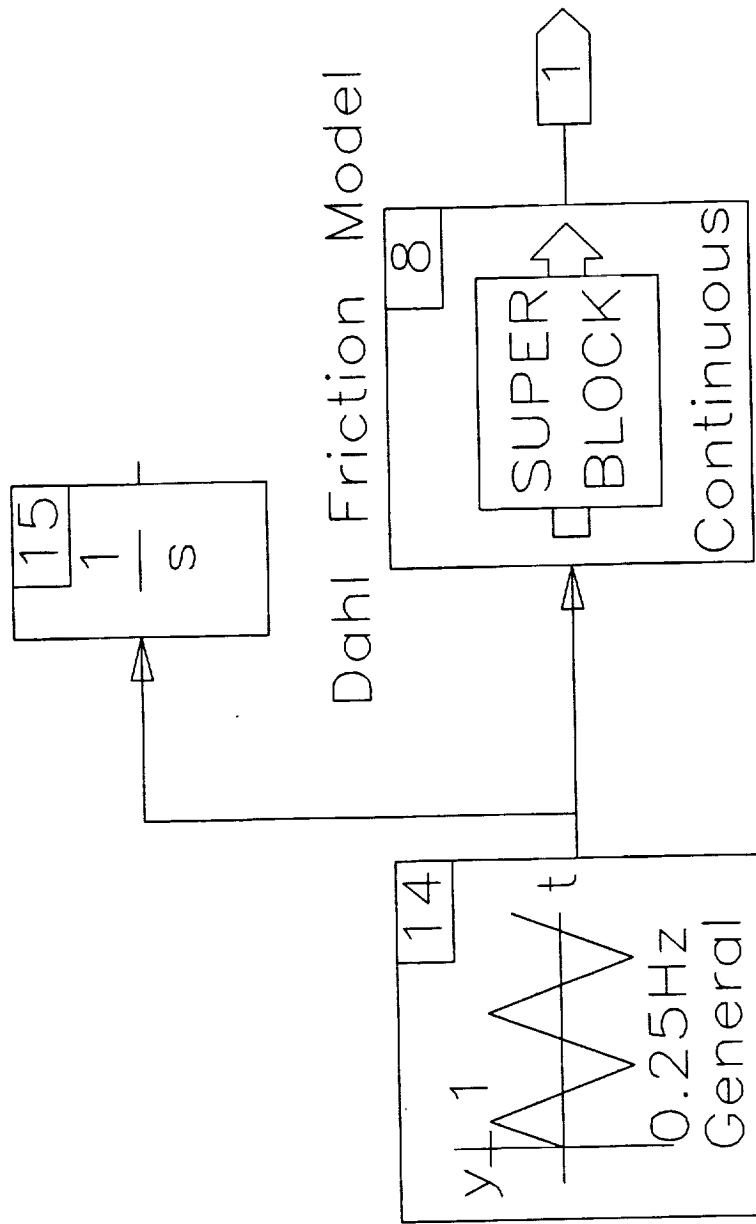


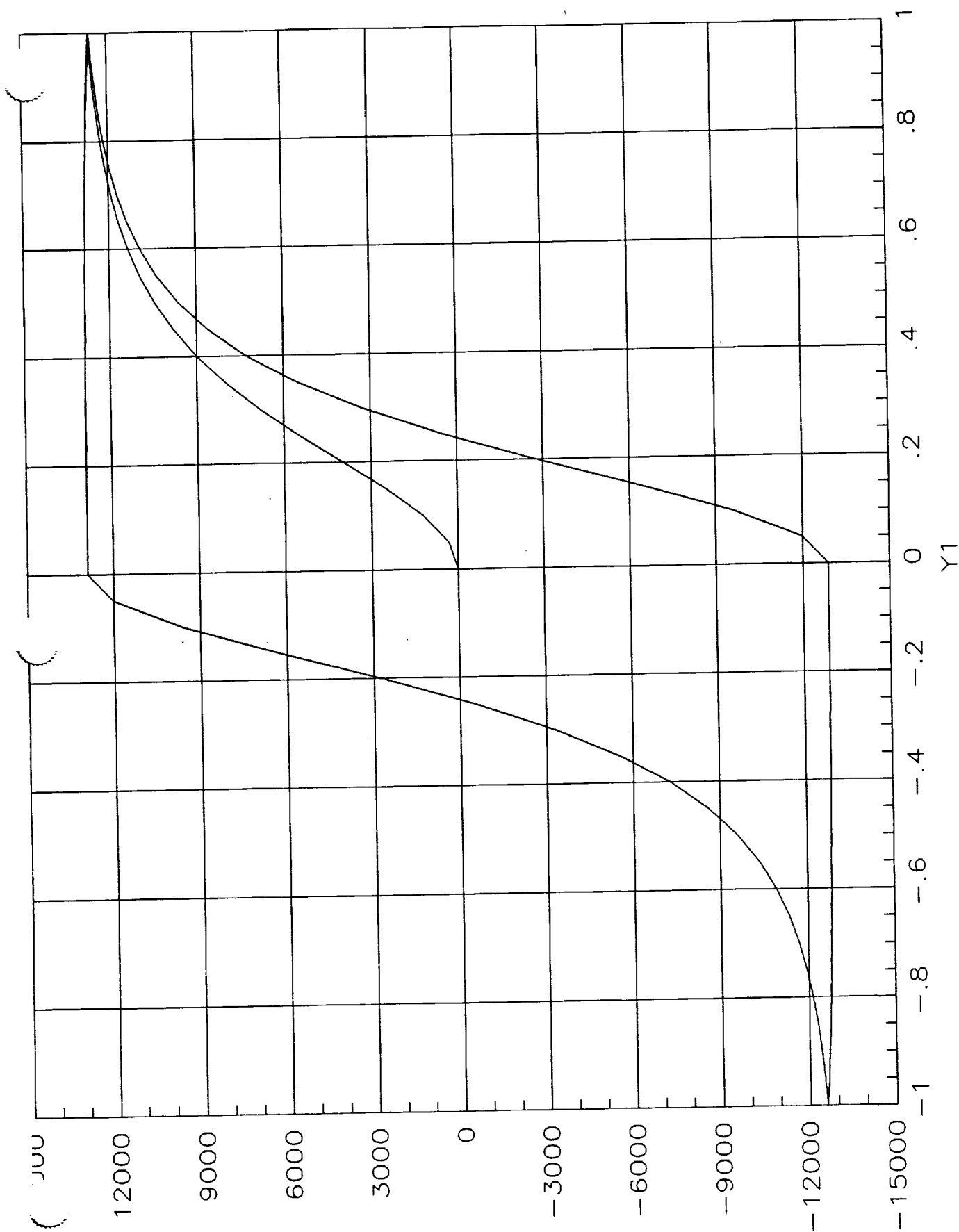
Continuous Super-Block
doane

Ext.In
1

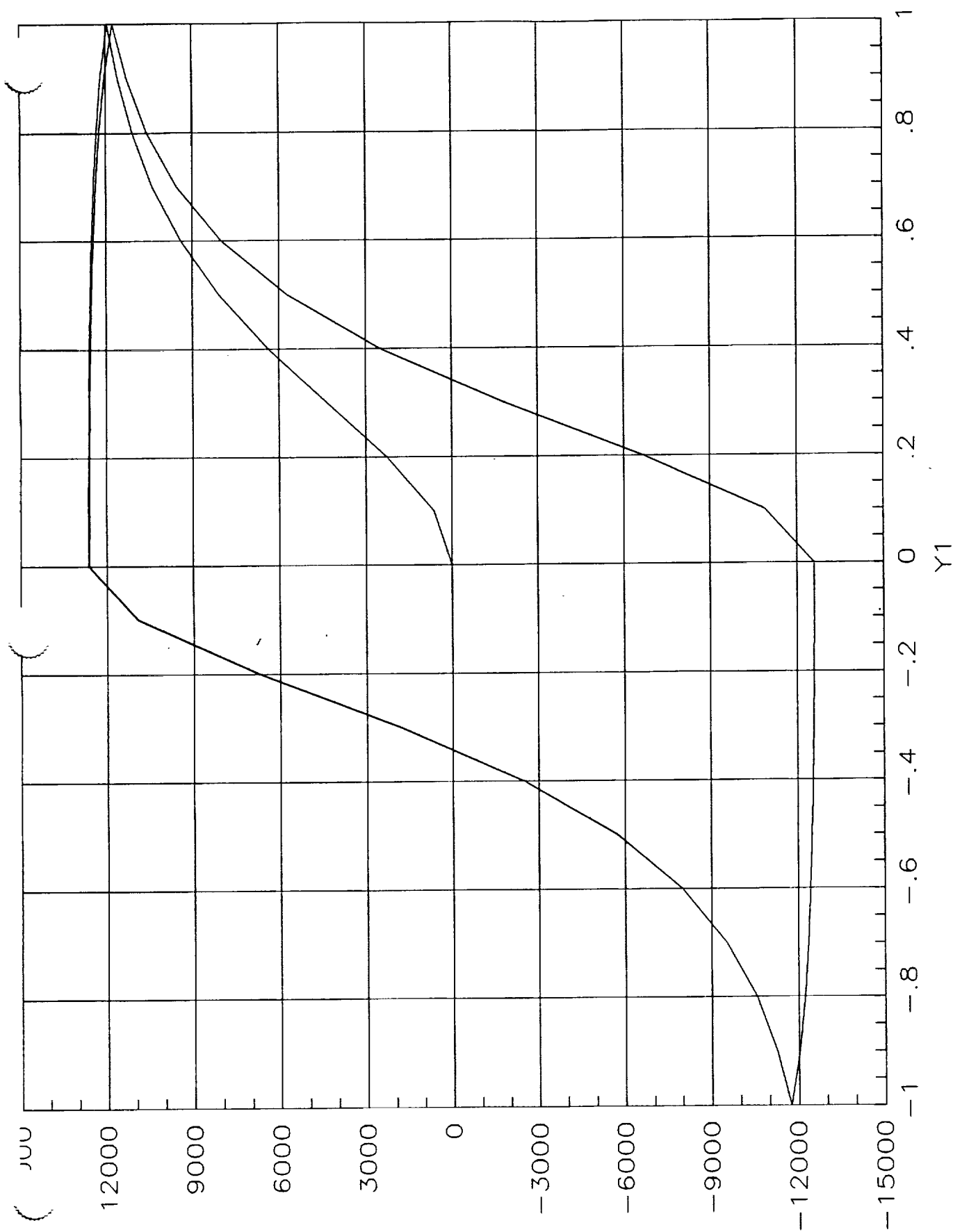
Ext.Out
1



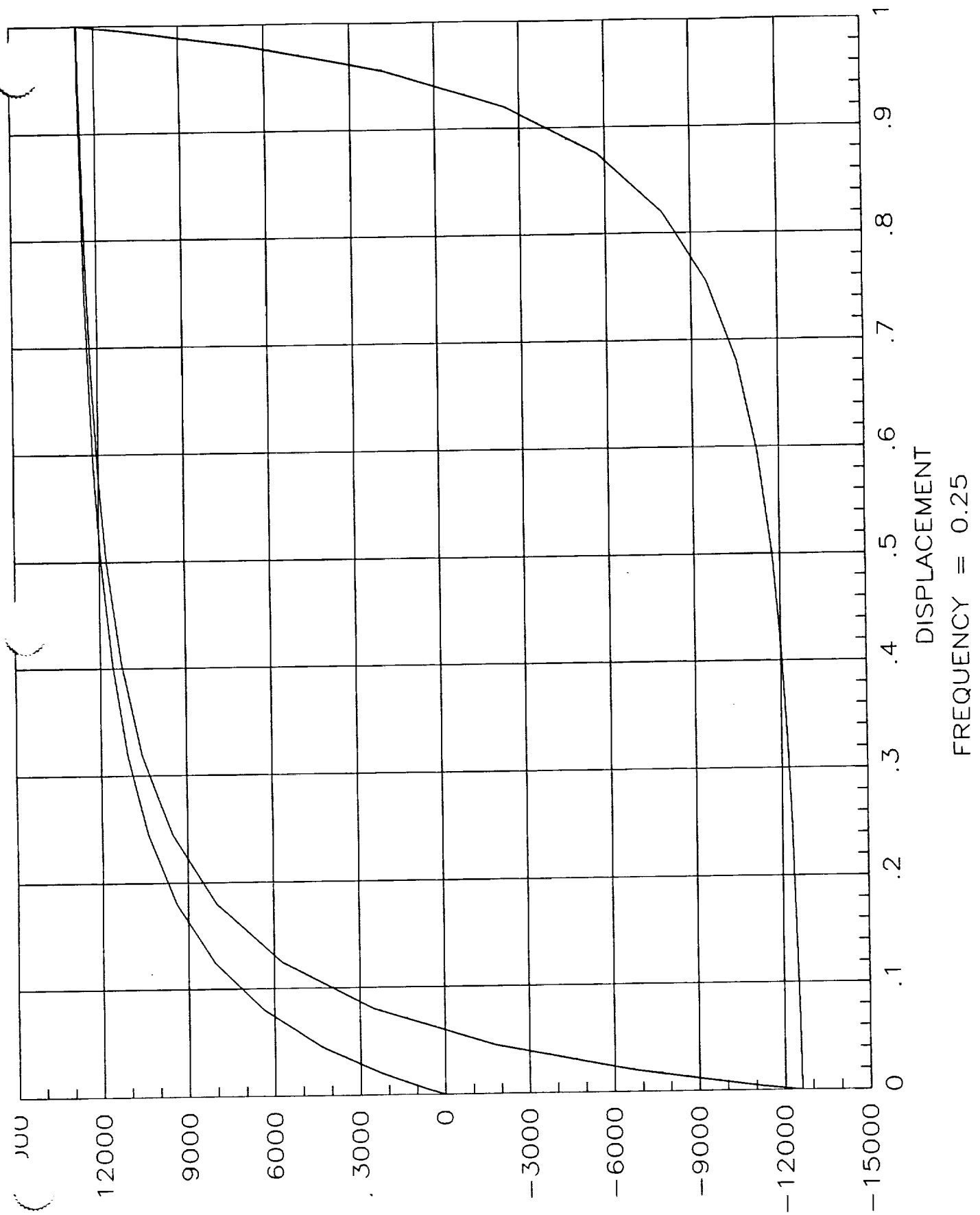




FREQUENCY = 0.125 HZ

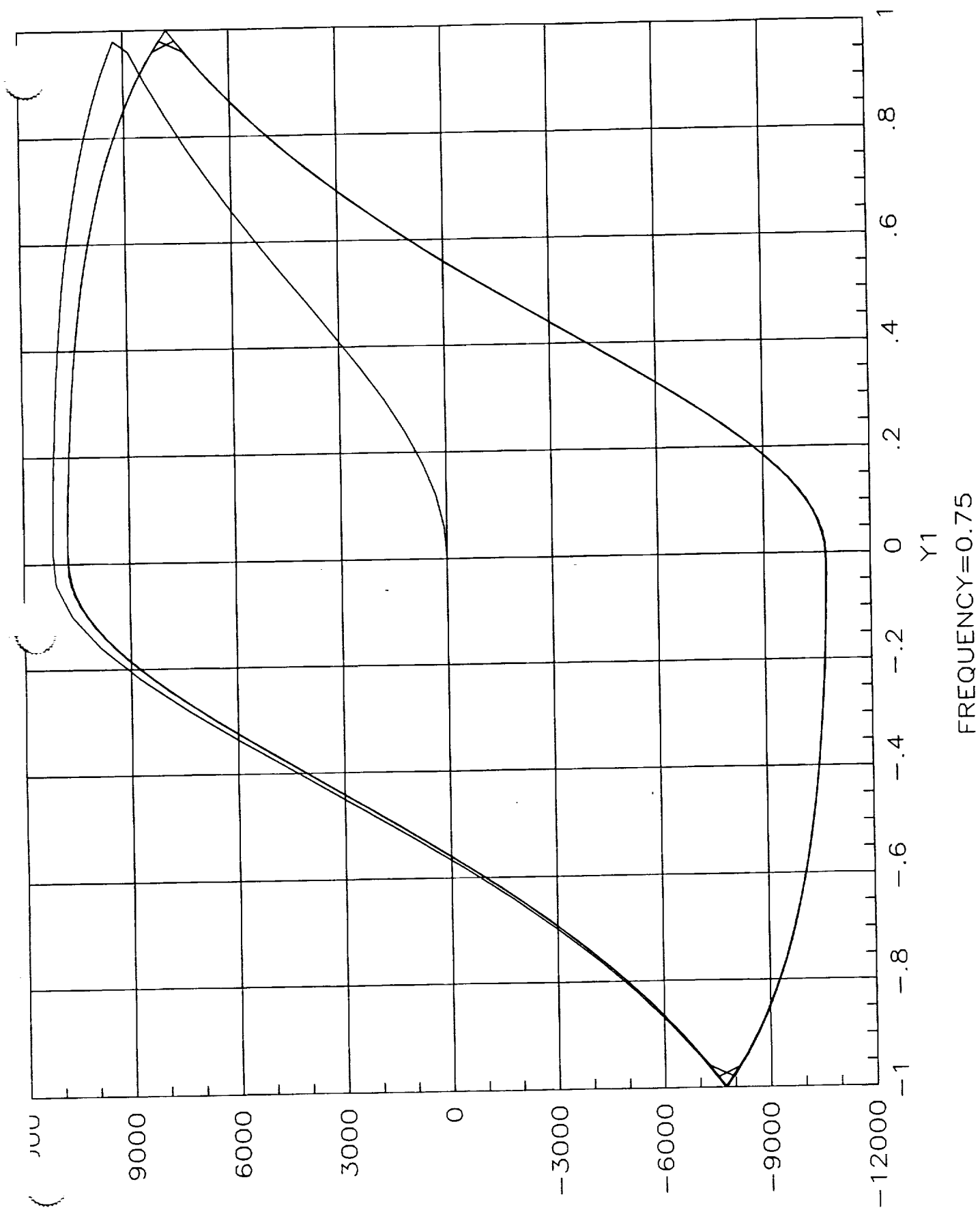


FREQUENCY=0.25 HZ



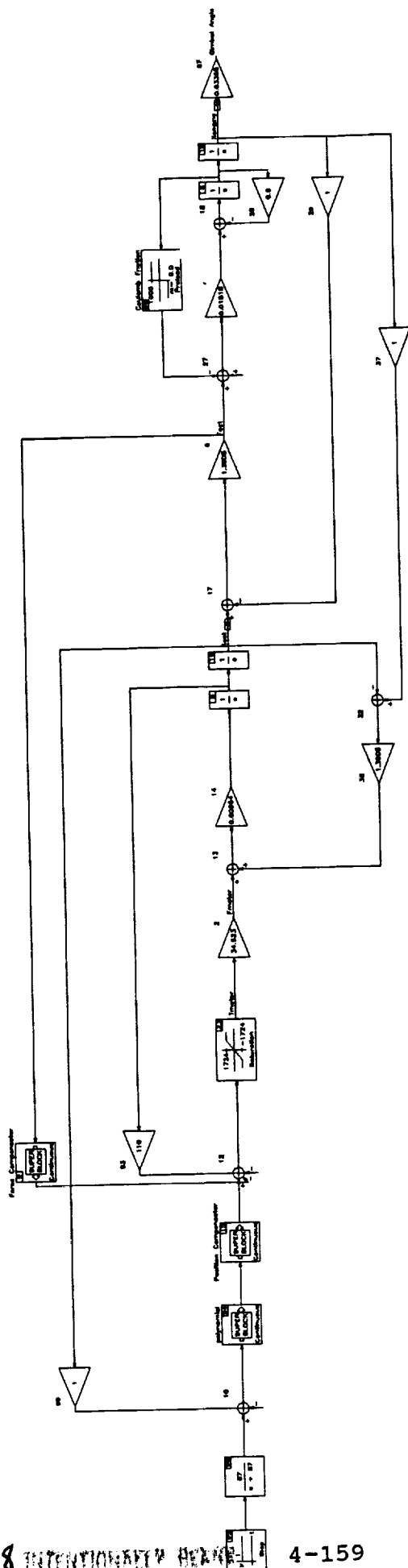
Y2

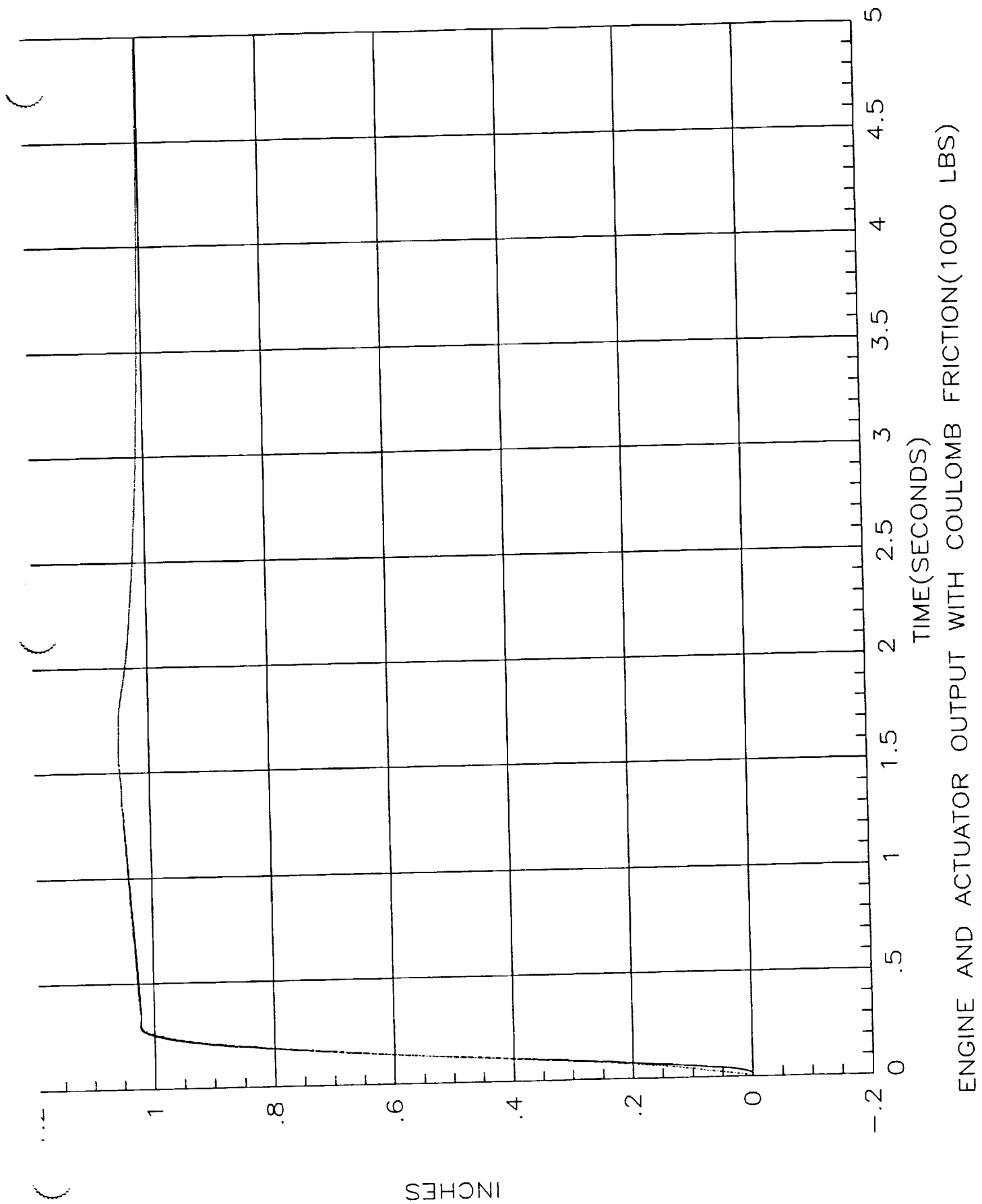
4-156



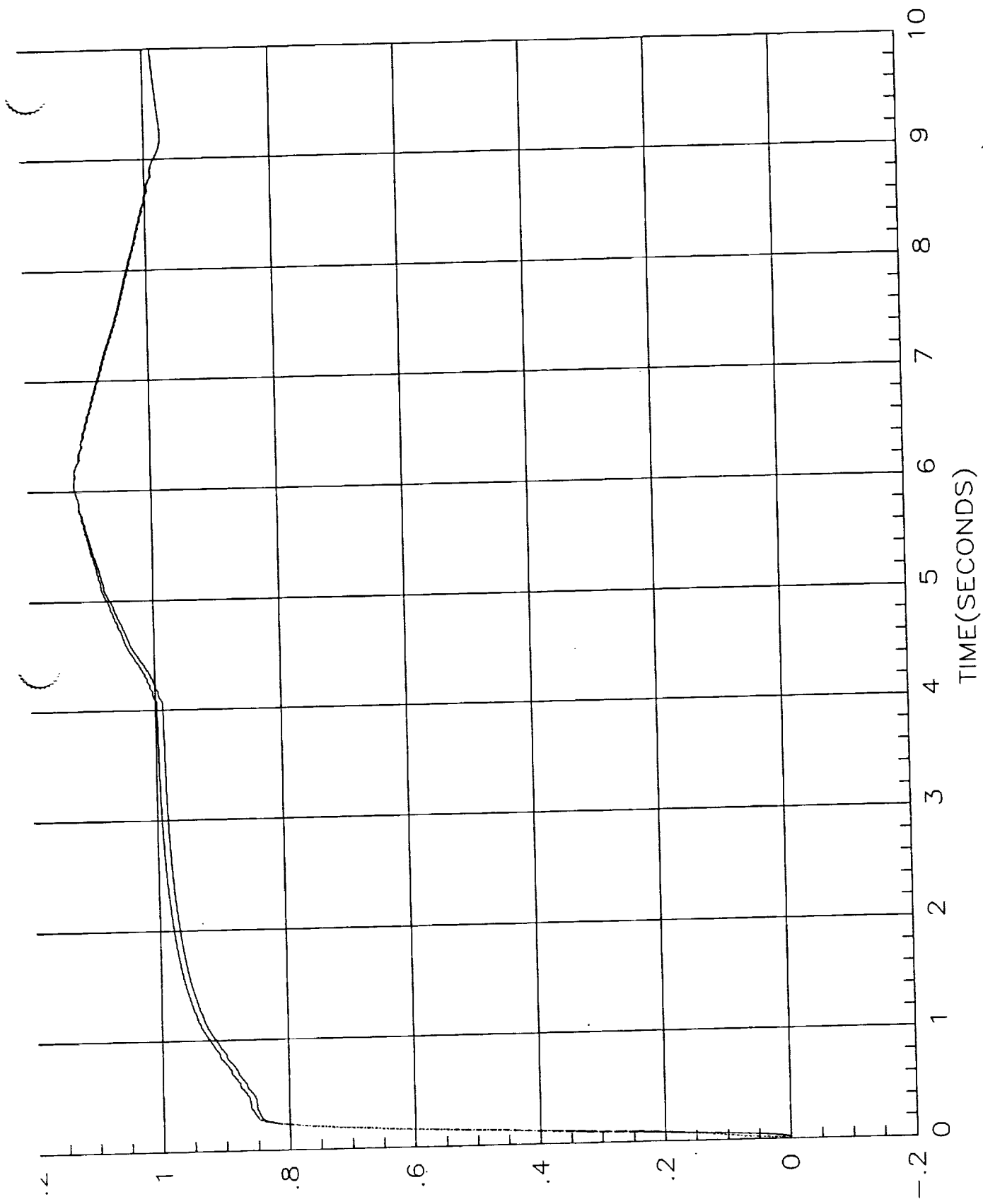
The other type of friction investigated was the classical Coulomb friction. This function in which the friction amplitude does not vary with relative velocity but does depends on the sign of the relative velocity so as to always oppose motion is a function built into the MATRIXx function library. The first figure shows the EMA simulation as before but with the Coulomb friction block added around the rocket engine so as to oppose its motion. Four simulations commanding one inch of motion were then run at varying levels of the Coulomb friction magnitude; these were 1000, 2000, 5000 and 13000 pounds. As might be expected the results varied markedly as the friction was increased. At the 1,000 pound friction level the motion was damped but the response was still quite fast and the result from a qualitative standpoint quite stable. At 2000 pounds the response was still fast but the response waveshape was becoming unfamiliar and may not be satisfactory. At 5,000 and 13,000 pounds the response waveform appeared unsatisfactory although it does appear that the response was settling into the commanded one inch.

This page intentionally left blank

$$\frac{1}{2} \text{Exl.und}$$
EXL.IN
0



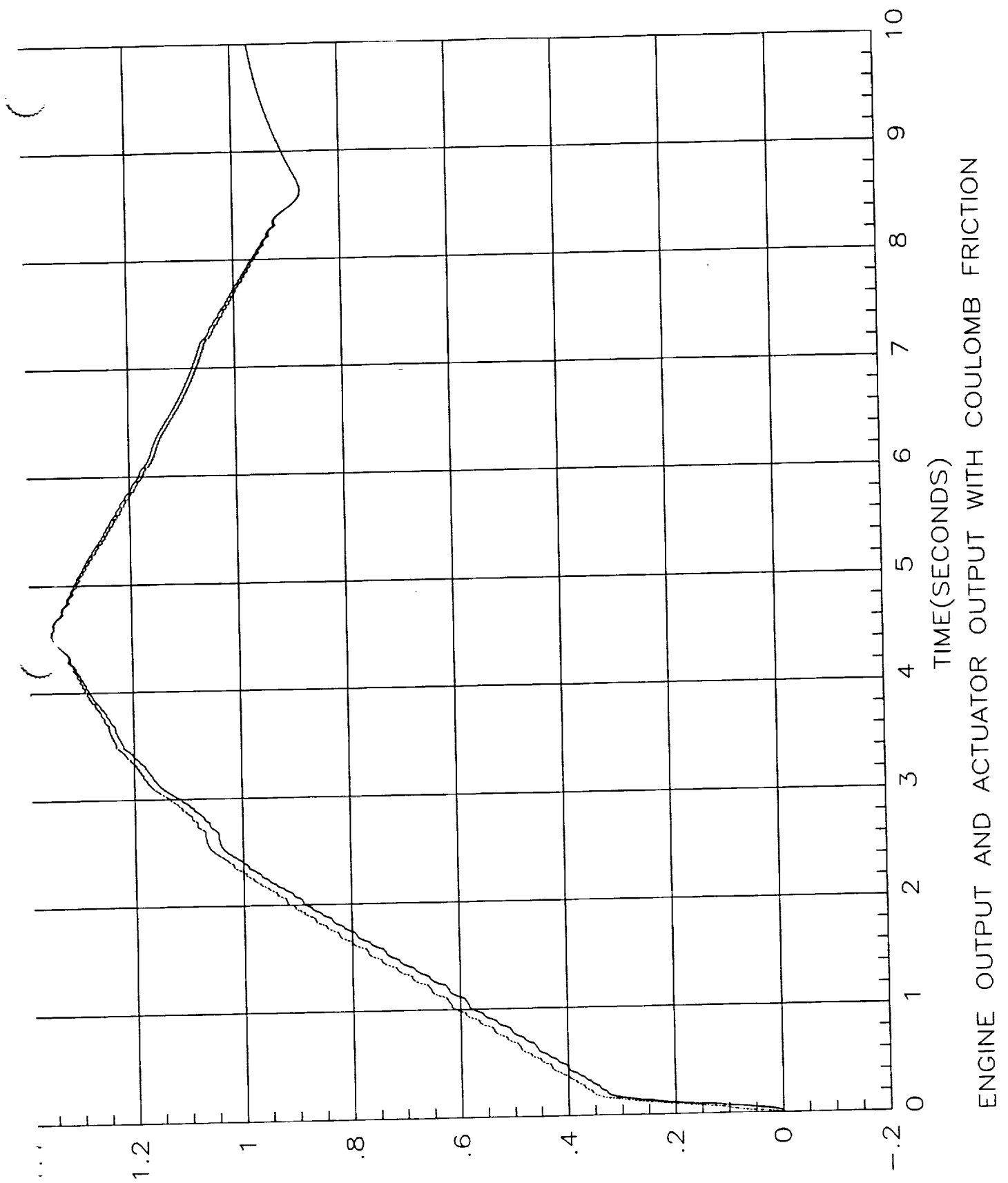
INCHES

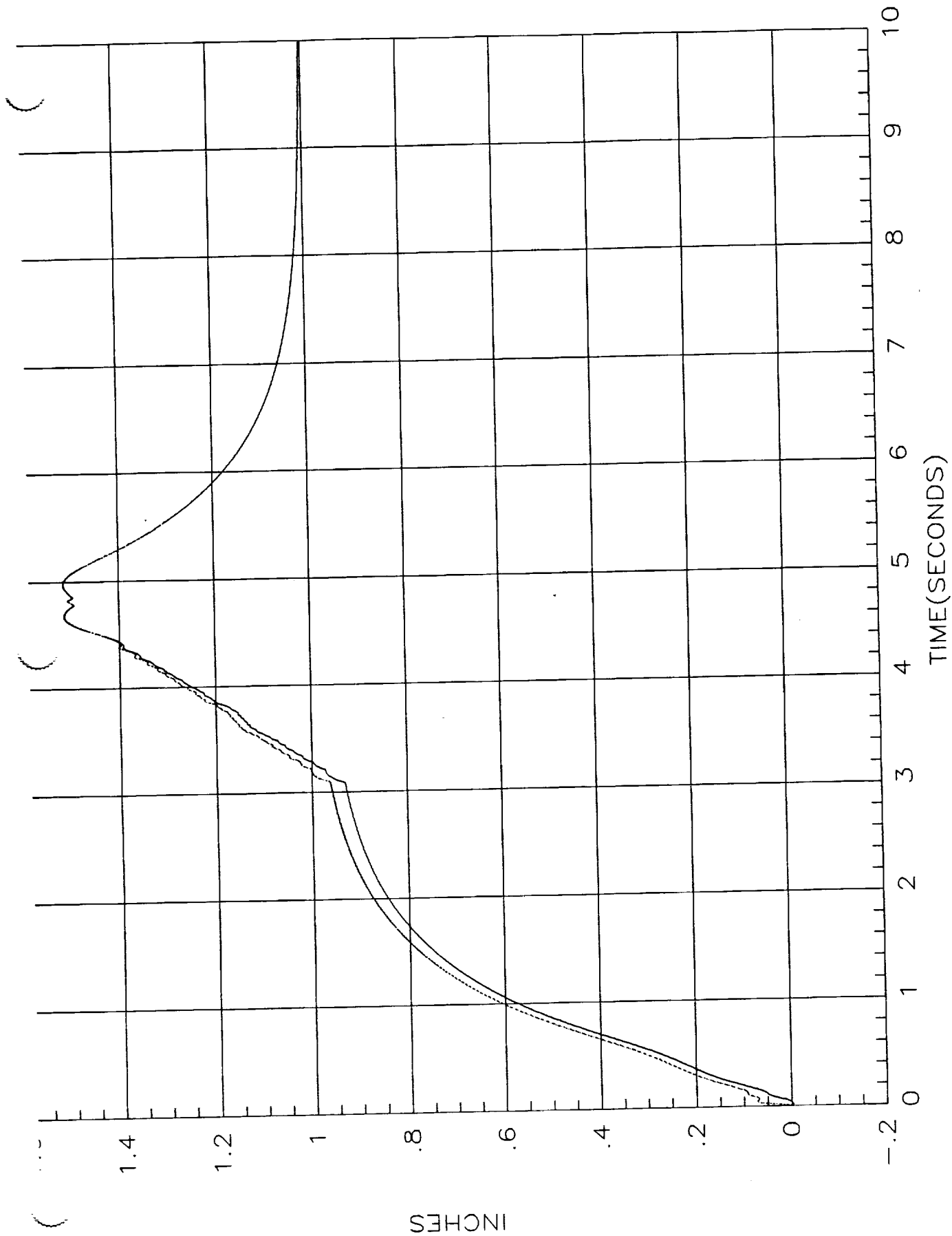


ENGINE AND ACTUATOR OUTPUT WITH COULOMB FRICTION(2000 LBS)

INCHES

4-162





ENGINE AND ACTUATOR OUTPUT WITH COULOMB FRICTION(13000LBS)

It could turn out that the actual friction is best modeled by some combination of friction models. In that case linear (viscous) friction could be added to the mix. Only time and hardware data will determine this. As is typical when dealing with nonlinear phenomena a great deal more investigation will be needed once the functional form of the friction is ascertained. The problem is in knowing how close to the boundary between satisfactory or unsatisfactory operation a given set of parameters may be. Usually the matter is investigated by running a significant number of simulations and of course by appropriate laboratory tests under varying conditions e.g. hot or cold, new or run in hardware, a high and low range of electronic gains etc.

It could turn out that the actual friction is best modeled by some combination of friction models. In that case linear (viscous) friction could be added to the mix. Only time and hardware data will determine this. As is typical when dealing with nonlinear phenomena a great deal more investigation will be needed once the functional form of the friction is ascertained. The problem is in knowing how close to the boundary between satisfactory or unsatisfactory operation a given set of parameters may be. Usually the matter is investigated by running a significant number of simulations and of course by appropriate laboratory tests under varying conditions e.g. hot or cold, new or run in hardware, a high and low range of electronic gains etc.

**ELECTRIC MOTOR
DESIGN**

K. Electric Motor Design Considerations

When designing an electric motor to fulfill the requirements of the EMA system there are two related sets of activities. One is to develop the system level motor specifications i.e. considering the motor as a subsystem component or "black box" in the overall EMA system design. The other is to take into account the component specifications and design a motor to meet them.

Developed first below are the specifications placed on the motor as an EMA system component. They include such things as the back-emf/torque constant and the armature resistance.

The torque/back-emf constant (K) of the electric motor and the motor armature resistance (R_a) have to meet certain requirements to be compatible with the overall actuator design. For instance if the motor constant is too large it will not be possible to put enough current into the motor at a 5 inches/second actuator stroking rate to develop 30 horsepower (i.e. 40KIPS); which is a specification. If, on the other hand, K is too small then the stall torque with the allowable current will be too little to meet the 60KIPS stall torque requirement. In a similar fashion limitations exist for R_a .

To calculate values for K and R_a one proceeds as follows. First assume that the motor model is that of a simple brush type permanent magnet armature controlled dc motor. This requires that the actual motor as a circuit element behave as the model motor; at this time the three phase winding data of the actual motor are still to be developed. Second assume that an efficient motor is being used i.e. the slope of the speed versus force curve from zero force to 40KIPS is small, say five percent (recall that a completely lossless motor would have zero slope to its speed torque curve, see "Control Systems Engineering" by J. E. Gibson and F. B. Tuteur, McGraw-Hill, 1958 pgs 210-212). Thus in this example the no load speed of the motor will be 3000 rpm (the speed at which it is to develop 10 horsepower) times 1.05 or 3150 rpm when excited with the bus voltage (assumed to be 240 volts). Because the calculations use radians per second 3000 rpm is converted to 314.1 radians per second.

The torque developed by each of the three motors when delivering 10 horsepower at 3000 rpm is 210 inch-pounds. 210 inch-pounds of torque equals 22.84 newton-meters of torque, a set of units also needed in the calculations (note that in a consistent set of units the back emf constant and the torque constant are numerically identical). Three motors would of course produce 68.5 newton-meters of torque. Proceed by writing a current balance equation

$$\frac{\text{Bus Voltage} - \text{Back EMF}}{R_a} = \frac{\text{Torque}}{K}$$

If the motor is running unloaded (i. e. is producing no torque) the back EMF must equal the bus voltage and hence

$$240 = K (329.8)$$

or

$$K = 0.7277 \text{ (Volts/Rad/Sec or Newton-Meters/Amp)}$$

So to this point

$$\frac{240 - (0.7277) \omega}{R_a} = \frac{\text{Torque}}{0.7277}$$

At 314.1 rad per second one motor must produce 22.84 Newton-Meters of torque. Thus

$$\frac{240 - (0.7277) (314.1)}{R_a} = \frac{22.84}{0.7277}$$

from which the armature resistance for one motor is 0.364 ohms.

The value of copper's electrical resistance varies with temperature. In the range from 0 degrees to 157 degrees Celsius it will increase 67%. Thus because the 0.364 ohms

figure represents the largest that R_a may be at 157 degrees Celsius it would have to be approximately 0.2 ohms at 0 degrees Celsius. Three motors in parallel would present to the line one third of these values. Thus the electronic amplifier would have to govern the current throughout the entire operating range to, among other things, avoid over current at the stalled, low temperature condition.

It has been demonstrated elsewhere in this report that given the ability to develop rated horsepower at a given rpm the least motor rotor mass polar moment of inertia consistent with such things as heat dissipation and torque generation will be beneficial in maximizing the load acceleration. Thus a long cylindrical ("hot dog") motor of modest radius is anticipated rather than an axially short, large radius ("pancake") one. In other words a maximization of the torque to inertia ratio would be beneficial within the other constraints (one should keep firmly in mind that in order to take advantage of any reduction in motor inertia the gear train ratios must be suitably adjusted). ANSYS, the finite element code used extensively in this design effort, has an optimization feature built into it. While the current effort did not exercise this feature, it will be applied during the next phase to improve the performance of the baseline design resulting from this task. The thermal model to be developed for the second phase will be three dimensional and thus have a completely different finite element arrangement than the

electromagnetic model. It is planned to imbed the thermal and magnetic models within an ANSYSIS controlled optimizer to improve overall characteristics subject to a general set of constraints (e.g. maximize torque to inertia ratio subject to no temperature greater than 150 degrees Celsius. When contemplating heat generation it should be noted that a slowly turning motor will generate less hysteresis loss per unit volume of ferromagnetic material than a corresponding motor turning faster because the B-H hysteresis loop is not traversed as often per unit time as in the case of the faster turning motor. Another feature of the motor which will have to be analyzed when a motor configuration is decided upon is that of the shaft critical speed. This is because of the large dynamic range of the commanded motor speed (positive and negative through zero) which requires that the shaft be operated suitably below the first critical speed to avoid any possibility of exciting any resonant response of the shaft lateral motion. This will also be explored in a future phase of the work. Another design parameter which will be evaluated with the model in the future is the leakage inductance of the windings. This is of importance when dealing with the failure mode in which the windings are shorted. It was shown by F. Nola and M. Hammond of MSFC that the leakage inductance limits the short circuit current in a way that reduces the retarding torque of the motor (acting as a shorted generator) when the motor

is turned faster than some given speed which is dependent upon the motor parameters e.g. the number of poles etc.

The reader is referred to the open literature for the very many treatises on the finite element method of solving distributed parameter problems. The technique appears to have gained its initial impetus in the structural analysis field before it began to spread to electrical engineering. Thus several of the codes used for solving electrical and magnetic (E & M) problems use the solution framework first built for structural problems.

As applied to problems of interest to electrical engineering the finite element codes solve Maxwell's equations. If one is considering high frequency problems such as occur in mega and giga Hertz radio link communication systems then all terms in the Maxwell's equations may be necessary to obtain a meaningful solution. However, in the class of problems which are of interest here i.e. motor design and analysis it is possible to decouple the four equations into two groups by assuming that the displacement current is negligible. This allows formulating the problem in terms of magnetic field intensity H , magnetic flux density B and electric current density J . This simplifies the problem as outlined in the ANSYS manuals and seminar notes. One reference specifically in the electrical engineering field is "Finite Elements for Electrical

Engineers" by P. P. Silvester and R. L. Ferrari, Cambridge University Press, 1990.

After establishing convenient access to the proper ANSYS-4.4A resource and obtaining the ANSYS manuals and seminar notes (30 some odd pounds worth) the first task was to comprehend the ANSYS language and how it is applied to analyze this type of problem. Next a motor geometry was selected and constructed in the code (see the figure entitled Motor Geometry). This was done based on past experience with previous motors but incorporating symmetry into the configuration so that only one sixth of the motor as viewed around the air gap had to be coded explicitly (the effect of the other five sixths was taken care of by the choice of periodic boundary conditions). It should be noted that not all motors as built are symmetrical. Some are "short pitched" or fractional slotted for various reasons (such as minimizing torque ripple or using the same lamination punching for a variety of motors) which destroys any symmetry. In this application it was judged initially that the conventional reasons for having unsymmetrical windings were not significant as, in all events, a lamination will be designed and fabricated that is tailored to this application.

The first geometry selected and coded is shown immediately below.

K. Electric Motor Design Considerations

When designing an electric motor to fulfill the requirements of the EMA system there are two related sets of activities. One is to develop the system level motor specifications i.e. considering the motor as a subsystem component or "black box" in the overall EMA system design. The other is to take into account the component specifications and design a motor to meet them.

Developed first below are the specifications placed on the motor as an EMA system component. They include such things as the back-emf/torque constant and the armature resistance.

The torque/back-emf constant (K) of the electric motor and the motor armature resistance (R_a) have to meet certain requirements to be compatible with the overall actuator design. For instance if the motor constant is too large it will not be possible to put enough current into the motor at a 5 inches/second actuator stroking rate to develop 30 horsepower (i.e. 40KIPS); which is a specification. If, on the other hand, K is too small then the stall torque with the allowable current will be too little to meet the 60KIPS stall torque requirement. In a similar fashion limitations exist for R_a .

To calculate values for K and Ra one proceeds as follows. First assume that the motor model is that of a simple brush type permanent magnet armature controlled dc motor. This requires that the actual motor as a circuit element behave as the model motor; at this time the three phase winding data of the actual motor are still to be developed. Second assume that an efficient motor is being used i.e. the slope of the speed versus force curve from zero force to 40KIPS is small, say five percent (recall that a completely lossless motor would have zero slope to its speed torque curve, see "Control Systems Engineering" by J. E. Gibson and F. B. Tuteur, McGraw-Hill, 1958 pgs 210-212). Thus in this example the no load speed of the motor will be 3000 rpm (the speed at which it is to develop 10 horsepower) times 1.05 or 3150 rpm when excited with the bus voltage (assumed to be 240 volts). Because the calculations use radians per second 3000 rpm is converted to 314.1 radians per second.

The torque developed by each of the three motors when delivering 10 horsepower at 3000 rpm is 210 inch-pounds. 210 inch-pounds of torque equals 22.84 newton-meters of torque, a set of units also needed in the calculations (note that in a consistent set of units the back emf constant and the torque constant are numerically identical). Three motors would of course produce 68.5 newton-meters of torque. Proceed by writing a current balance equation

$$\frac{\text{Bus Voltage} - \text{Back EMF}}{R_a} = \frac{\text{Torque}}{K}$$

If the motor is running unloaded (i. e. is producing no torque) the back EMF must equal the bus voltage and hence

$$240 = K (329.8)$$

or

$$K = 0.7277 \quad (\text{Volts/Rad/Sec or Newton-Meters/Amp})$$

So to this point

$$\frac{240 - (0.7277) \omega}{R_a} = \frac{\text{Torque}}{0.7277}$$

At 314.1 rad per second one motor must produce 22.84 Newton-Meters of torque. Thus

$$\frac{240 - (0.7277) (314.1)}{R_a} = \frac{22.84}{0.7277}$$

from which the armature resistance for one motor is 0.364 ohms.

The value of copper's electrical resistance varies with temperature. In the range from 0 degrees to 157 degrees Celsius it will increase 67%. Thus because the 0.364 ohms

figure represents the largest that R_a may be at 157 degrees Celsius it would have to be approximately 0.2 ohms at 0 degrees Celsius. Three motors in parallel would present to the line one third of these values. Thus the electronic amplifier would have to govern the current throughout the entire operating range to, among other things, avoid over current at the stalled, low temperature condition.

It has been demonstrated elsewhere in this report that given the ability to develop rated horsepower at a given rpm the least motor rotor mass polar moment of inertia consistent with such things as heat dissipation and torque generation will be beneficial in maximizing the load acceleration. Thus a long cylindrical ("hot dog") motor of modest radius is anticipated rather than an axially short, large radius ("pancake") one. In other words a maximization of the torque to inertia ratio would be beneficial within the other constraints (one should keep firmly in mind that in order to take advantage of any reduction in motor inertia the gear train ratios must be suitably adjusted). ANSYS, the finite element code used extensively in this design effort, has an optimization feature built into it. While the current effort did not exercise this feature, it will be applied during the next phase to improve the performance of the baseline design resulting from this task. The thermal model to be developed for the second phase will be three dimensional and thus have a completely different finite element arrangement than the

electromagnetic model. It is planned to imbed the thermal and magnetic models within an ANSYSIS controlled optimizer to improve overall characteristics subject to a general set of constraints (e.g. maximize torque to inertia ratio subject to no temperature greater than 150 degrees Celsius. When contemplating heat generation it should be noted that a slowly turning motor will generate less hysteresis loss per unit volume of ferromagnetic material than a corresponding motor turning faster because the B-H hysteresis loop is not traversed as often per unit time as in the case of the faster turning motor. Another feature of the motor which will have to be analyzed when a motor configuration is decided upon is that of the shaft critical speed. This is because of the large dynamic range of the commanded motor speed (positive and negative through zero) which requires that the shaft be operated suitably below the first critical speed to avoid any possibility of exciting any resonant response of the shaft lateral motion. This will also be explored in a future phase of the work. Another design parameter which will be evaluated with the model in the future is the leakage inductance of the windings. This is of importance when dealing with the failure mode in which the windings are shorted. It was shown by F. Nola and M. Hammond of MSFC that the leakage inductance limits the short circuit current in a way that reduces the retarding torque of the motor (acting as a shorted generator) when the motor

is turned faster than some given speed which is dependent upon the motor parameters e.g. the number of poles etc.

The reader is referred to the open literature for the very many treatises on the finite element method of solving distributed parameter problems. The technique appears to have gained its initial impetus in the structural analysis field before it began to spread to electrical engineering. Thus several of the codes used for solving electrical and magnetic (E & M) problems use the solution framework first built for structural problems.

As applied to problems of interest to electrical engineering the finite element codes solve Maxwell's equations. If one is considering high frequency problems such as occur in mega and giga Hertz radio link communication systems then all terms in the Maxwell's equations may be necessary to obtain a meaningful solution. However, in the class of problems which are of interest here i.e. motor design and analysis it is possible to decouple the four equations into two groups by assuming that the displacement current is negligible. This allows formulating the problem in terms of magnetic field intensity H , magnetic flux density B and electric current density J . This simplifies the problem as outlined in the ANSYS manuals and seminar notes. One reference specifically in the electrical engineering field is "Finite Elements for Electrical

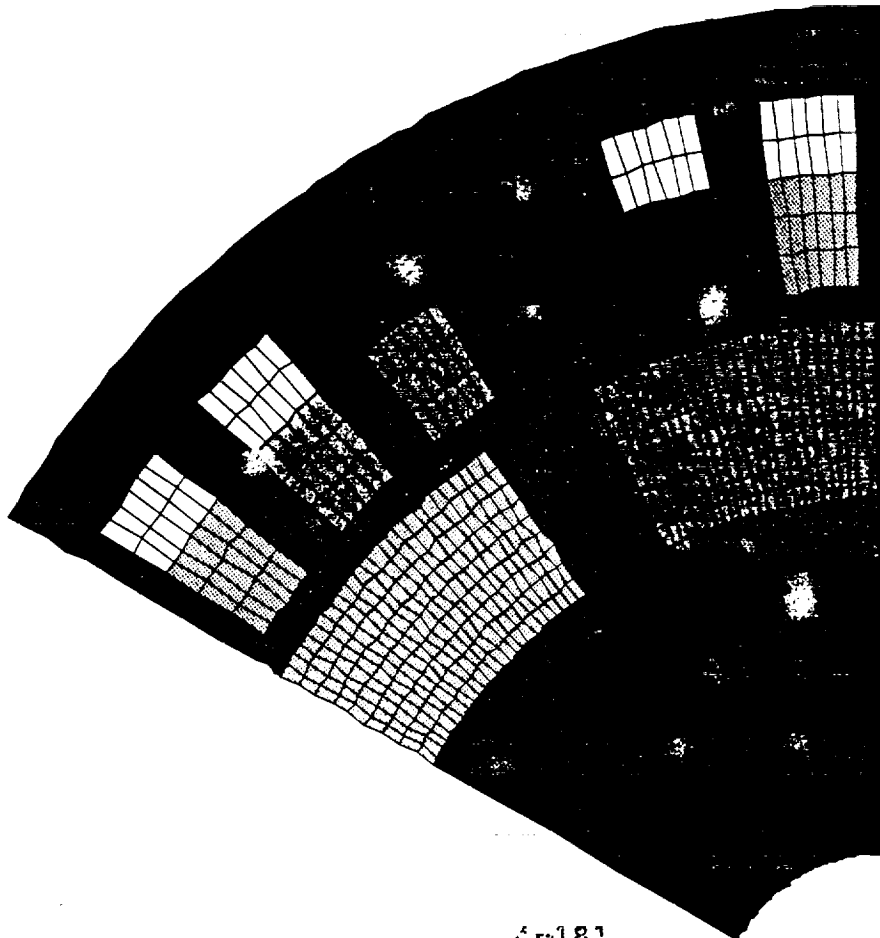
Engineers" by P. P. Silvester and R. L. Ferrari, Cambridge University Press, 1990.

After establishing convenient access to the proper ANSYS-4.4A resource and obtaining the ANSYS manuals and seminar notes (30 some odd pounds worth) the first task was to comprehend the ANSYS language and how it is applied to analyze this type of problem. Next a motor geometry was selected and constructed in the code (see the figure entitled Motor Geometry). This was done based on past experience with previous motors but incorporating symmetry into the configuration so that only one sixth of the motor as viewed around the air gap had to be coded explicitly (the effect of the other five sixths was taken care of by the choice of periodic boundary conditions). It should be noted that not all motors as built are symmetrical. Some are "short pitched" or fractional slotted for various reasons (such as minimizing torque ripple or using the same lamination punching for a variety of motors) which destroys any symmetry. In this application it was judged initially that the conventional reasons for having unsymmetrical windings were not significant as, in all events, a lamination will be designed and fabricated that is tailored to this application.

The first geometry selected and coded is shown immediately below.

ANSYS 4.4A
FEB 23 1992
17:33:16
PREP7 ELEMENTS
MAT NUM

ZV =1
DIST=0.02915
XF =0.0315
YF =0.025115



TITLE MOTOR GEOMETRY FOR TORQUE ANGLE ONE

Inspection of the figure will reveal that the motor has the following features.

Smooth rotor (but with air gaps between the magnets)

3 phase

full pitch (that is the two sides of a coil lie 180 electrical degrees from each other)

12 pole

36 slot (2 slots per pole per phase)

double layer windings

The soft iron assumed for the back iron is taken to be Carpenter Steel's Hi mu 49. This is so far the only suitable steel found in this country (the name of a French company, Metal Imphy was given but so far no representative has been found). Some of the alloys listed in the older references (such as Supermendur) led to Companies that no longer make this type of product. Normally Carpenter sells in large lots (one ton minimum) but they may make some smaller quantity available for Research and Development purposes.

The permanent magnet was taken to be made from Delco (General Motors) proprietary Neodymium-Iron-Boron material trademarked Magnequench. The particular version is the MQ3-F 30H variety. Its pertinent parameters are as follows.

Br of 11.3 KiloGauss (retentivity)
Hc of 10.4 KiloOersteds (coercive force)
BHmax of 30 MegaGaussOersteds (maximum energy
product)
Mur of 1.07 (recoil permeability)
Temperature coefficient of Br to 100 Degree
Celsius (0.09%/deg Celsius)
Temperature coefficient of Hci to 100 degrees
Celsius)
Maximum operating temperature 180 degrees Celsius
Curie Temperature 370 degrees Celsius
Mass density, rho, 7.55 gm/cm³
Hardness 60 Rockwell C

The principle dimensional parameters of this first geometry
are.

Magnet radial thickness, 1 cm.
Axle radius, 1 cm
Rotor OD 8 cm
Air gap 0.2 cm
Stator ID 8.2 cm
Stator OD 11.6 cm

The flux plots first generated were with a magnet angle of
50 degrees with an intervening air gap of 10 degrees (see
the figure denoted Motor Geometry For Torque Angle One).
ANSYS was used to calculate the developed torque due to this
configuration. The value was 10.8 Newton-Meter per Meter
length of the motor. The rotor was then clocked (i.e.

rotated with respect to the stator) by 5 mechanical degrees and the developed torque once again calculated. It was found to be 41.8 Newton-Meter per meter length of the motor. This is encouraging in that previous calculations indicate that a little over 60 Newton-Meters of torque will be required at stall for the point design. The torque generated at additional clocking angles will be evaluated to establish the functional relationship between the torque and the clocking angle. It is expected to approximate a sine wave in shape because of the smooth rotor design.

It is instructive to inspect the Torque Angle one and Torque Angle Two Flux Vector plots in the light of the formulation that is used by ANSYS to compute torque. This is because this inspection will explain the difference in the magnitude of the torque.

Generally speaking torque is calculated in one of two ways by the various finite element formulations. These are: one through the use of virtual work and two by the use of the Maxwell stresses. The virtual work approach involves calculating the magnetic energy stored at two relative positions of the rotor and stator. Maxwell's stresses are derived directly from Maxwell's equations. ANSYS uses the Maxwell stress approach. The torque is given by (note that this is a line integral).

$$T = \int [(B \cdot n) \left(\frac{r \times B}{\mu_0} \right) - \frac{|B|^2}{2\mu_0} (r \times n)] ds$$

A solid part for which the torque is to be calculated must be surrounded by air. In the case of the motor this is the motor rotor which is surrounded by the air gap. ANSYS has the means to designate a general path and perform a line integral along the designated path. In the case of an electric motor this path is a circle. This simple geometry allows a simplification of the general torque expression as given above. It becomes, upon manipulation,

$$T = \int [(B \cdot n) \left(\frac{r \times B}{\mu_0} \right)] ds$$

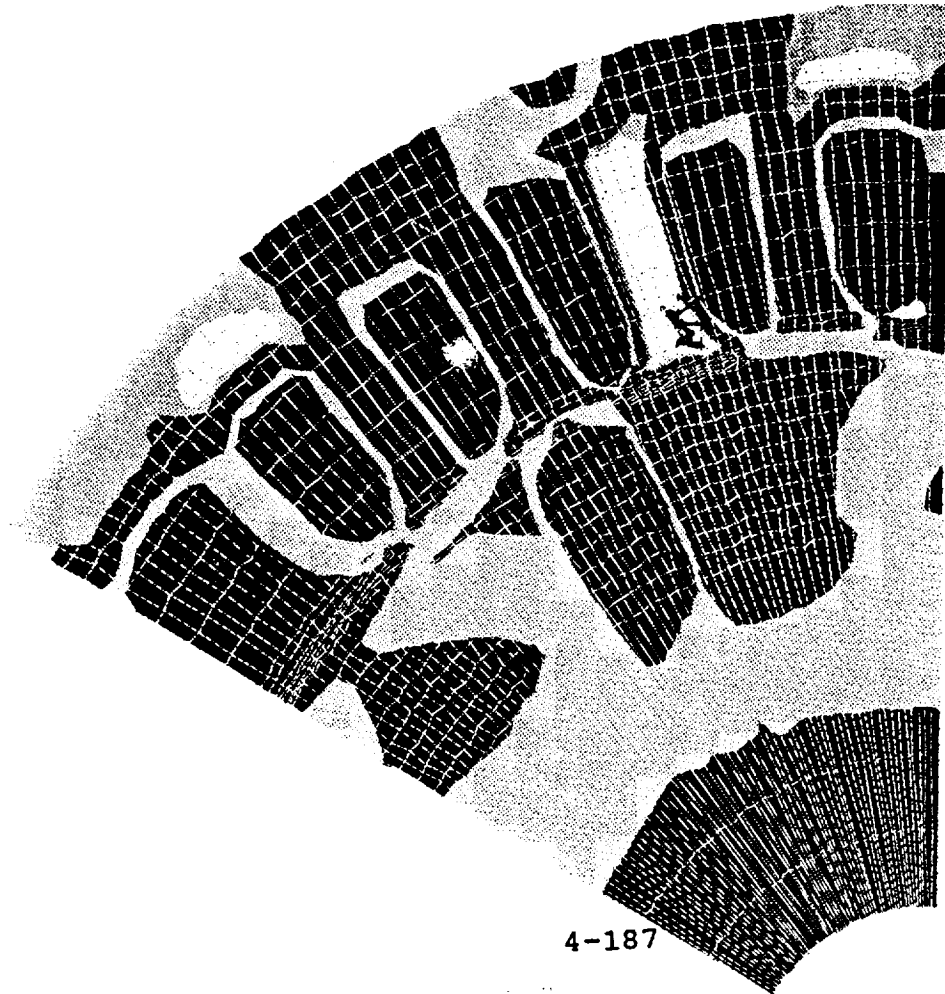
In this expression the r and n vectors are directed radially outward from the center line of the motor (i.e. orthogonal to the centerline of the motor shaft). The vector B is the flux vector existing at a point in the path along which the line integral is being evaluated. Noting that the cross or vector product of two vectors vanishes when they are colinear and that the scalar or dot product vanishes when its two vectors are orthogonal to each other it is seen that torque is developed in the motor only when the flux direction in the motor lies between the the normal and the tangential to the motor rotor surface (for a given magnitude of flux it can be shown that a crossing angle of 45 degrees

yields the maximum torque). Of course the torque is also dependent upon the physical dimensions of the motor.

With the foregoing in mind a comparison of the two Flux Vector plots reveals that in the case of the second torque angle plot as contrasted to the first torque angle plot there is more flux crossing the air gap and the crossing angle relative to the rotor surface appears to be much more favorable for torque generation (as is borne out by the torque calculation). Having completed the torque versus torque angle investigations for this geometry (see last page in this section) other magnet geometries will be tried with a view to optimizing the magnitude and angle of the flux producing torque. It is seen for instance that with these relatively wide magnets the centers of the magnets are contributing relatively little to torque generation (there is relatively little flux and the flux present crosses the air gap radially). Thus is suggested, during the next design iteration, the use of a larger number of narrower magnets to increase motor torque production.

ANSYS 4.4A
 FEB 23 1992
 16:21:11
 POST1: STRESS
 STEP=2
 ITER=10
 BSUM (AVG)
 SMN = 0.132E-03
 SMX = 0.791184

ZV = 1
 DIST = 0.02915
 XF = 0.0315
 YF = 0.025115
 0.132E-03
 0.088027
 0.175921
 0.263816
 0.351711
 0.439605
 0.527539
 0.615328
 0.791184



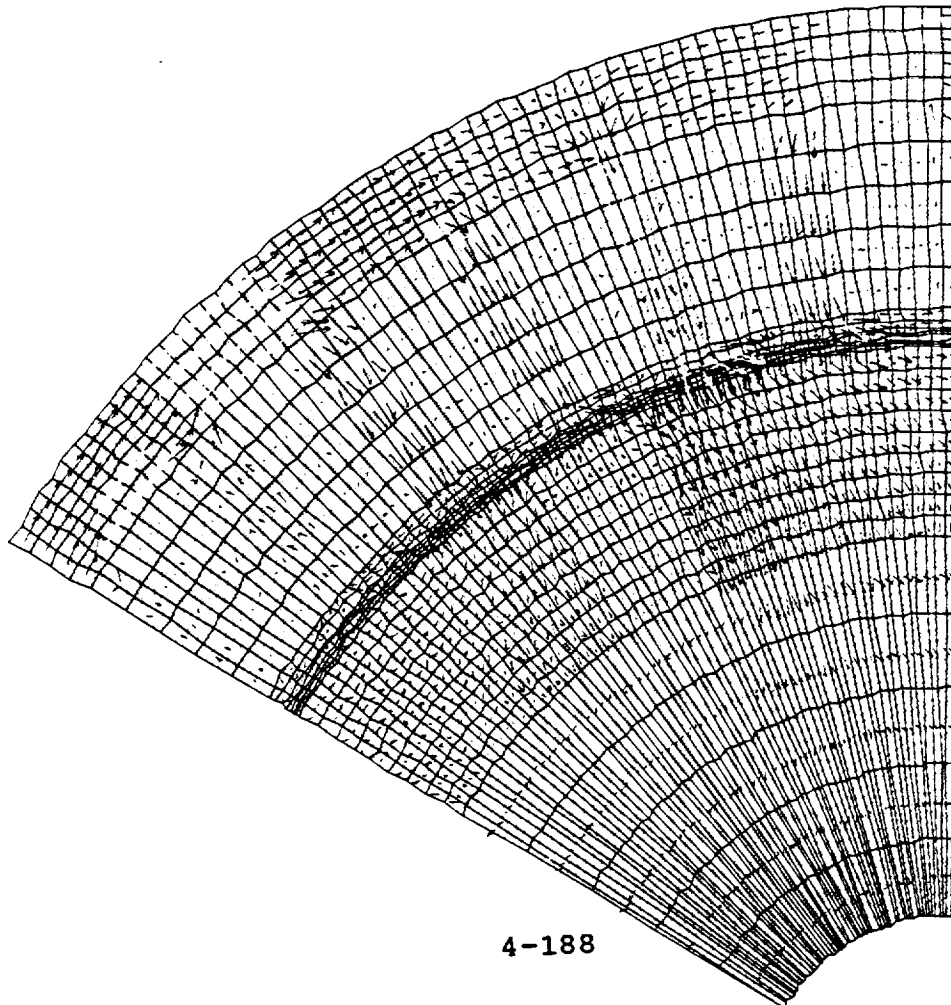
4-187

TITLE FLUX PLOT (TESLA) FOR TORQUE ANGLE ONE

ANSYS 4.4A
 FEB 23 1992
 16:42:41
 POST1 VECTOR
 STEP=2
 ITER=10
 BMAG
 ELEM=561
 0:094731
 0:188873
 0:283015
 0:377157
 0:471298

0.000000
 0.017000

ZV =1
 DIST=0.02915
 XF =0.0315
 YF =0.025115

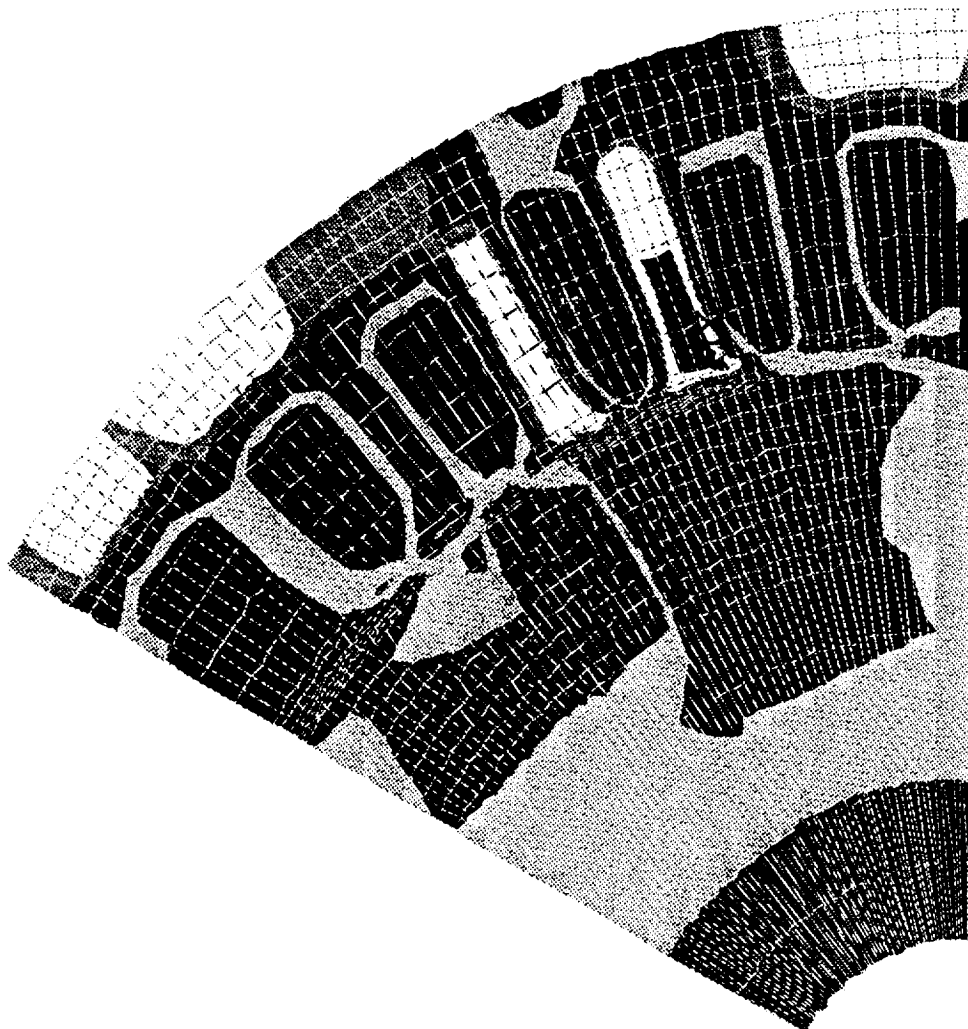


4-188

TITLE FLUX VECTOR (TESLA) PLOT FOR TORQUE ANGLE ONE

ANSYS 4.4A
 MAR 4 1992
 17:36:29
 POST1 STRESS
 STEP=2
 ITER=10 (AVG)
 BSUM = 0.232E-03
 SMN = 1.91
 SMX = 1.91

ZV = 1
 DIST = 0.02915
 XF = 0.0315
 YF = 0.025115
 0.232E-03
 0.212411
 0.42459
 0.63677
 0.848949
 1.0613
 1.24858
 1.4691

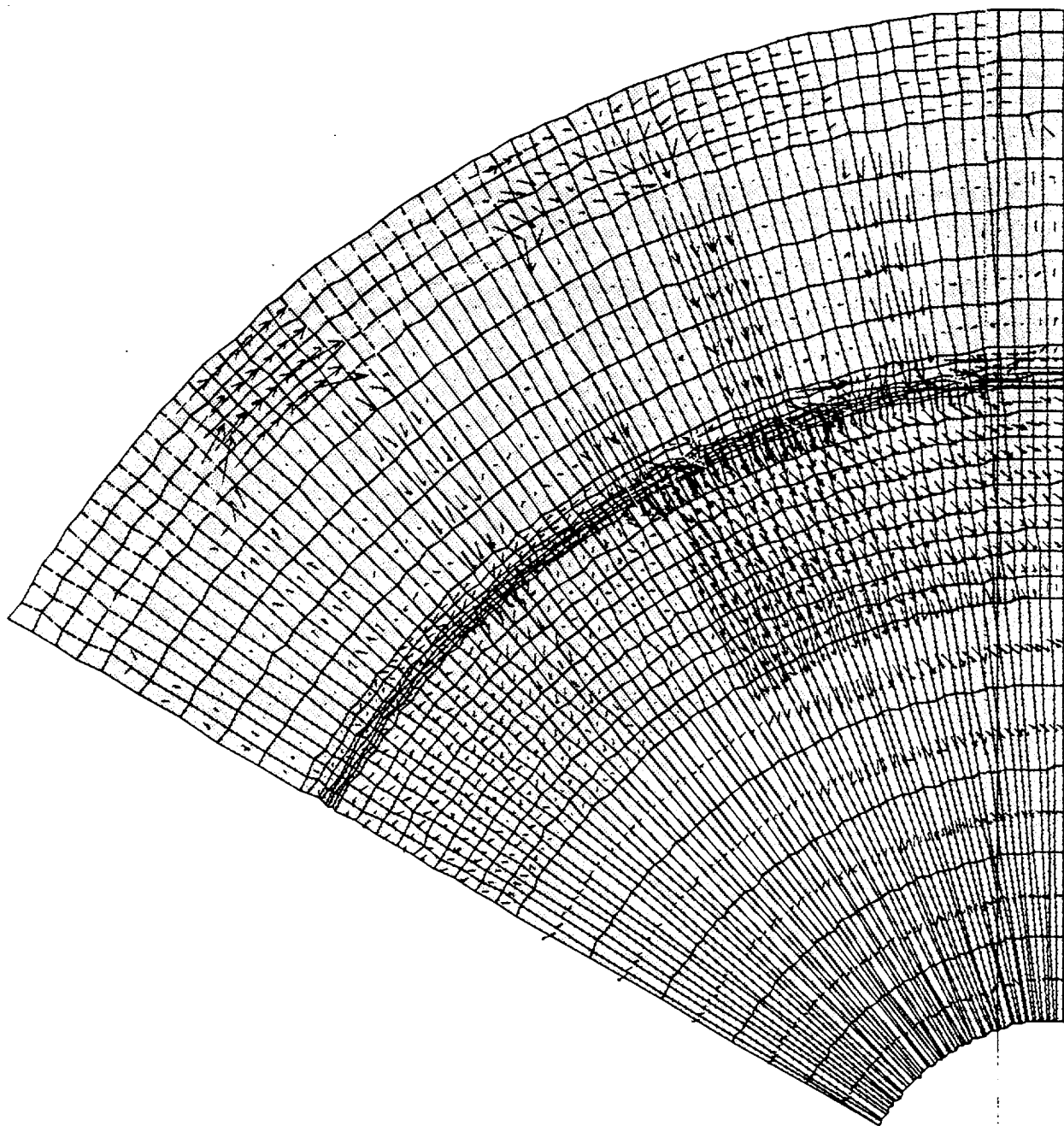


TITLE FLUX PLOT (TESLA) FOR TORQUE ANGLE TWO


```

ANSYS 4.4A
MAR 4 1992
17:59:01
POST1 VECTOR
STEP=2
ITER=10
BMAG
ELEM=561
0.208296
0.416031
0.62375
0.8315
1.039
1.662
1.87
ZV =1
DIST=0.02915
XF =0.0315
YF =0.025115

```



Out[4]=

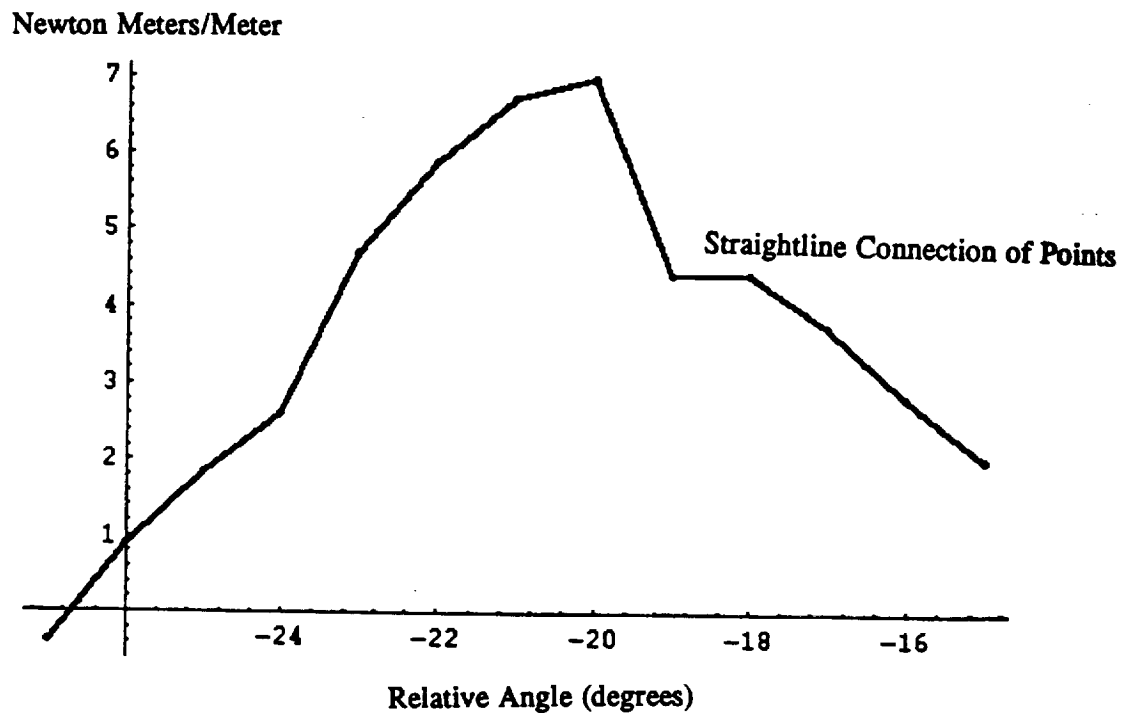
-Graphics-

```
tbl={{-27,-0.402},{-26,0.887},{-25,1.827},{-24,2.607},  
{-23,4.696},{-22,5.861},{-21,6.716},{-20,6.976},  
{-19,4.407},{-18,4.416},{-17,3.727},{-16,2.806},{-15,2.009}}
```

```
tblpts=ListPlot[tbl]
```

In[6]:=

```
Show[tblpts,stlin]
```



Torque Versus Torque Angle For First Motor Configuration

**DISCUSSION
OF
RESULTS**

DISCUSSION OF RESULTS

As mentioned in the APPROACH USED section there were three avenues of investigation followed in this research.

The first of these was the development of the power train optimization methodology. This method is in place. It allows the designer to determine the spur gear and roller screw reduction factors in such a way as to match the load (the rocket engine) to the actuator's electric motor in such a way as to obtain maximum load acceleration (and hence bandwidth) while at the same time minimizing the power needed by the actuator and attaining the required maximum horsepower and stall torque. The graphical presentations (3D and contour plots) which are used to display the results yield a "feel" for the relationships involved. The key to this investigation was the use of the relationship between the inertia of the pinion gear and its mating gear. Use of this relationship allowed finding a unique solution to the determination of the gear reduction factors. Without its use the two factors (n and l) involved are factors of each other and thus do not admit a unique but rather only a relative maximization of the load acceleration. Some further work is suggested to determine if the "detuning" process which is necessary to adjust the reduction factors from their maximum acceleration values so as to meet stall torque and maximum horsepower requirements can be improved. However, for the

slower turning motor selected in the point design the least detuning is required of all the motors tested.

The servoloop design procedure has been established. It involves the use of three loops utilizing the actuator delivered force, the actuator position and the actuator velocity as the three feedback quantities (note that the position, velocity, etc. of the rocket engine itself are stipulated to be unmeasurable). The key feature here is the use of the actuator force as a feedback quantity. Its use allows the rocket engine to follow the actuator motion over a wide bandwidth (4.2 Hertz in the point design) and controls the engine motion well in the face of disturbance forces applied to the rocket engine. The designs were carried out using classical root locus and frequency response methods on a linear model with the ground rules of having no conditionally stable loops and minimum electronic gain. Even so the electronic gain required in the position loop seems high, although of a value already attained in the MSFC building 4666 actuator laboratory. This is because of the large bandwidth required of this system. The electronic designers may have to expend effort in controlling the system noise to achieve the required gain levels. The point design was exercised in the simulations under a variety of nominal and off nominal conditions. These latter included limiting the torque from the electric motor, the additional of some friction acting on the rocket engine, the use of

elastic end of travel mechanical stops and the most undefined condition of all i.e. the introduction of various levels of start/stop induced disturbance forces on the rocket engine. This latter condition produced perhaps the most serious problem. At the larger values of force the engine traveled beyond any reasonable limit. A solution for this particular case was found which requires the reconfiguration of the electronic amplifier so that the motor acts as a current limited shorted generator (the electronic designers indicated this could be done relatively easily). Arguably the next most serious condition exists when the actuator hits the mechanical stops at the end of stroke. The results achieved in this study indicate that every effort should be made to avoid this condition but that if it does occur the softer the stop the better. For the relatively simple stop modeled a value of the compliance of the stop was obtained for stable operation of the actuator when contacting the stop ("bouncing on and off the stop"). The mechanical designers would have to be consulted to determine how soft a stop they could reasonably design.

The third area of investigation is that of the design of an electric motor to meet the demands of the point design. Progress to date includes setting up access to the ANSYS 4A finite element analysis code, obtaining the requisite manuals and tutorial materials, learning the computer languages involved and using the electromagnetic analysis of

the program. The electromagnetic analysis features have been applied to a first motor configuration and investigation is proceeding as to its torque producing capabilities. Physical interpretation of the flux vector plots in light of the Maxwell stress relationship is yielding valuable physical insight into the torque generation phenomena and has already resulted in suggesting directions which the next iteration of the motor configuration will take.

**CONCLUSIONS
AND
RECOMMENDATIONS**

CONCLUSIONS AND RECOMMENDATIONS

The overall conclusion is that the design and use of the electric actuator is feasible. The overall recommendation is that development be continued on three fronts. The first of the three is the continued design, fabrication and laboratory test of hardware. The second is the continued upgrading of the analytical models. The third is to continue work on optimizing the electric motor's various design features.

The power train design methodology is in place. The recommendation is to pursue a little more investigation into the detuning process. However, not too much change should be anticipated from the currently achieved values of reduction factors.

The servoloop design methodology is in place. The recommendation is that the models be continually updated as new data become available and that effort be continued to define the start/stop transient scenario. Some further level of detail in the representation of the pulse width modulated (PWM) amplifier is required if it is desired to calculate definitive profiles of the current and power drawn from the electrical supply. It is further recommended that the servo loops be mechanized in sample data form i.e. use a microprocessor in the next electronic iteration. Such mechanization would allow easy reconfiguration such as may

be needed to handle the start/stop transient. In general this would then require negligible hardware changes to accommodate changing loads, motors etc from application to application. Using a sampling frequency of a few hundred Hertz, which is well within the present state of the art, would necessitate only a straightforward design effort.

The electric motor design looks encouraging. Clearly several more design iterations are needed to optimize the torque production of the motor. After that the thermal models will have to be built and investigated. Whatever the configuration considered the shaft critical speed will have to be calculated as well as the stresses in the shaft under both nominal and off nominal conditions of operation.

APPENDICES

APPENDIX A:
MAXIMUM POWER TRANSFER CONSIDERATIONS

APPENDIX A: Maximum Power Transfer Considerations

Elsewhere in this report is derived an expression which if used in the design process will yield the maximum possible acceleration (and hence bandwidth) of the rocket engine for given electric motor, pinion and roller screw inertias. It was of course emphasized that this did not correspond to maximizing the acceleration of any other portion of the power train.

What will be shown in this appendix is that the determination of the most efficient transfer of power from the energy source (i.e. the power bus) to the rocket engine motion is satisfied by the same relationship as the requirement for maximum acceleration. Thus this happy result also satisfies one of the initial design goals, i.e. to minimize the required power while maximizing the acceleration or bandwidth possible when commanding the motion of the rocket engine.

In the context of regarding the actuator-rocket engine system as a linear network composed of lossless reactive circuit elements (the inertias) and a torque source, there are available a number of power transfer theorems from various sources (e.g. text books such as "Communications Circuits" by L. A. Ware and H. R. Reed, John Wiley and Sons, Second Edition, 1947). Most of the references are aimed specifically at electrical power transfer, but the analogies

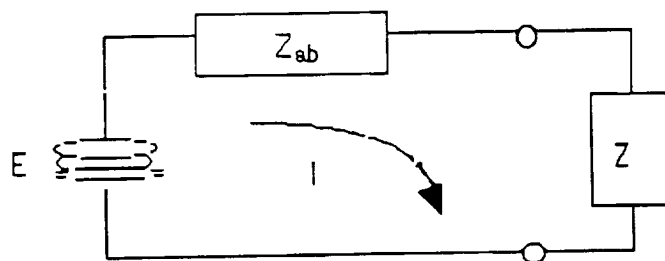
are straight forward, i.e. voltage to torque, current to velocity, capacitance to inertia etc. Thus they are readily used here.

The theorems take on a number of forms depending upon the specific situation (e.g. depending upon what is available or unavailable for change, i.e. tuning). The form applicable here is as follows.

If a generator which feeds through a network is to supply maximum power to an impedance Z (the load) and if the angle of Z is fixed (our case), then the absolute values of Z and Z_{ab} (the generator impedance) must be equal.

Note that the complex representation of impedance is being used here and that in our assumed representation (without energy dissipation) all the Z 's will be pure reactance, e.g. $j\omega l$ for an inertia.

Development of the proof applicable to this case follows the general development as follows.



$E \cong \text{Torque}$
 $I \cong \text{Velocity}$

$$I = \frac{E}{Z + Z_{ab}}; \text{ let } Z = R' + jX' \text{ and } Z_{ab} = R + jX$$

then

$$I = \frac{E}{R' + jX' + R + jX} = \frac{E}{(R' + R) + j(X' + X)}$$

rationalize

$$I = \frac{((R' + R) - j(X' + X))E}{(R' + R)^2 + (X' + X)^2}$$

There are several ways to calculate power using Cartesian complex representations of E (torque) and I (velocity). A very convenient one is the so called conjugate method of calculating real and reactive power. The method may be stated as follows:

If the conjugate of I, that is the Cartesian expression of I with the sign of the j or imaginary component reversed, is multiplied by E in Cartesian form, the result is a complex quantity the real part of which is the real power (i.e. the power that makes things hot etc.) and the j or imaginary part of which is the reactive or wattless power (i.e. causes power to oscillate in to and out of the circuit elements).

This form of the power expression may be found in "Alternating Current Circuits" by R.M. Kerchener and G. F. Corcoran, John Wiley, 1951, pgs 88-89. Applying this conjugate method the various powers associated with the circuit are given below.

Total power delivered by the source as shown immediately below.

$$P_{wr} = EI' = \frac{E^2 \{ (R' + R) - j(X' + X) \}}{(R' + R)^2 + (X' + X)^2}$$

From which the real power delivered is (i.e. that dissipated as heat)

$$P_{wr} - \text{real} = \frac{E^2 \{ (R' + R) \}}{(R' + R)^2 + (X' + X)^2}$$

in our case this zero because the source resistance and the load resistance are both zero.

The total reactive or wattless (i.e. non dissipative) power (which oscillates into and out of the load and source) is

$$P_{\text{VARs Developed}} = \frac{E^2 \{ (X' + X) \}}{(R' + R)^2 + (X' + X)^2} = \frac{(X' + X)E^2}{(X' + X)^2} = \frac{XE^2}{(X' + X)^2} + \frac{X'E^2}{(X' + X)^2}$$

the first term on the right is the power delivered to the reactive load i.e.

$$P_{\text{Load}} = \frac{X'E^2}{(X' + X)^2}$$

and the second, the power to the source reactance (inertia)

$$P_{\text{Source}} = \frac{XE^2}{(X' + X)^2}$$

To prove the theorem maximize the power to the load with respect to X' as

$$\frac{\partial \left(\frac{P_{\text{Load}}}{E^2} \right)}{\partial X'} = \frac{\partial \{ X[X' + X]^{-2} \}}{\partial X'}$$

$$= \frac{-2X'}{[X' + X]^3} + \frac{1}{[X' + X]^2} = 0$$

$$= \frac{-2X}{[X' + X]^3} + 1 = 0$$

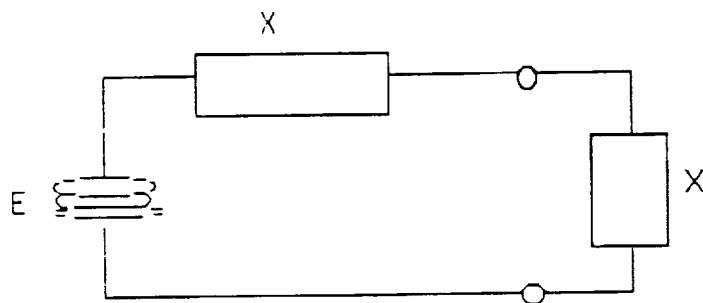
or $-2X' + X + X' = 0$

so $X = X'$

This best case then assures that for a given value of torque (E) available, the maximum amount of power will be delivered to the load (recall this applies to a linear system).

To further an appreciation of this theorem, consider three cases. These three are for the best (i.e. a perfect impedance match) and the cases where x' is less or greater than the best (mismatched impedances).

In general the equivalent circuit is



for generality let $X = \alpha X'$

$$\text{Power from source} = \frac{(X' + X)E^2}{(X' + X)^2} = \frac{E^2}{(X' + X)} = \frac{E^2}{(1 + \alpha)X} \equiv P_s$$

$$P_S = \frac{E^2}{(1+1/3)X} = \frac{3}{4} \frac{E^2}{X} = 0.75 \frac{E^2}{X}$$

$$P_{Load} = \frac{1/3 E^2}{(1+1/3)^2 X} = \frac{1/3}{(4/3)^2} \frac{E^2}{X} = \frac{3}{16} \frac{E^2}{X} = 0.1875 \frac{E^2}{X}$$

$$P_{Source} = \frac{E^2}{(1+1/3)^2 X} = \frac{9}{16} \frac{E^2}{X} = 0.5265 \frac{E^2}{X}$$

Note that for this case 50% more power is supplied by the source compared to the best or $\alpha=1$ case, but that the load receives only 75% of the power it did in the $\alpha=1$ case.

In the same spirit as was done previously, the following graphs are offered. There is however a complication involved. One has to be simultaneously aware of the power drawn from the source and of the power delivered to the load. The examples above show concrete evidence by example of this. Figures A-1 - A-3 are plots of the ratio of power actually drawn from the source to the power that would be drawn from the source under perfectly matched conditions. This is developed as follows.

$$\frac{\text{Power from source (actual)}}{\text{Power from source (matched)}} = \frac{\frac{E^2}{(1+\alpha)X}}{\frac{E^2}{2X}} = \frac{2}{(1+\alpha)}$$

Plots A-4 and A-5 are plots of the power delivered to the load divided by power supplied the network when the source and load impedances are matched. This is developed as

Immediately below is a plot of the ratio of the actual power delivered by the source to that which would be delivered if the load impedance matched the source impedance. In these two plots one notes that the power drawn from the source is ideally given by the ratio of one.

In[5]:=

$p1=2/(1+a)$

Plot[p1,{a,0,10}]

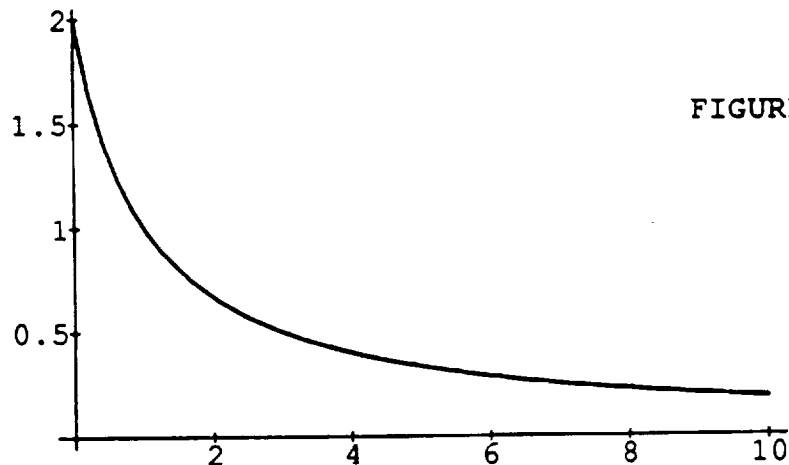


FIGURE A-1

This demonstrates the ideal value of the ratio (one occurring when alpha equals one). Note that as the value of alpha decreases the power ratio approaches two as compared to the ideal ratio of one when the load is matched to the source. As the mismatch parameter gets larger and larger less and less power is drawn from the source for use anywhere.

`In[6]:=`

```
p1=2/(1+a)  
Plot[p1,{a,0,2}]
```

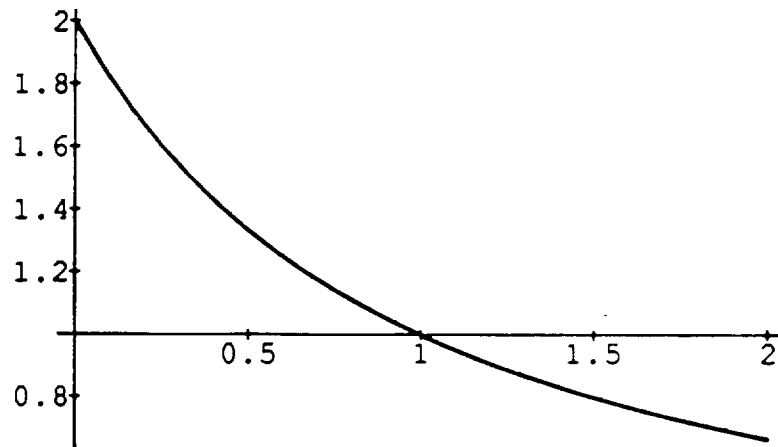


FIGURE A-2

This demonstrates the ideal value of the ratio (one, occurring when alpha equals one). Note that as the value of alpha decreases the power drawn from the source approaches two and that as it increases the power drawn from the source decreases toward zero.

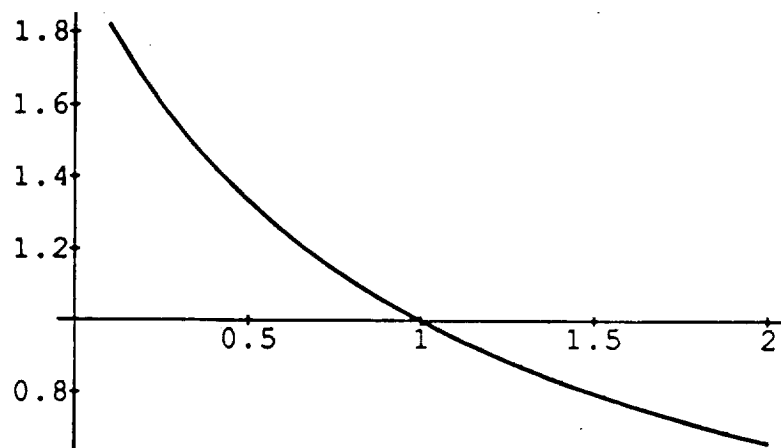


FIGURE A-3

The figures below plot the ratio of power actually delivered to the load to that which can be delivered to the load when the load is properly matched to the source (the maximum or best possible ratio is one-half the other half goes simultaneously to the source impedance).

In[1]:=

```
pwr3=(2*a)/((1+a)^2)  
Plot[pwr3,{a,0,10}]
```

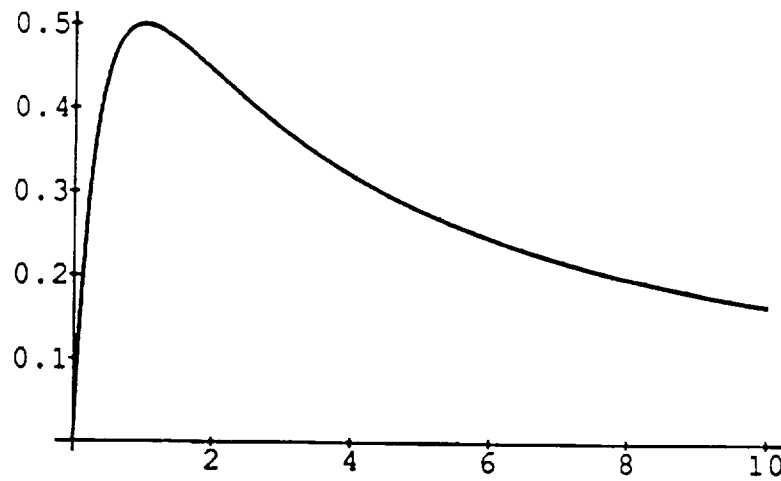


FIGURE A-4

The region around alpha equals one is expanded (as before) for clarity directly below. Recall the best value is one half.

In[2]:=

```
pwr3=(2*a)/((1+a)^2)  
Plot[pwr3,{a,0,2}]
```

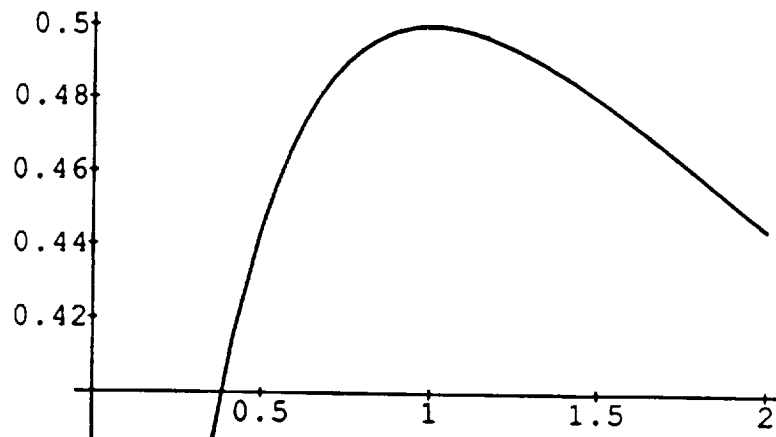


FIGURE A-5

Out[2]=

-Graphics-

In[4]:=

```
plt1=2/(1+a)  
plot1=Plot[plt1,{a,0,2}]
```

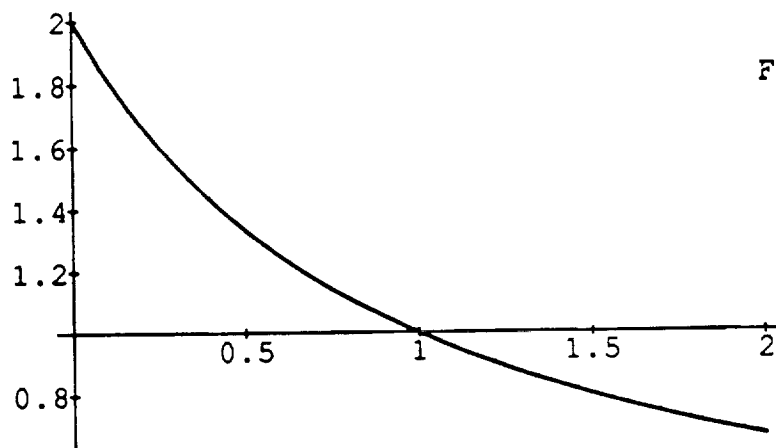


FIGURE A-6

Out[4]=

-Graphics-

In[5]:=

```
plt2=(2*aa)/((1+aa)^2)  
plot2=Plot[plt2,{aa,0,2}]
```

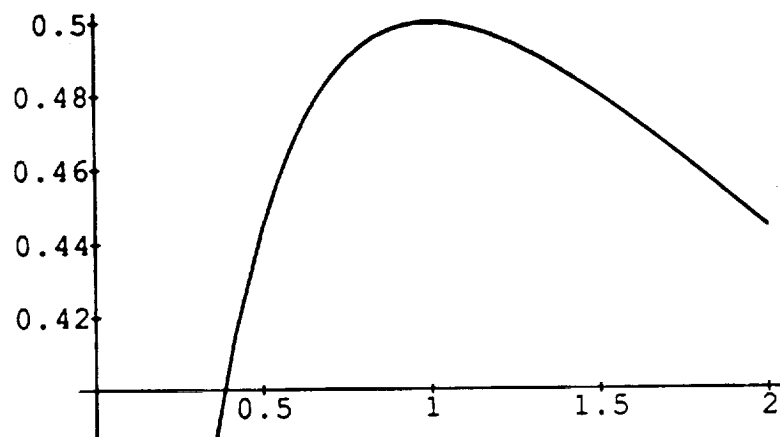


FIGURE A-7

Out[5]=

-Graphics-

$$\frac{\text{Power to Load (actual)}}{\text{Power from source (matched case)}} = \frac{\frac{\alpha E^2}{(1 + \alpha)^2 X}}{\frac{E^2}{2X}} = \frac{2\alpha}{(1 + \alpha)^2}$$

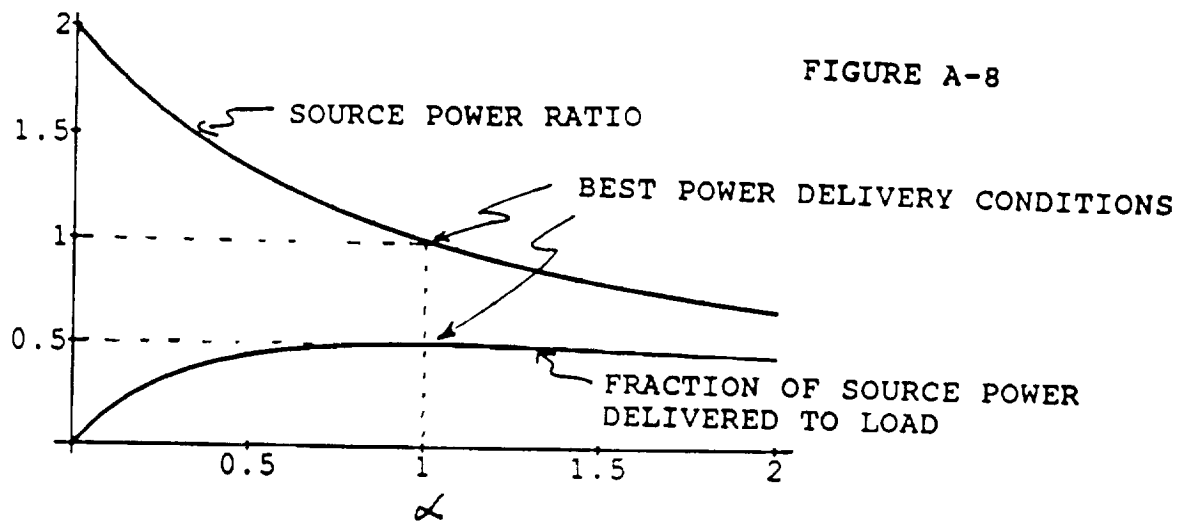
What the power maximization procedure does is select the values of circuit parameters which for a given torque level (E) transfers from the source to the load the maximum amount of power possible. This process involves both the power drawn from the source (a variable) and the fraction of that power actually delivered to the load.

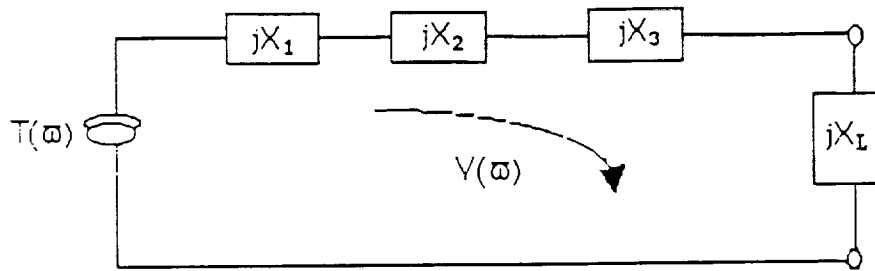
Arguably, Figure A-8 shows best that two ratios or conditions have to assume the proper values to achieve the maximum power transfer from the motor to the load at a given torque level.

A set of calculations such as were used in the examples (i.e., for $\alpha = 1/3, 1, 3$) may be used to evaluate the effect of a mismatch on power considerations.

As examples of the use of the maximum power transfer theorem consider the cases of the MSFC designed 2 motor case and then consider the best transient design case using the 15 HP Allied Signal data.

In each case the applicable equivalent circuit is given below.





In this equivalent circuit all the impedances except for the load itself are considered to be part of the source impedance. This is so because the desire is to move as much power as possible from the source to the load i.e, it is the load you are really interested in moving.

The first example considers the case of the MSFC designed 2 motor actuator. In this case all the inertias and gear ratios are given. Thus the power ratios developed earlier are evaluated only.

The next calculation considers the case in which the spur gear ratio and the roller screw lead were optimized for best transient response (all inertias and masses held at MSFC chosen values).

First example.

$$\begin{aligned}
 X \equiv X_1 + X_2 + X_3 &= J_M + (1 + n^2)J_p + \frac{J_{\text{Screw}}}{n^2} \\
 &= (2)(1.03)(10^{-2}) + (101)(19 \times 10^{-6}) + \frac{.064}{100}
 \end{aligned}$$

Note: The value of J_p (19×10^{-6}) was gotten from the undated Cornelius memo. Its value should be checked against a value calculated from the actual gear used.

$$X = 2.06 \times 10^{-2} + 0.1919 \times 10^{-2} + 6.4 \times 10^{-4} = 0.023159$$

$$X' = X_L = \frac{55}{\frac{2\pi(10)^2}{0.4}} = 2.23 \times 10^{-3}$$

$$\alpha = \frac{X_L}{X_1 + X_2 + X_3} = \frac{2.23 \times 10^{-3}}{2.3159 \times 10^{-2}} = 0.096$$

Recall: $\alpha = 1.0$ is a maximum power or perfect match.

$$\frac{\text{Power to Load (actual)}}{\text{Power from source (matched case)}} = \frac{2\alpha}{(1 + \alpha)^2} = \frac{(2)(0.096)}{1.096^2} = 0.1598$$

Recall: This ratio (above) is 0.5 in the best or matched case, thus 31.96% of the power ($0.1598/0.5$) is getting to the load that would get there in the matched case.

$$\frac{\text{Power from source (actual)}}{\text{Power from source (matched)}} = \frac{2}{(1 + \alpha)} = \frac{(2)}{1.096} = 1.825$$

Recall: This last ratio would be 1.0 for the best power matched case. Thus the motor must provide 82.5% more power for a given scenario than it would in the matched case.

Second example.

$$\begin{aligned} X &= (2)(1.03)(10^{-2}) + (1 + 7.62^2)(19 \times 10^{-6}) + \frac{0.064}{7.62^2} \\ &= 2.06 \times 10^{-2} + 0.112 \times 10^{-2} + 0.1102 \times 10^{-2} = 0.0228 \end{aligned}$$

$$X' = \frac{55}{\left[\frac{2\pi(7.62)}{1.312} \right]^2} = \frac{55}{1331.7} = 0.0413$$

$$\alpha = \frac{0.0413}{0.0228} = 1.811 \quad (\alpha = 1 \text{ is a perfect power match})$$

$$\frac{2\alpha}{(1+\alpha)^2} = \frac{2(1.811)}{(2.811)^2} = 0.4585 \quad (.5 \text{ is perfect})$$

$$\frac{2}{(1+\alpha)} = \frac{2}{1+1.811} = 0.712 \quad (1.0 \text{ is perfect})$$

Thus this system draws about 30% less power from the source than in the matched case.

In conclusion and summary it has been shown in the section beginning on pages 4-10 that proper matching (through the selection of the gear ratios) of the rocket engine mass to the actuator with its gearing and various masses results in maximum acceleration or deceleration of the rocket engine regardless of the particular time domain trajectory of the torque generated by the electromagnetics of the electric motor. This demonstration has also shown that the mass of the rocket engine and the mass of the actuator referred to any given point in the mechanical circuit (e.g. the tailstock or the shaft of the electric motor) are equal. Because mechanical kinetic energy is proportional to the square of the velocity of the mass involved and because the matching has maximized the acceleration/deceleration of the rocket engine mass then the first time integral of this quantity

which is velocity will likewise be extremized. Because the matched case results in the maximum velocity change of the rocket engine mass the maximum velocity change of the rocket engine mass the maximum energy is transferred to or from the rocket engine for a given torque profile. Because the masses of the rocket engine and the actuator are equal (when referred to the same coordinates) in this matched case there is equal kinetic energy stored in the rocket engine and the actuator masses in the best power transfer case. As the design is detuned (e.g. to meet stall torque specifications with a given electric motor) from the optimally matched case the power/energy transfer to or from the rocket engine mass will diminish for a given power input from the source thus requiring more power transfer between the source (ultimately the electrical bus) and the actuator than in the matched case to deliver the same amount of kinetic energy in the rocket engine (or to be dissipated in the case where the velocity is slowing down).

Thus it is seen that matching the rocket engine to the actuator in a manner so as to maximize its acceleration also results in best utilization of power and energy.

APPENDIX B:
WHY A SMALL MOTOR AND A LARGE
GEAR RATIO MAY NOT BE WHAT IS
WANTED

WHY A SMALL MOTOR AND A LARGE GEAR RATIO MAY NOT BE WHAT IS WANTED

It has been stated elsewhere in this report that to obtain maximum possible performance from a motor, gear train and load combination it is necessary to match carefully the motor to the load by careful selection of a gear ratio between the two and then repeat the matching process for a number of differing motors to ascertain the best possible load acceleration performance. The results may be counter intuitive to a casual observer because in many minds it is natural to think in terms of the motor and its speed and acceleration rather than the speed and acceleration of the load. In the present design environment it is possible to select motors of the same rated horsepower with different available torque capacities because of different speeds at which the motors are rated (and they therefore have differing attendant polar mass moments of inertia) as well as being able to select independently the gear ratio(s). Thus in the present case only the load is a fixed quantity - and it is the load in whose motion one is interested. The results of this procedure are presented in this report for the multipass gear train case but a simpler example will perhaps help to cement the principles involved.

Consider the case of a motor coupled to a load by a simple one pass gear train. Now examine the accelerations of the

motor and the load. The system inertia referred to the motor shaft will be given by

$$J_{tm} = J_m + J_l/n^2$$

while the system inertia referred to the load is given by

$$J_{tl} = n^2 J_m + J_l$$

where n is a step down gear ratio from the motor to the load and is greater than one in magnitude, J_t denotes a total inertia either at the load (l) or the motor (m), J_m is the motor rotor inertia and J_l is the load inertia.

The expression for the motor acceleration is given by

$$\text{accel}(m) = T/J_{tm} = T/(J_m + J_l/n^2)$$

and the load acceleration is

$$\text{accel}(l) = T n/(J_l + J_m n^2)$$

where T is the torque available from the motor.

Inspection of these expressions show immediately that to maximize the acceleration of a given motor n should be made as large as possible; in the limit the motor becomes

uncoupled from the load (J_l/n^2 approaches 0). Finding the maximum acceleration of the load is a more tedious matter but if the derivative of the load acceleration is taken with respect to n and the results set to zero the results become

$$n = \text{SquareRoot}[J_l/J_m]$$

$$\text{accel}(l)_{\text{max}} = T / (2 \text{ SquareRoot}[J_l J_m]).$$

Thus even in the simplest case finding the correct match of inertias through gear train ratio selection is more involved than maximizing the motor acceleration. And in this case for a given load different motors with different maximum torques and different inertias will produce different maximum load acceleration (which is desired for maximum bandwidth or speed of response). In this maximized load acceleration case the acceleration of the motor will be (by simple substitution) expressed by

$$\text{accel}(m) = T / (2 J_m)$$

which is certainly lower than could be achieved by a higher gear ratio (as n approaches infinity $\text{accel}(m)$ approaches T/J_m).

It is hoped that the simple example discussed above will help the intuitive reasoning process concerning motor and

gear ratio selection for a given load. Hopefully it lends insight into why the multipass gear case is somewhat involved to optimize with respect to load acceleration and motor-gear train selection, as has been done in this report.

Reference is made to Appendix G in which detailed calculations are presented. These detailed calculations result in choices of n and l , the spur gear and roller screw reduction ratios respectively. They show how in each case the selection of l is changed from its maximum acceleration producing value to another value. This is necessary because in addition to maximum acceleration (and minimum power consumption) the system is required to produce ten horsepower at an actuator velocity of five inches per second. Carrying on the theme of this Appendix these multipass results are plotted below. Note that the upper curve shows the maximum load acceleration possible with each of the motors investigated. Also note that the lower curve is a plot of the maximum acceleration possible after l is changed to meet the requirements as listed above. Examination of the figure shows that the choice a motor which develops its rated horsepower at a low rpm is the best choice from two viewpoints. First it is seen that the lower speed motor develops more load acceleration under all circumstances, thus producing the maximum bandwidth possibility. The second is that as the rated rpm decreases the difference between the maximum possible acceleration and

the "detuned" acceleration decreases. Thus the penalty of detuning from the maximum possible acceleration capability is minimized.

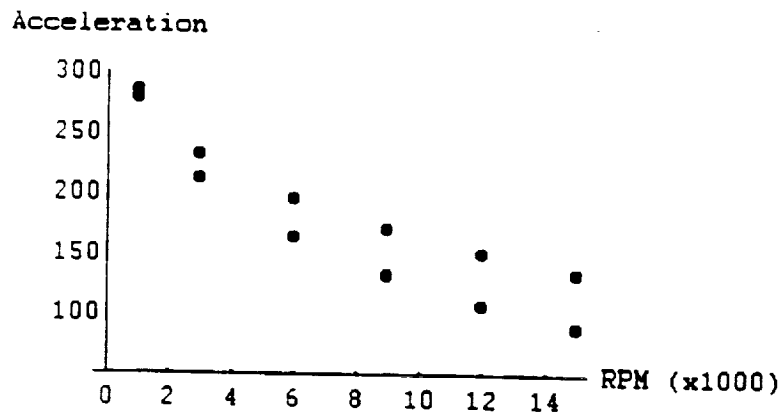
Comparison Plot Of Maximum Acceleration And Maximum Detuned Acceleration

In[93]:=

```
comp={{1,285.88},{1,278.448},
      {3,232.331},{3,211.703},
      {6,195.331},{6,163.757},
      {9,169.931},{9,131.194},
      {12,149.916},{12,106.407},
      {15,133.562},{15,87.114}}
```

In[103]:=

```
ListPlot[comp,Prolog->AbsolutePointSize[5],
          PlotRange->{50,300},AxesLabel->
          {"RPM (x1000)",
           "Acceleration"}]
```



Out[103]=

-Graphics-

**APPENDIX C:
VARIOUS ROLLER SCREW
RELATIONSHIPS**

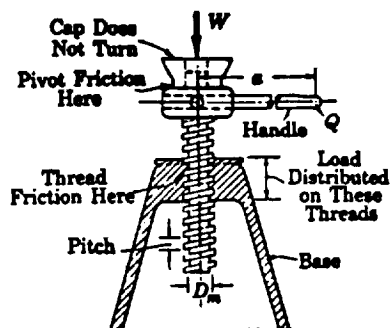
C. VARIOUS ROLLER SCREW RELATIONSHIPS

Modeling Roller Screw Kinematics and Dynamics

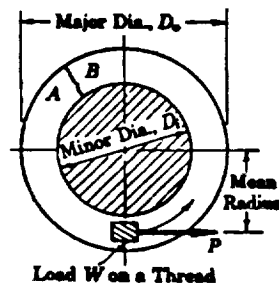
The first part of the following treatment concerning the force modeling draws heavily upon the same material in the book "Analytic Mechanics" by S.D. Chambers in collaboration with V.M. Faires, the MacMillan company, New York, 1949.

Screw threads are widely used not only to convert rotary motion to translational motion but also to achieve mechanical advantage. Examples of the use of screw threads to accomplish these types of ends include jacks, shaft straighteners, and a myriad of screw presses. In the present case a roller screw is used in the actuator to connect the rotary motion of an electric motor to the tailstock of the actuator thereby causing it to translate. This translation is in turn transmitted to the rocket engine by attaching the tailstock of the actuator to the structure of the rocket engine. With the foregoing in mind it is easily seen that mathematical relationships are required to relate the rotation of the shaft of the roller screw to the translation of the tailstock and to relate the various forces, torques and inertial effects to coordinate systems convenient for analysis.

To relate the forces and torques involved consider the picture of the screw jack shown below.



The first relationship to be developed is that between the axial screw force W and the torque applied to the jack handle (Q times a). Note that the load W produces a pressure between the threads in contact in the base of the jack. If the screw is turned the threads rub on each other so that the applied effort must be great enough not only to overcome the load W but also the frictional resistance. Observing that a thread is simply the equivalent to an inclined plane wrapped around a cylinder and that raising a load W on a jack is equivalent to pulling up a load along an inclined plane, the analysis is relatively easy to understand. One is never very sure what value the frictional resistance assumes but this development allows such data as are accumulated, especially by test, to be incorporated. Considering the next figure imagine the load W being pulled up the inclined plane by a force P perpendicular to the axis of the screw and always acting tangent to the mean circumference of the thread. The reduction of the area supporting the load does not affect the mechanics problem because the coefficient of friction is practically independent of the area. So, considering the thread to be unwrapped from the screw, one may picture the forces as shown on the second figure below.



R is the total plane reaction, the resultant of F' (the limiting frictional force) and N (the normal force). For these forces in equilibrium one writes from the sum of the forces in the x direction being identically zero (see figure below for the definition of the angles involved).

$$P=R \sin(\text{lamda}+ \text{phi})$$

Summing the forces in the y direction in a similar manner yields.

$$W=R \cos(\text{lamda}+\text{phi})$$

From dividing the two equations above one obtains the following.

$$P=W \tan(\text{lamda}+\text{phi})$$

Recalling that the force p is perpendicular to the axis of the screw shows that the torque or moment of P about the axis is

$$T= P \text{ Dm}/2$$

Thus if ones multiplies both sides of the expression for P by Dm/2, it is found that

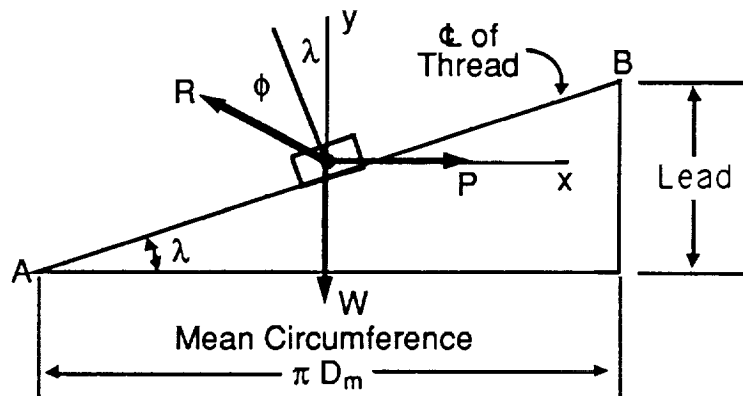
$$T=(W\text{Dm})/2 \tan(\text{Lamda}+\text{Phi})$$

and thus

$$T= (W\text{Dm})/2 ([\tan \text{Lamda}+\tan \text{Phi}]/[1-\tan\text{Lamda} \tan \text{Phi}])$$

where T is the torque that must be applied to the screw to raise the load W when the mean diameter of the thread is $\text{Dm}=(\text{Do}+\text{Di})/2$, where $\tan \text{Phi} = f$, the coefficient of friction, and where $\text{Lamda}=\arctan [\text{lead}/(\pi \text{ Dm})]$. The angle Lamda is called the lead angle. In single threads the lead is equal to the pitch, which is the axial distance between corresponding points on adjacent threads. Observe that the pitch is the reciprocal of the number of threads per unit

length. The larger diameter of the screw D_o is called the outside diameter or the major diameter; and the smaller diameter D_i is called the inside or minor diameter.



Note that

$$F = \tan \phi$$

which is by definition the coefficient of friction. If friction = 0 then

$$\tan \phi = 0$$

In which case

$$\text{Torque} = \frac{W D_m}{2} \tan \lambda ; \tan \lambda = \frac{\text{Lead}}{\text{Mean Circumference}} = \text{Constant}$$

$$\tan \lambda = \frac{\text{Lead}}{\pi D_m}$$

$$\text{Torque} = \left(\frac{W}{2}\right)(D_m)\left(\frac{\text{Lead}}{\pi D_m}\right) = \left(\frac{\text{Lead}}{2\pi}\right) W$$

Let

$$W = m \ddot{x}$$

$$T = \left(\frac{\text{Lead}}{2\pi}\right)(m \ddot{x}) = \left(\frac{m}{\frac{2\pi}{\text{Lead}}}\right) \ddot{x}$$

But

$$\theta = 2 \pi; x = \text{Lead}$$

$$\frac{\theta}{x} = \frac{2 \pi}{\text{Lead}}; \theta = \frac{2 \pi}{\text{Lead}} x; x = \frac{\text{Lead}}{2 \pi} \theta$$

So

$$x = \frac{\text{Lead}}{2 \pi} \ddot{\theta}$$

And

$$T = \left(\frac{m}{\left[\frac{2 \pi}{\text{Lead}} \right]} \right) \left(\frac{\text{Lead}}{2 \pi} \right) \ddot{\theta} = \left(\frac{m}{\left[\frac{2 \pi}{\text{Lead}} \right]^2} \right) \ddot{\theta} = J_{\text{eq}} \ddot{\theta}$$

So

$$J_{\text{eq}} = \frac{m}{\left[\frac{2 \pi}{\text{Lead}} \right]^2}$$

Observation

Unlike a spur gear ratio, which is dimensionless, the rotation to translation "gear ratio" has the dimension of 1/length. Thus more care than usual must be invoked with its use. For example if:

T is in lb - ft

m is in slug - ft²

J is in slug - ft²

Then

$$\frac{2 \pi}{\text{Lead}} \text{ is in ft}^{-1}$$

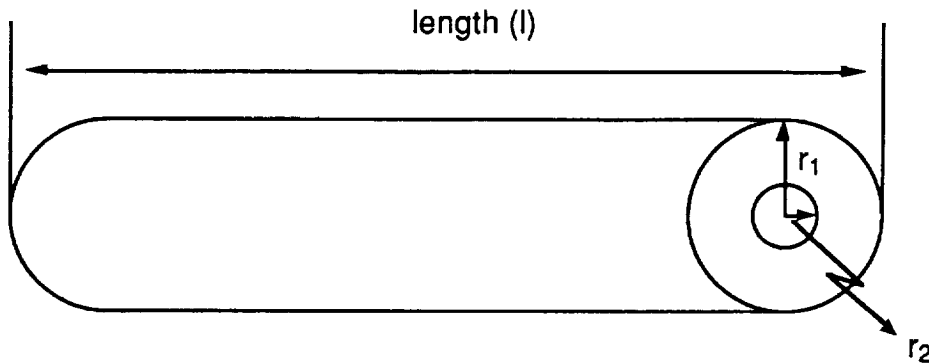
To validate

$$T = \left(\frac{m}{\left[\frac{2 \pi}{\text{Lead}} \right]^2} \right) \ddot{\theta}$$

$$lb - ft = \left(\frac{\left[\frac{lb - sec^2}{ft} \right]}{\left[\frac{1}{ft^2} \right]} \right) \left(\frac{1}{sec^2} \right) = lb - ft$$

So be careful of mixed units e. g. inches creeping into the calculations.

Effect Of Hollowing The Shaft Of The Roller Screw



One possible way to reduce the overall inertia of the system is to hollow out the inside of the roller screw. The following development investigates the effect that hollowing will have on the inertia contributed to the system by the roller screw. Treating the roller screw as a right cylinder, the inertia can be calculated as

$$J_{\text{Roller Screw}} = \frac{M r_1^2}{2}$$

where

$$M = \rho \pi r_1^2 l$$

ρ - Mass Density Of The Roller Screw Material

l - Length Of The Cylinder

r_1 - Radius Of The Roller Screw

Let the radius of the hollowed portion be

r_2

Then, the inertia of the hollowed portion is

$$J_{\text{Hollowed Portion}} = \frac{M r_2^2}{2}$$

where

$$M = \rho \pi r_2^2 l$$

ρ - Mass Density Of The Roller Screw Material

l - Length Of The Cylinder

r_2 - Radius Of The Hollowed Portion Of The Roller Screw

The total inertia of the roller screw is given by the following equation

$$J_{\text{Total Inertia}} = \frac{M r_1^2}{2} - \frac{M r_2^2}{2} = \frac{(\rho \pi l r_1^2) r_1^2}{2} - \frac{(\rho \pi l r_2^2) r_2^2}{2} = \frac{\rho \pi l}{2} (r_1^4 - r_2^4)$$

For an example, use a roller screw with the following characteristics

$$\rho = 7.3085 \times 10^{-4} \frac{\text{lbs} \cdot \text{sec}^2}{\text{in}^4} \quad (\text{Mass Density Of Steel})$$

$$l = 12.5 \text{ inches}$$

$$r_1 = 0.9449 \text{ inches}$$

Calculate the total inertia of the roller screw as the radius of the hollowed portion varies from 0 to 0.9449 inches.

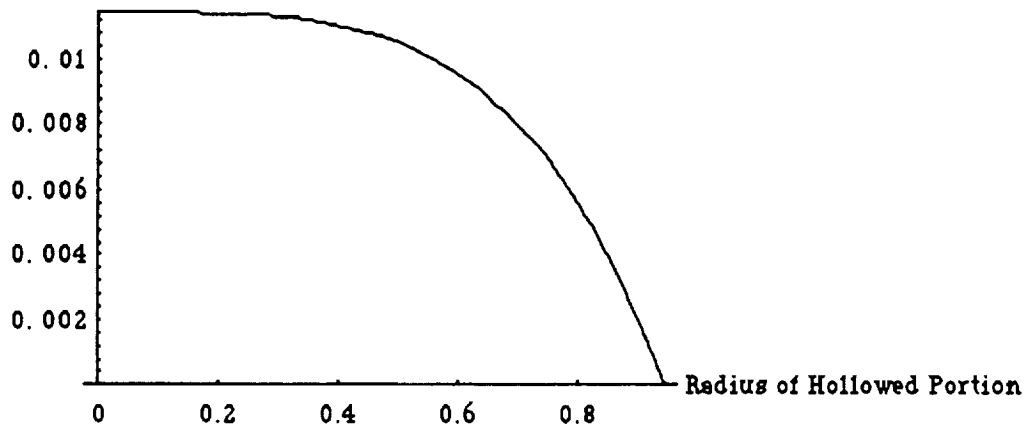
$$J_{\text{Total Inertia}} = 0.0143502[(0.9449)^4 - r_2^4] = 0.0114394 - 0.0143502 r_2^4$$

Define the total inertia of the roller screw as J

$$J = 0.0114394 - 0.0143502 * ((r_2)^{(4)})$$

Plot the roller screw inertia as the radius of the hollowed portion varies from 0 to 0.9449 inches

Total Inertia Of Roller Screw



The graph shows that as the roller screw is hollowed out, the total inertia does not change significantly until the radius of the hollowed portion becomes at least half the size of the original radius of the roller screw. An additional area of interest in considering hollowing shafts is the stress relationship in the shaft caused by pure torsion as a function of the radius of the hollowed portion of the shaft. The greatest stress will occur in the outside fibers and is given by the relationship

$$S_s = \frac{T r_1}{J}$$

where

T - Torque On The Shaft

r_1 - Outside Radius Of The Shaft

J - Polar Moment Of The Cross-Sections Area

$$[J = \frac{\pi}{2} (r_1^4 - r_2^4)]$$

Thus the ratio of stress to applied torque becomes

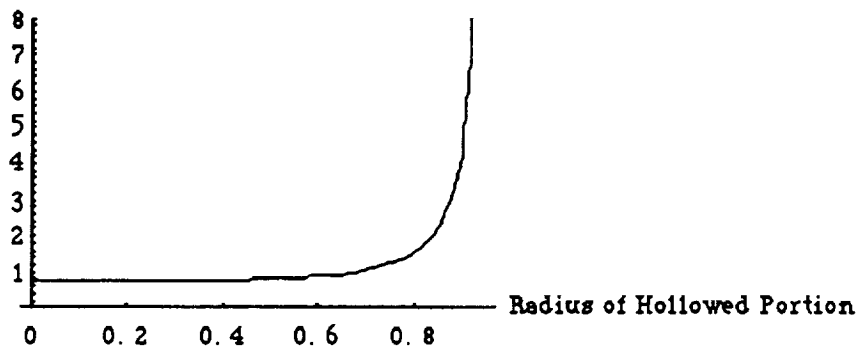
$$\frac{S_s}{T} = \frac{2 r_1}{\pi (r_1^4 - r_2^4)}$$

Define the ratio of stress to applied torque of the roller screw as RST

$$RST = 2 * (0.9449) / ((3.14159) * (((0.9449)^4) - (r_2^4)))$$

Plot the ratio of stress to torque as the radius of the hollowed portion varies from 0 to 0.9449 inches

Ratio of Stress To Torque



Comparing the two plots one observes that hollowing out the shaft does indeed reduce its mass moment of inertia but also increases the outer fiber stress. A value of about 0.65 inches would seem to be a compromise for this case. It would yield somewhat reduced inertia and not increase the outer fiber stress significantly. The buckling phenomenon and the combined stress problem would of course have to be evaluated by the designer to complete the design.

**APPENDIX D:
LOAD ANALYSIS**

D. LOAD ANALYSIS

Discussion Of Values Used For the Mass Of The Tailstock And Engine

The weight of the tailstock was estimated to be 100 lbs. This figure was based on data which was obtained from actuators which had actually been built previously. The mass of the engine referred to the actuator was estimated to be 55 lbs-sec²/in. This figure was taken from SSME data and is considered to be a representative estimate of the mass of the rocket engine referred to the actuator as it will be used on the National Launch System.

Calculation Of The Total Actuator Mass As Referred To The Tailstock

The total inertia seen at the tailstock is composed of five elements:

J_{Motor} ; $J_{\text{Pinion Gear}}$; $J_{\text{Bull Gear}}$; $J_{\text{Roller Screw}}$; $M_{\text{Tailstock}}$

The motor and pinion gear inertias must be reflected through both the spur gear train and the roller screw to the tailstock. The bull gear and the roller screw inertias must be reflected through the roller screw to the tailstock. To accomplish this multiply the motor and pinion gear inertias by the spur gear ratio(n) squared to reflect these inertias to the roller screw

$$(J_{\text{Motor}} + J_{\text{Pinion Gear}})n^2$$

Add the bull gear and roller screw inertias to this reflected inertia

$$(J_{\text{Motor}} + J_{\text{Pinion Gear}})n^2 + J_{\text{Bull Gear}} + J_{\text{Roller Screw}}$$

To reflect these inertias through the roller screw, multiply by the screw ratio $(2p/l)$ squared

$$[(J_{\text{Motor}} + J_{\text{Pinion Gear}})n^2 + J_{\text{Bull Gear}} + J_{\text{Roller Screw}}] \left(\frac{2\pi}{l}\right)^2$$

Finally, adding the mass of the tailstock this yields

$$[(J_{\text{Motor}} + J_{\text{Pinion Gear}})n^2 + J_{\text{Bull Gear}} + J_{\text{Roller Screw}}] \left(\frac{2\pi}{l}\right)^2 + M_{\text{Tailstock}}$$

The above equation is the total reflected actuator mass "seen" at the tailstock. From previous work (See MOTOR ANALYSIS) it has been shown that the mass of the motor dominates in the above equation. The mass of the pinion gear, bull gear, and roller screw contributes a small amount to the overall mass of the system and the mass of the tailstock is negligible.

APPENDIX E:
NASA/MSFC SPECIFICATIONS

E. NASA/MSFC SPECIFICATIONS

The following are the latest performance requirements obtained from MSFC. These specifications are based upon previously built actuators used on the SSME and were used as design points for the current electromechanical actuator. The current non-linear model shown previously meets all of these requirements.

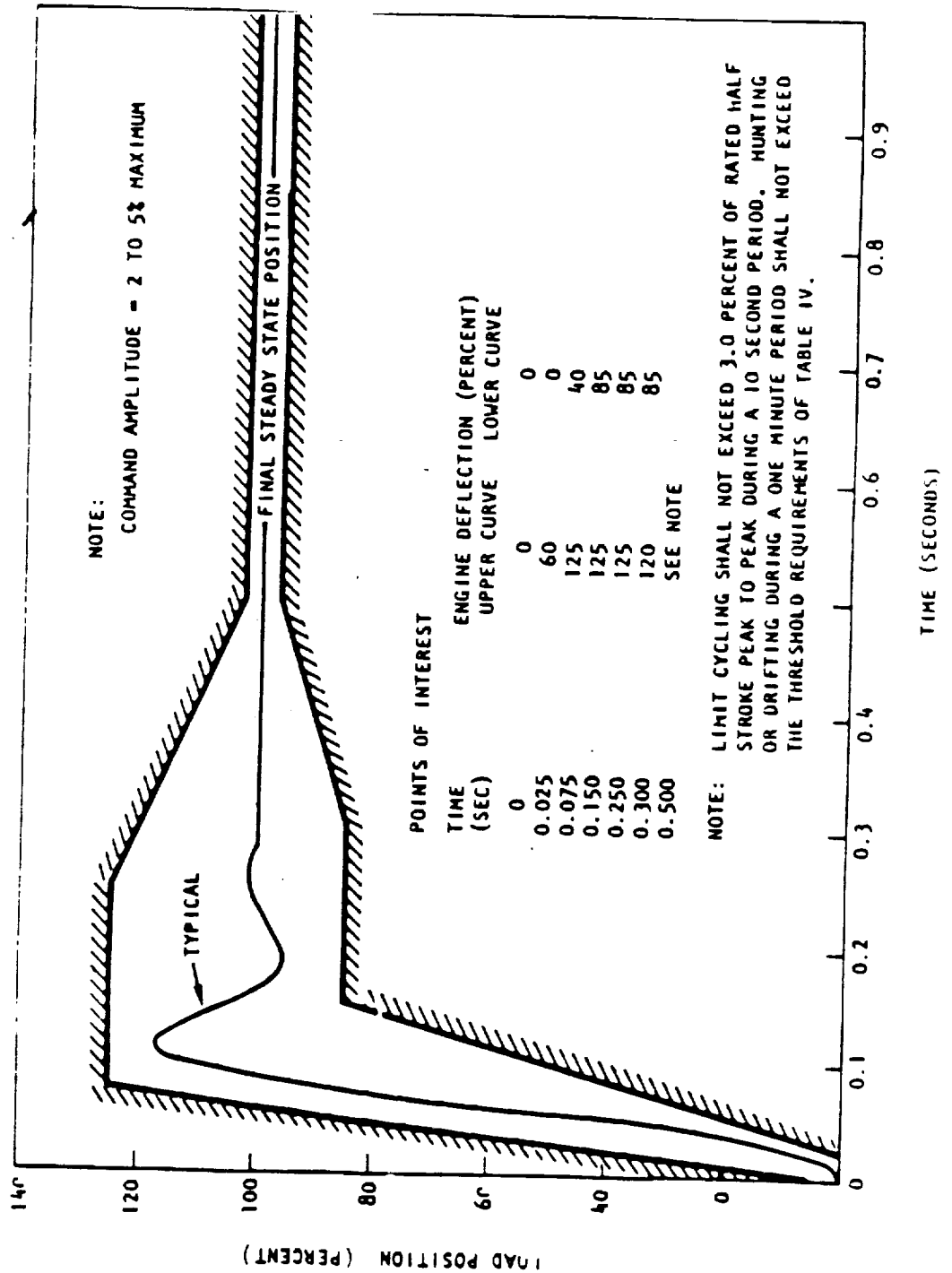
NUMBER

MC621-0015

REVISION LETTER

PAGE

32



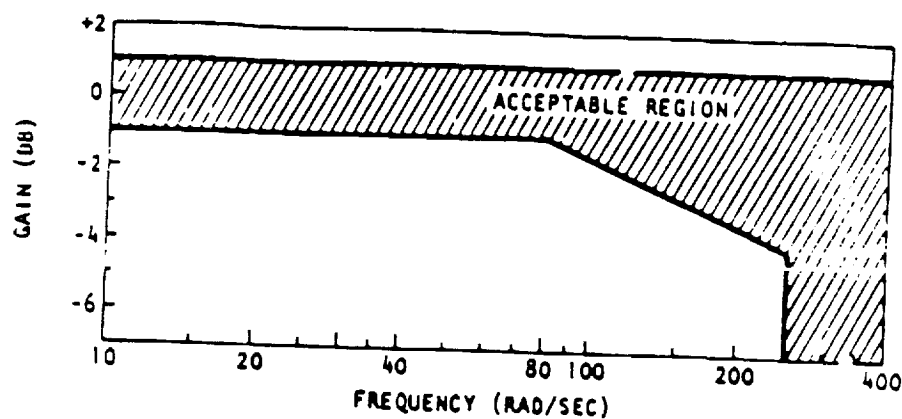


Figure 17a. Channel ΔP Transducer - Frequency Response Gain Requirements

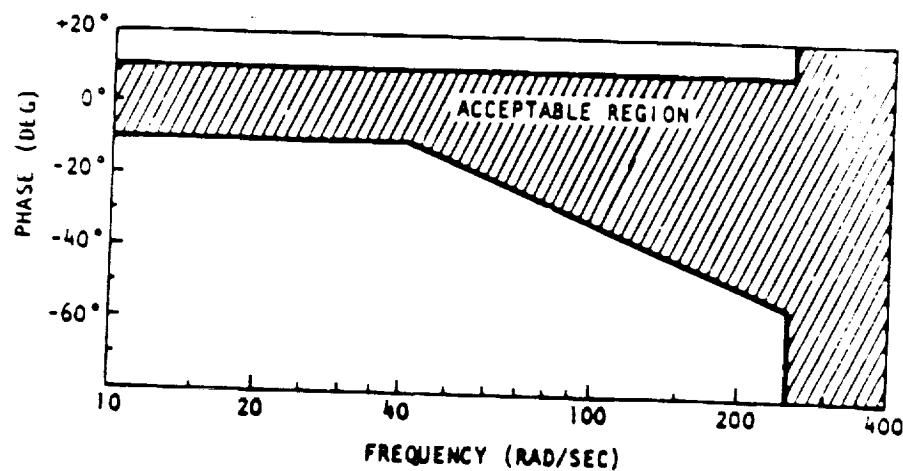
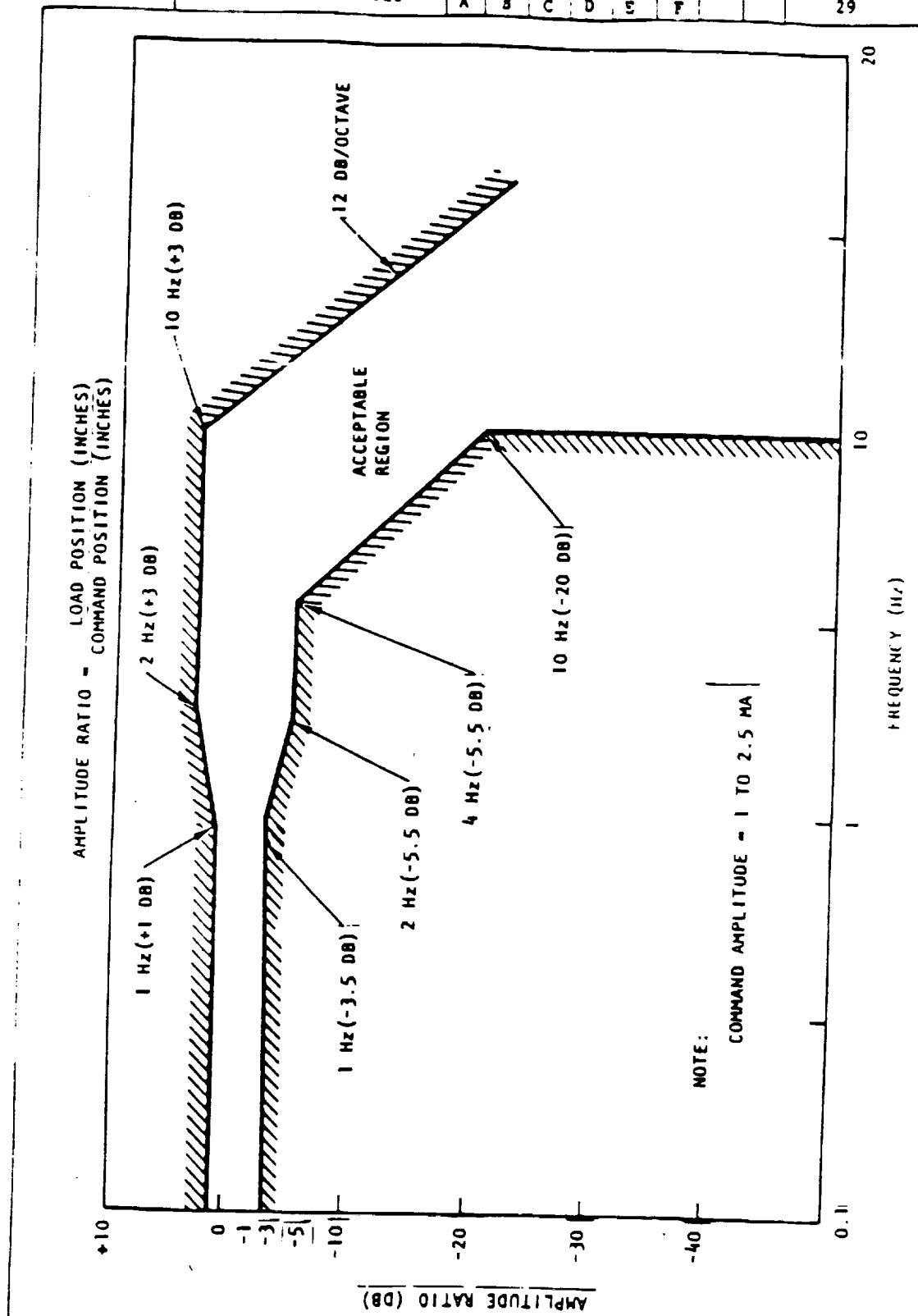
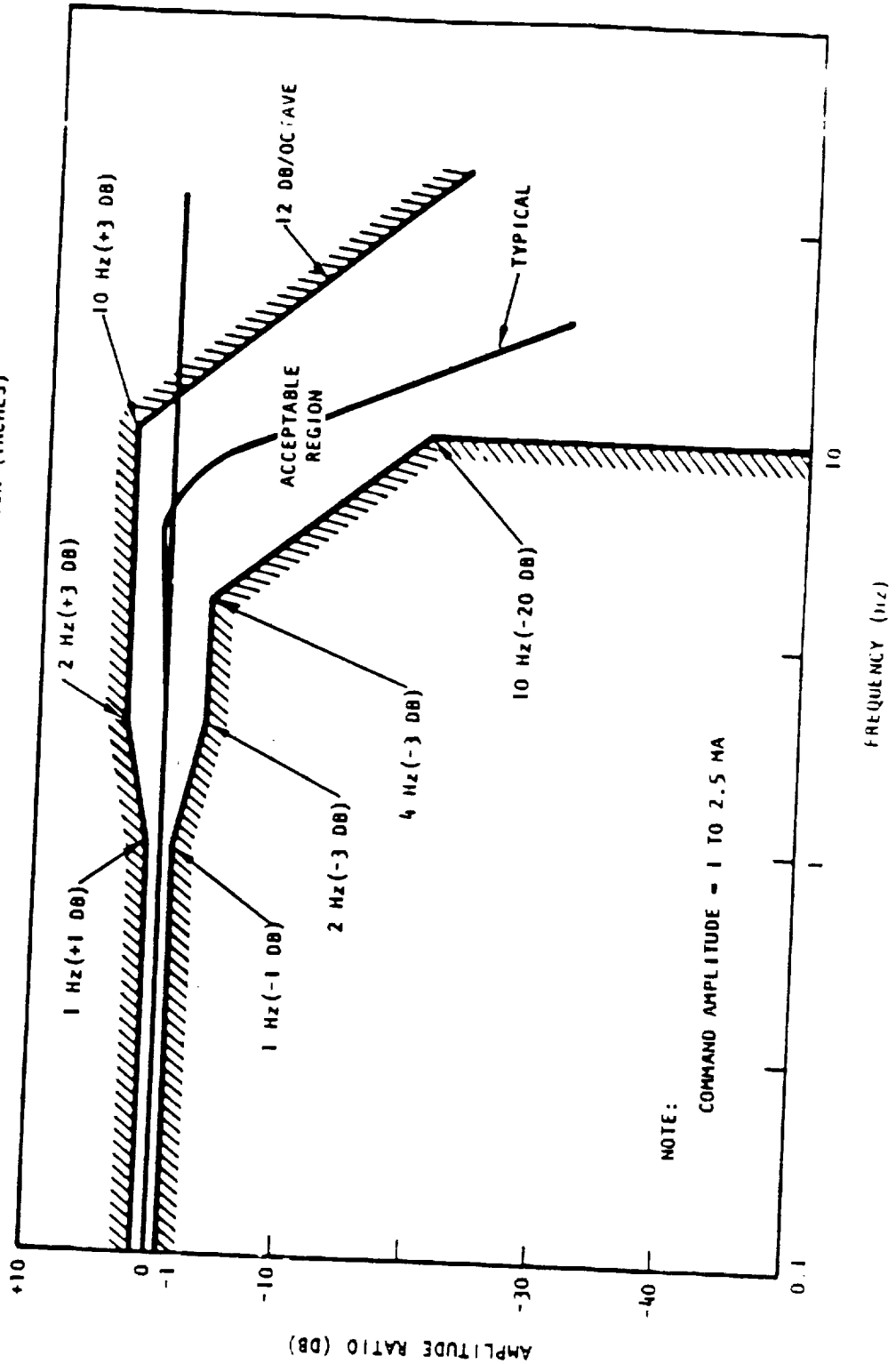


Figure 17b. Channel ΔP Transducer - Frequency - Phase Requirements



FORM M 131-4-2 REV 2-70

AMPLITUDE RATIO = $\frac{\text{LOAD POSITION (INCHES)}}{\text{COMMAND POSITION (INCHES)}}$



NOTE:

COMMAND AMPLITUDE = 1 TO 2.5 MA

NUMBER

MC621-0015

REVISION LETTER

PAGE

30

PHASE ANGLE = $\frac{\text{LOAD POSITION (INCHES)}}{\text{COMMAND POSITION (INCHES)}}$

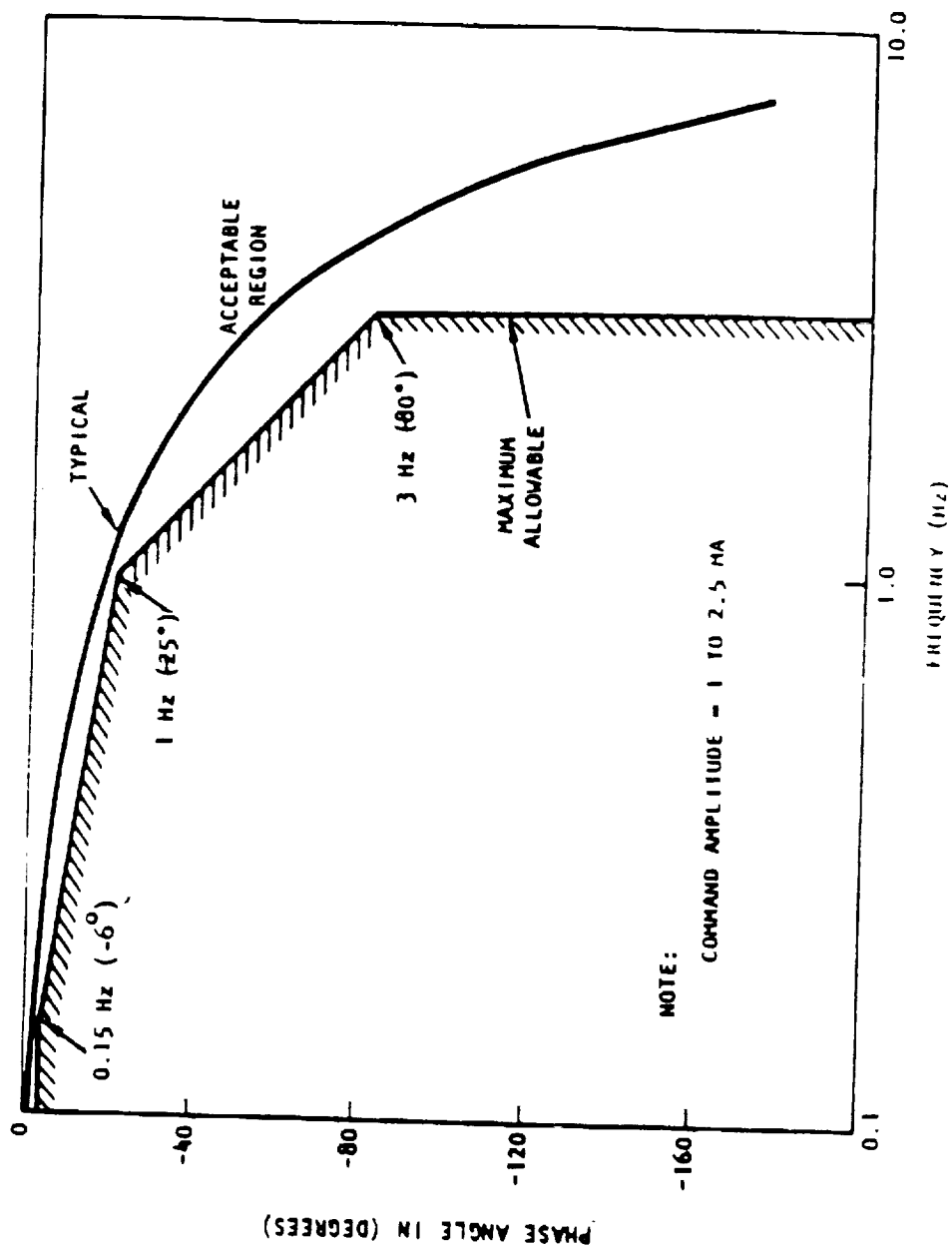


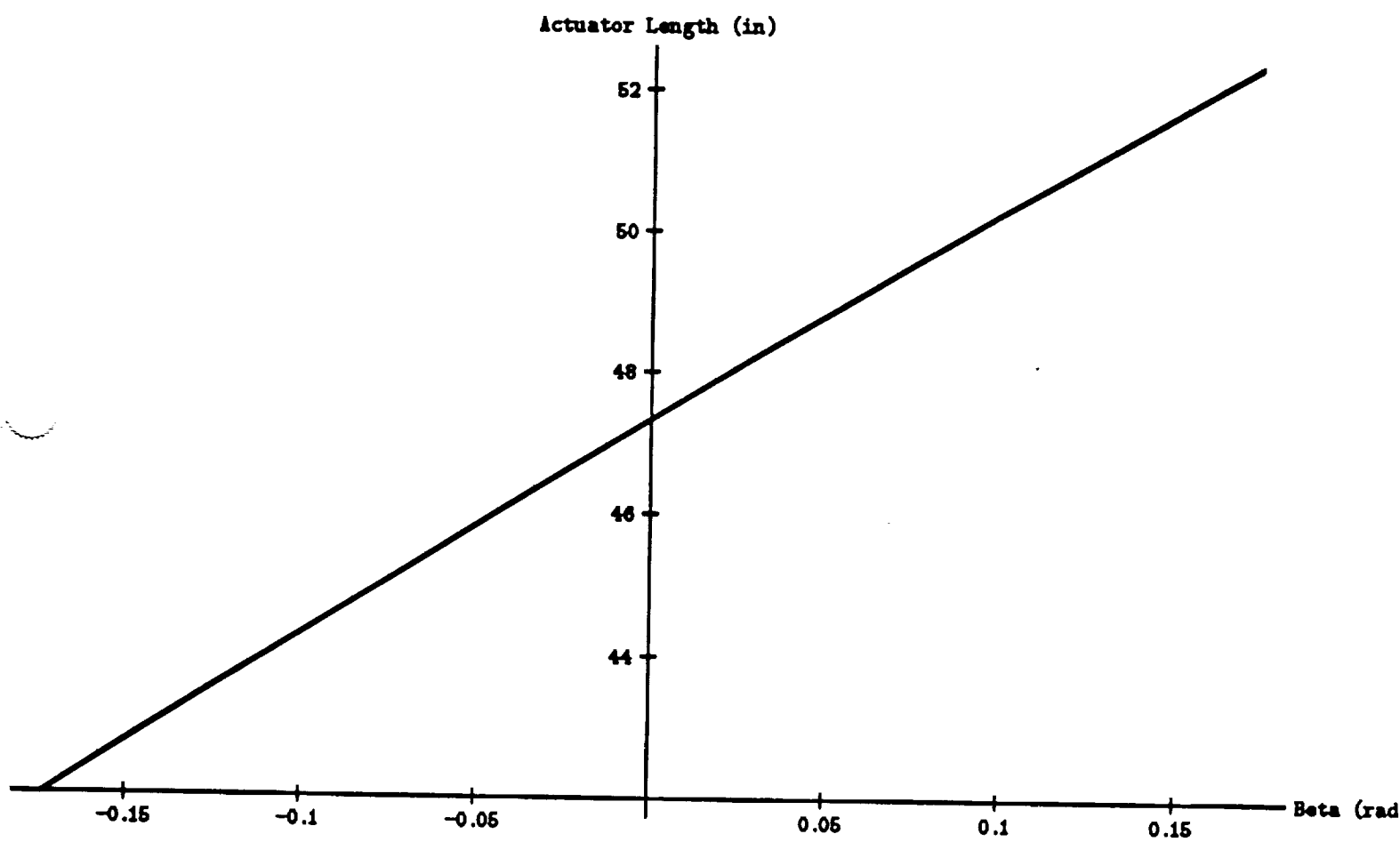
Figure 16. Frequency Response Phase Requirements

**APPENDIX F:
GEOMETRICAL AND
DISTURBANCE CALCULATIONS**

F. GEOMETRICAL AND DISTURBANCE CALCULATIONS

The first subject addressed in this appendix is the calculation of TVC actuator strokes and moment arms. The general formulation is contained in an MSFC internal memorandum dated August 16, 1972 from Mr. C. S. Cornelius to Mr. M. Kalange. A copy of this memorandum is enclosed in this appendix for ready reference.

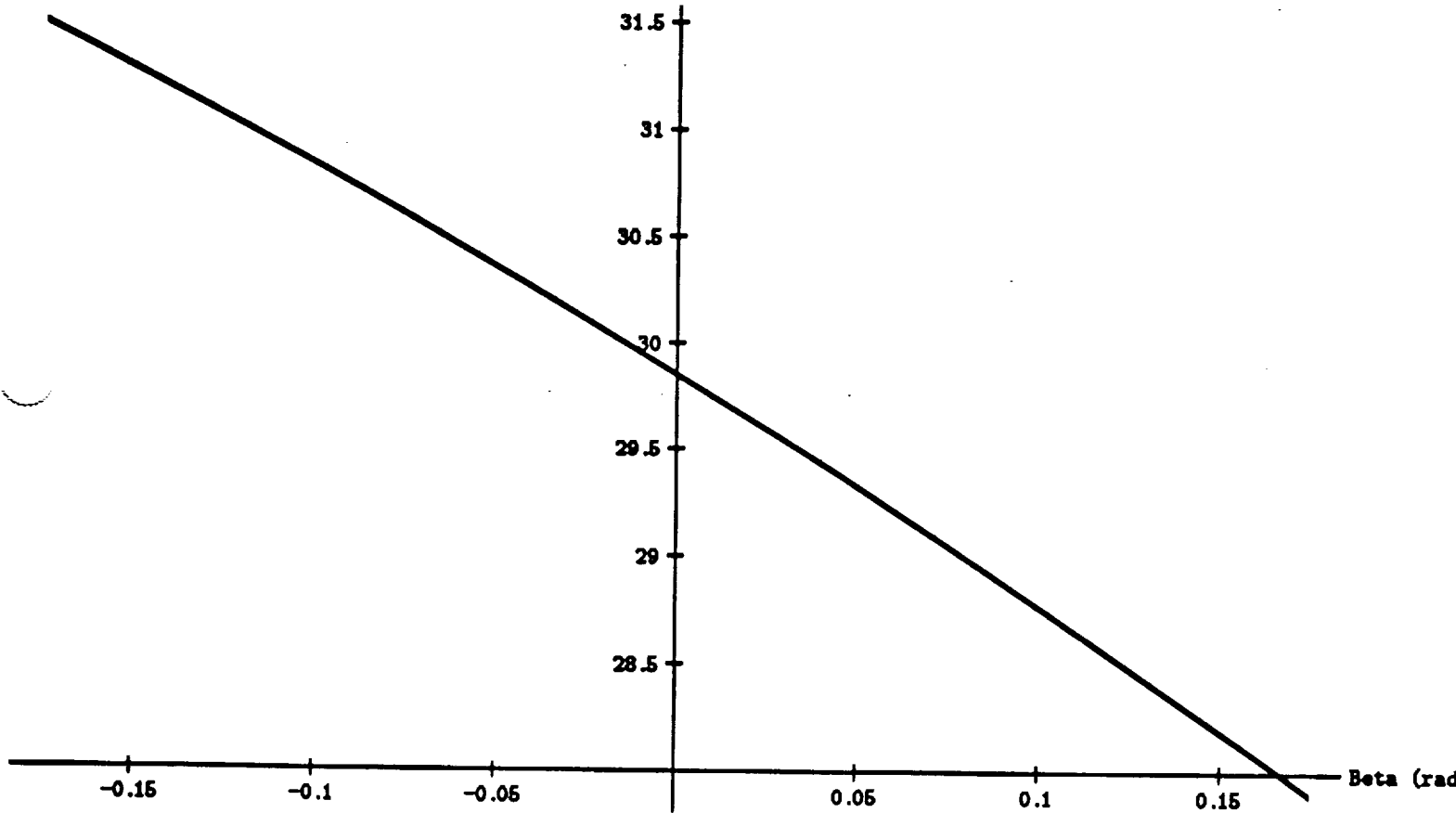
The first question addressed was the determination of the relationship between engine deflection angle, β , and the linear actuator stroke (L_a). This was accomplished by use of the formula contained in the referenced MSFC memorandum for L_a as a function of β , substituting in the values shown on the attached annotated figure 2 and programming the whole into MATHEMATICA then plotting the result. The result is shown in the accompanying figure with the resulting numerical formula at the bottom. From the figure it is seen that over the range of engine deflections anticipated the function approximates a straight line reasonably well and the actuator has a center point (i.e. β equal zero) value of 47.33 inches.



$$L_a = \left[2240.13 + 7684.3 \sin^2\left(\frac{\beta}{2}\right) - 8297.896 \sin\frac{\beta}{2} \cos\left(2.3.2 - \frac{\beta}{2}\right) \right]^{\frac{1}{2}}$$

The next question addressed was the relationship between the change in L_a to the change in the gimbal angle β . This function is useful when calculating the equivalent mass seen by the actuator when rotating the engine about its gimbal pivot point. Because of the varying length of the effective moment arm (d_a) between the actuator and the engine gimbal center the effective mass will in actuality vary as a function of β . In the design work a value corresponding to zero β angle is used as a nominal figure with which to design. The same evaluation procedure was used as in the previous evaluation for L_a versus β . In this case the computer was programmed to take the derivative of L_a with respect to β . The resulting expression is tabulated at the bottom of the following figure. The value of the derivative corresponding to a β of zero is 29.79 inches per radian and is the one that would be used to calculate the equivalent mass.

d/db(Actuator length (in/rad))

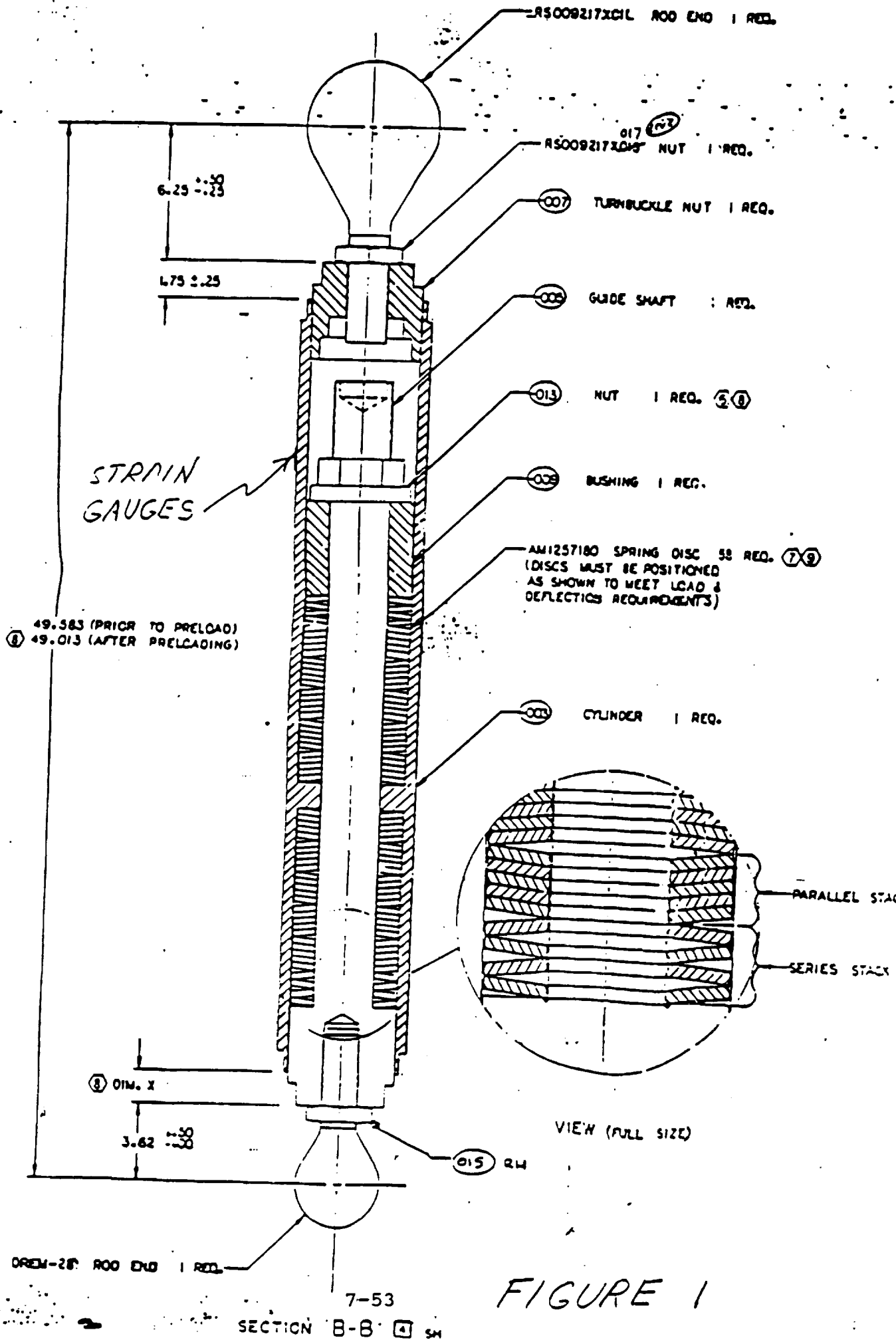


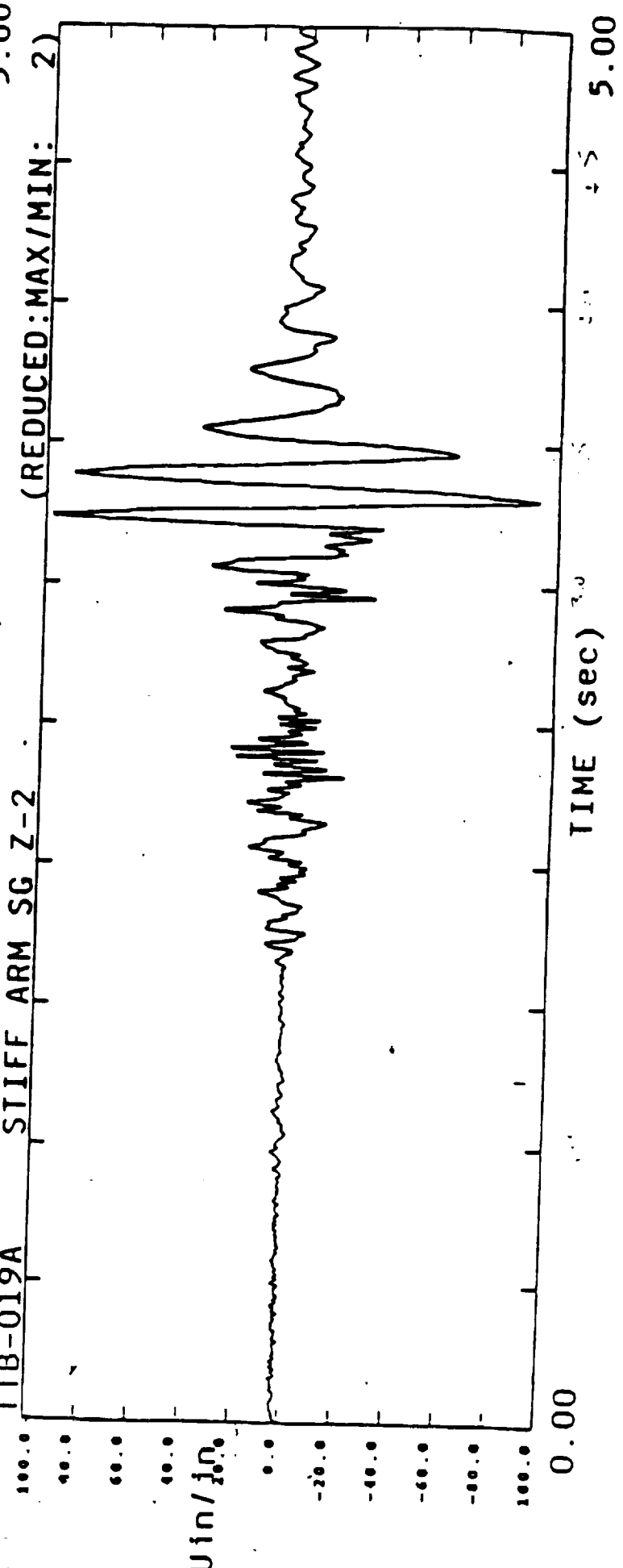
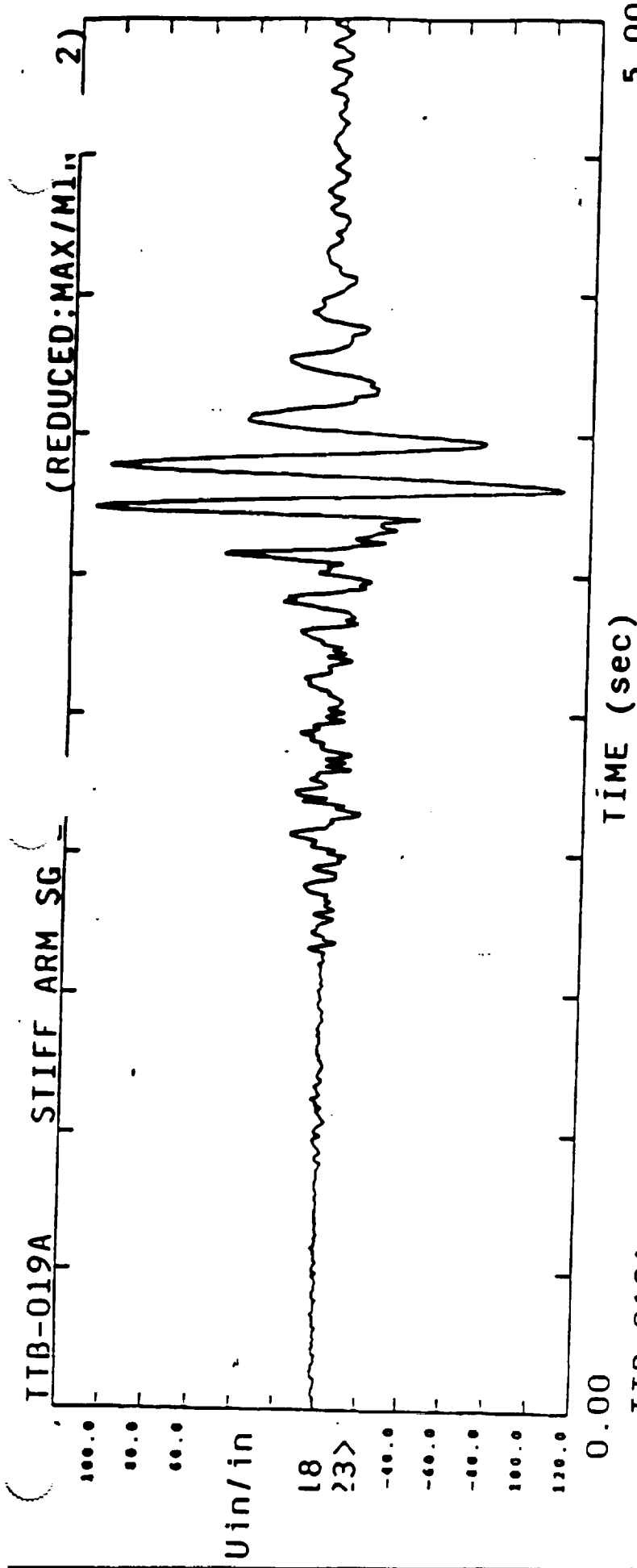
$$\frac{dL_a}{d\beta} = \frac{-4148.95 \cos\left(2.32 - \frac{\beta}{2}\right) \cos\left(\frac{\beta}{2}\right) + 7684.3 \cos\left(\frac{\beta}{2}\right) \sin\left(\frac{\beta}{2}\right) - 4148.95 \sin\left(2.32 - \frac{\beta}{2}\right) \sin\left(\frac{\beta}{2}\right)}{2 \left(2240.13 - 8297.9 \cos\left(2.32 - \frac{\beta}{2}\right) \sin\left(\frac{\beta}{2}\right) + 7684.3 \sin^2\left(\frac{\beta}{2}\right) \right)^{\frac{1}{2}}}$$

The next three figures address the test stand geometry used and the forces experienced during recent firings of an SSME type engine at MSFC. The first figure was obtained from Sverdrup and Parcel via MSFC. It defines the geometry of the test stand firing configuration of the "stiff arm" (i.e. the actuator substitute) and engine. Using the well known formula for calculating the distance from a point external to a line along a normal to the line results in a moment arm length of 36.92 inches (as has been added to the figure by hand). The next figure shows a cross section of the "stiff arm" showing that it is indeed not stiff but is in actuality a spring loaded strut (as one might expect, it has to absorb some force or "give" some amount to prevent damaging the engine). The third figure in this group shows a typical strain gage readout from the "stiff arm". As one might expect the motion is highly oscillatory and indicates a range of forces from 30 to 65 KIPS (which when multiplied by the 36.92 inch moment arm indicated a range of stiff arm associated moments of 90,000 to 200,000 lb-ft). Analysis would be required to determine if the frequency corresponds to the equivalent rigid mass of the engine resonating with the spring of the strut or whether there is some other phenomenon involved. It may well be profitable to pursue this analysis to determine if meaningful experimental data as to the actual engine caused start/stop transient forces themselves can be obtained. Certainly the whole TVC actuator design world would profit from such test data based

knowledge because the effects of this transient are the least known factors in the actuator design work and an accurate characterization of the transient force would be very beneficial. Information from the engine consortium (see the last chart) specifies a 30KIP start/stop force at the nozzle exit (it does not suggest either the duration or shape versus time of the transient, information needed to evaluate its effect on the actuator). The nozzle exit is 12.5 feet from the pivot point thus suggesting an actuator force of 147,000 pounds ($30,000 \times 12.5/2.5$) if the actuator were not to give which it certainly would have to do; thereby decreasing the actuator force by the amount "absorbed" by the acceleration of the engine mass. The consortium specified to the potential actuator vendor a start/stop actuator force of 100,000 pounds (duration and wave shape unknown).

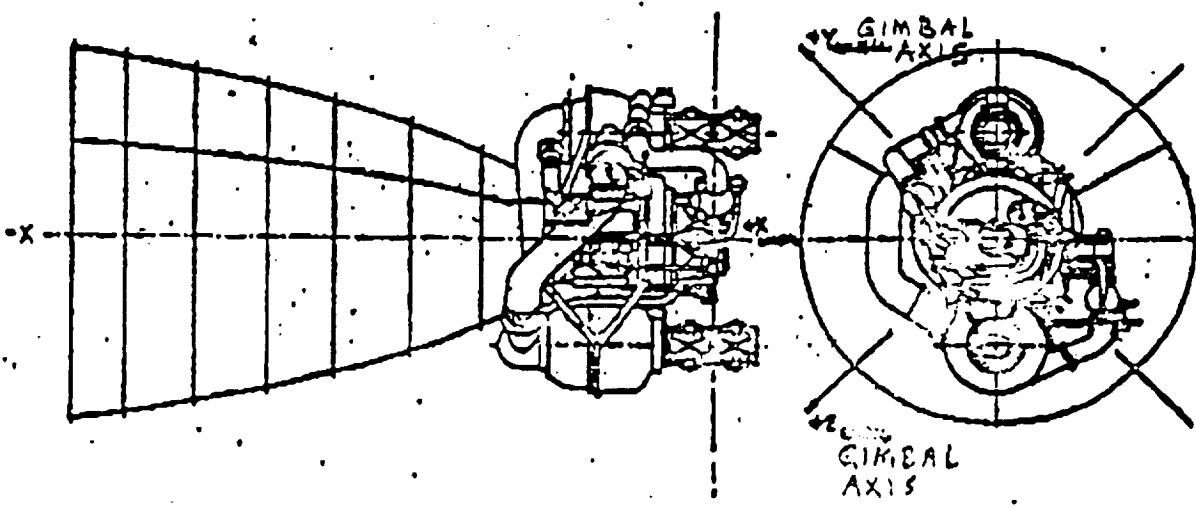
One additional calculation was made. It was assumed that the vehicle was accelerating along its center line at 4.5 g's. and that the engine was fully gimbaled. This worked out to be a load on the actuator of approximately 5,100 pounds. This appears to be negligible compared to the other loads being considered.





ALS

SPACE TRANSPORTATION ENGINE PROGRAM COORDINATION MEMO

CUSTOMER : DaWitt Westrope (NASA)	CM NO. HKO-078-14
COORDINATOR : (P & W) John Jergens for Alan Adams	INPUT/OUTPUT DATE 9/6/91
SUBJECT : STME Dry Weight, Center of Gravity, Moments of Inertia, and Side Loads	
REFERENCE : WESTROPE REQUEST	DUE DATE: 9/13/91
MESSAGE "Current Estimated Values" 1) <u>Engine System Dry Weight</u> = 8000 lbs. 2) <u>Engine Gimballed Mass Center of Gravity, Dry:</u> $x = -35.5, y = -1.5, z = +1.2$ 3) <u>Engine Gimballed Moments of Inertia, @ zero angle, Dry:</u> $I_{xx} = 6.4 \times 10^6 \text{ lbm in}^2, I_{yy} = 18.2 \times 10^6 \text{ lbm in}^2, I_{zz} = 18.4 \times 10^6 \text{ lbm in}^2$ 4) <u>Engine Side Load</u> = 30,000 lbs. @ nozzle exit (Occurs for start and shutdown transients). REFERENCE AXIS:	
 <p style="text-align: right;"><u>Example Engine Only</u></p>	



NATIONAL AERONAUTICS AND SPACE ADMINISTRATION
GEORGE C. MARSHALL SPACE FLIGHT CENTER
MARSHALL SPACE FLIGHT CENTER, ALABAMA 35812

REPLY TO
ATTN OF: S&E-ASTR-GMF *gmf*

August 16, 1972

TO: S&E-ASTR-GM/Mr. Kalange

FROM: S&E-ASTR-GMF/C. S. Cornelius

SUBJECT: Generalized Equations for Calculating TVC Actuator
Strokes and Moment Arms

The equations in paragraphs 2 and 3 below may be used to calculate the actuator length and effective moment arm as a function of the gimbal angle β . The gimbal angle β is considered positive when the actuator is extended and negative when retracted. Both schematics are shown for the actuator in the extended position; however, the equations hold for the retract positions. Definitions of the engine/actuator geometry is made consistent with the Space Shuttle Orbiter Vehicle/Engine ICD No. 13M15000E where the actuator pierce point in the Y-Z plane is defined.

Actuator stroke - Figure 1 shows a generalized schematic of a TVC Gimbal Actuator arrangement. With the configuration fixed, actuator strokes in the extend and retract directions can be calculated as a function of gimbal angle ($\pm \beta$). The following equations are used to calculate the actuator lengths.

$$L_6 = (L_4^2 + L_2^2)^{\frac{1}{2}}$$

$$L_1 = 2 L_6 \sin\left(\frac{\beta}{2}\right)$$

$$\phi_1 = \tan^{-1}\left(\frac{L_2}{L_4}\right)$$

$$\phi_0 = 270 - \phi_1 - \phi_2 - \frac{\beta}{2}$$

$$L_A = (L_0^2 + L_1^2 - 2 L_0 L_1 \cos \phi_0)^{\frac{1}{2}}$$

where β = gimbal angle

L_0 = actuator length at null position ($\beta = 0$)

L_A = actuator length at gimbal angle β

Actuator Moment Arm - Figure 2 shows a generalized gimbal actuator arrangement used to determine the effective moment arm as a function of gimbal angle ($\pm \beta$). The following equations are used to calculate the moment arms.

$$L_6 = (L_4^2 + L_2^2)^{\frac{1}{2}}$$

$$L_1 = 2 L_6 \sin\left(\frac{\beta}{2}\right)$$

$$\alpha_0 = \tan^{-1}\left(\frac{L_2}{L_4}\right) + \tan^{-1}\left(\frac{L_3}{L_5 - L_4}\right) - \sin^{-1}\left(\frac{L_1}{L_A} \sin \phi_0\right) - 90 + \beta$$

$$d_A = L_6 \cos \alpha_0$$

where β = gimbal angle

L_A = actuator length defined in paragraph 2

ϕ_0 = angle defined in paragraph 2

d_A = moment arm at gimbal angle β

H. H. H. H.

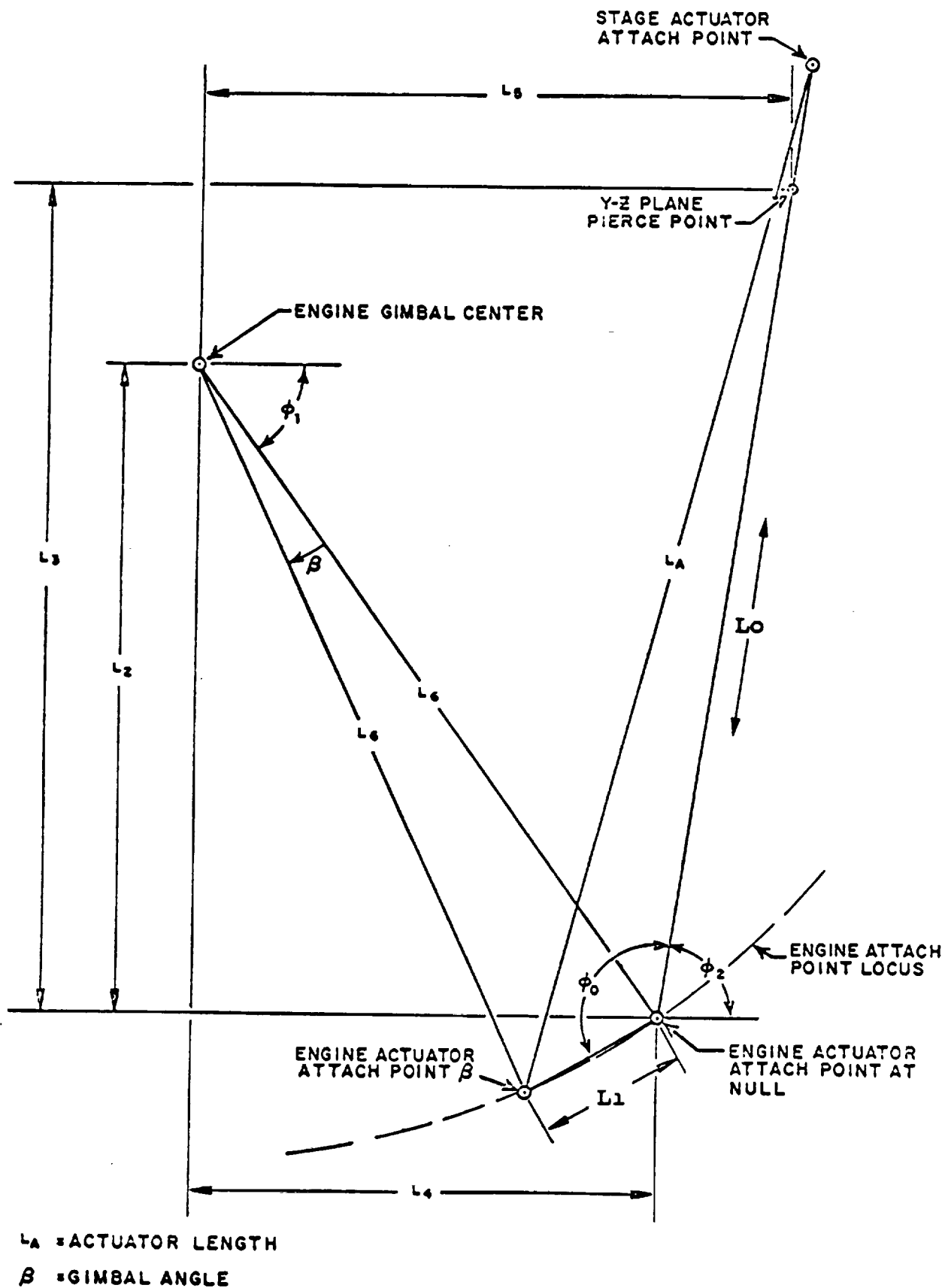
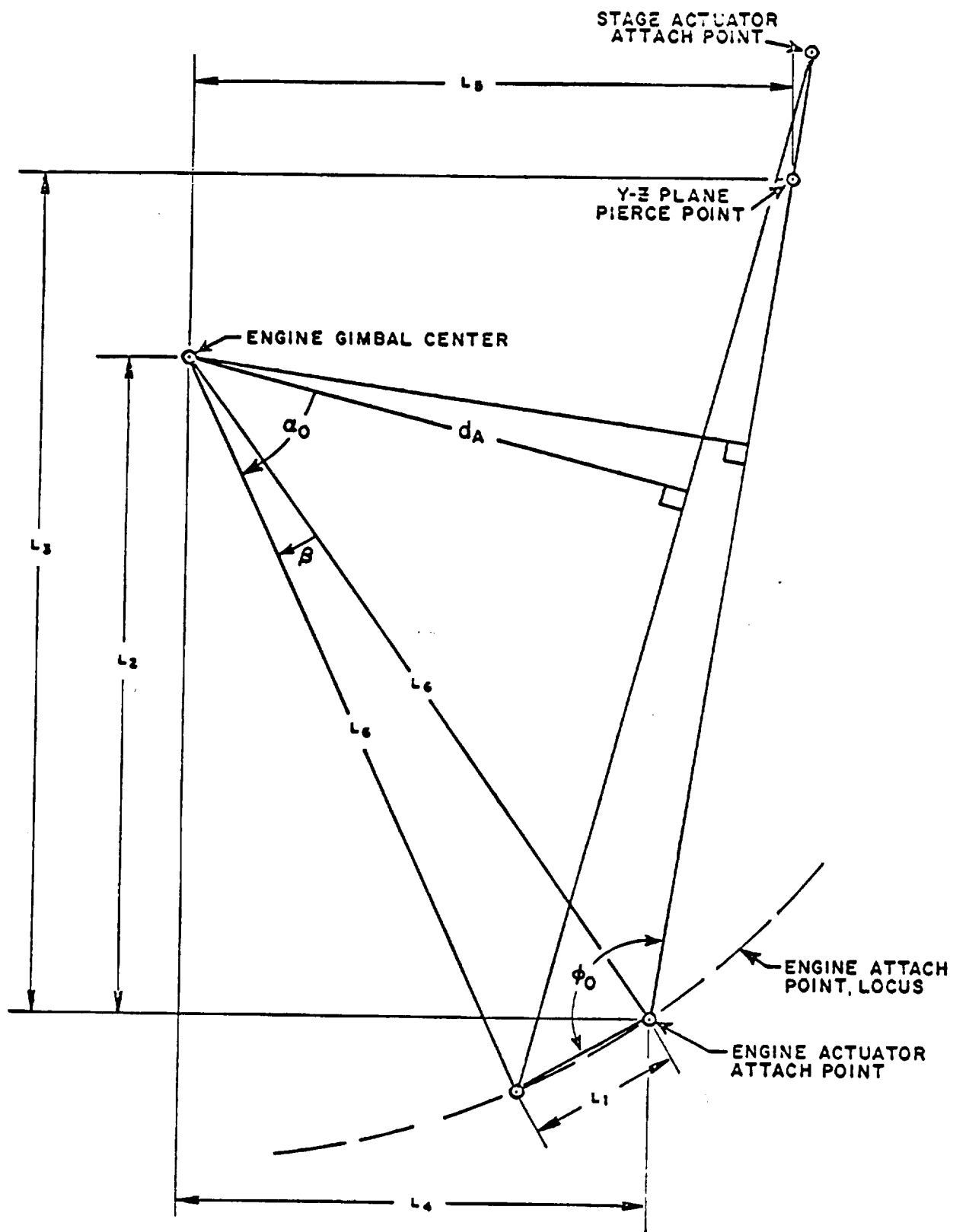


FIGURE 1 - ACTUATOR LENGTH SCHEMATIC



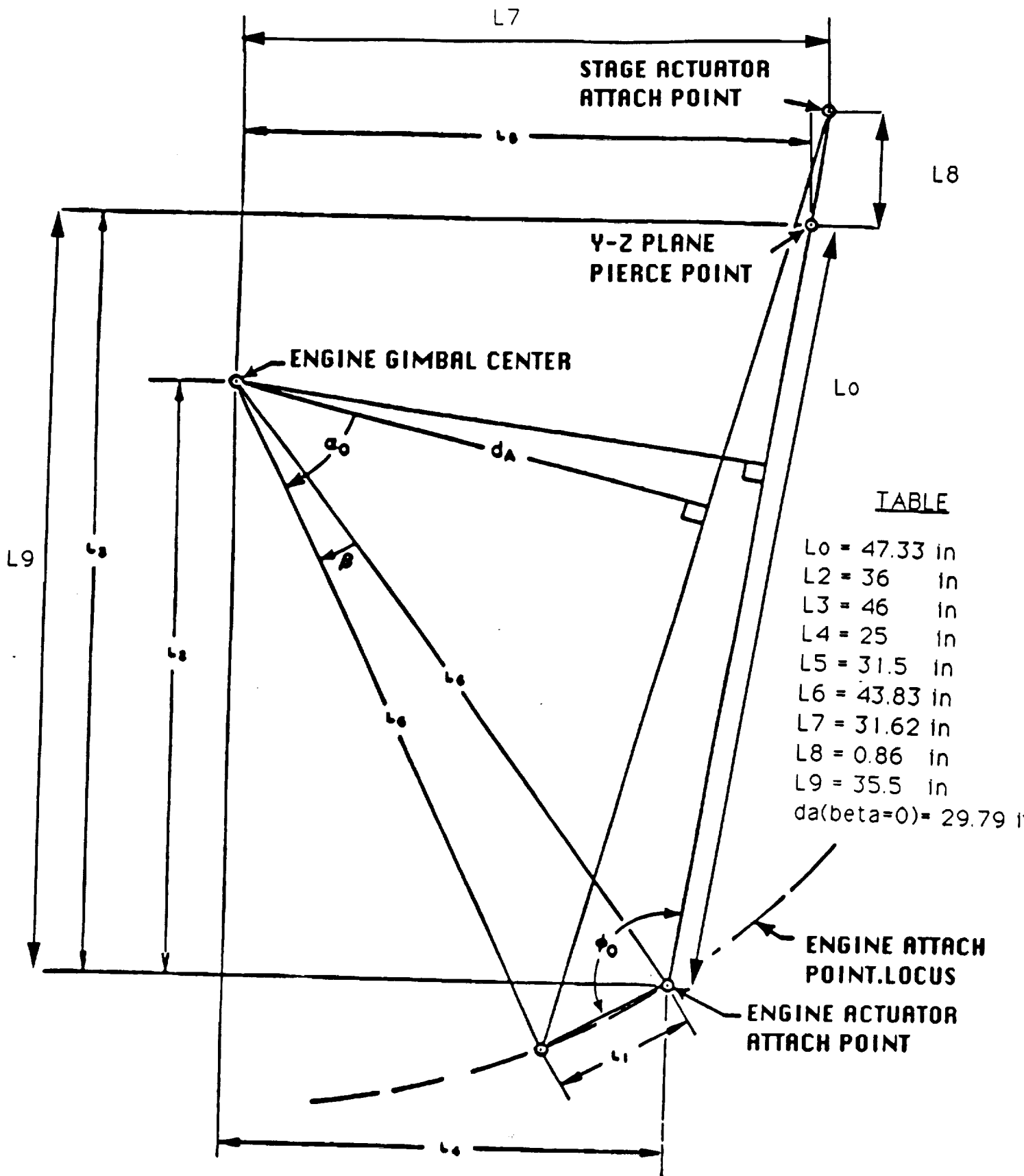
d_A = EFFECTIVE MOMENT ARM

β = GIMBAL ANGLE

FIGURE 2 - MOMENT ARM SCHEMATIC

7-59

PRECEDING PAGE BLANK NOT FILMED



TABLE

L_0	=	47.33	in
L_2	=	36	in
L_3	=	46	in
L_4	=	25	in
L_5	=	31.5	in
L_6	=	43.83	in
L_7	=	31.62	in
L_8	=	0.86	in
L_9	=	35.5	in
$d_A(\beta=0)$	=	29.79	in

d_A = EFFECTIVE MOMENT ARM

β = GIMBAL ANGLE

ANNOTATED MOMENT ARM SCHEMATIC

**APPENDIX G:
DEMONSTRATION OF OPTIMALITY
OF FINAL SELECTION OF GEAR
RATIO(n) AND LEAD(1) FOR
POINT DESIGN**

G. DEMONSTRATION OF OPTIMALITY OF FINAL SELECTION OF GEAR RATIO(n) AND LEAD(l) FOR POINT DESIGN

In previous sections, the value of n and l was calculated either to yield the maximum possible acceleration of the engine or to deliver 40,000 lbs to the engine at 5 in/sec. Recall that the l calculated for each case was different, while the value of n was held constant. As l varies the acceleration of the engine varies from its maximum value to some new smaller value. Notice that n could have been varied along with l to meet the requirements of the latter case.

The purpose of this section is to demonstrate that the choice of l obtained by fixing n provides the maximum detuned acceleration for the engine while delivering 40,000 lbs at 5 in/sec. It should be emphasized that the maximum detuned acceleration is less than the maximum acceleration calculated earlier. More importantly, as the rated RPM of the motor increases(i.e. 1000,3000,6000,...etc.), the difference between the maximum detuned acceleration and the maximum acceleration increases accordingly.

Case I: 1000 RPM, 15 HP Motor

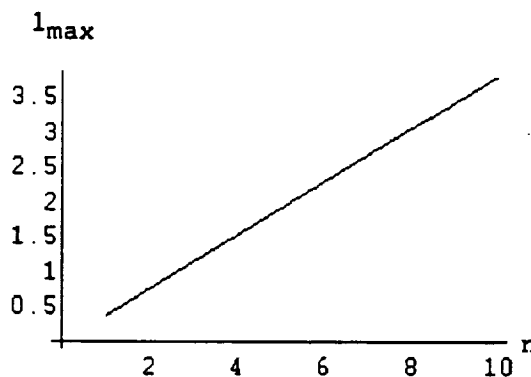
Recall that for maximum acceleration, $n=4.28$ and $l=1.61691$ inches. Define the overall gear ratio as

$$\text{ogr}_{\max} = \frac{2\pi n}{l} = \frac{2\pi(4.28)}{1.61691} = 16.6317 \text{ in}^{-1}$$

Using the above relationship for ogr_{\max} , solve for l_{\max}

$$l_{\max} = \frac{2\pi n}{16.6317}$$

If l_{\max} is treated as a function of n and n is varied over some range of values, a straight line plot is obtained



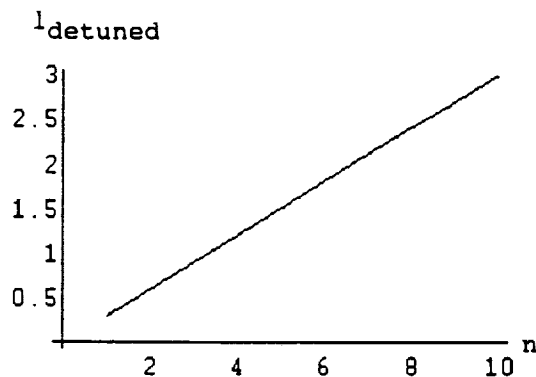
Recall that for the detuned acceleration, $n=4.28$ and $l=1.284$ inches. To meet the engine speed and force requirements, the overall gear ratio becomes

$$\text{ogr}_{\text{detuned}} = \frac{\dot{\theta}_{\text{motor}}}{\dot{x}_{\text{engine}}} = \frac{(1000 \frac{\text{rev}}{\text{min}})(2\pi \frac{\text{rad}}{\text{rev}})(\frac{1 \text{ min}}{60 \text{ sec}})}{5 \frac{\text{in}}{\text{sec}}} = 20.944 \quad (\dot{\theta}_{\text{motor}} = [\frac{2\pi n}{l}] \dot{x}_{\text{engine}})$$

Using the above relationship for $\text{ogr}_{\text{detuned}}$, solve for l_{detuned}

$$l_{\text{detuned}} = \frac{2\pi n}{20.944}$$

If l_{detuned} is treated as a function of n and n is varied over some range of values, a straight line plot is obtained

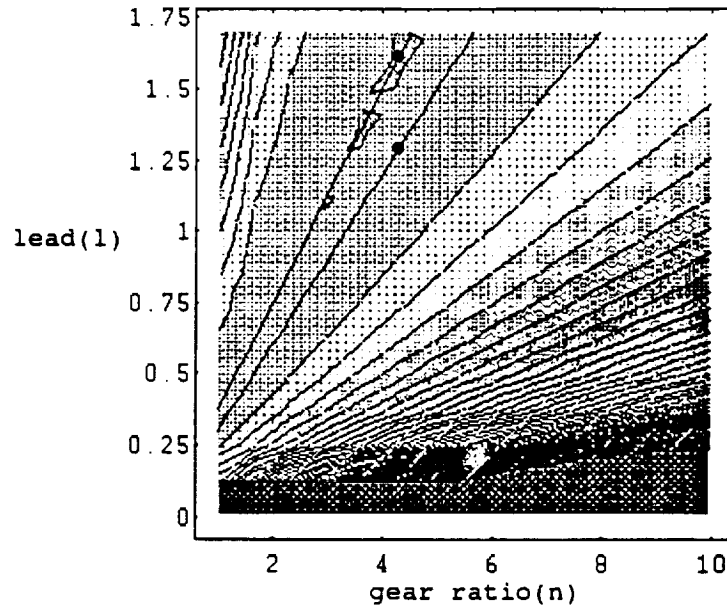


Recall that the total inertia seen by the motor is given by the following equation

$$\text{den} = [J_{\text{Motor}} \left(\frac{2\pi n}{l} \right) + J_{\text{PinionGear}} (3 + n^2) \left(\frac{2\pi n}{l} \right) + J_{\text{RollerScrew}} \left(\frac{2\pi}{nl} \right) + M_{\text{Engine}} \left(\frac{1}{2\pi n} \right)]$$

where the inertia and mass are known.

Superimpose the plots obtained for l_{max} and l_{detuned} onto a contour plot of den , and then plot the points that correspond to maximum acceleration and maximum detuned acceleration



Notice that the detuned acceleration is not the same as the maximum possible acceleration. The following will demonstrate that the assumption concerning n (i.e. fix $n=4.28$) yields the maximum possible acceleration in the detuned case.

Using $ogr_{detuned}$, solve for $l_{detuned}$

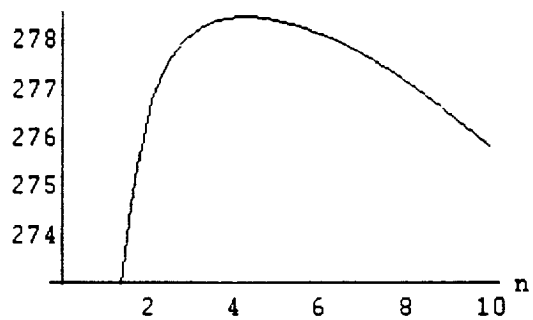
$$l_{detuned} = \frac{2\pi n(5)}{1000(2\pi / 60)}$$

Substituting the above value of $l_{detuned}$ into the equation of the total inertia seen by the motor yields an equation that is only a function of n . The available torque divided by the total inertia is the acceleration. The available torque is

$$\text{Torque} = \frac{(3)(10)(550)(12)}{1000(2\pi / 60)} = 1890.76$$

The following plot shows the acceleration of the engine as n varies from 1 to 10

Acceleration



It is clear from the above plot that the maximum acceleration occurs when n is equal to 4.28.

Case II: 3000 RPM, 15 HP Motor

Recall that for maximum acceleration, $n=4.28$ and $l=0.66319$.

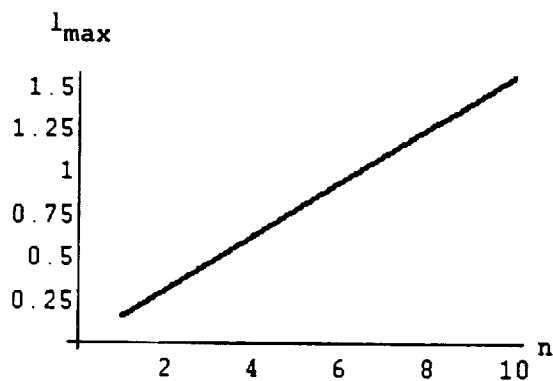
Define the overall gear ratio as

$$\text{ogr}_{\max} = \frac{2\pi n}{l} = \frac{2\pi(4.28)}{0.66319} = 40.5495 \text{ in}^{-1}$$

Using the above relationship for ogr_{\max} , solve for l_{\max}

$$l_{\max} = \frac{2\pi n}{40.5495}$$

If l_{\max} is treated as a function of n and n is varied over some range of values, a straight line plot is obtained



Recall that for the detuned acceleration, $n=4.28$ and $l=0.428$ inches. To meet the engine speed and force requirements, the overall gear ratio becomes

$$\text{ogr}_{\text{detuned}} = \frac{\dot{\theta}_{\text{motor}}}{\dot{x}_{\text{engine}}} = \frac{(3000 \frac{\text{rev}}{\text{min}})(2\pi \frac{\text{rad}}{\text{rev}})(\frac{1 \text{ min}}{60 \text{ sec}})}{5 \frac{\text{in}}{\text{sec}}} = 62.8319 \quad (\dot{\theta}_{\text{motor}} = [\frac{2\pi n}{l}]\dot{x}_{\text{engine}})$$

Using the above relationship for $\text{ogr}_{\text{detuned}}$, solve for l_{detuned}

$$l_{\text{detuned}} = \frac{2\pi n}{62.8319}$$

If l_{detuned} is treated as a function of n and n is varied over some range of values, a straight line plot is obtained

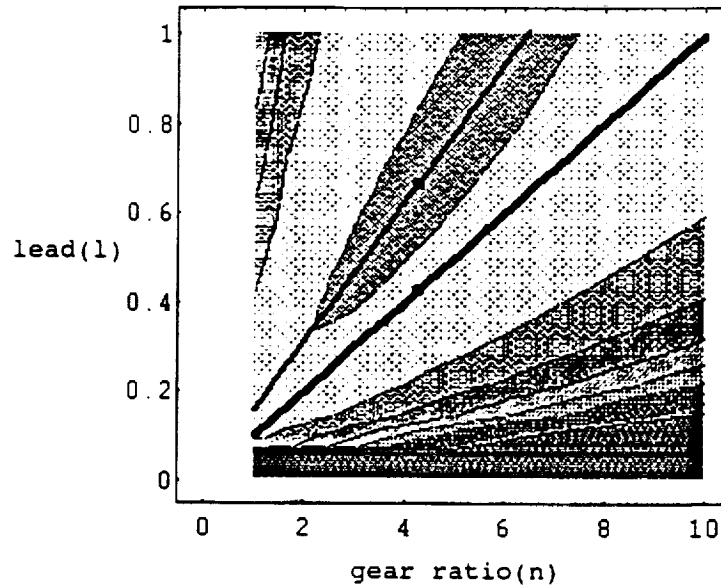


Recall that the total inertia seen by the motor is given by the following equation

$$\text{den} = [J_{\text{Motor}} \left(\frac{2\pi n}{l} \right) + J_{\text{PinionGear}} (3 + n^2) \left(\frac{2\pi n}{l} \right) + J_{\text{RollerScrew}} \left(\frac{2\pi}{nl} \right) + M_{\text{Engine}} \left(\frac{1}{2\pi n} \right)]$$

where the inertia and mass are known.

Superimpose the plots obtained for l_{max} and l_{detuned} onto a contour plot of den , and then plot the points that correspond to maximum acceleration and maximum detuned acceleration



Notice that the detuned acceleration is not the same as the maximum possible acceleration. The following will demonstrate that the assumption concerning n (i.e. fix $n=4.28$) yields the maximum possible acceleration in the detuned case.

Using $ogr_{detuned}$, solve for $l_{detuned}$

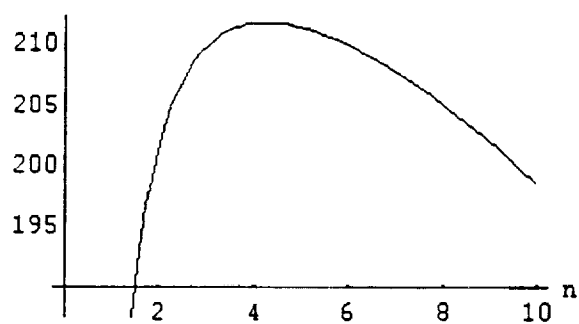
$$l_{detuned} = \frac{2\pi n(5)}{3000(2\pi / 60)}$$

Substituting the above value of $l_{detuned}$ into the equation of the total inertia seen by the motor yields an equation that is only a function of n . The available torque divided by the total inertia is the acceleration. The available torque is

$$\text{Torque} = \frac{(3)(10)(550)(12)}{3000(2\pi / 60)} = 630.254$$

The following plot shows the acceleration of the engine as n varies from 1 to 10

Acceleration



It is clear from the above plot that the maximum acceleration occurs when n is equal to 4.28.

Case III: 6000 RPM, 15 HP Motor

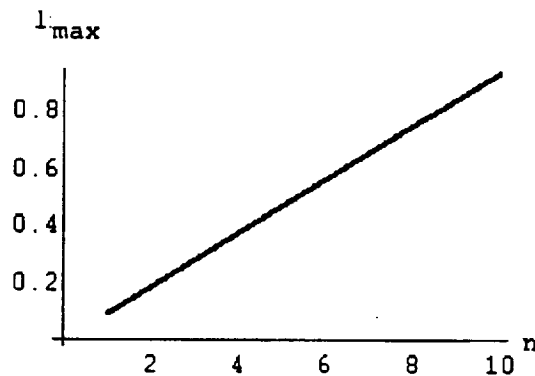
Recall that for maximum acceleration, $n=4.28$ and $l=0.39441$ inches. Define the overall gear ratio as

$$\text{ogr}_{\max} = \frac{2\pi n}{l} = \frac{2\pi(4.28)}{0.39441} = 68.1829 \text{ in}^{-1}$$

Using the above relationship for ogr_{\max} , solve for l_{\max}

$$l_{\max} = \frac{2\pi n}{68.1829}$$

If l_{\max} is treated as a function of n and n is varied over some range of values, a straight line plot is obtained



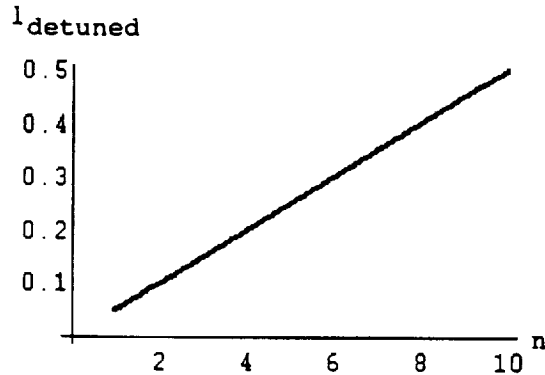
Recall that for the detuned acceleration, $n=4.28$ and $l=0.214$ inches. To meet the engine speed and force requirements, the overall gear ratio becomes

$$\text{ogr}_{\text{detuned}} = \frac{\dot{\theta}_{\text{motor}}}{\dot{x}_{\text{engine}}} = \frac{(6000 \frac{\text{rev}}{\text{min}})(2\pi \frac{\text{rad}}{\text{rev}})(\frac{1}{60} \frac{\text{min}}{\text{sec}})}{5 \frac{\text{in}}{\text{sec}}} = 125.664 \quad (\dot{\theta}_{\text{motor}} = [\frac{2\pi n}{l}] \dot{x}_{\text{engine}})$$

Using the above relationship for $\text{ogr}_{\text{detuned}}$, solve for l_{detuned}

$$I_{\text{detuned}} = \frac{2\pi n}{125.664}$$

If I_{detuned} is treated as a function of n and n is varied over some range of values, a straight line plot is obtained

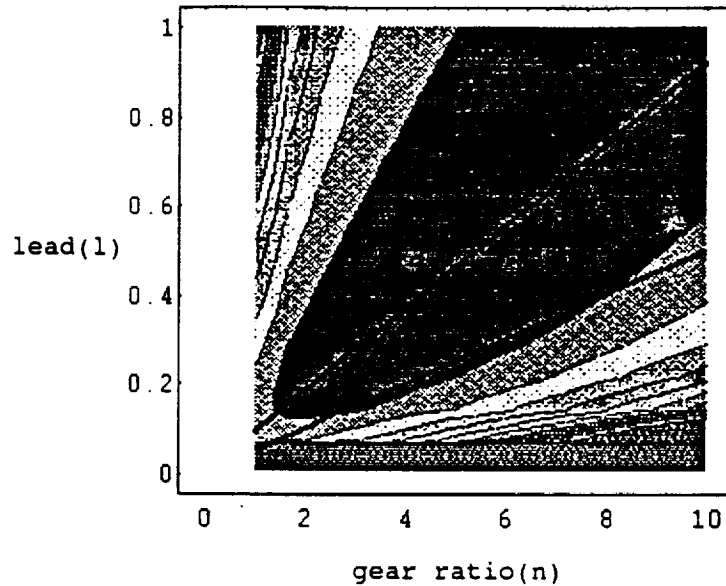


Recall that the total inertia seen by the motor is given by the following equation

$$\text{den} = [J_{\text{Motor}} \left(\frac{2\pi n}{l} \right) + J_{\text{PinionGear}} (3 + n^2) \left(\frac{2\pi n}{l} \right) + J_{\text{RollerScrew}} \left(\frac{2\pi}{nl} \right) + M_{\text{Engine}} \left(\frac{1}{2\pi n} \right)]$$

where the inertia and mass are known.

Superimpose the plots obtained for I_{max} and I_{detuned} onto a contour plot of den , and then plot the points that correspond to maximum acceleration and maximum detuned acceleration.



Notice that the detuned acceleration is not the same as the maximum possible acceleration. The following will demonstrate that the assumption concerning n (i.e. fix $n=4.28$) yields the maximum possible acceleration in the detuned case.

Using $ogr_{detuned}$, solve for $l_{detuned}$

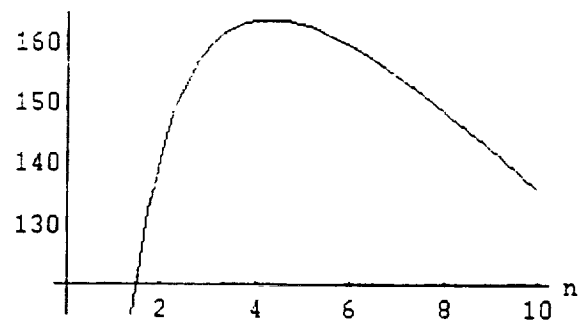
$$l_{detuned} = \frac{2\pi n(5)}{6000(2\pi / 60)}$$

Substituting the above value of $l_{detuned}$ into the equation of the total inertia seen by the motor yields an equation that is only a function of n . The available torque divided by the total inertia is the acceleration. The available torque is

$$\text{Torque} = \frac{(3)(10)(550)(12)}{6000(2\pi / 60)} = 315.127$$

The following plot shows the acceleration of the engine as n varies from 1 to 10

Acceleration



It is clear from the above plot that the maximum acceleration occurs when n is equal to 4.28.

Case IV: 9000 RPM, 15 HP Motor

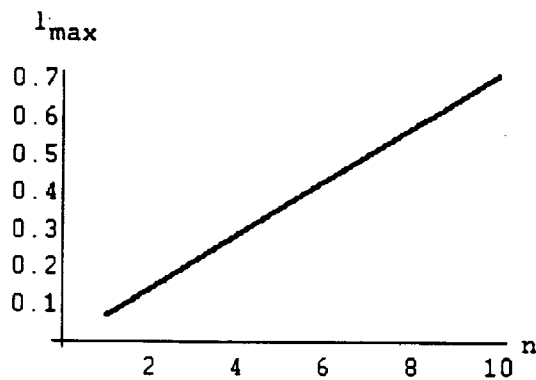
Recall that for maximum acceleration, $n=4.28$ and $l=0.30224$ inches. Define the overall gear ratio as

$$\text{ogr}_{\max} = \frac{2\pi n}{l} = \frac{2\pi(4.28)}{0.30224} = 88.9758 \text{ in}^{-1}$$

Using the above relationship for ogr_{\max} , solve for l_{\max}

$$l_{\max} = \frac{2\pi n}{88.9758}$$

If l_{\max} is treated as a function of n and n is varied over some range of values, a straight line plot is obtained



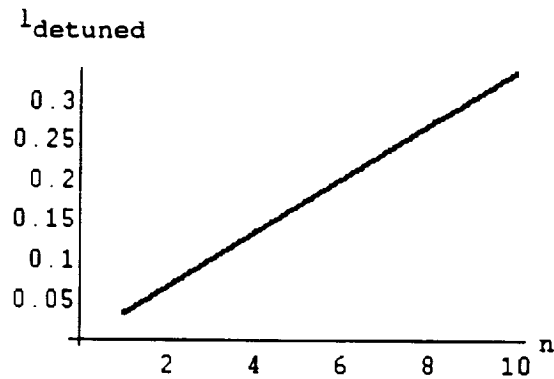
Recall that for the detuned acceleration, $n=4.28$ and $l=0.142667$ inches. To meet the engine speed and force requirements, the overall gear ratio becomes

$$\text{ogr}_{\text{detuned}} = \frac{\dot{\theta}_{\text{motor}}}{\dot{x}_{\text{engine}}} = \frac{(9000 \frac{\text{rev}}{\text{min}})(2\pi \frac{\text{rad}}{\text{rev}})(\frac{1 \text{ min}}{60 \text{ sec}})}{5 \frac{\text{in}}{\text{sec}}} = 188.496 \quad (\dot{\theta}_{\text{motor}} = [\frac{2\pi n}{l}]\dot{x}_{\text{engine}})$$

Using the above relationship for $\text{ogr}_{\text{detuned}}$, solve for l_{detuned}

$$l_{\text{detuned}} = \frac{2\pi n}{188.496}$$

If l_{detuned} is treated as a function of n and n is varied over some range of values, a straight line plot is obtained

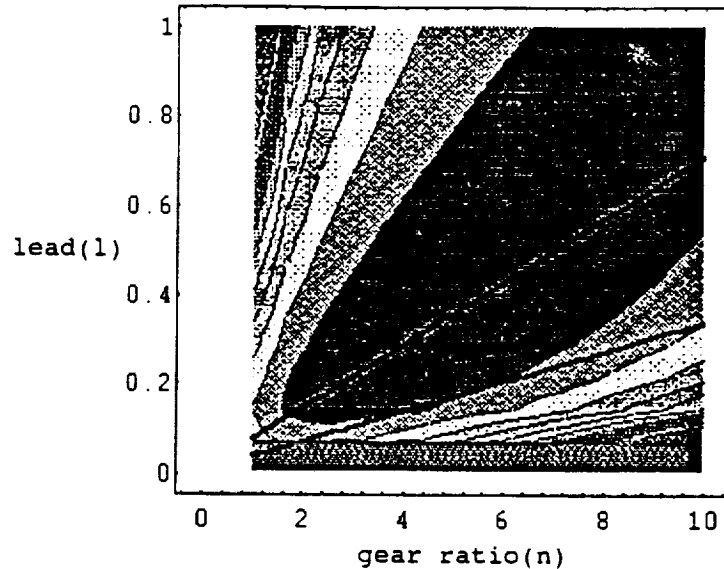


Recall that the total inertia seen by the motor is given by the following equation

$$\text{den} = [J_{\text{Motor}} \left(\frac{2\pi n}{l} \right) + J_{\text{PinionGear}} (3 + n^2) \left(\frac{2\pi n}{l} \right) + J_{\text{RollerScrew}} \left(\frac{2\pi}{nl} \right) + M_{\text{Engine}} \left(\frac{l}{2\pi n} \right)]$$

where the inertia and mass are known.

Superimpose the plots obtained for l_{max} and l_{detuned} onto a contour plot of den , and then plot the points that correspond to maximum acceleration and maximum detuned acceleration



Notice that the detuned acceleration is not the same as the maximum possible acceleration. The following will demonstrate that the assumption concerning n (i.e. fix $n=4.28$) yields the maximum possible acceleration in the detuned case.

Using $ogr_{detuned}$, solve for $l_{detuned}$

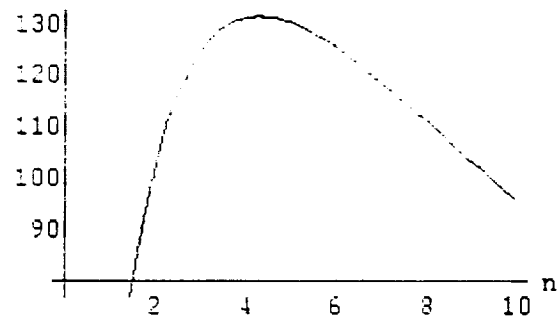
$$l_{detuned} = \frac{2\pi n(5)}{9000(2\pi / 60)}$$

Substituting the above value of $l_{detuned}$ into the equation of the total inertia seen by the motor yields an equation that is only a function of n . The available torque divided by the total inertia is the acceleration. The available torque is

$$\text{Torque} = \frac{(3)(10)(550)(12)}{9000(2\pi / 60)} = 210.084$$

The following plot shows the acceleration of the engine as n varies from 1 to 10

Acceleration



It is clear from the above plot that the maximum acceleration occurs when n is equal to 4.28.

Case V: 12000 RPM, 15 HP Motor

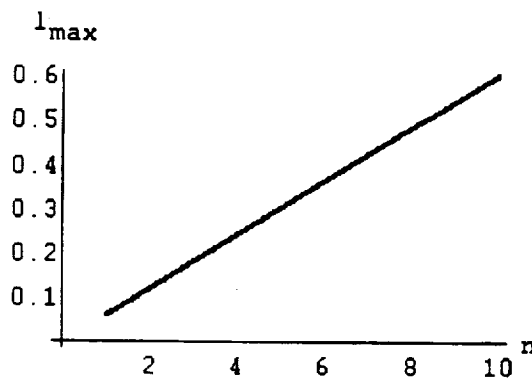
Recall that for maximum acceleration, $n=4.28$ and $l=0.256945$ inches. Define the overall gear ratio as

$$ogr_{\max} = \frac{2\pi n}{l} = \frac{2\pi(4.28)}{0.256945} = 104.661 \text{ in}^{-1}$$

Using the above relationship for ogr_{\max} , solve for l_{\max}

$$l_{\max} = \frac{2\pi n}{104.661}$$

If l_{\max} is treated as a function of n and n is varied over some range of values, a straight line plot is obtained



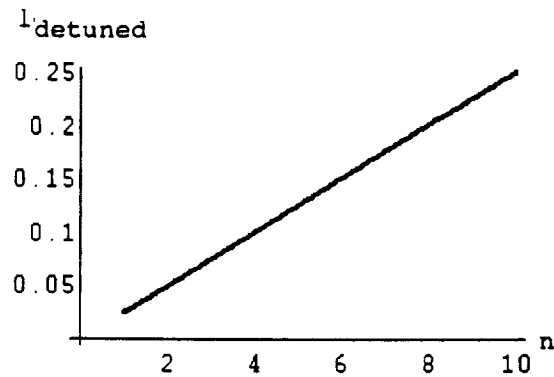
Recall that for the detuned acceleration, $n=4.28$ and $l=0.107$ inches. To meet the engine speed and force requirements, the overall gear ratio becomes

$$ogr_{\text{detuned}} = \frac{\dot{\theta}_{\text{motor}}}{\dot{x}_{\text{engine}}} = \frac{(12000 \frac{\text{rev}}{\text{min}})(2\pi \frac{\text{rad}}{\text{rev}})(\frac{1 \text{ min}}{60 \text{ sec}})}{5 \frac{\text{in}}{\text{sec}}} = 251.327 \quad (\dot{\theta}_{\text{motor}} = [\frac{2\pi n}{l}] \dot{x}_{\text{engine}})$$

Using the above relationship for ogr_{detuned} , solve for l_{detuned}

$$l_{\text{detuned}} = \frac{2\pi n}{251.327}$$

If l_{detuned} is treated as a function of n and n is varied over some range of values, a straight line plot is obtained

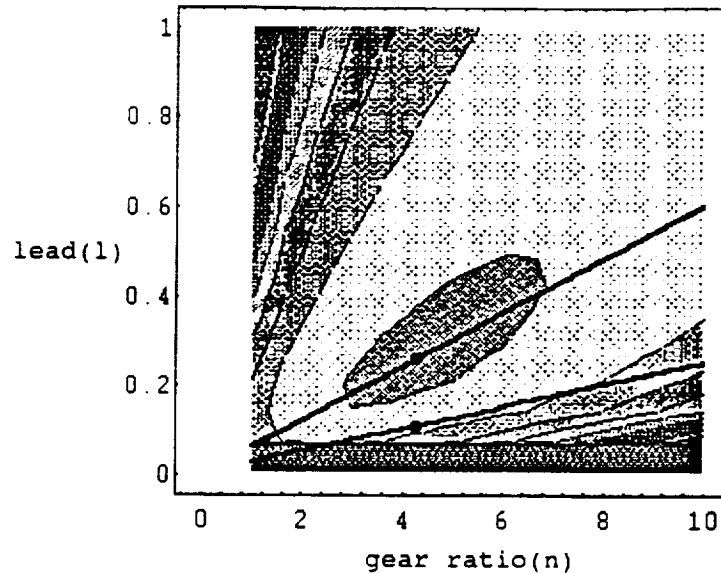


Recall that the total inertia seen by the motor is given by the following equation

$$\text{den} = [J_{\text{Motor}}(\frac{2\pi n}{l}) + J_{\text{PinionGear}}(3 + n^2)(\frac{2\pi n}{l}) + J_{\text{RollerScrew}}(\frac{2\pi}{nl}) + M_{\text{Engine}}(\frac{1}{2\pi n})]$$

where the inertia and mass are known.

Superimpose the plots obtained for l_{max} and l_{detuned} onto a contour plot of den , and then plot the points that correspond to maximum acceleration and maximum detuned acceleration.



Notice that the detuned acceleration is not the same as the maximum possible acceleration. The following will demonstrate that the assumption concerning n (i.e. fix $n=4.28$) yields the maximum possible acceleration in the detuned case.

Using $ogr_{detuned}$, solve for $l_{detuned}$

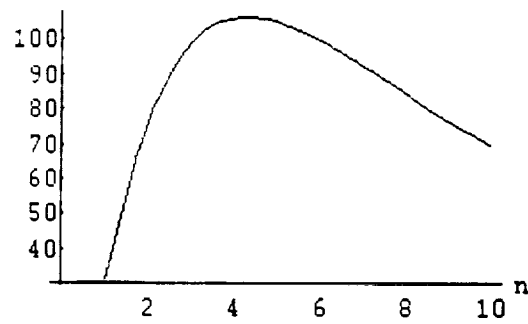
$$l_{detuned} = \frac{2\pi n(5)}{12000(2\pi / 60)}$$

Substituting the above value of $l_{detuned}$ into the equation of the total inertia seen by the motor yields an equation that is only a function of n . The available torque divided by the total inertia is the acceleration. The available torque is

$$\text{Torque} = \frac{(3)(10)(550)(12)}{12000(2\pi / 60)} = 157.563$$

The following plot shows the acceleration of the engine as n varies from 1 to 10

Acceleration



It is clear from the above plot that the maximum acceleration occurs when n is equal to 4.28.

Case VI: 15000 RPM, 15 HP Motor

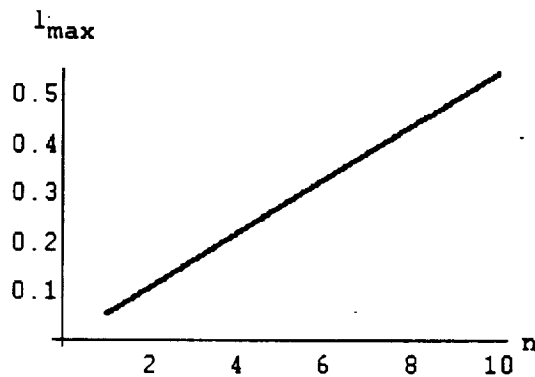
Recall that for maximum acceleration, $n=4.28$ and $l=0.230725$ inches. Define the overall gear ratio as

$$\text{ogr}_{\max} = \frac{2\pi n}{l} = \frac{2\pi(4.28)}{0.230725} = 116.554 \text{ in}^{-1}$$

Using the above relationship for ogr_{\max} , solve for l_{\max}

$$l_{\max} = \frac{2\pi n}{116.554}$$

If l_{\max} is treated as a function of n and n is varied over some range of values, a straight line plot is obtained



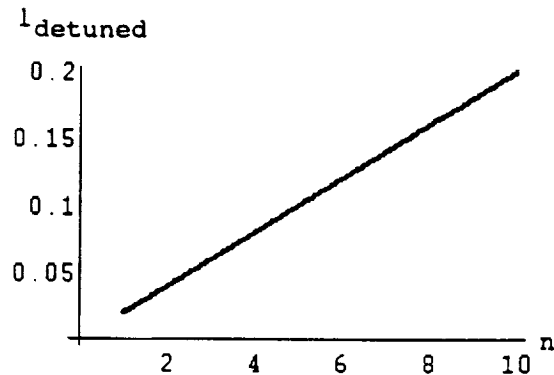
Recall that for the detuned acceleration, $n=4.28$ and $l=0.0856$ inches. To meet the engine speed and force requirements, the overall gear ratio becomes

$$\text{ogr}_{\text{detuned}} = \frac{\dot{\theta}_{\text{motor}}}{\dot{x}_{\text{engine}}} = \frac{(15000 \frac{\text{rev}}{\text{min}})(2\pi \frac{\text{rad}}{\text{rev}})(\frac{1 \text{ min}}{60 \text{ sec}})}{5 \frac{\text{in}}{\text{sec}}} = 314.159 \quad (\dot{\theta}_{\text{motor}} = [\frac{2\pi n}{l}] \dot{x}_{\text{engine}})$$

Using the above relationship for $\text{ogr}_{\text{detuned}}$, solve for l_{detuned}

$$l_{\text{detuned}} = \frac{2\pi n}{314.159}$$

If l_{detuned} is treated as a function of n and n is varied over some range of values, a straight line plot is obtained

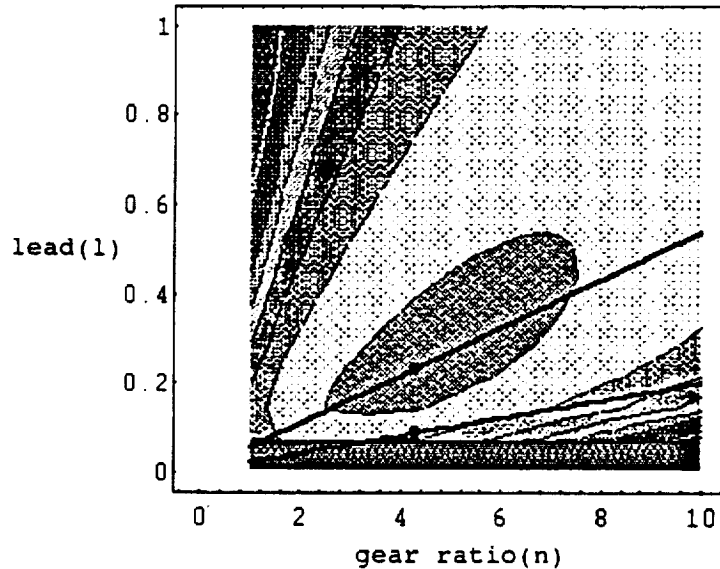


Recall that the total inertia seen by the motor is given by the following equation

$$\text{den} = [J_{\text{Motor}} \left(\frac{2\pi n}{l} \right) + J_{\text{PinionGear}} (3 + n^2) \left(\frac{2\pi n}{l} \right) + J_{\text{RollerScrew}} \left(\frac{2\pi}{nl} \right) + M_{\text{Engine}} \left(\frac{l}{2\pi n} \right)]$$

where the inertia and mass are known.

Superimpose the plots obtained for l_{max} and l_{detuned} onto a contour plot of den , and then plot the points that correspond to maximum acceleration and maximum detuned acceleration



Notice that the detuned acceleration is not the same as the maximum possible acceleration. The following will demonstrate that the assumption concerning n (i.e. fix $n=4.28$) yields the maximum possible acceleration in the detuned case.

Using $ogr_{detuned}$, solve for $l_{detuned}$

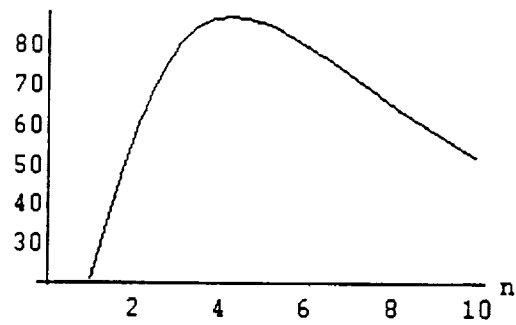
$$l_{detuned} = \frac{2\pi n(5)}{15000(2\pi/60)}$$

Substituting the above value of $l_{detuned}$ into the equation of the total inertia seen by the motor yields an equation that is only a function of n . The available torque divided by the total inertia is the acceleration. The available torque is

$$\text{Torque} = \frac{(3)(10)(550)(12)}{15000(2\pi/60)} = 126.0507$$

The following plot shows the acceleration of the engine as n varies from 1 to 10

Acceleration



It is clear from the above plot that the maximum acceleration occurs when n is equal to 4.28.